Synthesis and application of some novel functional polymers *via* controlled radical polymerization and click chemistry

by

Guang-zhao LI

A thesis submitted in partial fulfilment of the requirements for the degree

of

Doctor of Philosophy in Chemistry

Department of Chemistry

University of Warwick

March 2012

Table of Contents

List of Schemes

List of Figures

List of Tables

Abbreviations

ACN-d_3	deuterated acetonitrile
ACVA	4,4'-azobis(4-cyanopentanoic acid)
AIBN	azoisobutylnitrile
AROP	anionic ring-opening polymerization
ATR	attenuated total reflection
ATRA	atom transfer radical addition
ATRP	atom transfer radical polymerization
BHEDS	bis(2-hydroxyethyl) disulfide
BiBB	α-bromoisobutyryl bromide
Bipy	2,2'-bipyridine
bis-MPA	2,2-bis(hydroxymethyl)propionic acid
BM	benzyl mercaptan
BMP	methyl 2-bromopropionate
BSA	bovine serum albumin
CBB	carbonate-bicarbonate buffer
CCTP	cobalt-mediated catalytic chain-transfer polymerization
CoBF	bis(boron difluorodimethylglyoximate) cobalt(II)
Con A	concanavalin A
Conv.	conversion
CL	ε-caprolactone

CLRP	controlled/"living radical" polymerizations
CPDB	2-cyanoprop-2-yl dithiobenzoate
CROP	cationic ring-opening polymerization
CRP	controlled radical polymerizations
CTA	chain transfer agent
CuAAC	copper (I)-catalysed azide-alkyne cycloaddition
CuLRP	copper-catalysed living radical polymerization
DBU	1,8-diazabicyclo[5.4.0]undec-7-ene
DCC	*N, N'*-dicyclohexylcarbodiimide
DCM	dichloromethane
DCP	dicumyl peroxide
DC-SIGN	dendritic cell specific ICAM-3 grabbing nonintegrin
DCTB	trans-2-[3-(4-*tert*-butylphenyl)-2-methyl-2-propenylidene] malononitrile
DEGDMA	di(ethylene glycol) dimethacrylate
DEGMA	diethylene glycol methacrylate
DIPEA	diisopropylethylamine
DMAEMA	2-(dimethylamino)ethyl methacrylate
DMC	2-chloro-1,3-dimethylinidazolonium chloride
DMF	*N, N*-dimethyl formamide
DMI	1,3-dimethyl-2-imidazolidinone
DMPP	dimethyl phenyl phosphine

DMSO	dimethyl sulfoxide
DMSO-d_6	deuterated dimethyl sulfoxide
DP	degree of polymerization/kinetic chain length
DRI	differential refractive index
DT	dodecanethiol
EBiB	ethyl α-bromoisobutyrate
EDC·HCl	*N*-(3-dimethylaminopropyl)-*N'*-ethylcarbodiimide hydrochloride
ESI-MS	electrospray ionisation mass spectrometry
FITC	fluorescein isothiocyanate isomer I
FRP	free radical polymerization
FT-IR	fourier transform infrared spectroscopy
Gala	galactose
Glc	glucose
GPC	gel permeation chromatography
HA	hexylamine
HEMA	2-hydroxyethyl methacrylate
HEPES	4-(2-hydroxyethyl)piperazine-1-ethanesulfonic acid
HS-Glc	1-thiol-β-D-glucose sodium salt
I	initiator
IR	infrared
LCST	lower critical solution temperature

LRP	living radical polymerization
M	monomer
MA	methyl acrylate
MAA	methacrylic acid
MAIGlc	3-*O*-methacryloyl-1,2:5,6-di-*O*-isopropylidene- D-glucofuranose
MALDI	matrix assisted laser desorption ionisation mass spectroscopy
Mann	mannose
ME	mercaptoethanol
MeOH-d_4	deuterated methanol
Me_6-TREN	tris(2-(dimethylamino)ethyl)amine
MMA	methyl methacrylate
MPA	mercaptopropanoic acid
MS	mass spectrometry
M_n	number average molecular weight
$M_{n,NMR}$	M_n by nuclear magnetic resonance
$M_{n,GPC}$	M_n by gel permeation chromatography
$M_{n,th}$	theoretical number average molecular weight
M_p	peak molecular weight
MPC	5-methyl-5-propargyloxycarbonyl-1,3-dioxane-2-one
MUA	11-mercaptoundecanoic acid
Mw	molecular weight

M_w	weight average molecular weight
MWCO	molecular weight cut off
MWD	molecular weight distribution
NCA	*N*-carboxyanhydrides
NHS	*N*-hydroxy succinimide
NIPAAm	*N*-isopropyl-2-methyl-acrylamide
NMP	nitroxide-mediated polymerization
NMR	nuclear magnetic resonance
OEGMA	oligo(ethylene glycol) methacrylate
PAm	pentylamine
PBS	phosphate buffered saline
PCL	poly(ε-caprolactone)
PDi	polydispersity index
PDMA	poly(*N*,*N*-dimethylacrylamide)
PDMAEMA	poly(dimethylamino)ethyl methacrylate
PEG	poly(ethylene glycol)
PEGMEA	poly(ethylene glycol) methylether acrylate
PEGMEMA	poly(ethylene glycol) methyl ether methacrylate
PEO	poly(ethylene oxide)
PgMA	propargyl methacrylate
PLA	polylactide
PNA	peanut agglutinin

PMAGlc	poly- (3-*O*-methacryloyl-α,*β*-D-glucopyranose)
PMAlpGlc	poly(3-*O*-methacryloyl- 1,2:5,6-di-O-isopropylidene-D-glucofuranose)
PMDETA	*N,N,N',N'',N''*-pentamethyldiethylenetriamine
PMMA	poly(methyl methacrylate)
PNIPAM	poly(*N*-isopropylacrylamide)
PPgMA	poly(propargyl methacrylate)
ppm	parts per million
PS	polystyrene
PT	propanethiol
PVA	poly(vinyl alcohol)
QCM-D	quartz crystal microbalance biosensor with dissipation monitoring
RAFT	reversible addition fragmentation chain transfer
ROMP	ring opening metathesis polymerization
ROP	ring-opening polymerization
RROP	radical ring-opening polymerization
sCT	salmon calcitonin
SEM	scanning electron microscopy
SET-LRP	single electron transfer living radical polymerization
SPR	surface plasmon resonance
St	styrene

TBAF	tetra-*n*-butylammonium fluoride
TBTA	tris-(benzyl-triazolylmethyl)amine
TCEP	tris(2-carboxyethyl)phosphine hydrochloride
TEA	triethylamine
TEM	transmission electron microscopy
TEMPO	(2,2,6,6-Tetramethylpiperidin-1-yl)oxyl
TG	thioglycerol
TGA	thermal gravimetric analysis
THF	tetrahydrofuran
TIPS	triisopropylsilyl
TIPS-PMgA	TIPS-protected propargyl methacrylate
TMM-LRP	transition metal mediated living radical polymerization
TMS	trimethylsilyl
TMS-PMgA	TMS-protected propargyl methacrylate
TTCA	2-(dodecylthiocarbonothioylthio)-2-methylpropionic acid
VAc	vinyl acetate
VI	viscosity index
UV	ultraviolet
UV-VIS	ultraviolet-visible
WGA	wheat germ agglutinin
λ	wavelength (nm)

Acknowledgements

First and foremost I would like to thank Professor David M. Haddleton for all his help throughout my studies. His vision, positive encouragement, constant support and guidance give me the freedom to pursue various projects without objection.

I would like to thank Dr Giussepe Mantovani for your help at the beginning period of my Ph.D. studies.

I would like to thank the members of the polymer groups over the past three years. My thanks go to the Fina, Anne, Tomasz, Julien, Remzi, Flo, Paul, Jay, Mat, Ant, Raj, Stacy, George, Kayleigh, James, Muxiu, Yanzi, Zaidong, Jasmin, Chris, and Jamie.

A special mention goes to Qiang. Thank you so much for all your help throughout the printing process.

Finally, I would like to thank my family for their unconditional love and support. Love you forever!

Declaration

Experimental work contained in this thesis is original research carried out by the author, unless otherwise stated, in the Department of Chemistry at the University of Warwick, between October 2008 and October 2011. No material contained herein has been submitted for any other degree, or at any other institution.

Results from other authors are referenced in the usual manner throughout the text.

_____ Date: _____

Guang-zhao LI

Abstract

The objective of this thesis was to prepare thermoresponsive PEG-based homopolymers and copolymers by combination of cobalt-mediated catalytic chain-transfer polymerization (CCTP) and thiol-ene "click" chemistry and prepare well-defined glycopolymers *via* "living" polymerization and "click" chemistry.

The effect of different catalysts for the nucleophilic mediated thiol-ene reaction was investigated using model compounds, both monomers and oligomers obtained by CCTP. Different catalysts, including pentylamine and hexylamine (primary amines), triethylamine (tertiary amine), and two different phosphines, dimethylphenylphosphine (DMPP) and tris(2-carboxyethyl) phosphine (TCEP), were investigated in the presence of different thiols. The optimum reaction conditions for nucleophile mediated thiol-ene click reactions were investigated.

Thermoresponsive PEG-based homopolymers and copolymers of OEGMEMA obtained by CCT were modified using thiol-ene click chemistry with a variety of different functional thiol compounds to yield functional thermoresponsive polymers in high yield. The effect of different solvent systems for based catalyzed thiol-ene reaction was investigated in the presence of different functional thiols.

The ATRP polymerization of TMS-PgMA and TIPS-PgMA and ROP polymerization of aliphatic polyester were investigated. A maleimide functional initiator was used in order to achieve post conjugation of nanoparticles for drug delivery. Moreover, the disulfide based bifunctional initiator was introduced into the midpoint of the polymer chain, which could break down to afford the corresponding polymer chain with thiol end group under the reducing condition. The thiol-terminated polymer was also post-functionalized *via* thiol-ene click chemistry. In addition, the aliphatic polycarbonate is a biocompatible and biodegradable polymer, which is widely used in medical and pharmaceutical applications. The subsequent introduction of sugar moiety to the reactive polymer chain *via* CuAAC click reaction and then the interactions between glycopolymers and lectins were investigated by Surface Plasmon Resonance (SPR) and Quartz Crystal Microbalance with Dissipation (QCM-D).

The controlled SET-LRP polymerization of TMS-PgMA and SET-RAFT polymerization PgMA with the intact alkyne at ambient temperature were investigated. A maleimide functional initiator and CPDB, as the chain transfer agent have been employed. The introduction of maleimide moiety was to allow for post polymerization conjugation to peptides *via* reaction with cysteines. The subsequent introduction of sugar azides to click with the reactive polymer containing alkyne group and the glycopolymers through CuAAC was also investigated. The glycopolymer has been successfully prepared combining the SET-LRP/SET-RAFT and CuAAc click chemistry at ambient temperature.

Chapter 1. Synthesis of glycopolymers: An overview

1.1. Polymerization techniques

1.1.1. Living polymerization

Michael Szwarc first reported the anionic polymerization of styrene in THF solution by use of sodium and naphthalene yielding the naphthalene radical anion in 1956, **Figure 1.1**.[1, 2] Subsequently, the anionic polymerization of styrene and dienes in hydrocarbon solvent with alkyl lithium initiators were published and stimulated interest in this field, **Figure 1.2**.[3, 4]

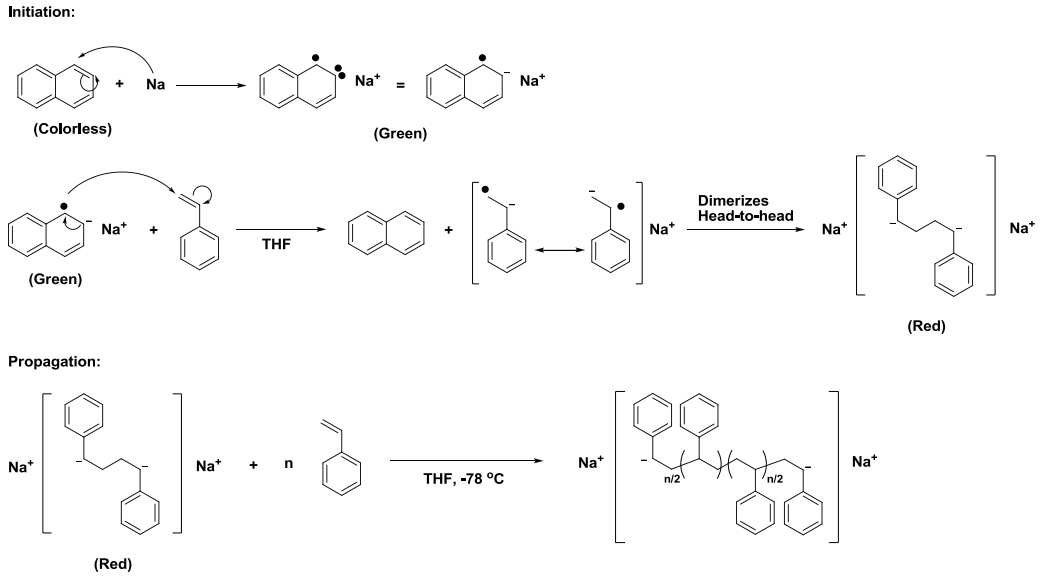

Figure 1.1 Anionic polymerization of styrene using sodium naphthalene as initiator in THF

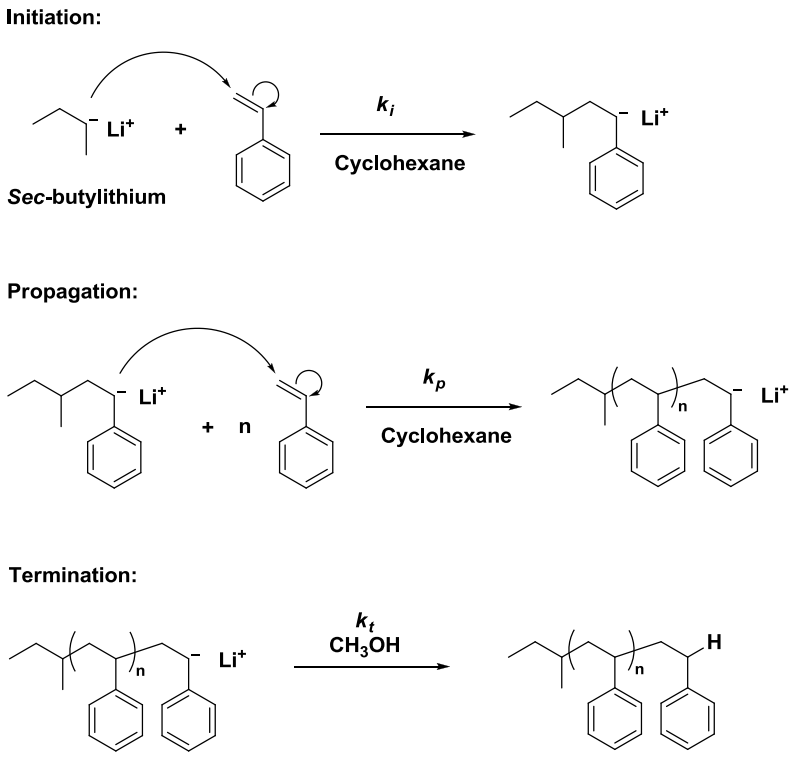

Figure 1.2 Anionic polymerization of styrene using *sec*-butyllithium as initiator in cyclohexane

This work inspired further research on the living polymerization in both academia and industry to synthesis well-defined block and graft copolymers, star polymers, telechelic polymers, cyclic and multi-cyclic polymers.[5-23] However, this polymerization is inherent sensitive towards protic species due to the high reactivity of carbanions, which requires the ultrapure regents and solvent, specially designed equipment as well as very low temperatures condition (usually -78 ℃) making the process is very expensive during commercial large-scale production. In addition, the types of available monomer necessary for ionic

polymerization are limited.

1.1.1.1. Definition of living polymerization

A living polymerization proceeds in the absence of the kinetic steps of chain termination and chain transfer. The following experimental criteria were used to diagnose whether a given polymerization is a living polymerization.[24, 25]

(1) Living polymerization proceeds until all monomers are consumed. The polymerization will continue growing if further monomers are added.

(2) The number average molecular weight of polymer increase in direct proportion to monomer conversion.

(3) The number of polymer molecules remains constant during the polymerization, which is independent of monomer conversion.

(4) The molecular weight of the polymer can be controlled by the stoichiometry of the reaction.

(5) The polymer with a narrow molecular weight distribution using a living polymerization

(6) Block copolymers can be synthesized by sequential monomer addition.

(7) Chain-end functionalized polymers can be gained in quantitative yield.

Generally, no one criterion is satisfactory to assess the living of polymerization; that is because different experimentally observable consequences and criteria have different sensitivities towards the chain termination and chain

transfer side reactions. In conclusion, a polymerization with each and every one of the above criteria can be termed living polymerization.

1.1.1.2. Living polymerization timescale

In the ideal situation living polymerization requires the absence of chain termination and chain transfer and yields polymers retaining their active centers, virtually indefinitely.

It is however, beneficial to assess the living polymerization based on a laboratory timescale. This means that no significant chain termination and chain transfer reactions occur within a sufficiently long time to complete the polymerization and carry out chain extension. Even some termination and chain transfer reactions may occur during this time, provide it is virtually undetectable and does not affect the result.

A relatively modest quantitative kinetic criterion for living polymerization was proposed by Matyjaszewski:[26]

$k_p/k_t > 10^4$ mol^{-1}L

$k_p/k_{tr} > 10^4$

$1/k_{t/tr} > 10^4$ s

where k_p is the propagation rate constant, k_t is the termination rate constant and k_{tr} is the chain transfer rate constant. The living polymerization system can provide a polymer with DP ≈100 and less than 10% chains deactivated by either transfer or termination in more than 1000 s (t ≈ 15 min).

1.1.2. Controlled radical polymerization (CRP)

Free radical polymerization is one of the most widely used polymerization methods. Nearly 50% of currently commercial synthetic polymers in the global market are prepared *via* radical polymerization. This can be explained in term of the main advantages of the radical polymerization which is the tolerance of a large range of available monomers and solvents, the relative insensitivity to water and impurities, the moderate wide reaction temperatures and many types of polymerization methods and technologies available, such as bulk, solution, suspension, emulsion, dispersion, precipitation polymerization, *etc*. However, there are some disadvantages of the radical polymerization which is poor control of the molecular weight and the polymer featuring broad molecular weight distribution. It is difficult to prepare copolymers with well-defined structures too. This due to the chain termination and chain transfer related to the mechanism of free radical polymerization.[27-30]

Controlled/"living" radical polymerization was developed in order to overcome some or all of these disadvantages. This controlled/"living" radical polymerization is based on the dynamic equilibrium between a low concentration of propagating radicals and various dormant species. Radicals may be involved in either a reversible deactivation/activation process or a ‘‘reversible transfer'', degenerative exchange process.[19, 31-34]

1.1.2.1. Nitroxide-mediated polymerization (NMP)

Nitroxide-mediated polymerization (NMP) was discovered firstly by Solomon *et al.* in 1985.[35] Sometimes NMP was also termed stable free radical polymerization (SFRP). It has received considerable attention only after the publication by Georges *et al.* in 1993 using 2,2,6,6-tetramethylpiperidynyl-1-oxy (TEMPO) as a mediator which showed a straightforward method for the controlled radical polymerization.[36] Numerous derivatives of TEMPO have been successfully employed in NMP, **Figure 1.3**. [119-122]

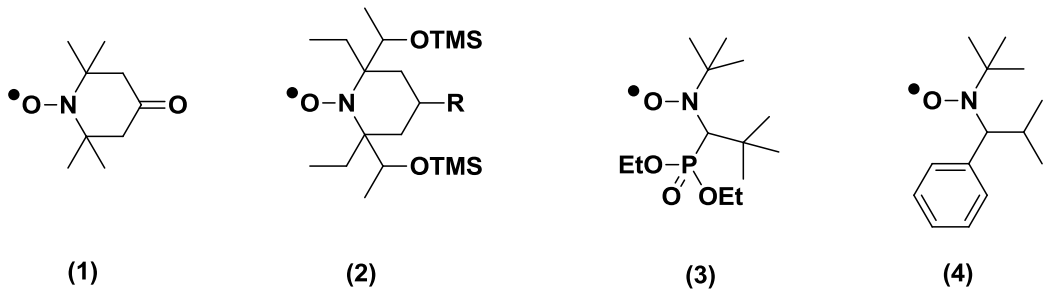

Figure 1.3 Structures of typical nitroxide derivatives used in NMP.

1.1.2.2. Atom Transfer Radical Polymerization (ATRP)

ATRP originates from the atom transfer radical addition (ATRA), also

referred to as Kharasch addition, which is widely used in organic chemistry. In this reaction, additional product was formed by alkyl halides and alkenes with transition metal catalyst.[37-42] ATRP was discovered independently reported by the group of Sawamoto[43] and Matyjaszewski.[44] In their first report, Sawamoto *et al.* employed $RuCl_2(PPh_3)_3$/$MeAl(ODBP)_2$ as a catalystic system and CCl_4 as a initiator in the polymerization of MMA.[43] Simultaneously the polymerization of styrene using CuCl/2,2'-bipyridine as the catalytic system and 1-phenylethyl chloride (1-PECl) as initiator by Matyjaszewski *et al.*[44]

Atom transfer radical polymerization (ATRP) relies on the reversible transfer of halogen atoms (usually Cl or Br), or pseudo-halogens, between a dormant species (P_n–X) and a transition metal catalyst (M_t^z - Y/Ligand) *via* redox process, **Figure 1.4**.

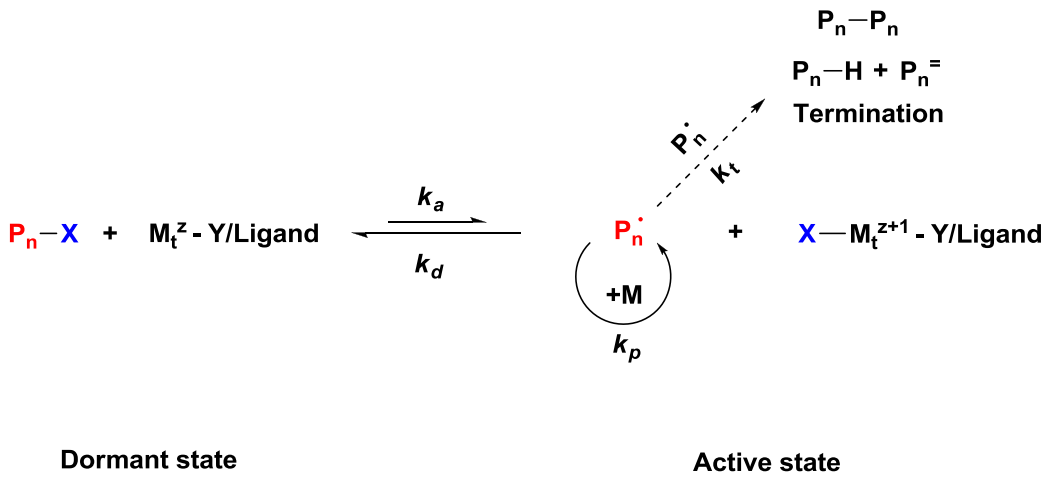

Figure 1.4 Proposed mechanism of atom transfer radical polymerization, the rate constant of activation (k_a), deactivation (k_d), propagation (k_p) and termination (k_t)

ATRP is a catalytic process and can be mediated by transition metal complex which exist in two different oxidation states during the polymerization. The lower oxidation state transition metal complex (M_t^z-Y/Ligand) is responsible for the homolytic cleavage of carbon-(pseudo)halogen bond in the ATRP initiator (alkyl (pseudo)halides, RX) to generates the corresponding higher oxidation state transition metal halide complex (X-M_t^{z+1}-Y/Ligand) and an active organic radical $P_n^{\bullet}$, proceeding with the rate constant of activation (k_a). The active radical $P_n^{\bullet}$ can react with vinyl monomer (M) to form growing polymer chain with the rate constant of propagation (k_p), or terminate by either bimolecular coupling or disproportionation reaction with the rate constant of termination (k_t), or be reversibly deactivated with the rate of deactivation (k_d) in this equilibrium by X-M_t^{z+1}-Y/Ligand complex to yield a halide-capped dormant polymer chain and M_t^z-Y/Ligand complex.

1.1.2.3. Single-Electron Transfer Living Radical Polymerization (SET−LRP)

In 2006, Percec group have reported the SET-LRP of vinyl monomers, including acrylates and vinyl halides, etc., mediated by Cu(0) using and alkyl halide as initiators in presence of nitrogen based ligands in polar solvent at 25 ^{o}C.[45-49] As described in these reports, the deactivating species in SET-LRP is

copper(II) halides similar to ATRP, however, the proposed activating is the zero-valent copper, in the form of a powder or wire, rather than Copper(I) halides.

This so-called SET-LRP process involves an equilibrium between active radicals $P_n^{\bullet}$ and dormant P_n-X species. The formation of active radicals, $P_n^{\bullet}$, and dormant species, P_n-X, proceeds by a heterolytic outer sphere electron transfer (OSET) process. The proposed mechanism is depicted in **Figure 1.5**. The reaction starts with between electron-donor Cu(0) species and the electron-acceptor halogen-containing dormant substrate (P_n-X). The P_n-X bond dissociation occurs through the formation and decomposition of the radical anion intermediates. The radical-anion pair and Cu^+/L counter cation must be close enough to promoting the decomposition of radical anion intermediates into the active radical $P_n^{\bullet}$ and Cu(I)X/L species. The resulting Cu(I)X/L complex spontaneously disproportionates into nascent Cu(0) species (activator) and Cu(II)X_2/L complex (deactivator) mediated by the polar media in presence of nitrogen containing ligands, which is the key part step in the SET-LRP mechanism. The absence of Cu(I)X/L complex during SET-LRP reveals that the Cu(II)X_2/L deactivator is only generated by spontaneous disproportionation of the Cu(I)X/L complex formed *in situ*. Besides, the reactivity of nascent atomic Cu(0) is higher than that of solid elemental Cu(0), so the main SET-LRP process is mediated by the nascent atomic Cu(0) in the presence of an equivalent amount of Cu(II)X_2/L complex. The deactivation process between an active radical $P_n^{\bullet}$ and the Cu(II)X_2/L complex (deactivator) in presence of the polar solvent is a more

complex reaction. One of the possible mechanisms may be the halide anion (X^-) in the Cu(II)X_2/L species (deactivator) transfer to the chain propagating radical $P_n^{\bullet}$ species, yielding radical anion intermediates composed of radical-anion pair and CuX^+/L counter cation.[45, 50-53]

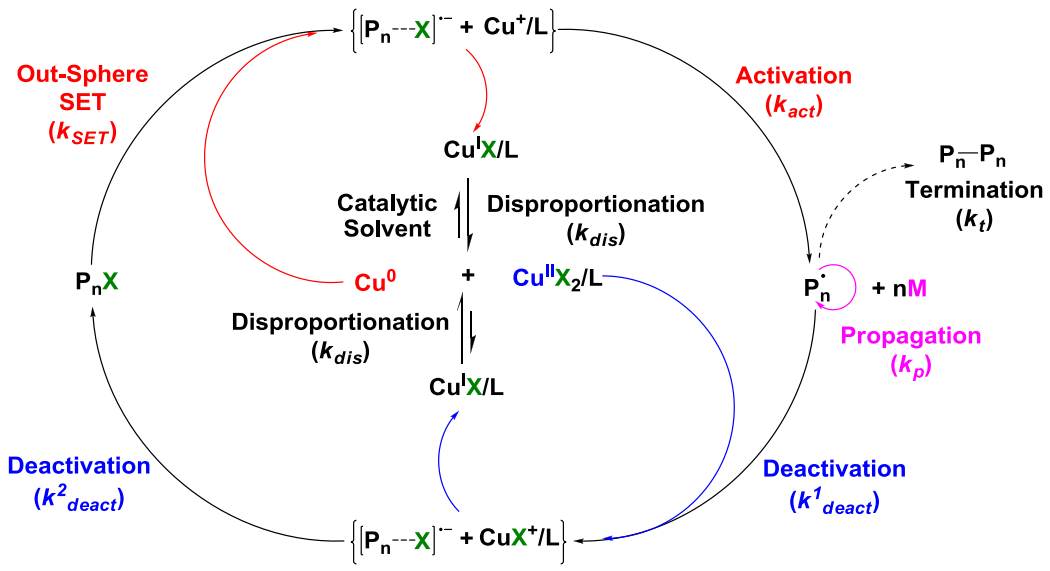

Figure 1.5 Proposed mechanism for SET-LRP mediated by Cu(0) species in polar solvent; P = polymer; X = halogen (Cl, Br, I); L = nitrogen-based ligand.

SET provides a technique for the ultrafast synthesis of predictable ultrahigh molecular weight polymers with narrow molecular weight distribution at ambient or sub-ambient temperature. The polymerization can proceed in a variety of solvents, including "green" and aqueous solvents, with excellent reaction rates. The Cu(0) catalyst is simple, inexpensive, highly active, easily recoverable and recyclable, leading to colorless polymers without the use of any special

purification. In addition, the acquired polymers have the perfect chain-end functionality.[45, 51]

1.1.2.4. Reversible Addition-Fragmentation Chain Transfer (RAFT) polymerization

RAFT polymerization was invented by Moad, Rizzardo and Thang *et al.* in 1998, [54] for controlled radical polymerization (CRP) and become currently one of the most popular CRP processes. This allows for the synthesis of polymers or copolymers with predetermined molecular weight and narrow molecular weight distributions. It is also tolerant to a wide range of monomers, initiators and reaction conditions. In addition, complex well-defined architecture including blocks, stars, branched, hyperbranched, gradient, microgel and supramolecular assemblies are accessible and the obtained polymers containing reactive terminal groups can be purposely manipulated, including further extensions of polymer chain. [55-65]

The unique feature of the mechanism of RAFT polymerization with thiocarbonylthio RAFT agent (RSC(Z)=S) is the sequence of reversible addition-fragmentation equilibria during the polymerization. The typical mechanism of RAFT polymerization is shown in **Figure 1.6**.

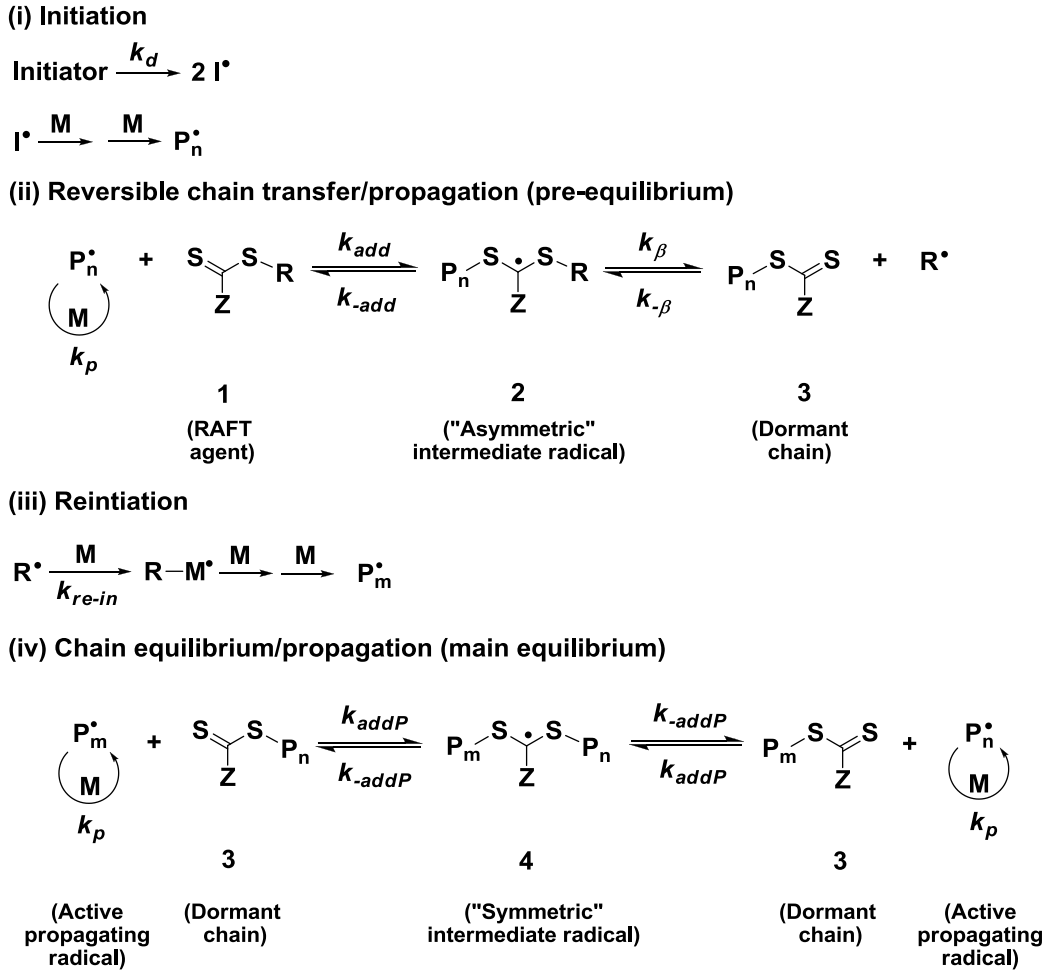

Figure 1.6 Mechanism of RAFT polymerization

The key to successful RAFT polymerization is the choice of favorable RAFT agents, a wide variety of RAFT agents have now been reported. Most contain thiocarbonlthio moieties belonging to one of the following general families of organic compounds: dithioesters (Z = alkyl, aryl) (A), trithiocarbonates (Z = S-alkyl, S-aryl) (B), xanthates (Z = O-alkyl, O-aryl) (C) and dithiocarbamates (Z =

NR'R"; R', R" = alkyl or aryl) (D), **Figure 1.7**.

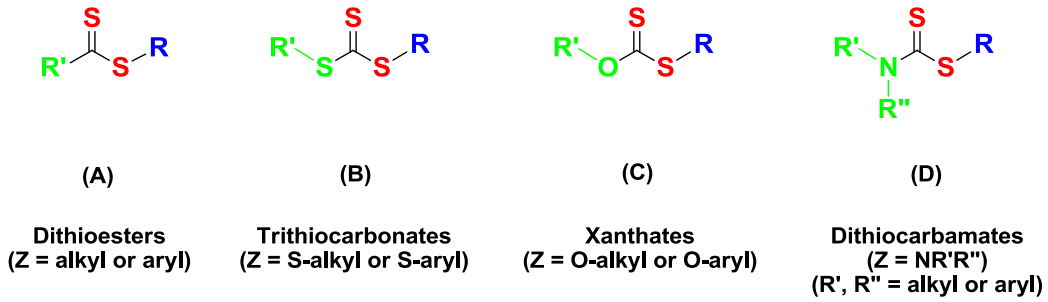

Figure 1.7 Structures of commonly used RAFT agents

The effectiveness of the RAFT agent bases on the monomer and is determined by the structures of the free radical (hemolytic) leaving group R and group Z. The Z group control the reactivity of the thiocarbonyl double bond (C=S) in the RAFT agent (**1**) towards to radical addition and modify the stability of the intermediate radicals (**2** or **4**, respectively). The choice of the R group allows for the fine tuning of the overall reactivity and initiates the growth of polymer chains, which must be a better free radical leaving group than the propagating radical and the radical is also capable of efficiently re-initiating polymerization. For an efficient RAFT polymerization (**Figure 1.6** and **Figure 1.8**):[55-57, 66]

(i) The reactive C=S double bond in initial RAFT agents (**1)** and the polymer RAFT agent (**3)** should have a high k_{add}.

(ii) The intermediate radicals (**2)** and (**4)** should fragment rapidly with high k_{β}, which possess weak S–R bond and have no side reactions.

(iii) The intermediate (**2)** should favor the formation of (**3**) ($k_{\beta} \geq k_{-add}$).

(iv) The expelled free radicals species ($R^{\bullet}$) from the hemolytic dissociation should efficiently re-initiate polymerization ($k_{re\text{-}in} > k_p$)

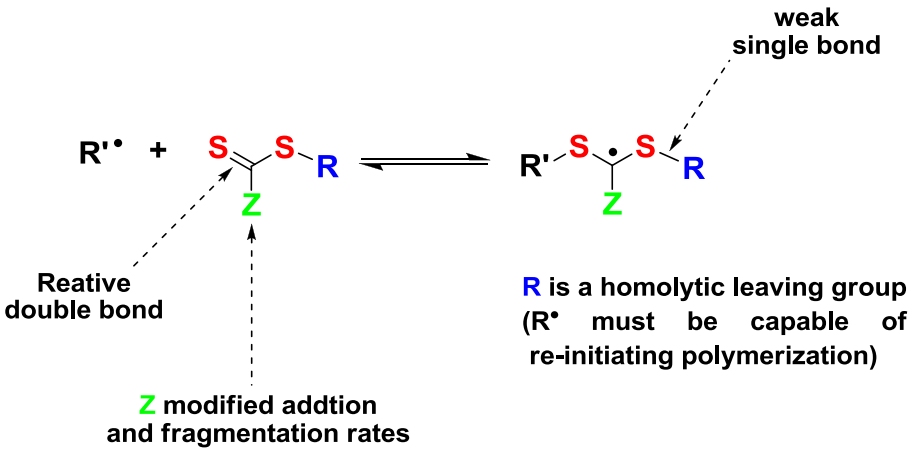

Figure 1.8 Generic structural features of thiocarbonylthio RAFT agent

1.1.2.5. Cobalt-Mediated Catalytic Chain-Transfer Polymerization (CCTP)

Smirnov, Morozova and Marchenko *et al.* discovered that Co(II) porphyrins (**Figure 1.9** (1)) catalyze the chain transfer reaction to monomer reaction in the early 1980s.[67-72] Some further research was carried out by Gridnev.[73, 74] Catalytic chain transfer polymerization is a very efficient and versatile free-radical polymerization technique for the synthesis of low molecular weight polymers with ω-unsaturated vinyl terminal groups which have been commercially used in

industry, such as DuPont, ICI/Zeneca and DSM.[75-79]

The best known CCT catalysts are Co(II) complexes with the following structures (**Figure 1.9**), where the substituent R group is used to modify solubility and activity.[75-79]

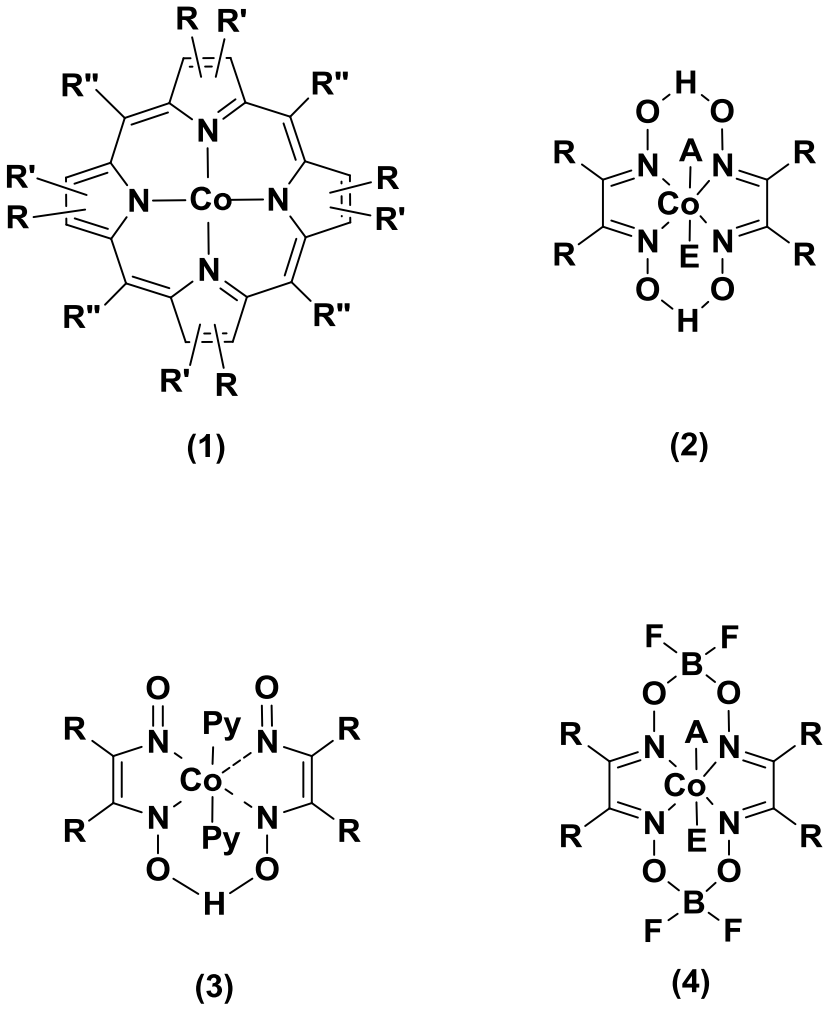

Figure 1.9 Examples of cobalt complexes in CCTP

1.2. Synthesis of glycopolymers

In 1998, Hirao *et al.* were the first group synthesis of glycopolymers by using the living anionic polymerization.[80] As shown in **Figure 1.10**, six styrene derivatives *meta*-substituted with acetal-protected glucofuranose (1) and (2), galactopyranose (3), fructopyranose (4) and sorbofuranose (5) and *para*-substituted with acetal-protected glucofuranose (6) were synthesized, and then they were all polymerized using *s*-BuLi as catalyst in THF at -78 ^{o}C for 30 mins.

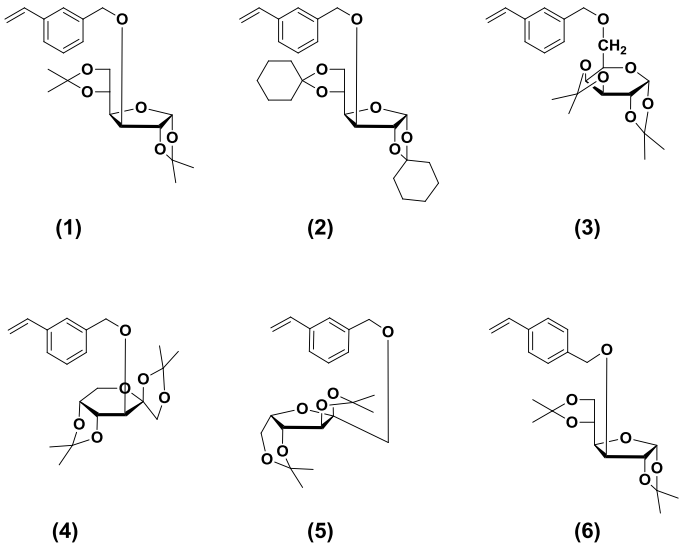

Figure 1.10 Styrene derivatives containing an acetal-protected sugar moiety

Glycopolymers have subsequently been prepared *via* living cationic polymerisation[81-86], ring-opening polymerization (ROP)[87-93], ring-opening

metathesis polymerization (ROMP)[94-102], cyanoxyl(OCN)-mediated free-radical polymerization[103-107], NMP[108-116], ATRP[117-137] and RAFT[138-150].

1.3. References

1. M. Szwarc, *Nature*, 1956, **178**, 1168-1169.
2. M. Szwarc, M. Levy and R. Milkovich, *J. Am. Chem. Soc.*, 1956, **78**, 2656-2657.
3. M. Morton, E. G. Bostich and R. A. Livigni, *Rubber Plast. Age.*, 1961, **42**, 397.
4. M. Morton and F. R. Ells, *J. Polym. Sci.*, 1962, **61**, 25-29.
5. D. Baskaran and A. H. E. Müller, *Controlled and Living Polymerizations: From Mechanisms to Materials. Chapter 1*, Wiley-VCH, Weinheim, 2009.
6. E. Franta, T. Hogen-Esch, M. Van Beylen and J. Smid, *J. Polym. Sci., Part A: Polym. Chem.*, 2007, **45**, 2576-2579.
7. D. Baskaran, *Prog. Polym. Sci.*, 2003, **28**, 521-581.
8. R. Jerome and J. D. Tong, *Curr. Opin. Solid State Mater. Sci.*, 1998, **3**, 573-578.

9. M. Vanbeylen, S. Bywater, G. Smets, M. Szwarc and D. J. Worsfold, *Adv Polym Sci*, 1988, **86**, 87-143.

10. P. Kubisa, I. Negulescu, K. Hatada, D. Lipp, J. Starr, B. Yamada and O. Vogl, *Pure Appl. Chem.*, 1976, **48**, 275-285.

11. A. Avila-Ortega and H. Vazquez-Torres, *J. Polym. Sci., Part A: Polym. Chem.*, 2007, **45**, 1993-2003.

12. A. Hirao, Y. Tsunoda, A. Matsuo, K. Sugiyarna and T. Watanabe, *Macromol. Res.*, 2006, **14**, 272-286.

13. M. H. Acar and K. Matyjaszewski, *Macromol. Chem. Phys.*, 1999, **200**, 1094-1100.

14. F. J. Hua and Y. L. Yang, *Polymer*, 2001, **42**, 1361-1368.

15. E. Ruckenstein and H. M. Zhang, *Macromolecules*, 1999, **32**, 6082-6087.

16. K. Se, H. Yamazaki, T. Shibamoto, A. Takano and T. Fujimoto, *Macromolecules*, 1997, **30**, 1570-1576.

17. A. C. M. Rizmi, E. Khosravi, W. J. Feast, M. A. Mohsin and A. F. Johnson, *Polymer*, 1998, **39**, 6605-6610.

18. S. K. Varshney, P. Bayard, C. Jacobs, R. Jerome, R. Fayt and P. Teyssie, *Macromolecules*, 1992, **25**, 5578-5584.

19. M. A. Tasdelen, M. U. Kahveci and Y. Yagci, *Prog. Polym. Sci.*, 2011, **36**, 455-567.

20. B. Lepoittevin and P. Hemery, *Polym. Adv. Technol.*, 2002, **13**, 771-776.

21. B. Lepoittevin and P. Hemery, *J. Polym. Sci., Part A: Polym. Chem.*, 2001, **39**, 2723-2730.

22. H. R. Kricheldorf, *J. Polym. Sci., Part A: Polym. Chem.*, 2010, **48**, 251-284.

23. H. Oike, H. Imaizumi, T. Mouri, Y. Yoshioka, A. Uchibori and Y. Tezuka, *J. Am. Chem. Soc.*, 2000, **122**, 9592-9599.

24. R. P. Quirk and B. Lee, *Polym. Int.*, 1992, **27**, 359-367.

25. T. R. Darling, T. P. Davis, M. Fryd, A. A. Gridnev, D. M. Haddleton, S. D. Ittel, R. R. Matheson, G. Moad and E. Rizzardo, *J. Polym. Sci., Part A: Polym. Chem.*, 2000, **38**, 1706-1708.

26. K. Matyjaszewski, *J. Polym. Sci., Part A: Polym. Chem.*, 1993, **31**, 995-999.

27. C. Walling, *Free radicals in solution.*, John Wiley and Sons,. Inc., New York, 1957.

28. C. H. Bamford, W. G. Barb, A. D. Jenkins and P. F. Onyon, *The kinetics of vinyl polymerization by radical mechanisms.*, Academic Press, New York, 1958.

29. K. Matyjaszewski and T. P. Davis, *Handbook of radical polymerization* Wiley-Interscience, Hoboken, 2002.

30. G. Moad and D. H. Solomon, *The Chemistry of Radical Polymerization, 2nd ed.*, Elsevier, Oxford, U.K., 2006.

31. K. Matyjaszewski, *Curr. Opin. Solid State Mater. Sci.*, 1996, **1**, 769-776.

32. W. A. Braunecker and K. Matyjaszewski, *Prog. Polym. Sci.*, 2007, **32**, 93-146.

33. M. Baumert, H. Frey, M. Holderle, J. Kressler, F. G. Sernetz and R. Mulhaupt, *Macromol. Symp.*, 1997, **121**, 53-74.

34. A. Goto and T. Fukuda, *Prog. Polym. Sci.*, 2004, **29**, 329-385.

35. Eur. Pat. Appl. EP135280, 1985.

36. M. K. Georges, R. P. N. Veregin, P. M. Kazmaier and G. K. Hamer, *Macromolecules*, 1993, **26**, 2987-2988.

37. M. S. Kharasch, E. V. Jensen and W. H. Urry, *Science*, 1945, **102**, 128.

38. M. S. Kharasch, W. H. Urry and E. V. Jensen, *J. Am. Chem. Soc.*, 1945, **67**, 1626-1626.

39. D. P. Curran, *Synthesis-Stuttgart*, 1988, 417-439.

40. D. P. Curran, *Synthesis-Stuttgart*, 1988, 489-513.

41. F. Minisci, *Acc. Chem. Res.*, 1975, **8**, 165-171.

42. R. A. Gossage, L. A. Van De Kuil and G. Van Koten, *Acc. Chem. Res.*, 1998, **31**, 423-431.

43. M. Kato, M. Kamigaito, M. Sawamoto and T. Higashimura, *Macromolecules*, 1995, **28**, 1721-1723.

44. J. S. Wang and K. Matyjaszewski, *J. Am. Chem. Soc.*, 1995, **117**, 5614-5615.

45. V. Percec, T. Guliashvili, J. S. Ladislaw, A. Wistrand, A. Stjerndahl, M. J. Sienkowska, M. J. Monteiro and S. Sahoo, *J. Am. Chem. Soc.*, 2006, **128**, 14156-14165.

46. G. Lligadas and V. Percec, *J. Polym. Sci., Part A: Polym. Chem.*, 2008, **46**, 2745-2754.

47. M. J. Sienkowska, B. M. Rosen and V. Percec, *J. Polym. Sci., Part A: Polym. Chem.*, 2009, **47**, 4130-4140.

48. T. Hatano, B. M. Rosen and V. Percec, *J. Polym. Sci., Part A: Polym. Chem.*, 2010, **48**, 164-172.

49. N. H. Nguyen, B. M. Rosen, G. Lligadas and V. Percec, *Macromolecules*, 2009, **42**, 2379-2386.

50. T. Guliashvili and V. Percec, *J. Polym. Sci., Part A: Polym. Chem.*, 2007, **45**, 1607-1618.

51. B. M. Rosen and V. Percec, *Chem. Rev.*, 2009, **109**, 5069-5119.

52. M. J. Monteiro, T. Guliashvili and V. Percec, *J. Polym. Sci., Part A: Polym. Chem.*, 2007, **45**, 1835-1847.

53. A. A. Isse, A. Gennaro, C. Y. Lin, J. L. Hodgson, M. L. Coote and T. Guliashvili, *J. Am. Chem. Soc.*, 2011, **133**, 6254-6264.

54. J. Chiefari, Y. K. Chong, F. Ercole, J. Krstina, J. Jeffery, T. P. T. Le, R. T. A. Mayadunne, G. F. Meijs, C. L. Moad, G. Moad, E. Rizzardo and S. H. Thang, *Macromolecules*, 1998, **31**, 5559-5562.

55. G. Moad, E. Rizzardo and S. H. Thang, *Aust. J. Chem.*, 2005, **58**, 379-410.

56. G. Moad, E. Rizzardo and S. H. Thang, *Aust. J. Chem.*, 2006, **59**, 669-692.

57. G. Moad, E. Rizzardo and S. H. Thang, *Aust. J. Chem.*, 2009, **62**, 1402-1472.

58. G. Moad, E. Rizzardo and S. H. Thang, *Polymer*, 2008, **49**, 1079-1131.

59. C. Barner-Kowollik and S. Perrier, *J. Polym. Sci., Part A: Polym. Chem.*, 2008, **46**, 5715-5723.

60. P. Vana, *Macromol. Symp.*, 2007, **248**, 71-81.

61. E. Rizzardo, M. Chen, B. Chong, G. Moad, M. Skidmore and S. H. Thang, *Macromol. Symp.*, 2007, **248**, 104-116.

62. A. D. Peklak and A. Butte, *Macromol. Theory Simul.*, 2006, **15**, 546-562.

63. A. Butté, A. D. Peklak, G. Storti and M. Morbidelli, *Macromol. Symp.*, 2007, **248**, 168-181.

64. D. Colombani, *Prog. Polym. Sci.*, 1999, **24**, 425-480.

65. B. Yamada, P. B. Zetterlund and E. Sato, *Prog. Polym. Sci.*, 2006, **31**, 835-877.

66. A. B. Lowe and C. L. McCormick, *Prog. Polym. Sci.*, 2007, **32**, 283-351.

67. B. R. Smirnov, I. S. Morozova, A. P. Marchenko, M. A. Markevich, L. M. Pushchaeva and N. S. Enikolopyan, *Dokl. Akad. Nauk SSSR*, 1980, **253**, 891.

68. B. R. Smirnov, A. P. Marchenko, G. V. Korolev, I. M. Bel'govskii and N. S. Yenikolopyan, *Polym. Sci. U.S.S.R.*, 1981, **23**, 1158-1168.

69. B. R. Smirnov, A. P. Marchenko, V. D. Plotnikov, A. I. Kuzayev and N. S. Yenikolopyan, *Polym. Sci. U.S.S.R.*, 1981, **23**, 1169-1178.

70. B. R. Smirnov, A. P. Marchenko, V. D. Plotnikov, A. I. Kuzaev and N. S. Yenikolopyan, *Vysokomol. Soedin., Ser. A*, 1981, **23**, 1051-1058.

71. B. R. Smirnov, V. D. Plotnikov, B. V. Ozerkovskii, V. P. Roshchupkin and N. S. Yenikolopyan, *Polym. Sci. U.S.S.R.*, 1981, **23**, 2807-2816.

72. N. S. Enikolopyan, B. R. Smirnov, G. V. Ponomarev and I. M. Belgovskii, *J. Polym. Sci., Part A: Polym. Chem.*, 1981, **19**, 879-889.

73. A. A. Gridnev, P. M. Belgovskii and N. S. Enikolopyan, *Vysokomol. Soedin., Ser. B*, 1981, **28**, 85.

74. A. A. Gridnev, *Polym. Sci. U.S.S.R.*, 1989, **31**, 2369-2376.

75. A. A. Gridnev and S. D. Ittel, *Chem. Rev.*, 2001, **101**, 3611-3659.

76. D. M. Haddleton, E. Depaquis, E. J. Kelly, D. Kukulj, S. R. Morsley, S. A. F. Bon, M. D. Eason and A. G. Steward, *J. Polym. Sci., Part A: Polym. Chem.*, 2001, **39**, 2378-2384.

77. A. Debuigne, R. Poli, C. Jerome, R. Jerome and C. Detrembleur, *Prog. Polym. Sci.*, 2009, **34**, 211-239.

78. A. Gridnev, *J. Polym. Sci., Part A: Polym. Chem.*, 2000, **38**, 1753-1766.

79. J. P. A. Heuts and N. M. B. Smeets, *Polym. Chem.*, 2011, **2**, 2407-2423.

80. S. Loykulnant, M. Hayashi and A. Hirao, *Macromolecules*, 1998, **31**, 9121-9126.

81. M. Minoda, K. Yamaoka, K. Yamada, A. Takaragi and T. Miyamoto, *Macromol. Symp.*, 1995, **99**, 169-177.

82. K. Yamada, M. Minoda and T. Miyamoto, *J. Polym. Sci., Part A: Polym. Chem.*, 1997, **35**, 751-757.

83. K. Yamada, K. Yamaoka, M. Minoda and T. Miyamoto, *J. Polym. Sci., Part A: Polym. Chem.*, 1997, **35**, 255-261.

84. K. Yamada, M. Minoda and T. Miyamoto, *Macromolecules*, 1999, **32**, 3553-3558.

85. K. Yamada, M. Minoda, T. Fukuda and T. Miyamoto, *J. Polym. Sci., Part A: Polym. Chem.*, 2001, **39**, 459-467.

86. J. Bernard, M. Schappacher, A. Deffieux, P. Viville, R. Lazzaroni, M. H. Charles, M. T. Charreyre and T. Delair, *Bioconjugate Chem.*, 2006, **17**, 6-14.

87. K. Aoi, H. Suzuki and M. Okada, *Macromolecules*, 1992, **25**, 7073-7075.

88. K. Aoi, K. Tsutsumiuchi and M. Okada, *Macromolecules*, 1994, **27**, 875-877.

89. K. Aoi, K. Tsutsumiuchi, E. Aoki and M. Okada, *Macromolecules*, 1996, **29**, 4456-4458.

90. K. Tsutsumiuchi, K. Aoi and M. Okada, *Macromolecules*, 1997, **30**, 4013-4017.

91. M. Okada, K. Aoi and K. Tsutsumiuchi, *Proc. Jpn. Acad. Ser. B Phys. Biol. Sci.*, 1997, **73**, 205-209.

92. C. H. Lu, Q. Shi, X. S. Chen, T. C. Lu, Z. G. Xie, X. L. Hu, J. Ma and X. B. Jing, *J. Polym. Sci., Part A: Polym. Chem.*, 2007, **45**, 3204-3217.

93. F. Suriano, R. Pratt, J. P. K. Tan, N. Wiradharma, A. Nelson, Y. Y. Yang, P. Dubois and J. L. Hedrick, *Biomaterials*, 2010, **31**, 2637-2645.

94. K. H. Mortell, M. Gingras and L. L. Kiessling, *J. Am. Chem. Soc.*, 1994, **116**, 12053-12054.

95. C. Fraser and R. H. Grubbs, *Macromolecules*, 1995, **28**, 7248-7255.

96. K. Nomura and R. R. Schrock, *Macromolecules*, 1996, **29**, 540-545.

97. K. H. Mortell, R. V. Weatherman and L. L. Kiessling, *J. Am. Chem. Soc.*, 1996, **118**, 2297-2298.

98. D. D. Manning, L. E. Strong, X. Hu, P. J. Beck and L. L. Kiessling, *Tetrahedron*, 1997, **53**, 11937-11952.

99. D. D. Manning, X. Hu, P. Beck and L. L. Kiessling, *J. Am. Chem. Soc.*, 1997, **119**, 3161-3162.

100. M. Kanai, K. H. Mortell and L. L. Kiessling, *J. Am. Chem. Soc.*, 1997, **119**, 9931-9932.

101. C. W. Cairo, J. E. Gestwicki, M. Kanai and L. L. Kiessling, *J. Am. Chem. Soc.*, 2002, **124**, 1615-1619.

102. J. E. Gestwicki, C. W. Cairo, L. E. Strong, K. A. Oetjen and L. L. Kiessling, *J. Am. Chem. Soc.*, 2002, **124**, 14922-14933.

103. D. Grande, S. Baskaran, C. Baskaran, Y. Gnanou and E. L. Chaikof, *Macromolecules*, 2000, **33**, 1123-1125.

104. D. Grande, S. Baskaran and E. L. Chaikof, *Macromolecules*, 2001, **34**, 1640-1646.

105. S. Baskaran, D. Grande, X. L. Sun, A. Yayon and E. L. Chaikof, *Bioconjugate Chem.*, 2002, **13**, 1309-1313.

106. X. L. Sun, D. Grande, S. Baskaran, S. R. Hanson and E. L. Chaikof, *Biomacromolecules*, 2002, **3**, 1065-1070.

107. S. J. Hou, X. L. Sun, C. M. Dong and E. L. Chaikof, *Bioconjugate Chem.*, 2004, **15**, 954-959.

108. K. Ohno, Y. Tsujii, T. Miyamoto, T. Fukuda, M. Goto, K. Kobayashi and T. Akaike, *Macromolecules*, 1998, **31**, 1064-1069.

109. K. Ohno, T. Fukuda and H. Kitano, *Macromol. Chem. Phys.*, 1998, **199**, 2193-2197.

110. K. Ohno, Y. Izu, S. Yamamoto, T. Miyamoto and T. Fukuda, *Macromol. Chem. Phys.*, 1999, **200**, 1619-1625.

111. Y. Chen and G. Wulff, *Macromol. Chem. Phys.*, 2001, **202**, 3426-3431.

112. Y. Chen and G. Wulff, *Macromol. Chem. Phys.*, 2001, **202**, 3273-3278.

113. A. Narumi, T. Matsuda, H. Kaga, T. Satoh and T. Kakuchi, *Polym. J.*, 2001, **33**, 939-945.

114. A. Narumi, T. Satoh, H. Kaga and T. Kakuchi, *Macromolecules*, 2002, **35**, 699-705.

115. A. Narumi, T. Matsuda, H. Kaga, T. Satoh and T. Kakuchi, *Polymer*, 2002, **43**, 4835-4840.

116. H. Gotz, E. Harth, S. M. Schiller, C. W. Frank, W. Knoll and C. J. Hawker, *J. Polym. Sci., Part A: Polym. Chem.*, 2002, **40**, 3379-3391.

117. K. Ohno, Y. Tsujii and T. Fukuda, *J. Polym. Sci., Part A: Polym. Chem.*, 1998, **36**, 2473-2481.

118. Y.-Z. Liang, Z.-C. Li, G.-Q. Chen and F.-M. Li, *Polym. Int.*, 1999, **48**, 739-742.

119. Z. C. Li, Y. Z. Liang and F. M. Li, *Chem. Commun.*, 1999, 1557-1558.

120. Z. C. Li, Y. Z. Liang, G. Q. Chen and F. M. Li, *Macromol. Rapid Commun.*, 2000, **21**, 375-380.

121. M. Ejaz, K. Ohno, Y. Tsujii and T. Fukuda, *Macromolecules*, 2000, **33**, 2870-2874.

122. Y. Z. Liang, Z. C. Li and F. M. Li, *Chem. Lett.*, 2000, 320-321.

123. Y. M. Chen and G. Wulff, *Macromol. Rapid Commun.*, 2002, **23**, 59-63.

124. L. C. You, F. Z. Lu, Z. C. Li, W. Zhang and F. M. Li, *Macromolecules*, 2003, **36**, 1-4.

125. C. M. Dong, X. L. Sun, K. M. Faucher, R. P. Apkarian and E. L. Chaikof, *Biomacromolecules*, 2004, **5**, 224-231.

126. C. M. Dong, K. M. Faucher and E. L. Chaikof, *J. Polym. Sci., Part A: Polym. Chem.*, 2004, **42**, 5754-5765.

127. F. Z. Lu, J. Q. Meng, F. S. Du, Z. C. Li and B. Y. Zhang, *Macromol. Chem. Phys.*, 2005, **206**, 513-520.

128. J. Q. Meng, F. S. Du, Y. S. Liu and Z. C. Li, *J. Polym. Sci., Part A: Polym. Chem.*, 2005, **43**, 752-762.

129. V. Ladmiral, L. Monaghan, G. Mantovani and D. M. Haddleton, *Polymer*, 2005, **46**, 8536-8545.

130. S. Muthukrishnan, H. Mori and A. H. E. Muller, *Macromolecules*, 2005, **38**, 3108-3119.

131. S. Muthukrishnan, D. P. Erhard, H. Mori and A. H. E. Muller, *Macromolecules*, 2006, **39**, 2743-2750.

132. S. Muthukrishnan, M. Nitschke, S. Gramm, Z. Ozyurek, B. Voit, C. Werner and A. H. E. Muller, *Macromol. Biosci.*, 2006, **6**, 658-666.

133. R. Narain and S. P. Armes, *Chem. Commun.*, 2002, 2776-2777.

134. R. Narain and S. P. Armes, *Macromolecules*, 2003, **36**, 4675-4678.

135. R. Narain and S. P. Armes, *Biomacromolecules*, 2003, **4**, 1746-1758.

136. S. Sen Gupta, K. S. Raja, E. Kaltgrad, E. Strable and M. G. Finn, *Chem. Commun.*, 2005, 4315-4317.

137. V. Vazquez-Dorbatt and H. D. Maynard, *Biomacromolecules*, 2006, **7**, 2297-2302.

138. Y. Tsujii, M. Ejaz, K. Sato, A. Goto and T. Fukuda, *Macromolecules*, 2001, **34**, 8872-8878.

139. A. B. Lowe, B. S. Sumerlin and C. L. McCormick, *Polymer*, 2003, **44**, 6761-6765.

140. L. Albertin, C. Kohlert, M. Stenzel, L. J. R. Foster and T. P. Davis, *Biomacromolecules*, 2004, **5**, 255-260.

141. L. Albertin, M. Stenzel, C. Barner-Kowollik, L. J. R. Foster and T. P. Davis, *Macromolecules*, 2004, **37**, 7530-7537.

142. L. Albertin, M. H. Stenzel, C. Barner-Kowollik, L. J. R. Foster and T. P. Davis, *Macromolecules*, 2005, **38**, 9075-9084.

143. J. Bernard, A. Favier, L. Zhang, A. Nilasaroya, T. P. Davis, C. Barner-Kowollik and M. H. Stenzel, *Macromolecules*, 2005, **38**, 5475-5484.

144. J. Bernard, X. J. Hao, T. P. Davis, C. Barner-Kowollik and M. H. Stenzel, *Biomacromolecules*, 2006, **7**, 232-238.

145. L. Albertin, M. H. Stenzel, C. Barner-Kowollik and T. P. Davis, *Polymer*, 2006, **47**, 1011-1019.

146. M. H. Stenzel, L. Zhang and W. T. S. Huck, *Macromol. Rapid Commun.*, 2006, **27**, 1121-1126.

147. S. G. Spain, L. Albertin and N. R. Cameron, *Chem. Commun.*, 2006, 4198-4200.

148. M. Ahmed and R. Narain, *Biomaterials*, 2011, **32**, 5279-5290.

149. O. Abdelkader, S. Moebs-Sanchez, Y. Queneau, J. Bernard and E. Fleury, *J. Polym. Sci., Part A: Polym. Chem.*, 2011, **49**, 1309-1318.

150. S. R. S. Ting, A. M. Granville, D. Quemener, T. P. Davis, M. H. Stenzel and C. Barner-Kowollik, *Aust. J. Chem.*, 2007, **60**, 405-409.

Chapter 2. Investigation into thiol-(meth)acrylate Michael addition

2.1. Introduction

Over the last decade, click chemistry has opened new avenues to design and synthesize tailor-made macromolecules for different applications in chemistry as well as for the functionalization of nanoparticles and polymers.[1-5] Although, numerous organic reactions have been described in the literature as ‘‘click reactions’’, the copper catalyzed [3 + 2] Huisgen cycloaddition reaction has been widely employed in conjunction with metal-mediated controlled radical polymerization.[6-9] However, the residual amount of copper and the ligand content in the final product gives constraints and limits the application of Huisgen cycloaddition, especially for biological applications. This has directed research towards metal-free synthesis techniques.[10-12] One of the most attractive and long time known organic reactions, thiol-ene addition, has become popular in polymer chemistry.[13-18]

Thiol-ene addition reactions can proceed by two routes: (i) anti-Markovnikov radical addition and (ii) base or nucleophile catalyzed Michael addition reaction, **Scheme 2.1**. [19-26]

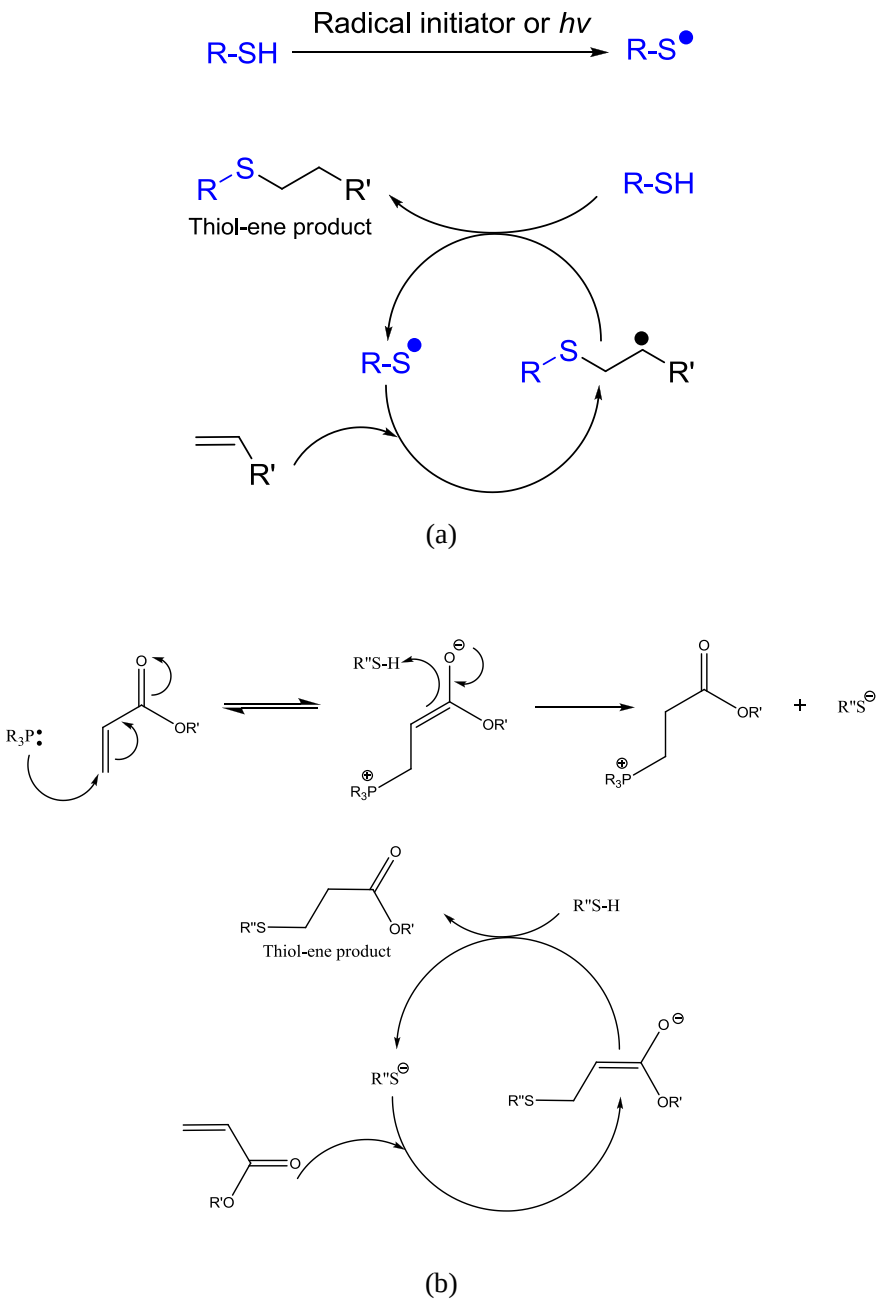

Scheme 2.1 (a) Mechanism for the anti-Markovnikov radical addition (b) Mechanism for the nucleophilic mediated hydrothiolation of an acrylic carbon–carbon bond under phosphine catalysis

The thiol-ene/yne radical addition mechanism requires an external radical source and energy to generate radicals, which may be *via* azo-initiators or photo-initiators using thermal or UV light energy.[27-32] Moreover, it should be noted

that thiol compounds may reaction-selectively with any type of vinyl bond within the polymer. Despite the few drawbacks of thiol-ene radical addition reactions, it is possible to reach near quantitative conversions in relatively short periods by its high reactivity for low molecular weight compounds, as described recently.[33]

In the case of the Michael addition reaction, this is a facile reaction between nucleophilic species and activated olefins under basic conditions.[34] The Michael reaction benefits from mild reaction conditions, minimal by-product formation, high functional group tolerance and high conversions, when optimized. Various amines, enolates, thiols and phosphines can react with (meth)acrylates, (meth)acrylamides, maleimides, acrylonitriles and cyanoacrylates, which are Michael donors and Michael acceptors, respectively.[35, 36] There are a few parameters that should be taken into account when optimizing the synthetic protocol, such as the nucleophile type, solvent and substrate, all of which have been systematically investigated in this present study.

The synthesis of end functional polymers with high fidelity is challenging, even though several controlled radical polymerization techniques have been developed.[37] Metal mediated radical polymerization techniques have been widely employed to obtain bromide or chloride end-functionalized polymers that can be converted into azide groups to subsequently facilitate Cu-catalyzed azide-alkyne click reactions. Similarly, reversible addition-fragmentation chain transfer (RAFT) polymerization has been used to give thiol terminated polymers following the cleavage of the chain transfer agent.[38-42] In general practice, amines have been

used in excess to cleave the chain transfer agent from the chain end, however, the bulky structure of the polymer may reduce the cleavage efficiency. Additionally, the free thiol terminal-groups can be oxidized to disulfides. To avoid this side reaction CAMD has developed a strategy proposing the in situ aminolysis of RAFT end-groups in the presence of pyridyl disulfide to yield a thiol protected polymer.[43] In addition, RAFT polymerization requires dedicated chain transfer agents (CTA) designed according to the monomer structure and also optimized reaction conditions such as initiator/CTA ratio, solvent type and reaction temperature.[44-51] Nevertheless, thiol terminated polymers have been successfully used in thiol-ene, thiol-yne, thiol-bromo, thiol-isocyanate and thiol-maleimide click reactions.[52-60]

Alternatively, vinyl terminated polymers have been prepared to react with thiol compounds.[61-63] One of the most successful techniques to obtain vinyl-terminated polymers is catalytic chain transfer polymerization (CCTP) that proceeds *via* a free-radical mechanism in the presence of certain low-spin Co(II) catalysts.[64-68] In particular, this is an ideal technique to synthesize very short oligomers, i.e. dimer, trimer and tetramer, with very high end group fidelity. This technique has been generally employed for the preparation of macromonomers and has been used successfully for a wide range of methacrylates. Advantageously, CCTP requires a very low amount of catalyst (in low ppm levels), yielding quasi-pure polymers with a very low amount of residual catalyst.

In this present work, the effect of different catalysts for the nucleophilic

mediated thiol-ene reaction is described using model compounds, both monomers and oligomers obtained by CCTP. Different catalysts, including pentylamine and hexylamine (primary amines), triethylamine (tertiary amine), and two different phosphines, dimethylphenylphosphine (DMPP) and tris(2-carboxyethyl) phosphine (TCEP), were investigated in the presence of different thiols, **Scheme 2.2**. This study had the objective to determine the optimum reaction conditions for nucleophile mediated thiol-ene click reactions.

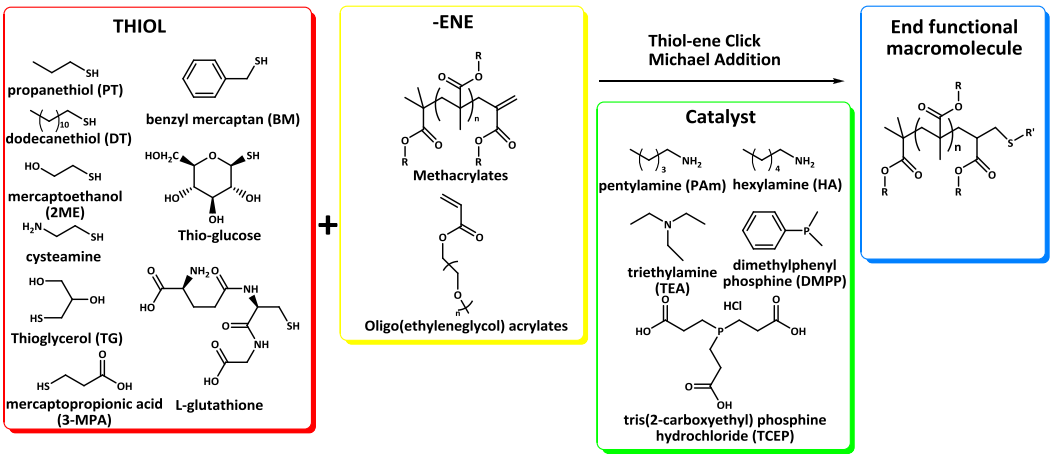

Scheme 2.2 Summary of the different thiols, thiol-enes and catalysts investigated in this study.

2.2. Experimental part

2.2.1. Materials

Methyl methacrylate (MMA, 99%, Sigma-Aldrich), 2-hydroxyethyl methacrylate (HEMA, 97%, Sigma-Aldrich), poly(ethylene glycol) methylether acrylate ($PEGMEA_{454}$, Sigma-Aldrich), poly(ethylene glycol) methyl ether

methacrylate ($PEGMEMA_{475}$, Sigma-Aldrich), 2,2' -azoisobutyronitrile (AIBN), 2-mercaptoethanol (2-ME, 99%, Fluka, Sigma-Aldrich), 1-thioglycerol (TG, 98%, Sigma-Aldrich), 1-propanethiol (PT, 99%, Sigma-Aldrich), 1-dodecanethiol (DT, 98+%, Sigma-Aldrich), benzyl mercaptan (BM, 99%, Sigma-Aldrich), glutathione (98%, Sigma-Aldrich), 1-thiol-β-D-glucose sodium salt (thiol-glucose, 99%, Sigma-Aldrich), 3-mercaptopropanoic acid (3-MPA, 99%, Sigma-Aldrich), dimethylphenylphosphine (DMPP, 99%, Aldrich), tris(2-carboxyethyl)phosphine hydrochloride (TCEP, 98%, Alfa Aesar), triethylamine (TEA, 99%, Fisher Scientific UK Ltd.), pentylamine (PAm, 99%, Sigma-Aldrich), hexylamine (HA, 99%, Sigma-Aldrich), dimethyl sulfoxide-d_6 (DMSO-d_6, 99.9%, atom %D, Sigma-Aldrich) and acetone-d_6 (99.9% atom %D, Sigma-Aldrich), acetonitrile-d_3 (ACN-d_3, 99.8% atom %D, Sigma-Aldrich) and deuterium oxide (D_2O, 99.9% atom %D, Sigma-Aldrich) were used as received. PBS buffer (pH 7.1, 0.5M) was made up of NaH_2PO_4 (99.85%, Fisher Scientific UK Ltd.), carbonate-bicarbonate (CBB) buffer (pH 9.2, 0.2 M) was made of Na_2CO_3 (0.2 M) (99%, BDH, VWR International Ltd.) and $NaHCO_3$ (0.2 M) (99%, Fisher Scientific UK Ltd.). Bis(boron difluorodimethylglyoximate) cobaltate(II) bis(methanol) complex, $(CH_3OH)_2Co$-$(dmgBF_2)_2$(CoBF), as prepared according to the method of Bakac *et al.*[69] The activity of the synthesized CCT agent was tested with CCTP of MMA yielding a C_s value = 25000.

2.2.2. Characterization

^{1}H NMR spectroscopy was used to determine the monomer conversion. NMR spectra were recorded on a Bruker DPX-300 MHz and a Bruker DPX-400 MHz spectrometer at 25 ^{o}C on approximately 10% w/v solutions in deuterated NMR solvents from Sigma-Aldrich. All chemical shifts are reported in ppm (δ) relative to tetramethylsilane (TMS), referenced to the chemical shifts of residual solvent resonances (^{1}H and ^{13}C). The following abbreviations were used to explain the multiplicities: s = singlet, d = doublet, dd = doublet of doublets, t = triplet, m = multiplet.

Mass spectra were recorded on either Bruker UHR-Q-TOF MaXis or Thermo Finnigan LCQ. ESI-MS was obtained using Thermo Finnigan LCQ Deca quadrupole ion trap mass spectrometer (Thermo Finnigan, San Jose, CA), equipped with an atmospheric pressure ionization source operating in the nebulizer assisted electrospray mode and was used in positive ion mode. Mass calibration was performed using caffeine, MRFA, and Ultramark 1621 in the m/z range of 195-1822 Da. All spectra were acquired within the m/z range of 150-2000 Da, and typical instrumental parameters were a spray voltage of 4.5 kV, a capillary voltage of 44 V, a capillary temperature of 275 ^{o}C and flow rate of 5 μL min $^{-1}$. Nitrogen was used as sheath gas (flow: 50% maximum) and helium was used as auxiliary gas (flow: 5% maximum), 30 microscans, with maximum inject time of 10 ms per microscan. For each respective scan, approximately 35 scans were signal averaged to obtain the final spectrum. Solvent used was 3 : 1 mixture of

DCM : methanol with sodium acetate concentration of 0.3 mM. Sodium acetate was added to the solvent prior to analysis to ensure that ionization would occur and to suppress potassium salt peaks. All data processing was done using Xcalibur™ included together with Thermoproducts. Mass spectra were recorded on a Bruker UHR-Q-TOF MaXis equipped with electrospray ionisation source in positive mode; samples were directly infused at 2 μL min^{-1} with a syringe pump. Nitrogen was used as nebulizer gas (0.4 bar) and dry gas (4 L min^{-1} at 180 ^{o}C). Capillary voltage was set at -3000 V. Data were acquired in the 50-2000 m/z range. Calibration was carried out with sodium formate solution (10 mM in 50% IPA). Mass spectra were acquired by MALDI-ToF (matrix-assisted laser desorption and ionization time-of-flight) mass spectrometry using a Bruker Daltonics Ultraflex II MALDI-ToF mass spectrometer, equipped with a nitrogen laser delivering 2 ns laser pulses at 337 nm with positive ion ToF detection performed using an accelerating voltage of 25 kV.

2.2.3. Catalytic chain transfer polymerization (CCTP)

2.2.3.1. Preparation of MMA dimer

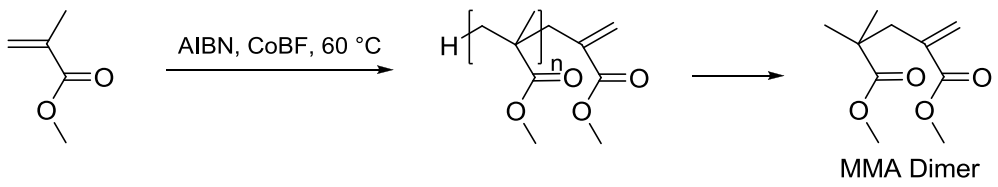

Scheme 2.3 Synthesis of MMA dimer *via* catalytic chain transfer polymerization

Methyl methacrylate dimer macromonomer was prepared by CCTP of MMA with CoBF as chain transfer agent and AIBN as the initiator. MMA (250 mL) was used as supplied and degassed by bubbling through with nitrogen for at least 2 hours prior to use, then CoBF (0.25 g) and AIBN (0.5 g) were added to the Schlenk tube filled with nitrogen prior to addition of MMA. The reaction was carried out in an oil bath at 60 ^{o}C for three days, after which the unreacted MMA was removed using a rotary evaporator. Hydroquinone (100 ppm) was added to inhibit subsequent polymerization of products during the removal of MMA dimer. A crude separation was carried out using a Kugelrohr apparatus and MMA dimer was collected at 125-135 ^{o}C, 0.12 mbar. MMA dimer was further purified by reduced pressure distillation at 130 ^{o}C, 0.12 mbar, **Scheme 2.3**. The purity of the macromonomers was verified by ^{1}H NMR, ^{13}C NMR and ESI-MS.

^{1}H NMR (400 MHz, acetone-d_6, 298 K), δ (ppm) = 6.15 (d, J = 1.6 Hz, 1H, 1/2 CH_2=C), 5.57 (d, J = 1.3 Hz, 1H, 1/2 CH_2=C), 3.69 (s, 3H, CH_2=C-COOCH_3), 3.59 (s, 3H, CH_3-C-COOCH_3), 2.59 (s, 2H, CH_2=C-CH_2), 1.12 (s, 6H, C(CH_3)$_2$).

^{13}C NMR (100 MHz, acetone-d_6, 298K), δ (ppm) = 177.44 (1C, CH_3-C-*C*=O), 168.26 (1C, CH_2=C-*C*=O), 138.74 (1C, CH_2=*C*), 128.25 (1C, *C*H_2=C), 52.36 (1C, CH_3-C-COO*C*H_3), 52.06 (1C, CH_2=C-COO*C*H_3), 43.46 (1C, CH_2), 42.02 (1C, *C*(CH_3)$_2$), 25.40 (2C, C(*C*H_3)$_2$).

Mass spectrometry: ESI-MS Calcd. for $C_{10}H_{16}NaO_4^+$ (M+Na^+)=223.09, Found 223.09.

2.2.3.2. Preparation of HEMA dimer.

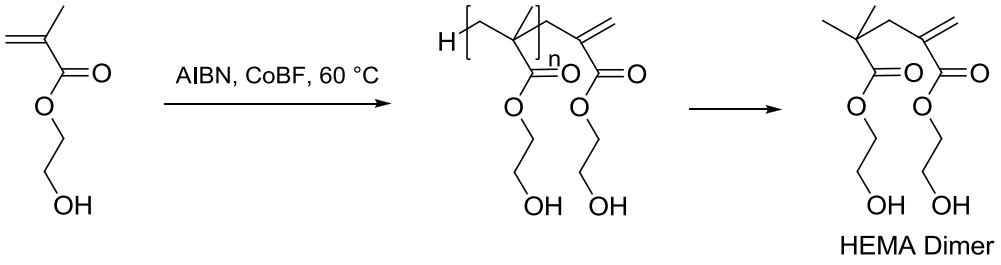

Scheme 2.4 Synthesis of HEMA dimer *via* catalytic chain transfer polymerization

Hydroxyethyl methacrylate dimer macromonomer was prepared by CCTP of HEMA in the presence of CoBF as chain transfer agent initiated by AIBN. CoBF (0.1 g) and AIBN (0.5 g) were dissolved in a mixture of HEMA (150 mL) and methyl ethyl ketone (MEK) (150 mL). All reagents were degassed by three freeze-pump-thaw cycles prior to use. The reaction mixture was placed in an oil bath at 60 ^{o}C for 48 h under nitrogen, and then the MEK was removed by rotary evaporation. Hydroquinone (100 ppm) was added to inhibit subsequent polymerization of products during the removal of both HEMA and HEMA dimer. A crude separation was carried out using a Kugelrohr apparatus, HEMA was collected at 60-150 ^{o}C, 0.3 mbar, HEMA dimer was collected at 170-180 ^{o}C, 0.4 mbar. HEMA dimer was further purified by reduced pressure distillation, HEMA removed at 113 ^{o}C, 1 mbar, and HEMA dimer was collected at 202 ^{o}C, 1 mbar, **Scheme 2.4**. The purity of the macromonomers was verified by ^{1}H NMR and ESI-MS.

^{1}H NMR (400 MHz, D_2O, 298 K) δ = 6.33 (d, *J* = 0.9 Hz, 1H, 1/2 CH_2=C), 5.75 (d, *J* = 0.5 Hz, 1H, 1/2 CH_2=C), 4.25-4.27 (m, 2H, $COOCH_2$), 4.14-4.16 (m, 2H, $COOCH_2$), 3.85-3.87 (m, 2H, C*H*$_2$OH), 3.81-3.83 (m, 2H, C*H*$_2$OH), 2.67 (s, 2H, CH_2=C-C*H*$_2$), 1.21 (s, 6H, $C(CH_3)_2$)

Mass spectrometry: ESI-MS Calcd. for $C_{12}H_{20}NaO_6^+$ ($M+Na^+$) = 283.12, Found 283.12.

2.2.3.3. Preparation of PEGMEMA$_{475}$ oligomers.

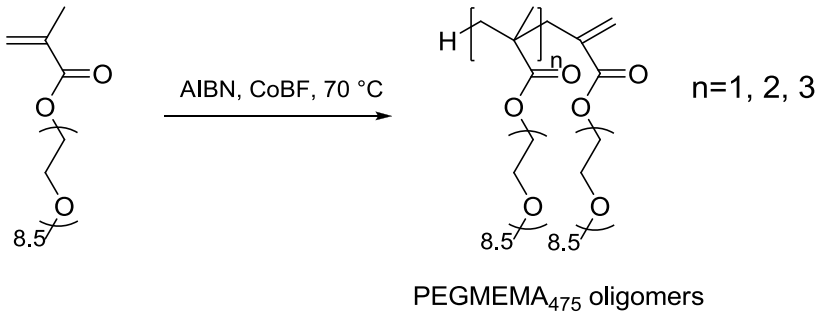

Scheme 2.5 Synthesis of PEGMEMA475 oligomers *via* catalytic chain transfer polymerization

The monomer, PEGMEMA$_{475}$ (5 g, 10.5 mmol), in acetonitrile (5 mL) was deoxygenated by purging with N_2 gas for at least one hour prior to use. A stock solution of CoBF was prepared by dissolving CoBF (1.3 mg) in acetonitrile (10 mL) followed by purging with N_2 gas for at least one hour. AIBN (12.5 mg, 0.0761 mmol) was then weighed in a Schlenk flask and mixed with the deoxygenated PEGMEMA$_{475}$ and the CoBF stock solution (4 mL). The mixture was then

subjected to three freeze–pump–thaw cycles to ensure removal of oxygen. The mixture was then placed in an oil bath at 70 ^{o}C for 14 hours. The reaction was stopped by exposure to air and quenched in ice bath. The resulting product was a mixture of $PEGMEMA_{475}$ monomer, dimer, and trimer, **Scheme 2.5**.

2.2.4. Thio-click reactions

2.2.4.1. TEA catalyzed thio-click reactions.

The MMA, MMA dimer, HEMA, $PEGMEA_{454}$ or $PEGMEMA_{475}$, thiols, TEA were added into an NMR tube containing acetone-d_6 or acetonitrile-d_3 or DMSO-d_6. The reactions were carried out at ambient temperature and monitored by ^{1}H NMR spectroscopy. In a typical reaction, 1 eq. (0.05 g) of monomer, 1.5 eq. thiol, 0.5 eq. of TEA were added into an NMR tube containing deuterated solvent (0.5 mL).

2.2.4.2. PAm catalyzed thio-click reactions.

The MMA, MMA dimer, HEMA, $PEGMEA_{454}$ or $PEGMEMA_{475}$, thiols, PAm were added into an NMR tube containing acetone-d_6 or actonitrile-d_3 or DMSO-d_6. The reactions were carried out at ambient temperature and monitored by ^{1}H NMR spectroscopy. In a typical reaction, 1 eq. (0.05 g) of monomer, 1.5 eq. thiol, 5 eq. of PAm were added into an NMR tube containing deuterated solvent (0.5 mL).

2.2.4.3. HA catalyzed thio-click reactions.

The $PEGMEMA_{475}$ oligomers were placed in glass vials with hexylamine, water or acetonitrile as solvent, and thiol. In a typical reaction, 100 mg of $PEGMEMA_{475}$ oligomers, 5 eq. thiol, and 5 eq. hexylamine were mixed in a flask and then purged for 15 minutes with N_2 and placed into 40 ^{o}C oil bath and reacted for 14 hours before and the products were purified using dialysis.

2.2.4.4. DMPP or TCEP catalyzed thio-click reactions.

The MMA, MMA dimer, HEMA, HEMA dimer, $PEGMEA_{454}$, $PEGMEMA_{475}$ or oligo($PEGMA_{475}$), thiols, DMPP or TCEP were added into an NMR tube containing acetone-d_6, actonitrile-d_3, DMSO-d_6 or D_2O. The reactions were carried out at ambient temperature and monitored by ^{1}H NMR spectroscopy. In a typical reaction, 1 eq. (0.05 g) of monomer, 1.5 eq. thiol and 0.05 eq. (1.7 mg) of DMPP were added into an NMR tube containing deuterated solvent (0.5 mL).

2.3. Results and discussion

The optimal conditions for the thiol-ene reaction were investigated using primary amines, tertiary amine and phosphines at different temperatures and in

different solvents using a broad range of monomers or oligomers. The synthesis of short oligomers bearing a terminal vinyl group was carried out using CCTP. [23, 61, 62, 70-75] This method has been successfully exploited for the synthesis of MMA and HEMA dimers (after separation from higher adducts) and OEGMA oligomers. The oligomers were tested using different thiol-ene reactions with a large range of thiol compounds and catalyst systems.

2.3.1. Triethylamine catalyzed thiol-ene reactions

The Michael addition between a thiol and an activated (electron deficient) vinyl group was carried out in the presence of triethylamine as catalyst at ambient temperature. **Table 2.1** presents the results from using MMA, MMA dimer (dMMA), poly(ethylene glycol) acrylate ($PEGMEA_{454}$) and poly(ethylene glycol) methacrylate ($PEGMEMA_{475}$) in the presence of 1-thio-glycerol (TG), 1-dodecanethiol (DT), 2-mercaptoethanol (2-ME), 1-propanethiol (PT) and benzyl mercaptan (BM).

Table 2.1 Optimization reactions using triethylamine as catalyst with different monomers/dimers and thiols

Run	Monomer/dimer	Thiol	Ratios [M]:[T]:[cat][a]	React. Time /h	Conv. (%)
T1	MMA	TG	1:1:0.5	96	69
T2	MMA	DT	1:1:0.5	96	2

T3	MMA	DT	1:1.5:0.5	96	3
T4	dMMA	2-ME	1:1.5:0.1	15	42
T5	dMMA	PT	1:1.5:0.5	96	11
T6	dMMA	PT	1:1.5:1.1	97	18
T7	dMMA	BM	1:1.5:1.1	87	70
T8	$PEGMEA_{454}$	2-ME	1:1.2:0.3	2	97
T9	$PEGMEMA_{475}$	2-ME	1:1.2:1.1	72	81
T10	$PEGMEMA_{475}$	2-ME	1:1.2:2.2	72	89
T11	$PEGMEMA_{475}$	2-ME	1:1.2:4.5	72	88
T12	$PEGMEMA_{475}$	2-ME	1:1.2:9.0	72	88

[a] [M]:[T]:[cat] = monomer/dimer : thiol : triethylamine. All reactions were performed at ambient temperature in acetone-d_6. Conversion values were calculated by ^{1}H NMR following the disappearance of the vinyl bond.

Different thiol-ene reactions were conducted using five different thiols in the presence of a low concentration of triethylamine as the catalyst, **Figure 2.1** and **Figure 2.2**.

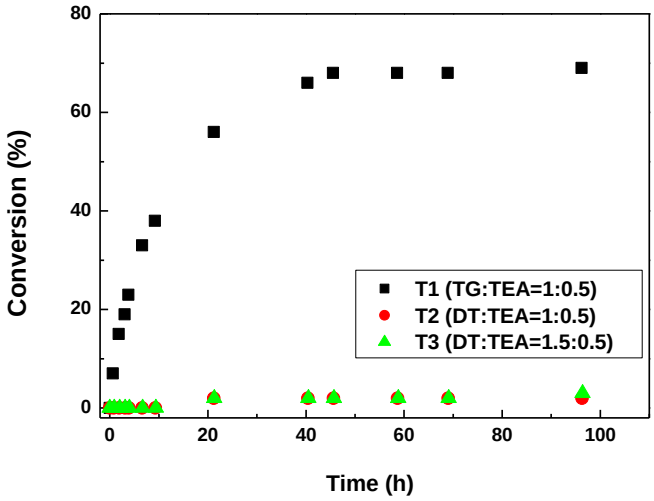

Figure 2.1 Vinyl bond conversion *vs.* time plots for MMA reacting with different thiols in the presence of triethylamine as catalyst. Note: Conversion values were calculated by ^{1}H NMR based on the consumption of the vinylic bonds.

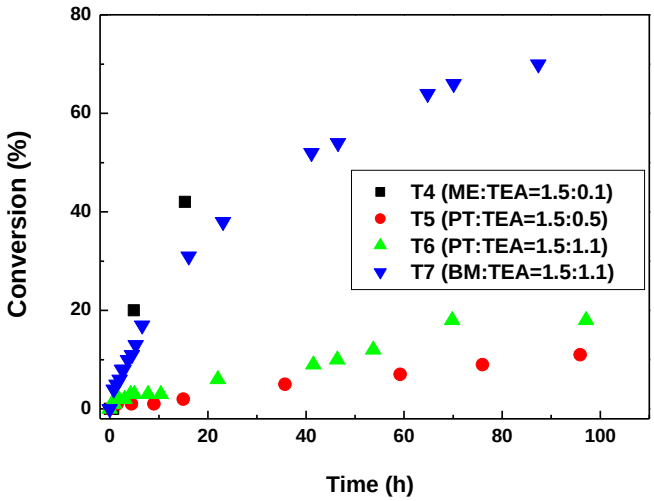

Figure 2.2 Vinyl bond conversion *vs.* time plots for MMA dimer reacting with different thiols in the presence of triethylamine as catalyst. Note: Conversion

values were calculated by ^{1}H NMR based on the consumption of the vinylic bonds.

The reaction rates differ depending on the thiol structure. For example, 1-dodecanethiol (DT) has the slowest rate (2% conversion in 96 hours, T2; 3% conversion in 96 hours, T3) in comparison to all other thiols used in this study. The reaction with 1-thioglycerol (TG), T1, achieved 69% conversion after 4 days of reaction, **Figure 2.3**. The reaction MMA dimer with 1-propanethiol (PT) in present of 0.5 equivalents of triethylamine as catalyst was only 11% conversion after 4 days of reaction, T5. Even if 1.1 equivalents of triethylamine catalyst was used, the reaction was still 18% conversion after 4 days of reaction, T6. Nevertheless, 70% conversion was achieved for MMA dimer using a [BM]/[TEA] ratio equal to 1.5/1.1 after 87 hours, T7 (**Figure 2.4**).

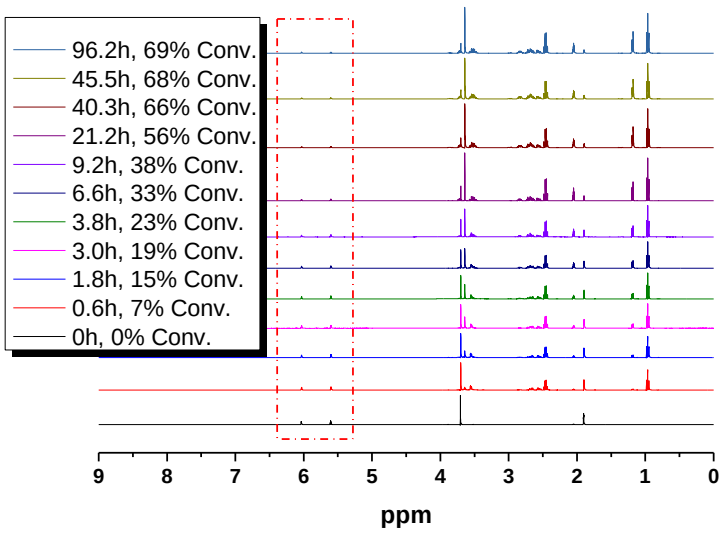

(a)

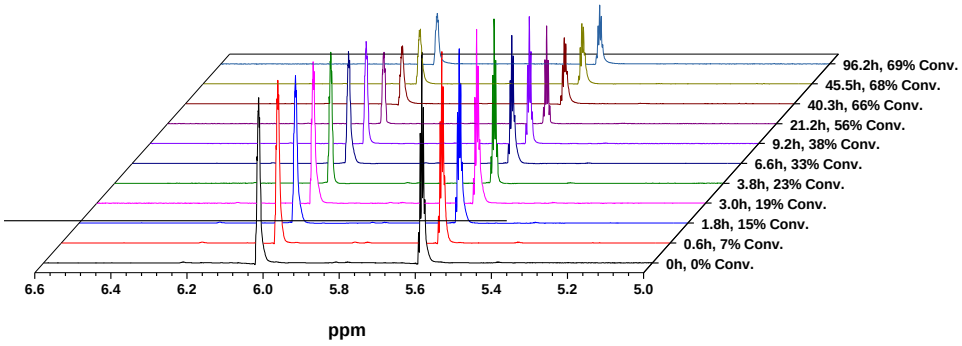

(b)

Figure 2.3 Thiol-Michael addition of MMA with 1-thioglycerol (TG) using 0.5 eq. of TEA in acetone-d_6 followed by ^{1}H NMR, T1. The vinyl groups represented by ^{1}H-NMR peaks at 6.05-6.06 ppm and 5.57-5.58 ppm have almost disappeared, indicating the formation of the thioether compound.

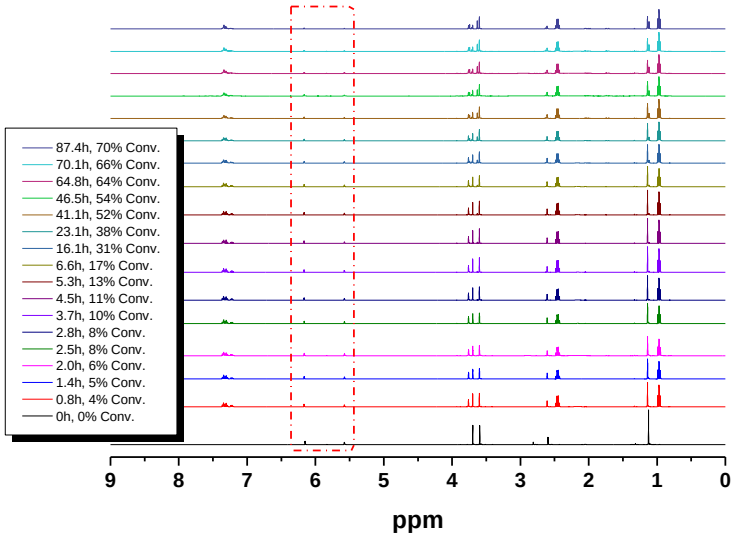

(a)

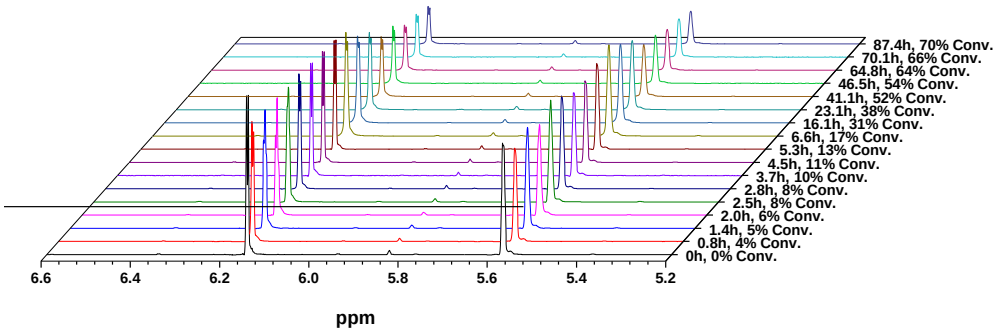

(b)

Figure 2.4 Thiol-Michael addition of MMA with 1-thioglycerol (TG) using 0.5 eq. of TEA in acetone-d6 followed by ^{1}H NMR, T7

A relatively fast reaction rate was observed for $PEGMEA_{454}$ with the reaction T8 catalyzed by a [TEA]/[thiol] ratio of 1.2/0.3 reaching quantitative conversions after 2 hours. However, in the case of methacrylates, even at extended reaction periods, i.e. 72 h, it was not possible to reach quantitative conversion values. Nevertheless, more than 80% conversion was measured for $PEGMEMA_{475}$ using a [thiol]/[TEA] ratio equal to 1.2/1.1 after 3 days. To accelerate this reaction, the [monomer]/[thiol]/[TEA] ratio was varied from 1.0/1.2/1.1 to 1.0/1.2/9.0 (T9-T12) and the kinetics followed by ^{1} H NMR, **Figure 2.5**.

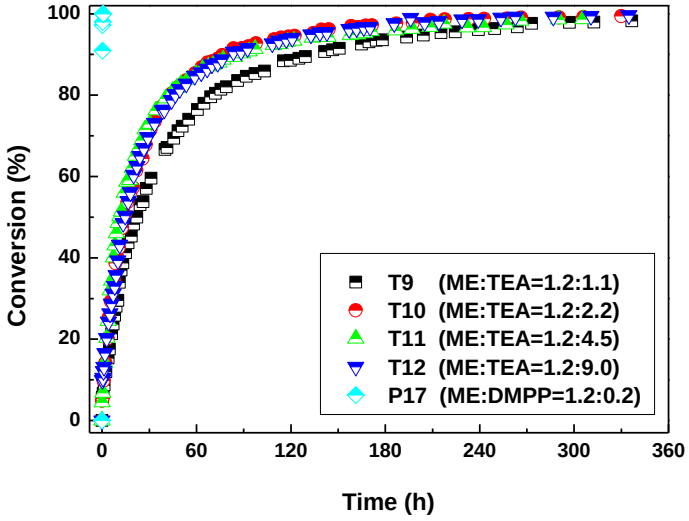

Figure 2.5 Conversion *vs.* time plot for the reaction of $PEGMEMA_{475}$ with 2-ME in the presence of varying concentrations of TEA or DMPP. Conversion values were calculated by ^1H NMR following the disappearance of the vinyl group

There was no significant difference in the kinetic behavior as the ratios were varied. Thus, excess TEA does not accelerate the thiol-ene reaction with methacrylic vinyl groups. ^{1} H NMR and ESI-MS does not show any formation of side products. The DMPP catalyzed reaction P17 is included as a comparison in **Figure 2.5**, which reached quantitative conversions in few minutes; this will be discussed further in the following sections.

2.3.2. Primary amine catalyzed thiol-ene reactions

In order to accelerate the rate of reaction, primary amines were examined as catalysts at ambient temperature. It was noted that primary amines were more

nucleophilic than tertiary amines. The formation of thiolate should be followed by a nucleophilic addition onto the vinyl group. $PEGMEA_{454}$, $PEGMEMA_{475}$ and $PEGMEMA_{2080}$ monomers were reacted with 2-ME, 3-MPA and 1-dodecanethiol (DT), **Table 2.1**. Higher ratios of catalyst were used to compensate for the lower reactivity of methacrylates relative to acrylates.

Table 2.2 Optimized reactions using n-pentylamine as catalyst with different monomers and thiols

Run	Monomer	Thiol	Ratios [M]:[T]:[cat][a]	React. time /h	Conv. (%)
PAm1	$PEGMEA_{454}$	DT	1:1.2:0.1	24	10
PAm2	$PEGMEA_{454}$	3-MPA	1:1.2:0.1	24	20
PAm3	$PEGMEA_{454}$	BM	1:1.2:0.1	24	78
PAm4	$PEGMEA_{454}$	2-ME	1:1.2:0.1	24	93
PAm5	$PEGMEA_{454}$	2-ME	1:1.2:0.3	0.5	93
PAm6	$PEGMEMA_{475}$	DT	1:1.2:1.7	4	5
PAm7	$PEGMEMA_{475}$	3-MPA	1:1.2:1.4	4	3
PAm8	$PEGMEMA_{475}$	BM	1:1.2:1.4	4	17
PAm9	$PEGMEMA_{475}$	TG	1:1.2:1.4	4	77
PAm10	$PEGMEMA_{475}$	2-ME	1:1.2:1.3	4	33
PAm11	$PEGMEMA_{475}$	2-ME	1:1.2:2.7	4	49
PAm12	$PEGMEMA_{475}$	2-ME	1:1.2:5.4	4	74
PAm13	$PEGMEMA_{475}$	2-ME	1:1.2:10.8	4	95
PAm14	$PEGMEMA_{475}$	-	1:0:1.4	137	0
PAm15	$PEGMEMA_{475}$	-	1:0:5.4	137	0
PAm16	$PEGMEMA_{475}$	-	1:0:10.8	137	0
PAm17	$PEGMEMA_{2080}$	2-ME	1:1.2:5.0	4	60

PAm18	$PEGMEMA_{2080}$	2-ME	1:1.2:10.0	4	69
PAm19	$PEGMEMA_{2080}$	2-ME	1:1.2:20.0	4	87
PAm20	$PEGMEMA_{2080}$	2-ME	1:1.2:40.0	4	99

[a] [M] : [T] : [cat] = monomer : thiol : *n*-pentylamine. All reactions were performed at ambient temperature in acetone-d_6 as solvent. Conversion values were calculated by ^{1}H NMR based on the consumption of the vinylic bonds.

Different thiol-ene reactions were conducted using 4 different thiols in the presence of a low concentration of *n*-pentylamine as the catalyst ([M]/[T]/[amine] = 1.0/1.1/0.1), **Figure 2.6**.

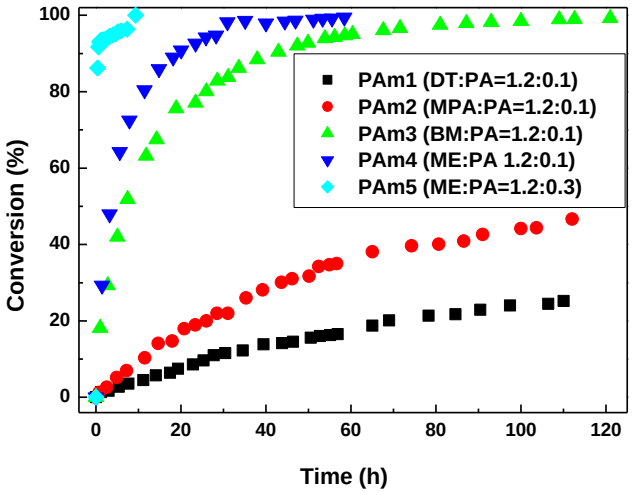

(a)

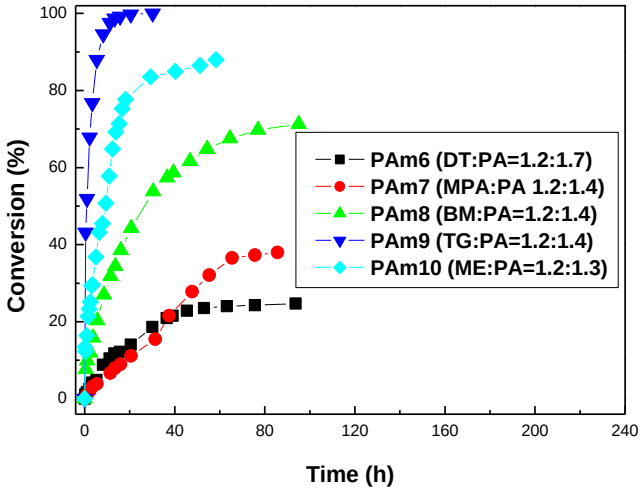

(b)

Figure 2.6 Vinyl bond conversion *vs.* time plots for $PEGMEA_{454}$ (a) and $PEGMEMA_{475}$ (b) reacting with different thiols in the presence of *n*-pentylamine as catalyst. Note: Conversion values were calculated by ^{1}H NMR based on the consumption of the vinylic bonds.

The reactions were monitored for up to 5 days and the vinyl bond conversion versus time was plotted, **Figure 2.6**. The reaction rates differ depending on the thiol structure. For example, 1-dodecanethiol (DT) has the slowest rate (10% conversion in 24 hours, PAm1) in comparison to all other thiols used in this study. The reaction with 3-mercaptopropionic acid (3-MPA), PAm2, did not exceed 50% conversion, even after 4 days of reaction. However, benzyl mercaptan (BM) had a faster reaction rate PAm3 with 78% after 24 hours. One explanation of the low reactivity of 3-MPA is the presence of carboxylic acid functionality (PAm2) resulting in potentially the enolate quenching and the subsequent non-generation of thiolate.

It is evident that benzyl mercaptan (BM) and 2-ME react with $PEGMEA_{454}$ relatively faster than DT and 3-MPA, PAm3-PAm5, PAm1 and PAm2, respectively. Quantitative conversions were obtained in < 3 days by reacting BM in the presence of n-pentylamine, PAm3. The final product of PAm3 was characterized using MALDI-TOF MS confirming the expected structure, **Figure 2.7**.

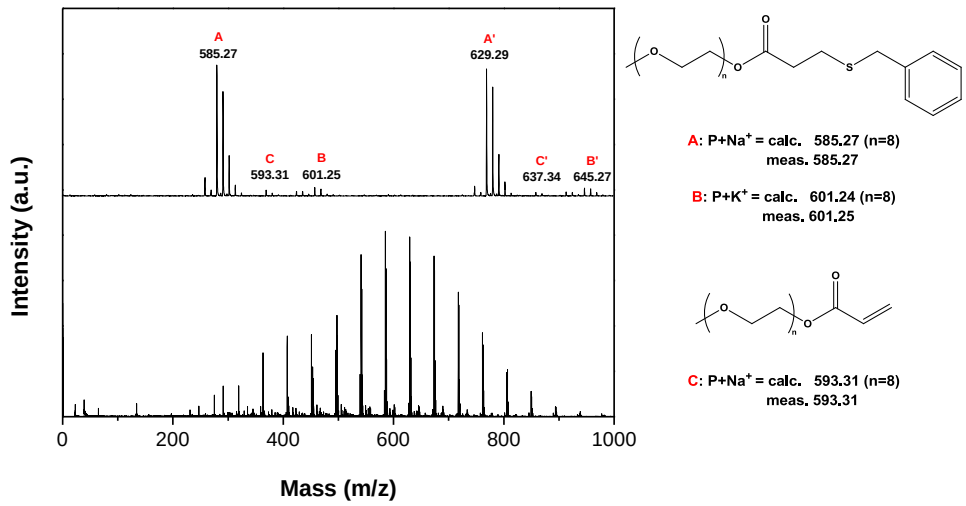

Figure 2.7 MALDI-TOF MS analysis of the final product of $PEGMEA_{454}$ reacted with benzyl mercaptan (BM) PAm3 in the presence of *n*-pentylamine.

All peaks can be assigned and the main distribution (labeled as A and B ionized with Na^+ or K^+ salt, respectively) can be assigned to BM conjugated $PEGMEA_{454}$ (a trace amount of un-reacted monomer (labeled as C) is also detected).

The catalyst concentration was varied as 0.1 PAm4 and 0.3 PAm5 for the reaction of $PEGMEA_{454}$ and 2-ME. The reactions reached ~90% conversion after

24 hours and 0.5 hours using 0.1 and 0.3 equivalents of PA, respectively. There is a significant difference in the reaction rate by changing the catalyst concentration (in contrast to the TEA catalyzed reactions). The reaction kinetics with acrylates was followed by ^{1}H NMR and all corresponding peaks of the starting material and the products are assigned, **Figure 2.8**. Using relatively short oligomer chains has facilitated the characterization of both the products and the side products in detail.

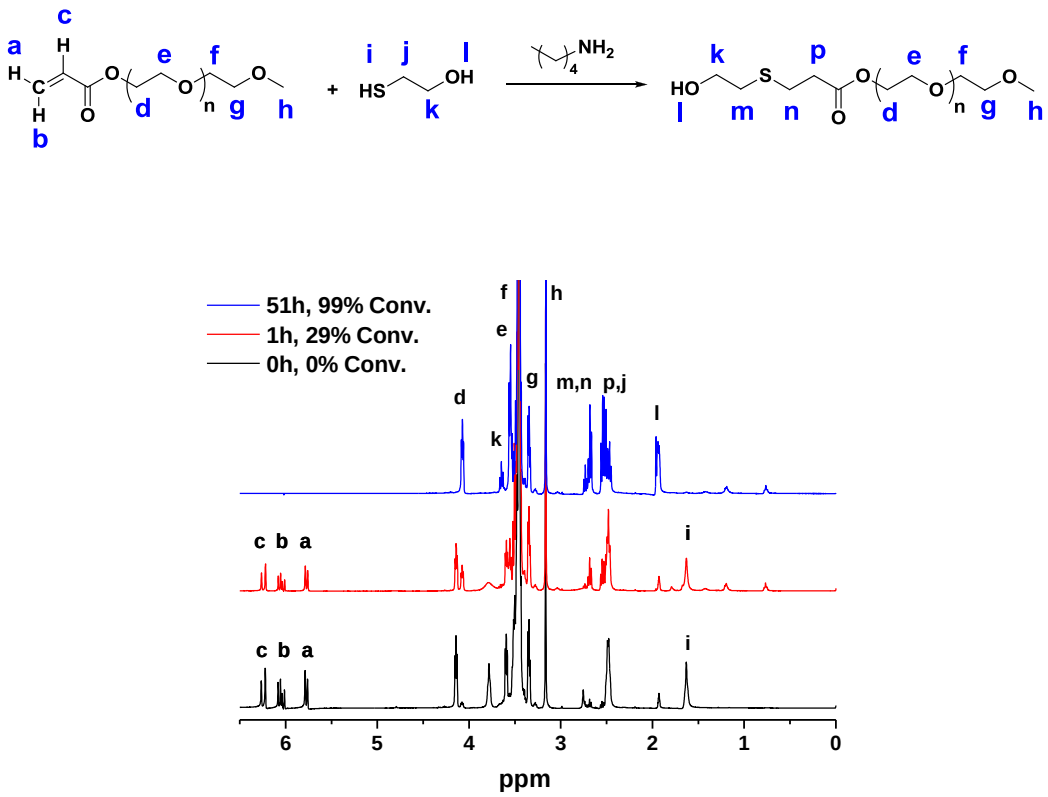

Figure 2.8 ^{1}H NMR spectra for Michael addition of $PEGMEA_{454}$ and ME, using 0.1 eq. of *n*-pentylamine in acetone-d_6, PAm4

The effect of the pentylamine concentration on the Michael addition reaction of 2-ME in the presence of $PEGMEMA_{475}$ or $PEGMEMA_{2080}$ was investigated in

experiments, PAm10-PAm13 and PAm17-PAm20, **Table 2.2**. The reaction kinetics of methacrylates with 2-ME PAm10-PAm13 and PAm17-PAm20 was followed using ^{1}H NMR, **Figure 2.9**.

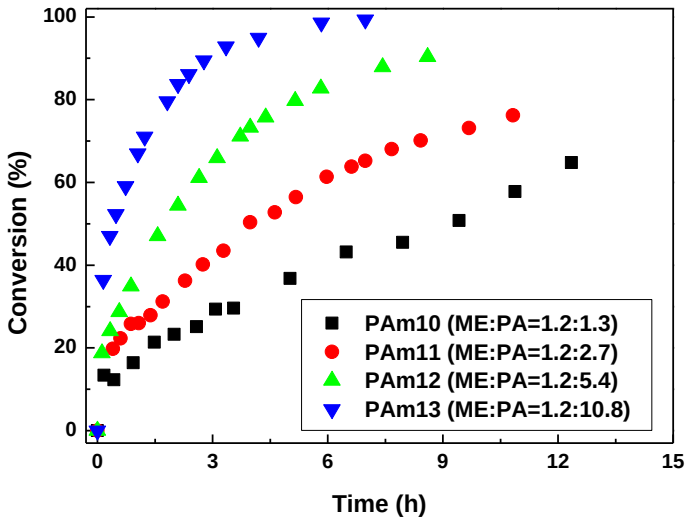

(a)

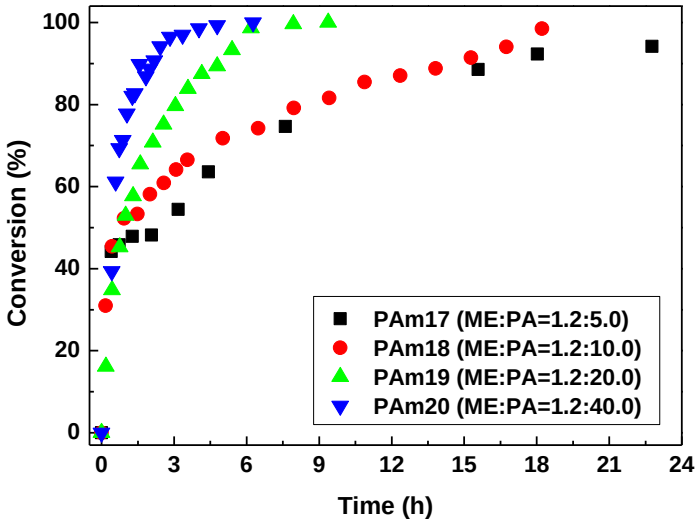

(b)

Figure 2.9 Michael addition of $PEGMEMA_{475}$ (a) or $PEGMEMA_{2080}$ (b) with 2-ME in different amounts of *n*-pentylamine. The reaction was performed in 0.5 mL acetone-d_6 and monitored *via* ^{1}H NMR.

An excess of catalyst was used in these experiments for two reasons: (i) it has been shown that methacrylates react very slowly with thiols in the presence of amines, (ii) $PEGMEMA_{2080}$ is a more sterically hindered molecule with reduced accessibility to the vinyl bonds. In these experiments, it is shown that the reaction proceeds much faster with a higher amount of catalyst present.

The excess of catalyst was used in the reaction without the thiols in order to evaluate whether the *n*-pentylamine can react with the vinyl group. After 5 days, the presence of vinyl group was monitored by ^{1}H NMR and it was found that vinyl groups were not reacted with amine as the monomer to DMPP ratio changed from 1.4 to 10.8, **Figure 2.10**.

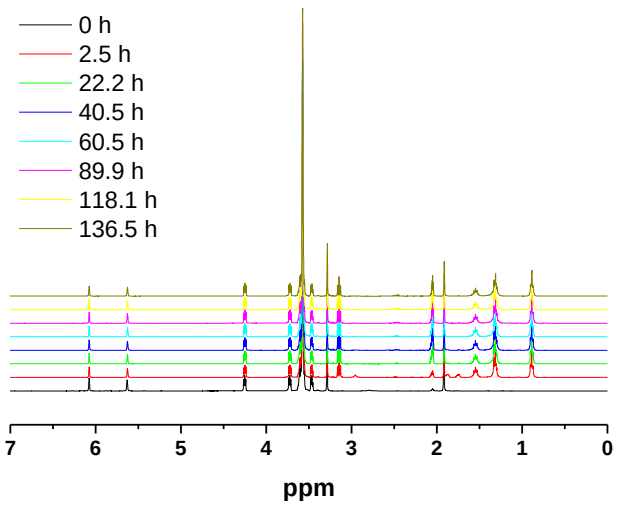

(a)

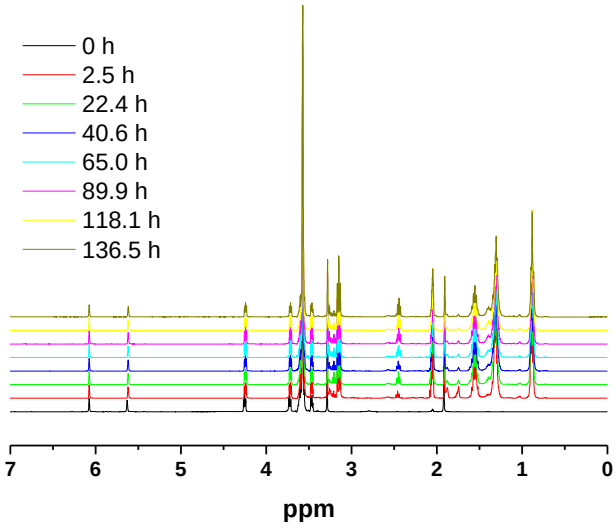

(b)

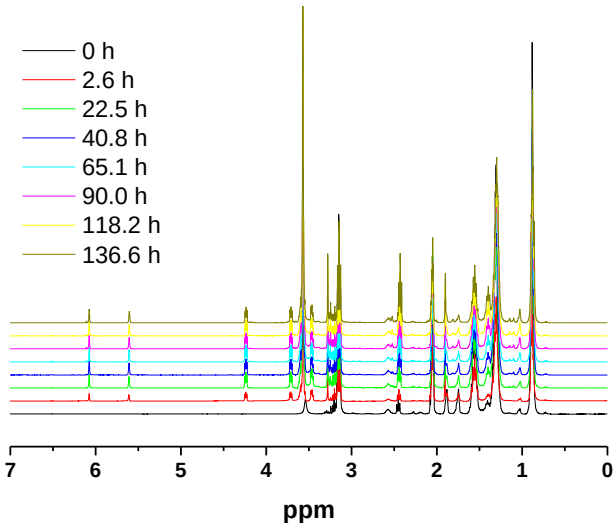

(c)

Figure 2.10 Effect of adding excess of *n*-pentylamine to $PEGMEMA_{475}$ in acetone-d_6 as followed by ^1H NMR. (a) 1.4 equivalents of *n*-pentylamine, PAm14, (b) 5.4 equivalents of *n*-pentylamine, PAm15, (c) 10.8 equivalents of *n*-pentylamine, PAm16.

However, it was noted that when using a large excess of *n*-pentylamine provides an intermediate species in the nucleophile mediated hydrothiolation reaction was seen. These intermediates were identified using MALDI-TOF MS from the reaction of $PEGMEMA_{2080}$ and 2-ME, **Figure 2.11**.

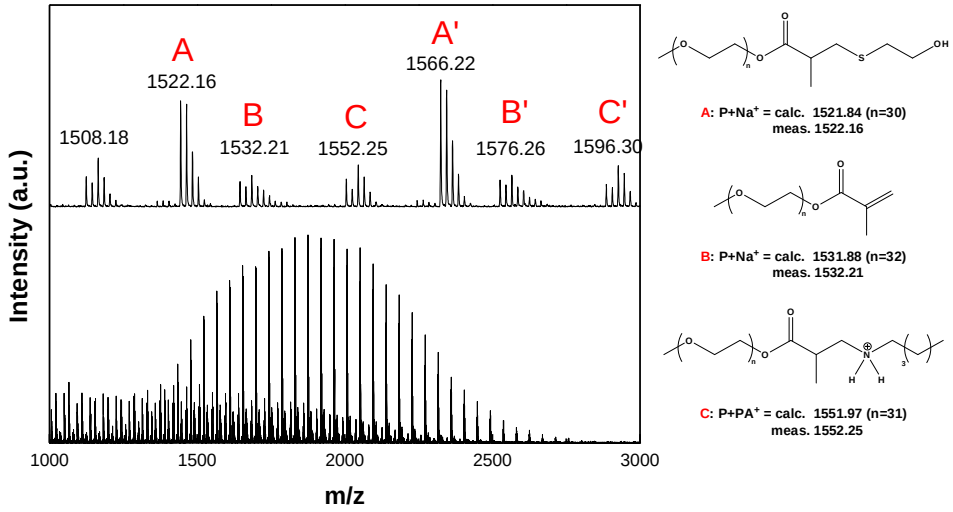

Figure 2.11 MALDI-TOF MS spectrum of $PEGMEMA_{2080}$ reacted with 2-ME in the presence of 40.0 eq. of *n*-pentylamine PAm20

The main distribution (labeled as A and A') belonged to the product at 1521.9 Da (n = 30) and 1565.9 Da (n = 31). Moreover, starting material could be identified (labeled as B and B', 1531.9 Da and 1575.9 Da) and the intermediates (labeled as C and C', 1552.2 Da and 1596.3 Da) observed in the spectrum. The intermediate was assigned as a compound formed from the reaction of $PEGMEMA_{2080}$ and *n*-pentylamine. Even though thiols were better nucleophiles than amines with a large excess of amine (or with a higher [amine]/[thiol] ratio),

such as in PAm20, these intermediates were visible by this technique. It is also noted that MALDI-TOF MS does not provide quantitative information due to potentially different ionization efficiencies of each compound. For instance, compound C was protonated and ionizes without forming a sodium adduct, as calculated from the spectra. It was interesting to note that MALDI-TOF MS analysis showed the presence of starting material, while almost full conversion was calculated from ^{1}H NMR. Based on these results, it appeared that vinyl terminated species ionizes more efficiently than the thiol or amine substituted species.

CCTP was used to synthesize oligo(PEGMEMA$_{475}$) to give mixtures of dimers, trimers, tetramers and higher adducts, that were used directly for subsequent thiol addition reactions. The CCTP product mixture was reacted with six different thiols, 2-ME, BM, 3-MPA, cysteamine, glutathione and thiol–glucose, **Table 2.3**.

Table 2.3 Optimization reactions using *n*-hexylamine as catalyst with oligo(PEGMEMA)$_{475}$ and various thiols

Run	Oligomer	Thiol	Ratio [M]:[T]:[cat][a]	Solvent	Conv. (%)
HA1	oligo(PEGMEMA$_{475}$)	2-ME	1:5:5	ACN	100
HA2	oligo(PEGMEMA$_{475}$)	BM	1:5:5	ACN	100
HA3	oligo(PEGMEMA$_{475}$)	3-MPA	1:5:5	ACN	100
HA4	oligo(PEGMEMA$_{475}$)	Cysteamine	1:5:5	D_2O	100
HA5	oligo(PEGMEMA$_{475}$)	Glutathione	1:5:5	D_2O	100

HA6	oligo($PEGMEMA_{475}$)	HS-Glc	1:5:5	D_2O	100

[a] [M]:[T]:[cat] = oligo($PEGMEMA_{475}$) : thiol : hexylamine. Conversion values were calculated by ^1H NMR with respect to vinyl peaks. All reactions were performed at 40 °C for 14 hours.

The mixtures were reacted overnight at 40 °C. To improve the yield of the reaction using primary amine, reactions were carried out using [ene]/[thiol]/[amine] = 1/5/5 at 40 °C in organic solvents and aqueous solution. After 14 hours, a complete conversion of oligo($PEGMEMA_{475}$) was observed by ^1H NMR, **Table 2.3**, and by ESI-MS, **Figure 2.12**. ESI-MS spectra show the quantitative formation of expected product, i.e. thiol conjugated to oligo($PEGMEMA_{475}$), without the formation of by-products.

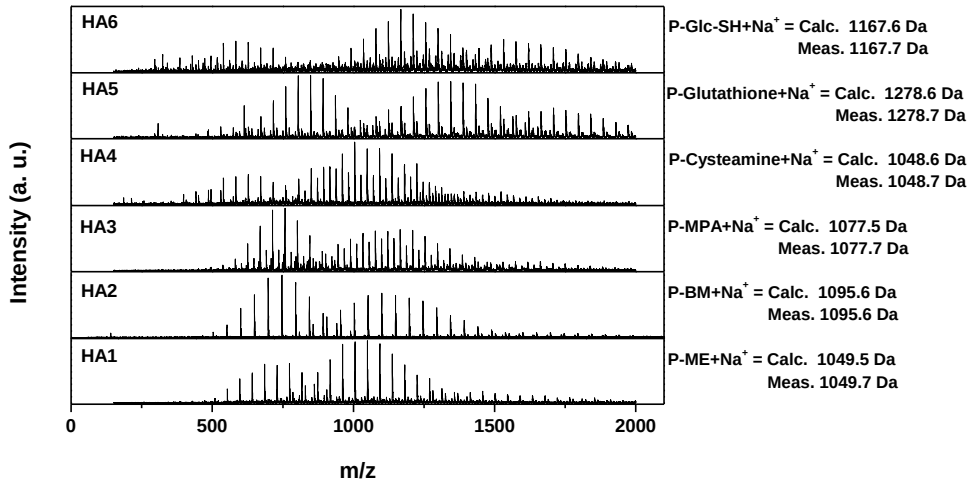

Figure 2.12 ESI-MS result of oligo($PEGMEMA_{475}$) reacted with various thiol compounds. Note: all the populations are attributed to expected compounds quaternized with Na^+ and H^+

in the case of HA3-HA6, and quaternized with Na^+ for HA1 and HA2. The populations were spaced by 44 Da corresponding to ethylene glycol unit.

Characterization was also carried out using ESI-MS, **Figure 2.12**. The top spectra show the presence of monomer, dimer, trimer and also tetramer distributions modified by thiol-glucose (HA6). Similar results were obtained for the 2-ME, BM, 3-MPA, cysteamine and glutathione conjugated oligomers HA1-HA5. ESI-MS results confirm the synthesis of expected products. The presence of two main distributions observed for HA1, HA2, HA3 and HA6 can be attributed to the expected products. The two populations can be assigned to differently ionized forms (ionized with sodium or hydrogen). The calculated and measured molecular weight was found to have maximum error of 0.2 Da, well within the inherent 0.3 Da error of the instrument. Moreover, it can also be seen from the mass spectra that there is no starting material or side products. As explained above, mass spectroscopy is more sensitive than ^{1}H NMR analysis, giving confidence that the reactions were complete, without detectable side products. The absence of addition of amine onto methacrylic bonds can be explained by the use of low [thiol]/[amine] ratio = 1 at 40 ^{o}C. In summary, hexylamine is an efficient catalyst for the Michael reaction of thiol/acrylates at ambient temperature without observation of any side products when the [amine]/[thiol] ratio is kept close to 1.0. The use of a higher ratio yields a side product which can be attributed to the addition of amine onto vinyl bonds. A slight increase of the temperature (at 40 ^{o}C) and the amount of thiol allow us to obtain a

quantitative reaction with monomer or oligomer bearing a methacrylic double bond.

2.3.3. Phosphine catalyzed thiol-ene reactions

Lowe has reported that phosphine based catalysts are known as very reactive catalysts for Michael addition reactions.[18] However, the highly reactive phosphine compound can also react with the vinyl group (methacrylate or acrylate) resulting in the formation of side products. Therefore, we initially performed some test reactions P1 and P2 by mixing MMA in the presence of different amounts of dimethylphenylphosphine (DMPP) in acetone, **Table 2.4**.

Table 2.4 Optimization reactions using DMPP as catalyst with different monomers and thiols

Run	Monomer /oligomer	Thiol	Base	Ratios [M]:[T]: [cat][a]	Solvent	React. time /h	Conv. (%)
P1	MMA	-	DMPP	1:0:0.1	Acetone	96	4
P2	MMA	-	DMPP	1:0:1.0	Acetone	96	23
P3	MMA	TG	DMPP	1:1:0.05	Acetone	1	100
P4	MMA	DT	DMPP	1:1:0.05	Acetone	3.5	93
P5	dMMA	TG	DMPP	1:1:0.05	Acetone	1	97
P6	dMMA	DT	DMPP	1:1:0.05	Acetone	4	81
P7	dMMA	DT	DMPP	1:1.5:0.05	ACN	2	83
P8	dMMA	DT	DMPP	1:1.5:0.05	DMSO	2	95
P9	dMMA	PT	DMPP	1:1.5:0.05	Acetone	9	72

P10	dMMA	PT	DMPP	1:2.5:0.05	Acetone	8	85
P11	dMMA	PT	DMPP	1:1.5:0.05	ACN	9	98
P12	dMMA	PT	DMPP	1:1.5:0.05	DMSO	1	100
P13	dMMA	PT	DMPP	1:1.5:0	DMSO	96	5
P14	dMMA	MPA	DMPP	1:1.5:0.05	Acetone	88	18
P15	dMMA	MPA	DMPP	1:1.5:0.05	DMSO	88	48
P16	dMMA	BM	DMPP	1:1.5:0.05	Acetone	1	90
P17	$PEGMEMA_{475}$	2-ME	DMPP	1:1.2:0.2	Acetone	0.5	100

[a] [M]: [T]: [cat]= monomer or oligomers : thiol : DMPP. Conversion values were calculated by ^{1}H NMR. All reactions were performed at ambient temperature.

The expected reaction is the nucleophilic addition of the phosphine to the vinyl group. After 4 days, the presence of vinyl group was monitored by ^{1}H NMR and it was found that 4% and 23% of vinyl groups were reacted with a monomer to DMPP ratio equal to 0.1 and 1.0, respectively. Subsequently, a 1 : 1 ratio of [MMA]/[thiols] (TG or DT) were reacted in the presence of [vinyl group]/[thiol]/[DMPP] = 1/1/0.05 as catalyst in acetone solution. Full conversion was obtained in an hour for the reaction of TG (P3, **Figure 2.13**, **Figure 2.14**) and ≥93% conversion was calculated for the reaction of DT (P4, **Figure 2.15**-**Figure 2.17**). Similar reaction rates were observed when the dimer of MMA was used in place of the monomer (P5, **Figure 2.18**, **Figure 2.19**; P6, **Figure 2.20**, **Figure 2.21** and P16).

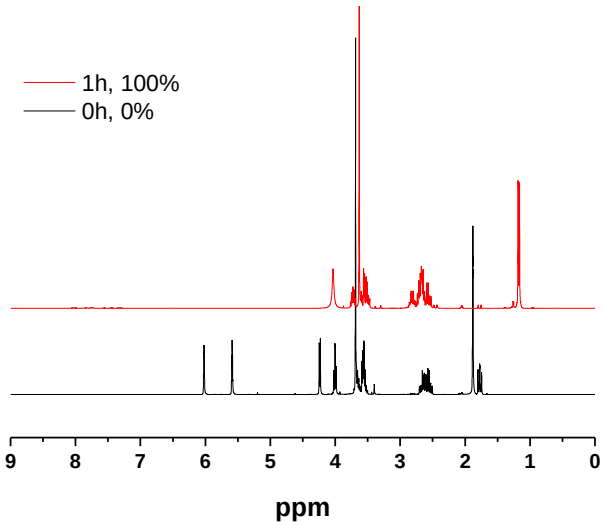

Figure 2.13 Thiol-Michael addition of MMA with 1-thioglycerol (TG) using 0.05 eq. of DMPP in acetone-d_6 followed by ^{1}H NMR, P3

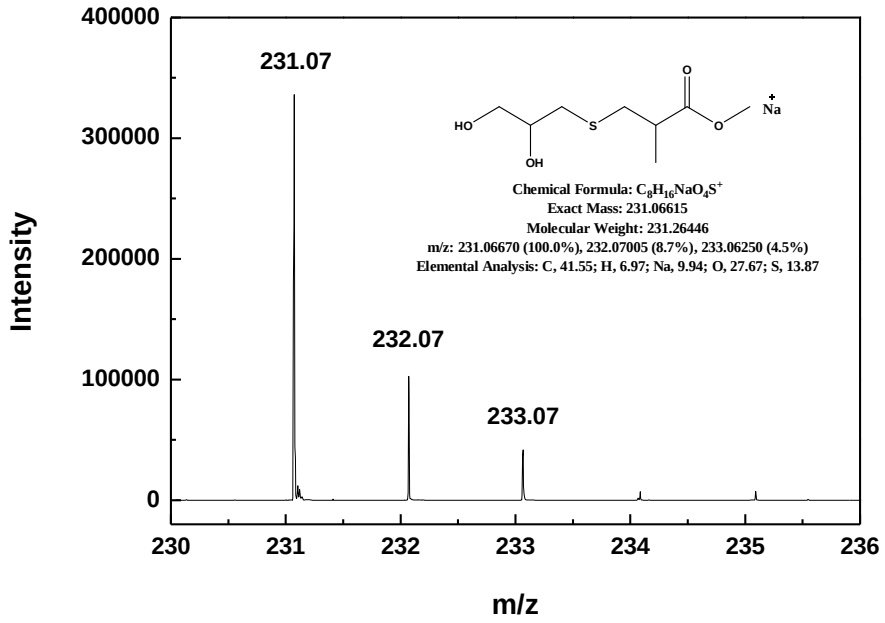

Figure 2.14 ESI-Mass spectrum of MMA-TG (P3)

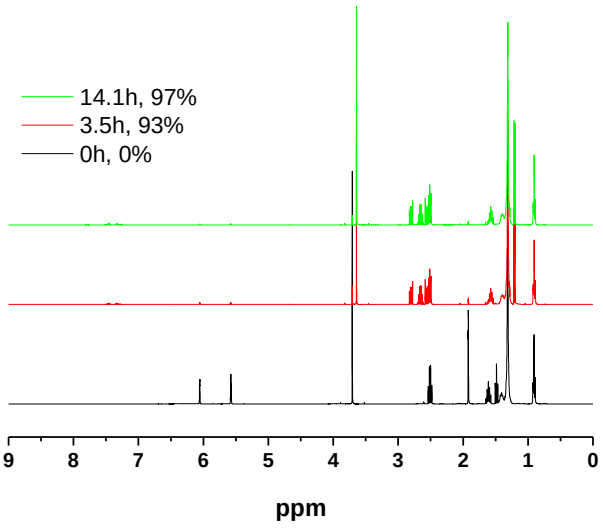

Figure 2.15 Thiol-Michael addition of MMA with 1-dodecanethiol (DT) using 0.05 eq. of DMPP in acetone-d_6 followed by ^{1}H NMR, P4

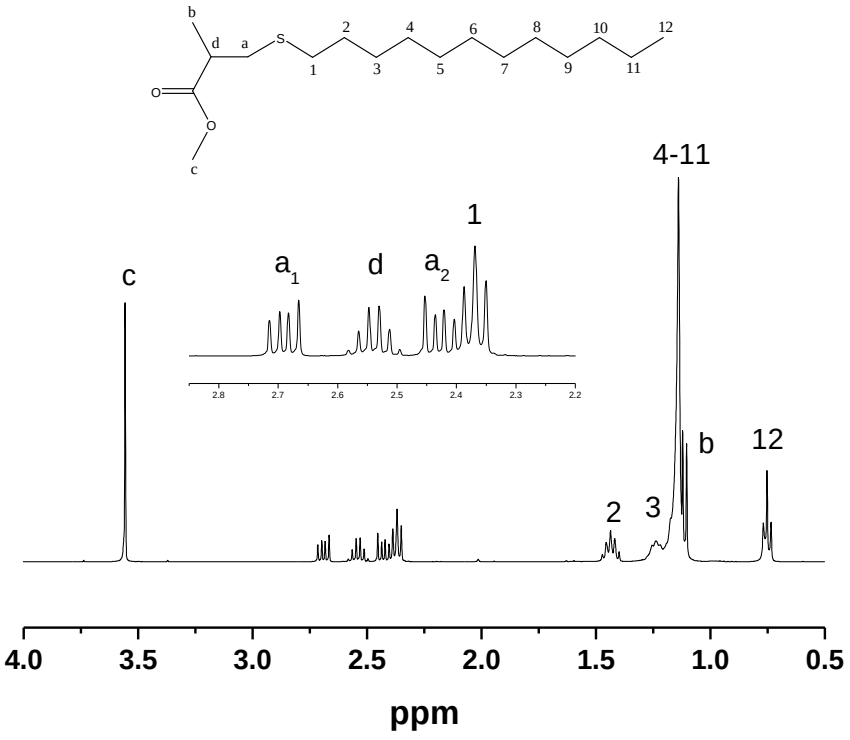

(a)

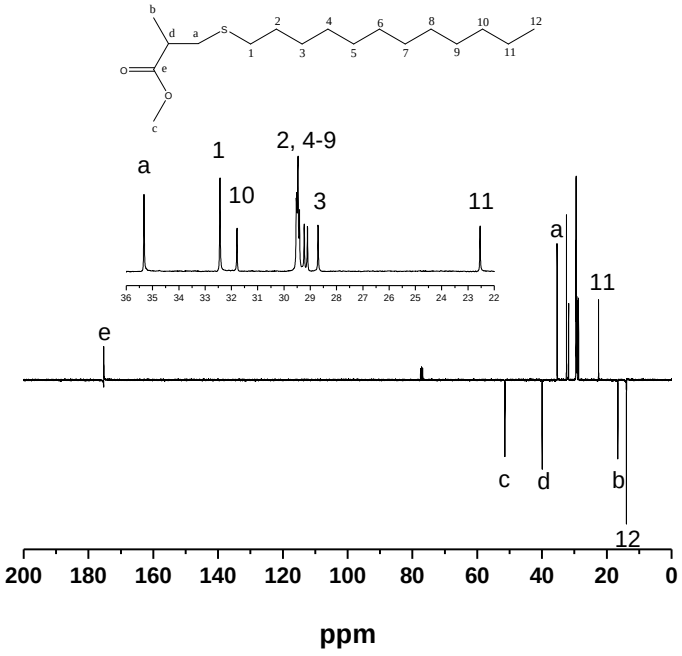

(b)

Figure 2.16 ^{1}H NMR (a) spectra ($CDCl_3$, 400 MHz, 298 K) and ^{13}C NMR (b) spectra ($CDCl_3$, 100 MHz, 298 K) of MMA-DT (P4)

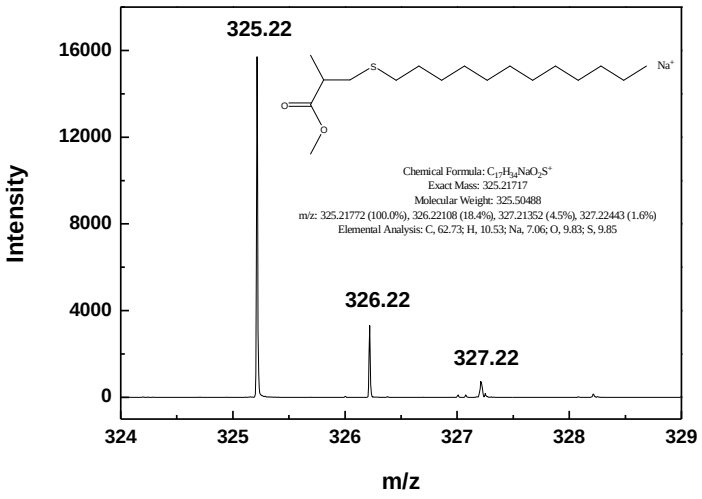

Figure 2.17 ESI-Mass spectrum of MMA-DT (P4)

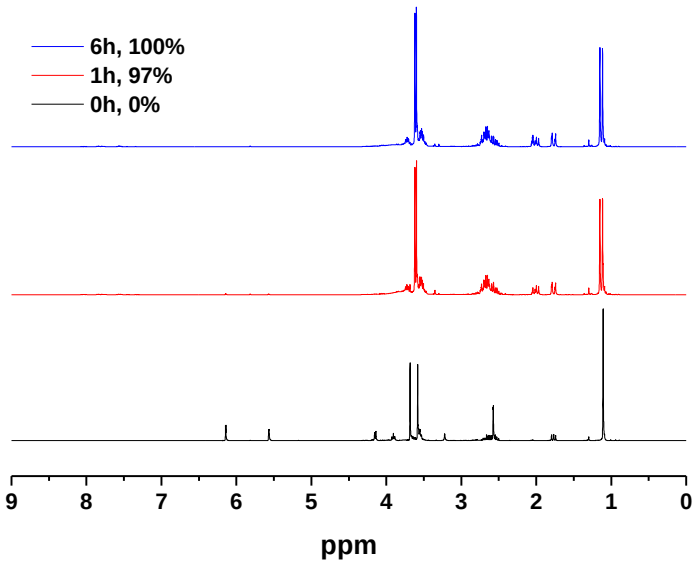

Figure 2.18 Thiol-Michael addition of MMA dimer with 1-thioglycerol (TG) using 0.05 eq. of DMPP in acetone-d_6 followed by ^{1}H NMR, P5

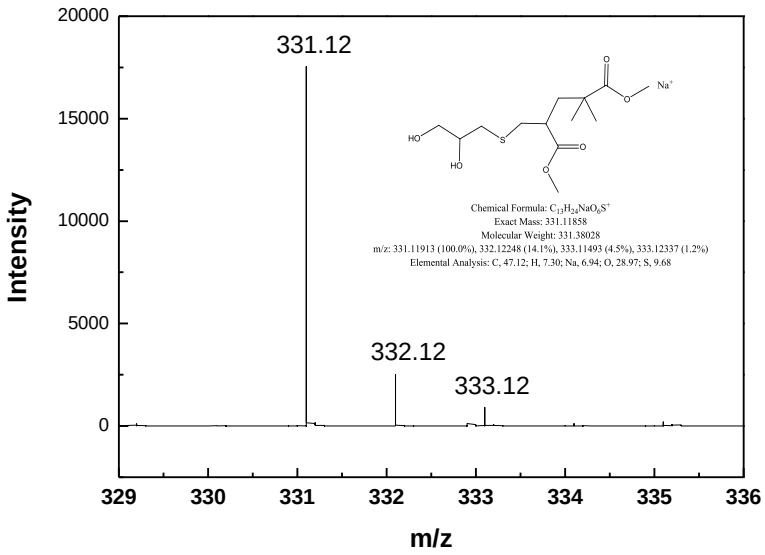

Figure 2.19 ESI-Mass spectrum of MMA dimer-TG (P5)

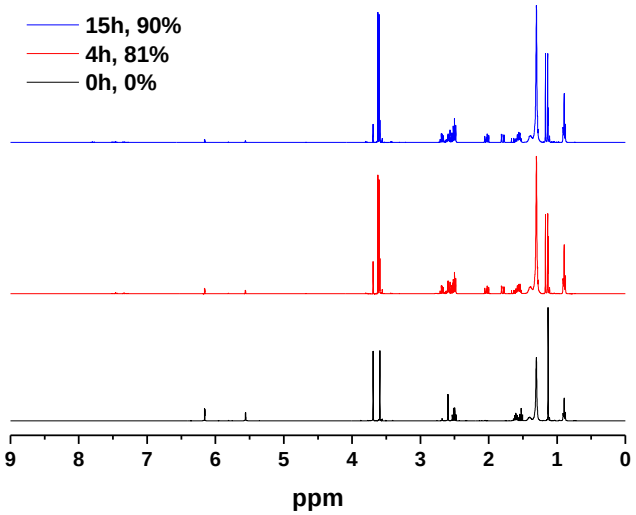

Figure 2.20 Thiol-Michael addition of MMA dimer with 1-dodecanethiol (DT) using 0.05 eq. of DMPP in acetone-d_6 followed by ^{1}H NMR, P6

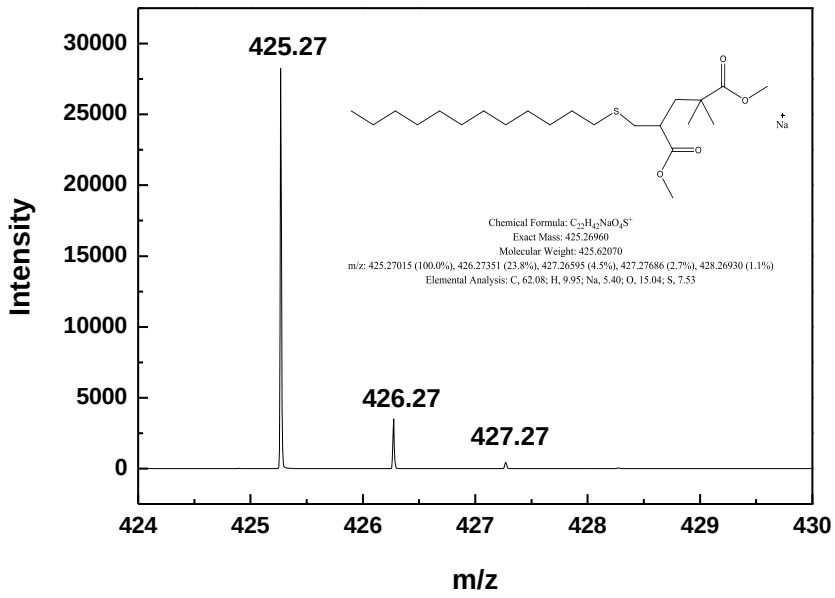

Figure 2.21 ESI-Mass spectrum of MMA dimer-DT (P6)

As expected, solvent selection has a great influence on the reaction rates. Therefore, we tested acetone, acetonitrile (ACN) and DMSO with the reaction in DMSO displaying faster kinetics in comparison to ACN and acetone (P7 and P8) attributable to the higher polarity of DMSO. The high polarity of DMSO should allow for a better stabilization of thiolate ion, and favors its formation. Solvent effects were also tested by using 1-propanethiol (PT) in all three solvents. The reaction in acetone was the slowest and in DMSO the fastest (P9, P11 and P12), **Figure 2.22** and **Figure 2.23**. Similar reaction rates were observed when the 3-mercaptopropionic acid (3-MPA) was used instead of PT (P14 and P15), **Figure 2.24**. In reactions P9 and P10, a higher ratio of thiol provided higher conversion values at the same reaction time. Finally, $PEGMEMA_{475}$ monomer was reacted with 2-ME in the presence of DMPP and full conversion was observed after 30 minutes P17, **Table 2.4**.

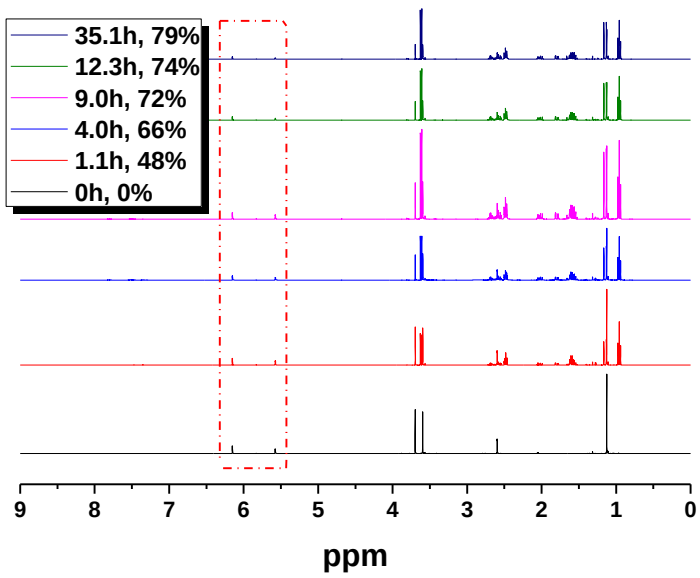

(a)

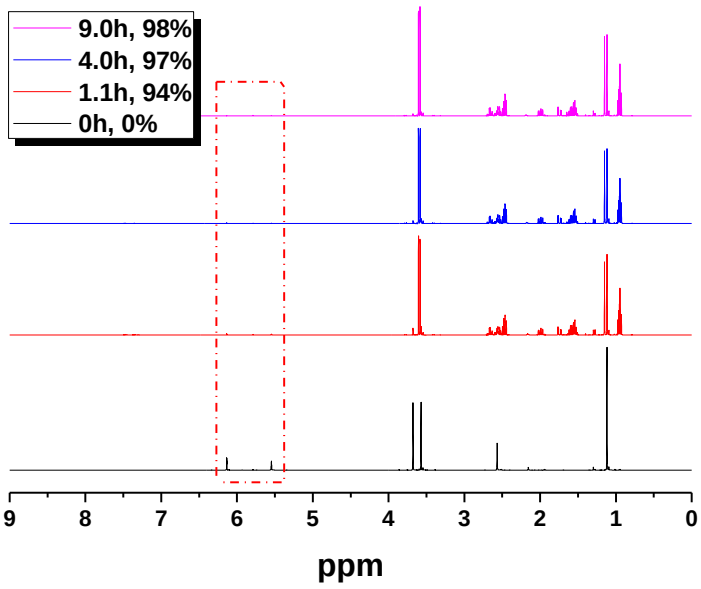

(b)

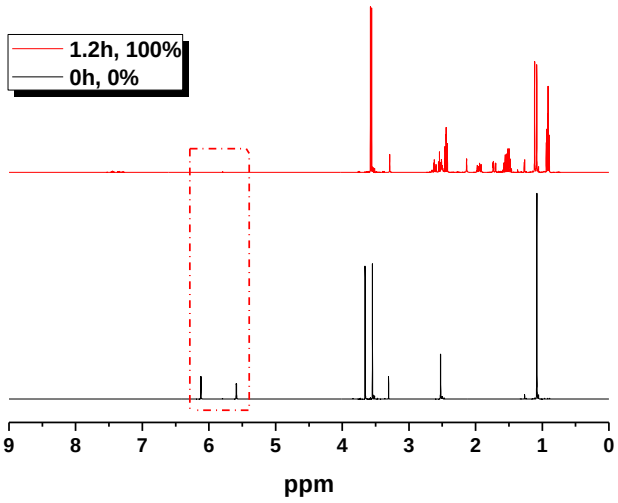

(c)

Figure 2.22 Thiol-Michael addition of MMA dimer with 1-propanthiol (PT) using 0.05 eq. of DMPP in different solvents followed by ^{1}H NMR (a) acetone-d_6, P9; (b) acetonitrile-d_3, P11; (c) DMSO-d_6, P12.

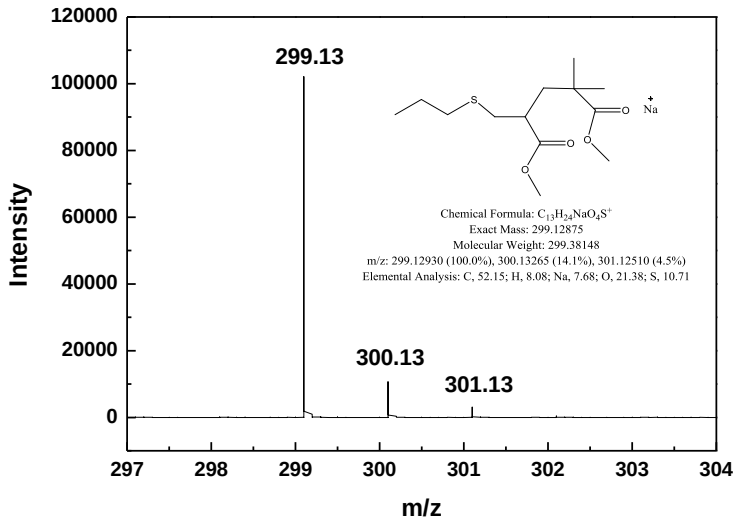

Figure 2.23 ESI-Mass spectrum of MMA dimer-PT (P11)

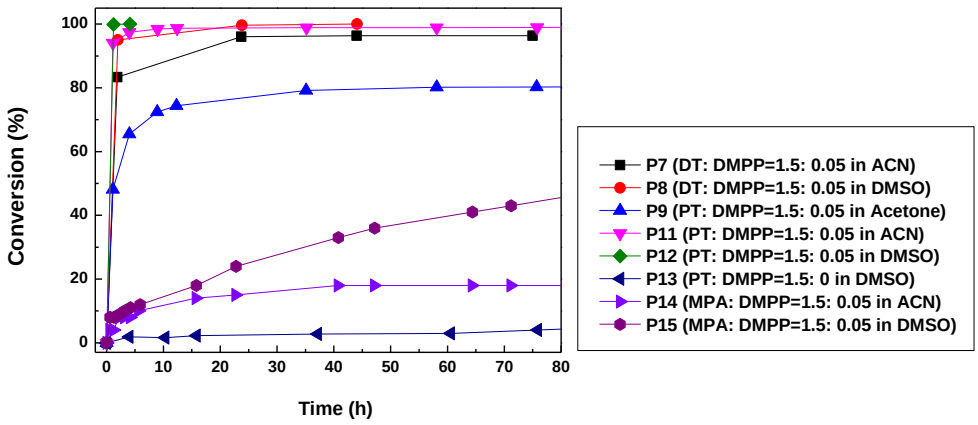

Figure 2.24 Vinyl bond conversion vs. time for MMA dimer in the presence of different thiols and solvents.

Furthermore, the addition reaction on oligo($PEGMEMA_{475}$) was investigated using DMPP and TCEP as catalysts, **Table 2.5**.

Table 2.5 Michael addition reactions to show evidence of side reactions

Run	Oligomer	Ratios [M]:[T]:[B]:[P][a]	Reac. Temp / ℃	React. Time /h	Cat.
S1	o(PEGMEMA $_{475}$)	1:5:0:2.5	ambient	14	TCEP (pH 8)
S2	o(PEGMEMA $_{475}$)	1:5:0:2.5	ambient	14	TCEP (pH 3)
S3	o(PEGMEMA $_{475}$)	1:5:2.5:2.5	40	14	DMPP/HA

[a] [M] : [T] : [B] : [P] = o(PEGMEMA$_{475}$) : 2-ME : hexylamine : phosphine.

However, side reactions occur when an excess of catalyst was used and this should be taken into account when designing experimental conditions S1-S3. The presence of side reactions was investigated with ESI-MS, **Figure 2.25**. In the presence of a large excess of DMPP or TCEP, by-products were clearly identified, corresponding to the presence of mono-addition of phosphine onto vinyl group for TCEP and DMPP.

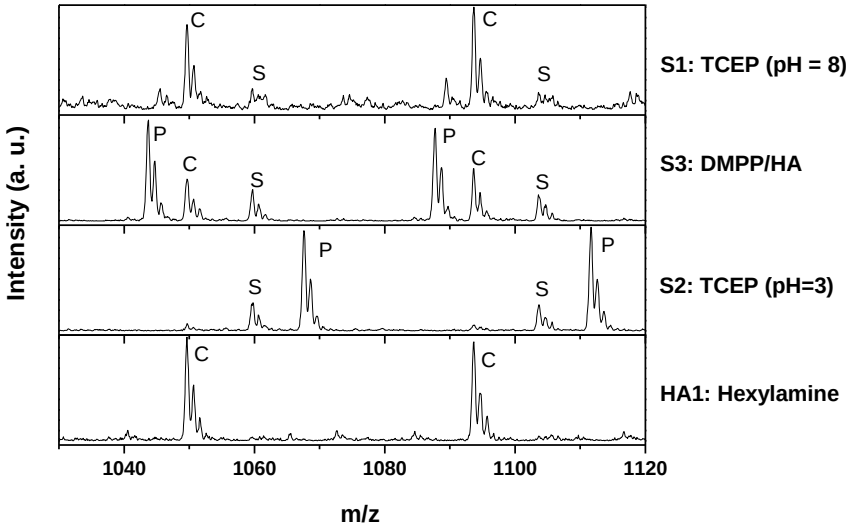

Figure 2.25 ESI-MS of oligo(PEGMEMA475) synthesized by CCTP used to identify the side reaction of phosphine catalyst. S = starting material, P = phosphine conjugated species, C = desired thiol–oligomer conjugate. Spectra were obtained with ESI-MS LCQ-Deca quadrupole.

In the case of TCEP, the pH has a large effect on the amount of side products formed. Indeed, at low pH, the major population observed corresponds to the presence of phosphine reacted polymers, while at high pH values the excepted product (thiol–oligomer conjugate) is present in large amounts. As expected, low pH does not favor the formation of thiolate anion ($R\text{-}S^-$). These experiments show that the concentration of phosphine should be kept relatively low (or the [phosphine]/[thiol] ratio should be kept very low) to minimize side product formation.

According to **Table 2.6**, the pH value has an effect on the reaction rates. When the TCEP was added in the reaction of HEMA dimer and 2-ME in D_2O,

the mixture pH = 1.8 and 4% conversion was observed after 16 hours (TP1). However, the reaction of HEMA dimer and 2-ME in PBS buffer pH 7.1 took 1.5 hours and 43 hours to reach 57% and 92%, respectively (TP2, **Figure 2.26**). Both DMPP and TCEP dissolve in DMSO, but DMPP had a higher efficient catalyst than TCEP to the thiol-ene click reaction in DMSO solvent. For example, the reaction of MMA dimer with PT (TP3) did not exceed 3% conversion in presence of 0.05 eq. of TCEP catalyst after 96 hours while the full conversion was reached using the same amount of DMPP catalyst in 1 hour (P12). Similar results could be observed in the reaction of MMA dimer with DT, TP4 and P8.

Table 2.6 Michael addition reactions using TCEP as catalyst with different monomers and thiols

Run	Monomer /dimer	Thiol	Ratios [M]:[T]:[Cat][a]	Solvent	React. time /h	Conv. (%)
TP1[b]	dHEMA	2-ME	1:1.5:0.1	D_2O	16	4
TP2[c]	dHEMA	2-ME	1:1.5:0.1	D_2O	43	92
TP3	dMMA	PT	1:1.5:0.05	DMSO	96	3
TP4	dMMA	DT	1:1.5:0.05	DMSO	24	0

[a] [M] : [T] : [Cat] = monomer or dimer : thiol : TCEP. Conversion values were calculated by ^{1}H NMR. All reactions were performed at ambient temperature. [b] Deuterium oxide (D_2O) was used. [c] PBS buffer was used at a pH value of 7.1.

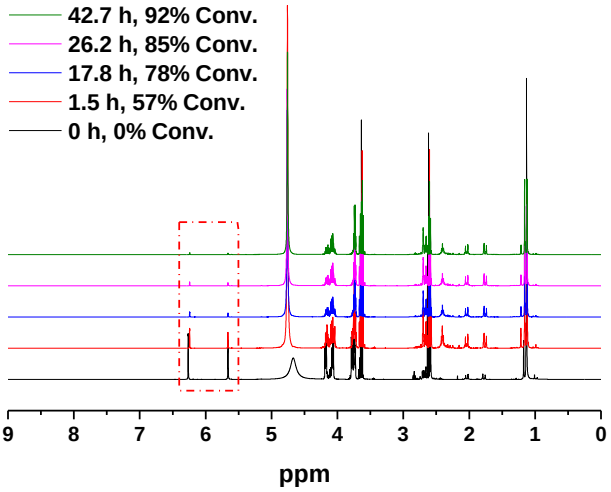

Figure 2.26 Thiol-Michael addition of HEMA dimer with 2-mercaptoethanol (2-ME) using 0.1 eq. of TCEP in PBS buffer (pH =7.1) followed by ^{1}H NMR, TP2.

Although the aim of this study was to investigate the effect of catalysts on thiol-ene click reactions, it was also observed that 2-hydroxyethyl methacrylate (HEMA) monomer and dimer (dHEMA) (water soluble) can react with 2-ME in water in the absence of catalyst, **Table 2.7**.

Table 2.7 Optimization reactions with different monomers/dimers and thiols in the absence of catalysts

Run	Monomer /dimer	Thiol	Ratios [M]:[T][a]	Solvent	React. time /h	Conv. (%)
N1[b]	HEMA	2-ME	1:1.5	D_2O	4	84
N2[c]	HEMA	2-ME	1:1.5	D_2O	4	100
N3[c]	dHEMA	2-ME	1:1.5	D_2O	0.5	60
N4[b]	dHEMA	HS-Glc	1:1.5	D_2O	44	91

[a] [M] : [T] = monomer or dimer : thiol. Conversion values were calculated by ^{1}H NMR. All reactions were performed at ambient temperature. [b] PBS buffer was used at a pH value of 7.1. [c] CBB buffer was used at a pH value of 9.2.

However, it is crucial to control the pH of the solution in the right range.[76] For instance, when PBS or CBB buffer was used and the pH was set to 7.1 and 9.2 for the reaction of HEMA and 2-ME in D_2O after 4 hours 84% and 100% of conversion was observed for N1 and N2, respectively (**Figure 2.27** and **Figure 2.28**). Pure dimer of HEMA synthesized by CCTP[77] was reacted with 2-ME under basic conditions in D_2O and 60% of conversion was obtained in 30 minutes N3. However, the reaction with thiol-glucose took relatively longer time to reach more than 90% conversion N4.

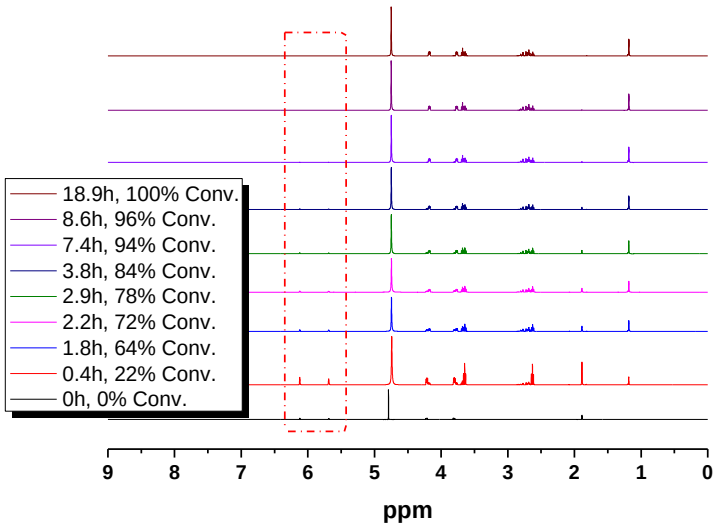

Figure 2.27 Thiol-Michael addition of HEMA with 2-mercaptoethanol (2-ME) in PBS buffer (pH = 7.1) followed by ^{1}H NMR, N1

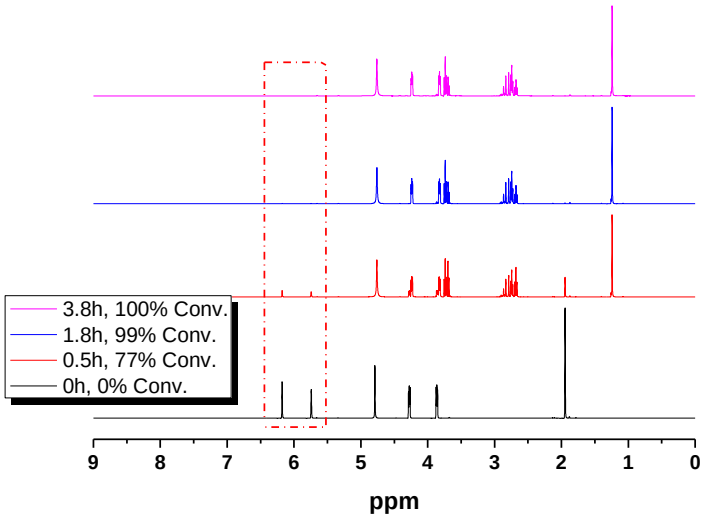

Figure 2.28 Thiol-Michael addition of HEMA with 2-mercaptoethanol (2-ME) in CBB buffer (pH = 9.2) followed by ^{1}H NMR, N2

2.4. Conclusion

A detailed study on the effect of catalyst on nucleophilic thiol-ene click reactions was described. It has been shown that when triethylamine was used as catalyst, even in excess amounts, it did not give any noticeable side reactions since mechanistically it was operating differently from pentylamine, hexylamine, DMPP and TCEP. Moreover, primary amines, pentylamine and hexylamine, were tested as appropriate catalysts. However, these can react with the vinyl group and form stable species which can also be monitored by MALDI-TOF MS and ESI-MS. Phosphine catalysts provided the fastest reaction, which also brought the

highest amount of side reactions. Nevertheless, using the catalyst in catalytic amounts provided relatively fast reaction rates for the desired compounds. It should also be noted that the effect of solvent, type of thiol and the basicity of the medium have a great role on this reaction and should be selected with care based on these optimization reactions. These model reactions were performed on monomers, dimers and oligomers and will form the basis of our following studies on thiol-click reactions with vinyl-terminated polymers.

2.5. References

1. W. H. Binder and R. Sachsenhofer, *Macromol. Rapid Commun.*, 2007, **28**, 15-54.
2. C. J. Hawker and K. L. Wooley, *Science*, 2005, **309**, 1200-1205.
3. H. C. Kolb, M. G. Finn and K. B. Sharpless, *Angew. Chem. Int. Ed.*, 2001, **40**, 2004-2021.
4. H. C. Kolb and K. B. Sharpless, *Drug Discov. Today*, 2003, **8**, 1128-1137.
5. C. R. Becer, S. Hahn, M. W. M. Fijten, H. M. L. Thijs, R. Hoogenboom and U. S. Schubert, *J. Polym. Sci., Part A: Polym. Chem.*, 2008, **46**, 7138-7147.
6. V. Ladmiral, G. Mantovani, G. J. Clarkson, S. Cauet, J. L. Irwin and D. M.

Haddleton, *J. Am. Chem. Soc.*, 2006, **128**, 4823-4830.

7. B. Gacal, H. Durmaz, M. A. Tasdelen, G. Hizal, U. Tunca, Y. Yagci and A. L. Demirel, *Macromolecules*, 2006, **39**, 5330-5336.

8. A. Dag, H. Durmaz, E. Demir, G. Hizal and U. Tunca, *J. Polym. Sci., Part A: Polym. Chem.*, 2008, **46**, 6969-6977.

9. B. S. Sumerlin, N. V. Tsarevsky, G. Louche, R. Y. Lee and K. Matyjaszewski, *Macromolecules*, 2005, **38**, 7540-7545.

10. C. R. Becer, R. Hoogenboom and U. S. Schubert, *Angew. Chem. Int. Ed.*, 2009, **48**, 4900-4908.

11. J. F. Lutz, *Angew. Chem. Int. Ed.*, 2008, **47**, 2182-2184.

12. P. V. Chang, J. A. Prescher, E. M. Sletten, J. M. Baskin, I. A. Miller, N. J. Agard, A. Lo and C. R. Bertozzi, *Proc. Natl. Acad. Sci. USA*, 2010, **107**, 1821-1826.

13. M. J. Kade, D. J. Burke and C. J. Hawker, *J. Polym. Sci., Part A: Polym. Chem.*, 2010, **48**, 743-750.

14. N. Gupta, B. F. Lin, L. Campos, M. D. Dimitriou, S. T. Hikita, N. D. Treat, M. V. Tirrell, D. O. Clegg, E. J. Kramer and C. J. Hawker, *Nat. Chem.*, 2010, **2**, 138-145.

15. M. W. Jones, G. Mantovani, S. M. Ryan, X. X. Wang, D. J. Brayden and D. M. Haddleton, *Chem. Commun.*, 2009, 5272-5274.

16. C. Boyer, A. Granville, T. P. Davis and V. Bulmus, *J. Polym. Sci., Part A Polym. Chem.*, 2009, **47**, 3773-3794.

17. R. K. Iha, K. L. Wooley, A. M. Nystrom, D. J. Burke, M. J. Kade and C. J. Hawker, *Chem. Rev.*, 2009, **109**, 5620-5686.

18. A. B. Lowe, *Polym. Chem.*, 2010, **1**, 17-36.

19. T. Clark, L. Kwisnek, C. E. Hoyle and S. Nazarenko, *J. Polym. Sci., Part A: Polym. Chem.*, 2008, **47**, 14-24.

20. L. A. Connal, C. R. Kinnane, A. N. Zelikin and F. Caruso, *Chem. Mater.*, 2009, **21**, 576-578.

21. K. L. Killops, L. M. Campos and C. J. Hawker, *J. Am. Chem. Soc.*, 2008, **130**, 5062-5064.

22. J. W. Chan, C. E. Hoyle and A. B. Lowe, *J. Am. Chem. Soc.*, 2009, **131**, 5751-5753.

23. L. Nurmi, J. Lindqvist, R. Randev, J. Syrett and D. M. Haddleton, *Chem. Commun.*, 2009, 2727-2729.

24. A. Geissler, M. F. Vallat, P. Fioux, J. S. Thomann, B. Frisch, J. C. Voegel, J. Hemmerle, P. Schaaf and V. Roucoules, *Plasma Process. Polym.*, 2010, **7**, 64-77.

25. Y. Li and T. Michinobu, *Polym. Chem.*, 2010, **1**, 72-74.

26. J. W. Chan, H. Wei, H. Zhou and C. E. Hoyle, *Eur. Polym. J.*, 2009, **45**, 2717-2725.

27. D. Konkolewicz, A. Gray-Weale and S. Perrier, *J. Am. Chem. Soc.*, 2009, **131**, 18075-18077.

28. N. ten Brummelhuis, C. Diehl and H. Schlaad, *Macromolecules*, 2008, **41**,

9946-9947.

29. A. Gress, A. Volkel and H. Schlaad, *Macromolecules*, 2007, **40**, 7928-7933.

30. M. Uygun, M. A. Tasdelen and Y. Yagci, *Macromol. Chem. Phys.*, 2010, **211**, 103-110.

31. Z. Jia, J. Liu, T. P. Davis and V. Bulmus, *Polymer*, 2009, **50**, 5928-5932.

32. D. Valade, C. Boyer, T. P. Davis and V. Bulmus, *Aust. J. Chem.*, 2009, **62**, 1344-1350.

33. S. P. S. Koo, M. M. Stamenovi, cacute, R. A. Prasath, A. J. Inglis, F. E. D. Prez, C. Barner-Kowollik, W. V. Camp and T. Junkers, *J. Polym. Sci., Part A: Polym. Chem.*, 2010, **48**, 1699-1713.

34. B. D. Mather, K. Viswanathan, K. M. Miller and T. E. Long, *Prog. Polym. Sci.*, 2006, **31**, 487-531.

35. C. Gimbert, M. Lumbierres, C. Marchi, M. Moreno-Manas, R. M. Sebastian and A. Vallribera, *Tetrahedron*, 2005, **61**, 8598-8605.

36. C. Gimbert, M. Moreno-Manas, E. Perez and A. Vallribera, *Tetrahedron*, 2007, **63**, 8305-8310.

37. Y. Yagci and M. A. Tasdelen, *Prog. Polym. Sci.*, 2006, **31**, 1133-1170.

38. C. Boyer, V. Bulmus, T. P. Davis, V. Ladmiral, J. Liu and S. Perrier, *Chem. Rev.*, 2009, **109**, 5402-5436.

39. J. T. Xu, C. Boyer, V. Bulmus and T. P. Davis, *J. Polym. Sci., Part A: Polym. Chem.*, 2009, **47**, 4302-4313.

40. H. Willcock and R. K. O'Reilly, *Polym. Chem.*, 2010, **1**, 149-157.

41. S. Perrier, P. Takolpuckdee and C. A. Mars, *Macromolecules*, 2005, **38**, 2033-2036.

42. G. Moad, Y. K. Chong, A. Postma, E. Rizzardo and S. H. Thang, *Polymer*, 2005, **46**, 8458-8468.

43. C. Boyer, V. Bulmus and T. P. Davis, *Macro. Rapid Comm.*, 2009, **30**, 493-497.

44. G. Moad, E. Rizzardo and S. H. Thang, *Aust. J. Chem.*, 2006, **59**, 669-692.

45. G. Moad, E. Rizzardo and S. H. Thang, *Aust. J. Chem.*, 2009, **62**, 1402-1472.

46. G. Moad and S. H. Thang, *Aust. J. Chem.*, 2009, **62**, 1379-1381.

47. G. Moad, E. Rizzardo and S. H. Thang, *Acc. Chem. Res.*, 2008, **41**, 1133-1142.

48. G. Moad, E. Rizzardo and S. H. Thang, *Polymer*, 2008, **49**, 1079-1131.

49. M. Benaglia, J. Chiefari, Y. K. Chong, G. Moad, E. Rizzardo and S. H. Thang, *J. Am. Chem. Soc.*, 2009, **131**, 6914-6915.

50. C. R. Becer, A. M. Groth, R. Hoogenboom, R. M. Paulus and U. S. Schubert, *QSAR Comb. Sci.*, 2008, **27**, 977-983.

51. R. M. Paulus, C. R. Becer, R. Hoogenboom and U. S. Schubert, *Aust. J. Chem.*, 2009, **62**, 254-259.

52. J. T. Xu, L. Tao, C. Boyer, A. B. Lowe and T. P. Davis, *Macromolecules*,

2010, **43**, 20-24.

53. M. Semsarilar, V. Ladmiral and S. Perrier, *Macromolecules*, 2010, **43**, 1438-1443.

54. B. M. Rosen, G. Lligadas, C. Hahn and V. Percec, *J. Polym. Sci., Part A: Polym. Chem.*, 2009, **47**, 3931-3939.

55. M. Li, P. De, S. R. Gondi and B. S. Sumerlin, *J. Polym. Sci., Part A: Polym. Chem.*, 2008, **46**, 5093-5100.

56. H. Li, B. Yu, H. Matsushima, C. E. Hoyle and A. B. Lowe, *Macromolecules*, 2009, **42**, 6537-6542.

57. R. M. Hensarling, V. A. Doughty, J. W. Chan and D. L. Patton, *J. Am. Chem. Soc.*, 2009, **131**, 14673-14675.

58. A. B. Lowe, C. E. Hoyle and C. N. Bowman, *J. Mater. Chem.*, 2010, **20**, 4745-4750.

59. C. E. Hoyle, A. B. Lowe and C. N. Bowman, *Chem. Soc. Rev.*, 2010, **39**, 1355-1387.

60. C. Boyer and T. P. Davis, *Chem. Comm.*, 2009, 6029-6031.

61. T. P. Davis, D. M. Haddleton and S. N. Richards, *J. Macromol. Sci., Rev. Macromol. Chem. Phys.*, 1994, **C34**, 243-324.

62. T. P. Davis, D. Kukulj, D. M. Haddleton and D. R. Maloney, *Trends Polym. Sci.*, 1995, **3**, 365-373.

63. D. Kukulj, T. P. Davis, K. G. Suddaby, D. M. Haddleton and R. G. Gilbert, *J. Polym. Sci., Part A: Polym. Chem.*, 1997, **35**, 859-878.

64. K. G. Suddaby, D. R. Maloney and D. M. Haddleton, *Macromolecules*, 1997, **30**, 702-713.

65. R. A. Sanayei and K. F. Odriscoll, *J. Macromol. Sci., Chem.*, 1989, **A26**, 1137-1149.

66. J. P. A. Heuts, D. Kukulj, D. J. Forster and T. P. Davis, *Macromolecules*, 1998, **31**, 2894-2905.

67. A. Gridnev, *J. Polym. Sci., Part A: Polym. Chem.*, 2000, **38**, 1753-1766.

68. J. P. A. Heuts, G. E. Roberts and J. D. Biasutti, *Aust. J. Chem.*, 2002, **55**, 381-398.

69. A. Bakac, M. E. Brynildson and J. H. Espenson, *Inorg. Chem.*, 1986, **25**, 4108-4114.

70. T. Y. J. Chiu, J. P. A. Heuts, T. P. Davis, M. H. Stenzel and C. Barner-Kowollik, *Macromol. Chem. Phys.*, 2004, **205**, 752 - 761.

71. D. M. Haddleton, E. Depaquis, E. J. Kelly, D. Kukulj, S. R. Morsley, S. A. F. Bon, M. D. Eason and A. G. Steward, *J. Polym. Sci., Part A: Polym. Chem.*, 2001, **39**, 2378-2384.

72. D. M. Haddleton, D. R. Maloney, K. G. Suddaby Adam Clarke and S. N. Richards, *Polymer*, 1997, **38**, 6207-6217.

73. D. M. Haddleton, D. R. Maloney, K. G. Suddaby, A. V. G. Muir and S. N. Richards, *Macromol. Symp.*, 1996, **111**, 37-46.

74. D. M. Haddleton, D. R. Maloney and K. G. Suddaby, *Macromolecules*, 1996, **29**, 481-483.

75. D. M. Haddleton, M. C. Crossman, K. H. Hunt, C. Topping, C. Waterson and K. G. Suddaby, *Macromolecules*, 1997, **30**, 3992-3998.

76. E. S. Read, K. L. Thompson and S. P. Armes, *Polym. Chem.*, 2010, **1**, 221-230.

77. J. D. Biasutti, G. E. Roberts, F. P. Lucien and J. P. A. Heuts, *Eur. Polym. J.*, 2003, **39**, 429-435.

Chapter 3. Synthesis and modification of PDEGMEMA and POEGMEMA via CCTP and thiol-ene click reactions

3.1. Introduction

Catalytic chain transfer polymerization is a very efficient and versatile free-radical polymerization technique for the synthesis of macromonomers with ω-unsaturated vinyl terminal groups.[1, 2] It is used commercially by DSM and DuPont for the production of coatings, viscosity modifiers and engine additives for the automotive industry. The reaction is mediated by the ability of certain low-spin Co(II) complexes, such as Cobaloximes, to efficiently catalyze the chain transfer to monomer reaction.[3, 4] A widely investigated Co(II) transfer agent is bis(boron difluorodimethylglyoximate) cobalt(II) (CoBF).[1, 2, 5-7] The chain transfer constant of CoBF is typically between 10^2 and 10^4 for monomers containing an α-methyl group, such as methacrylates. CCT occurs *via* a mechanism characterized by two consecutive steps:[3, 4, 8] Firstly, the Co(II) complex abstracts a hydrogen from the propagating radical to form a dead polymer chain and a Co(III)-H complex; then this complex reacts with another monomer molecule to produce the original Co(II) complex and another propagating radical (**Scheme 3.1**).

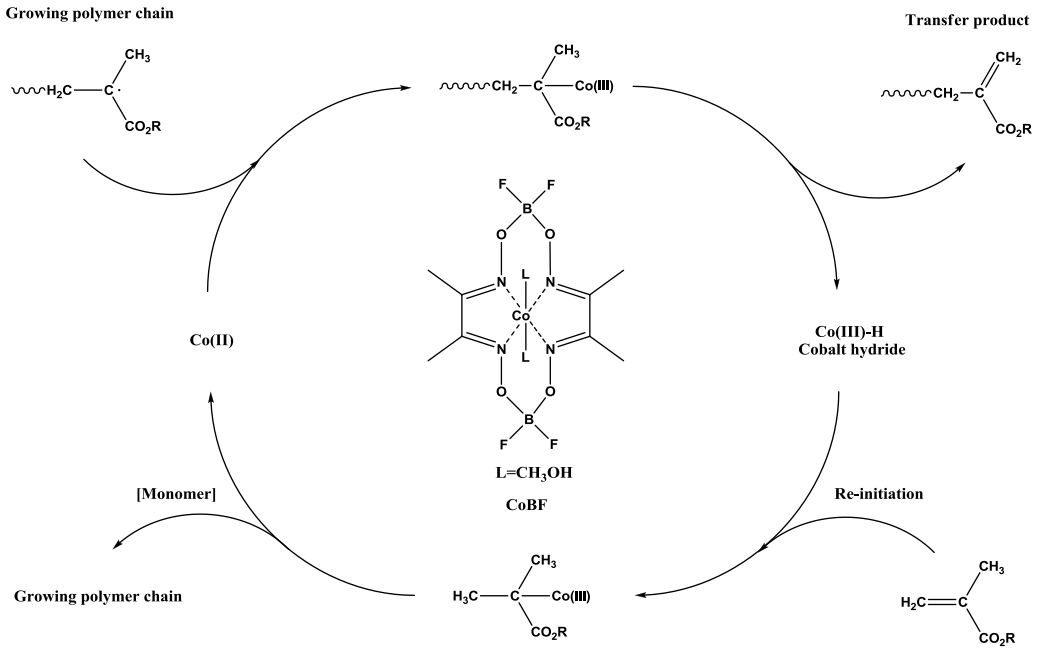

Scheme 3.1 General mechanism for Catalytic Chain Transfer Polymerization (CCTP).

The Co(II) complex acts in a catalytic fashion and is not consumed in the process. CCT is a very powerful technique used to synthesize low molecular weight polymers/oligomers terminated by a vinyl end-group (macromonomers) with a large range of functional or non-functional monomers. CCT polymerization can be performed in a large range of solvents, ranging from aqueous to nonpolar organic media.[9, 10]

Inspired by the work reported by Ishizone *et al*.[11] and later by Lutz and Hoth[12] and others, the preparation of thermoresponsive, antifouling PEG based polymers is of increasing interest for the preparation of thermoresponsive micelles, hybrid organic/inorganic nanoparticles,[13-16] surface modification,[17-20] hyper-branched/nanogels and protein–polymer conjugates.[21-27] As illustrated by

the recent publication of Dong and Matyjaszewski who describe the first preparation of thermally responsive poly-(oligo(ethylene glycol) methyl ether methacrylate) *via* AGET ATRP in miniemulsion.[28] In this current study, the synthesis of thermoresponsive PEG based macromonomers by the copolymerization of OEGMEMA and DEGMEMA using CCT is described. The lower critical solution temperature (LCST) was tuned by altering the composition of the polymer with these two monomers to yield thermoresponsive polymers with LCSTs ranging from 16 to 95 ^{o}C. An advantage of CCT is that the resulting polymer chains have unsaturated vinylic end-groups (with very high chain-end fidelity; close to 100%) which create a large range of synthetic options for end-group modification with simple organic compounds. Furthermore, CCTP requires a very low amount of catalyst (in low ppm levels), yielding very pure polymers with a very low amount of residual catalyst complex. Over the last decade, ‘‘click’’ chemistry has opened new avenues for the design and creation of tailor-made macromolecules.[29-31] Thiol-ene ‘‘click’’ chemistry, in which thiols react quantitatively by addition to double bonds, has been shown to be highly efficient in a large range of solvents, without the addition of metals, under mild conditions.[32-41]

There are two types of thiol-ene reaction: (i) Base catalyzed Michael addition and (ii) the anti-Markovnikov radical UV initiated click reaction. Both of these approaches have been used for the functionalization of polymers[33, 42] or for the design of complex macromolecules.[35, 43-47]

In this study, thermoresponsive PEG-based copolymers and homopolymers of OEGMEMA obtained by CCT were modified using thiol-ene click chemistry with a variety of different functional thiol compounds to yield functional thermoresponsive polymers in high yield. The effect of different solvent systems for based catalyzed thiol-ene reaction was investigated in the presence of different functional thiols. The optimal conditions for thiol-ene click chemistry to obtain a very high degree of functionality (solvent and nature of the catalyst) are reported here. The polymers were characterized *via* electrospray mass spectrometry (ESI-MS), ^{1}H NMR spectroscopy and MALDI-ToF MS analysis. In addition, the thermoresponsive properties (LCST) and thermal properties (glass transition and decomposition temperatures) of the copolymers were determined before and after thiol-ene modification.

3.2. Experimental

3.2.1. Materials

The CCT agent bis(methanol) complex, $(CH_3OH)_2Co$-$(dmgBF_2)_2$ (CoBF), was synthesized according to the method of Bakac *et al.* [48, 49] The CTA transfer efficiency was checked by CCT polymerization of methyl methacrylate (MMA) which yielded a C_S value = 25 000. The monomers, $OEGMEMA_{475}$ (95%, Sigma-Aldrich), DEGMEMA (95%, Sigma-Aldrich) and $OEGMEMA_{1100}$ (95%,

Sigma-Aldrich) were used as received. The initiator 4,4'-azobis-(4-cyanovaleric acid) (ACVA, 98%, Sigma-Aldrich) was used as received and 2,2'-azobisisobutyronitrile (AIBN, 98%, Sigma-Aldrich) was purified by recrystallization twice from methanol. The thiols, 2-mercaptoethanol (2-ME, 99%, Sigma-Aldrich), 1-dodecanethiol (DT, 98+%, Sigma-Aldrich), benzyl mercaptan (BM, 99%, Sigma-Aldrich), 1-propanethiol (PT, 99%, Sigma-Aldrich), 3-mercaptopropionic acid (3-MPA, 99%, Sigma-Aldrich), 1-thiol-β-D-glucose sodium salt (HS-Glc, 99%, Sigma-Aldrich) were used as received. The catalyst triethylamine (TEA, 99%, Fisher Scientific UK Ltd.), hexylamine (HA, 99%, Sigma-Aldrich), and dimethylphenylphosphine (DMPP, 99%, Aldrich) were used as received. Sodium iodide (NaI, 99+%, Sigma-Aldrich), trans-2-[3-(4-*tert*-butylphenyl)-2-methyl-2-propenylidene] malononitrile (DCTB, 99+%, Fluka, Sigma-Aldrich), acetone-d_6 (99.9% atom %D, Sigma-Aldrich), acetonitrile-d_3 (ACN-d_3, 99.8% atom %D, Sigma-Aldrich) and dimethylsulfoxide-d_6 (DMSO-d_6, 99.9% atom %D, Sigma-Aldrich) were used as received.

3.2.2. Catalytic chain transfer (CCT) homopolymerization

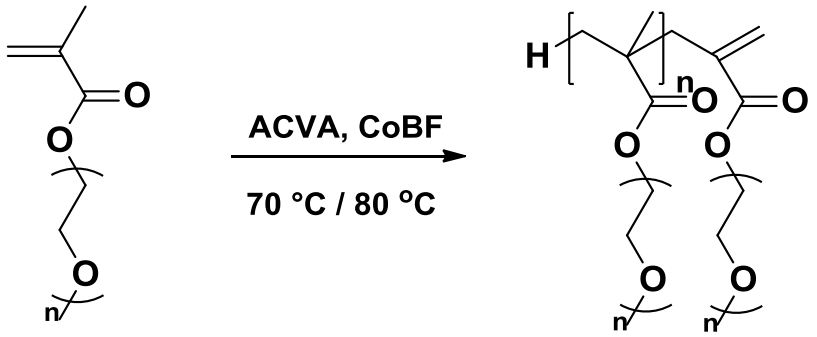

Scheme 3.2 Synthesis of OEGMEMA homopolymers *via* catalytic chain transfer polymerization.

The general catalytic chain transfer polymerizations (CCTPs) were performed as follows: monomers (DEGMEMA, $OEGMEMA_{475}$, and $OEGMEMA_{1100}$) and solvents (acetonitrile, methanol or methanol/water mixture) were purged with nitrogen for at least an hour prior to use. Stock solutions of CoBF were also weighed and purged with nitrogen prior to use. AIBN or ACVA was weighed into Schlenk flasks. All reaction mixtures were then mixed under nitrogen. To ensure the absence of oxygen, the reaction mixtures were subjected to at least three freeze-pump-thaw cycles. Polymerizations were performed at a constant temperature of 70 ^{o}C or 80 ^{o}C. The polymerization mixture was sampled periodically using an airtight degassed syringe for molecular weight and conversion analysis. Polymerizations were stopped by cooling and subsequent exposure to air. Polymers were then purified by precipitation and dialysis. Poly(OEGMEMA) was precipitated in diethyl ether and poly(DEGMEMA) was precipitated in water or cold petroleum ether (40-60 ^{o}C). For semi-batch

polymerizations, the procedure was the same, however, the monomer and CoBF solutions were added at a rate of 1 mL min^{-1} throughout the reactions.

3.2.3. Catalytic chain transfer (CCT) copolymerization

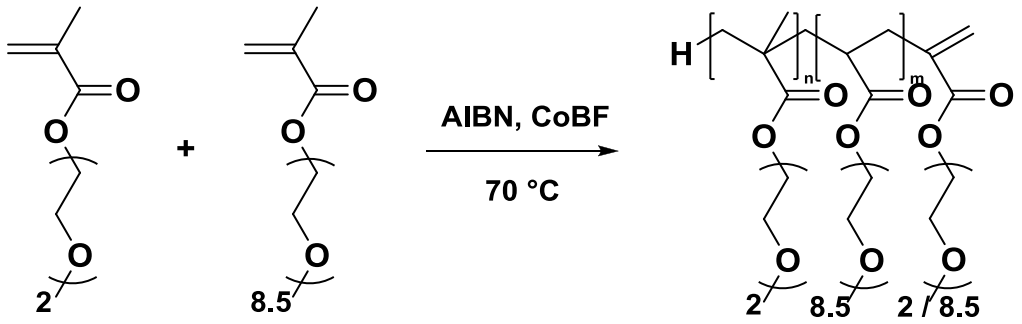

Scheme 3.3 Synthesis of OEGMEMA copolymers *via* catalytic chain transfer polymerization.

The general CCT copolymerization procedure was as follows: monomers $OEGMEMA_{475}$ and DEGMEMA with different compositions and solvents (acetonitrile or water/methanol mixture) were mixed with AIBN and purged with nitrogen at least one hour before use. Stock solutions of CoBF were prepared and purged before use. All reaction mixtures were then mixed under nitrogen and to ensure the absence of oxygen, the reaction mixtures were then subjected to at least three freeze-pump-thaw cycles. Polymerizations were performed at a constant temperature of 70 ^{o}C. Polymerizations were stopped by cooling and subsequent exposure to air and copolymers were then purified by dialysis in water/acetone.

3.2.4. Triethylamine (TEA) catalyzed thio-click reactions

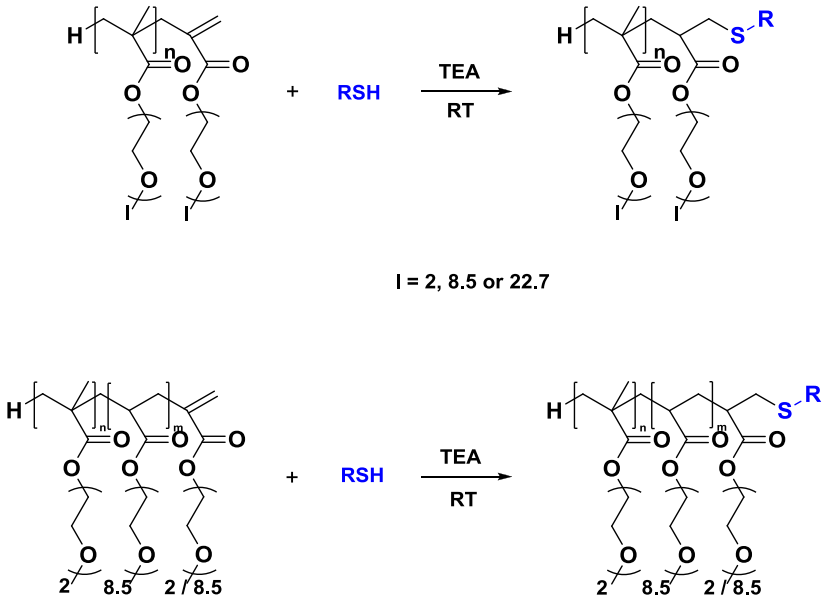

Scheme 3.4 Thiol-ene click reactions of OEGMEMA polymers with different of thiols in presence of triethylamine.

Poly(OEGMEMA) was mixed with triethylamine, water, acetone, acetonitrile or DMSO as solvents, and thiol reagent. In a typical reaction, 1.0 eq. of poly(OEGMEMA) (100 mg), 2.0 eq. of thiol, and 3.0 eq. of triethylamine were added into a flask and then purged for 15 minutes with nitrogen. The vial was then placed at ambient temperature or in a 40 ^{o}C oil bath before the reaction was stopped. The reaction mixtures were purified *via* precipitation in cold petroleum ether or dialysis. The reaction was monitored by the disappearance of the vinyl bond seen at 5.6-6.1 ppm.

3.2.5. *n*-Hexylamine (HA) catalyzed thio-click reactions

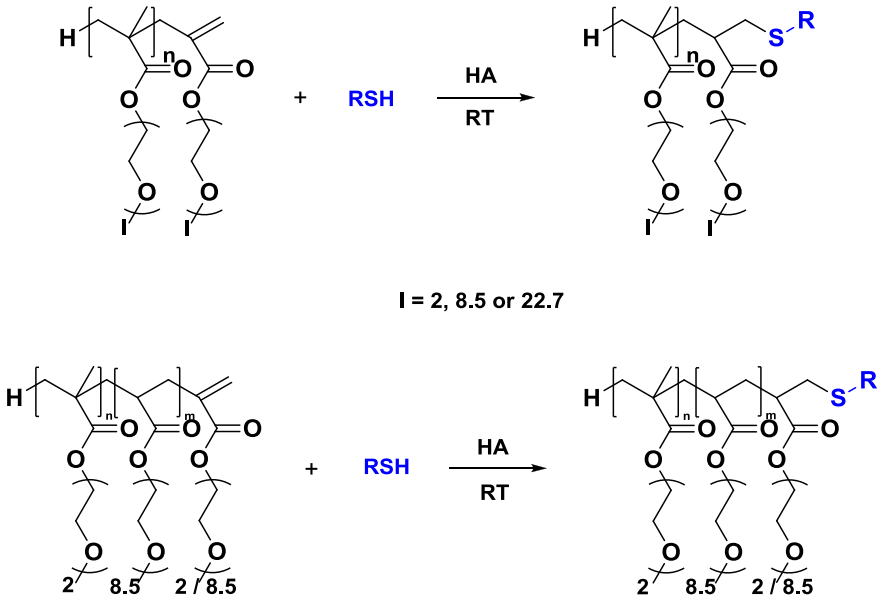

Scheme 3.5 Thiol-ene click reactions of OEGMEMA polymers with different of thiols in presence of hexylamine (HA).

Poly(OEGMEMA) was mixed with hexylamine, water, acetone, acetonitrile or DMSO used as solvents, and thiol reagent. In a typical reaction, 1.0 eq. of poly(OEGMEMA) (100 mg), 2.0 eq. of thiol, and 3.0 eq. of hexylamine were added into a flask and then purged for 15 minutes with nitrogen. The vial was then placed at ambient temperature or in a 40 ^{o}C for 14 hours before the reaction was stopped. The reaction mixtures were purified *via* precipitation in cold petroleum ether or dialysis. The reaction was monitored by the disappearance of the vinyl bond seen at 5.6-6.1 ppm.

3.2.6. DMPP catalyzed thio-click reactions

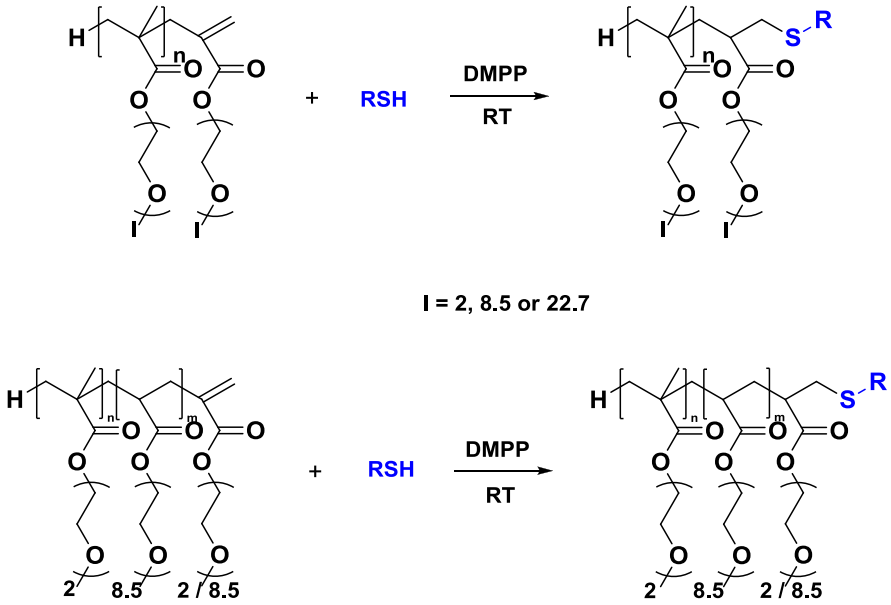

Scheme 3.6 Thiol-ene click reactions of OEGMEMA polymers with different of thiols in presence of dimethylphenylphosphine (DMPP).

Poly(OEGMEMA), thiols and DMPP were mixed in a NMR tube containing acetone-d_6, acetonitrile-d_3 or DMSO-d_6. The reactions were performed at ambient temperature and monitored by ^{1}H NMR spectroscopy. In a typical reaction, 1.0 eq. of polymer (0.05 g), 2.0 eq. of thiol and 0.1 eq. of DMPP were added to a NMR tube containing 0.55 mL of deuterated solvent. The reaction was monitored by the disappearance of the vinyl bond seen at 5.6-6.1 ppm.

3.3. Characterization

3.3.1. Gel permeation chromatography (GPC).

Gel permeation chromatography (GPC) was used to determine molecular weights and polydispersity ratio (M_w/M_n) of polymer samples.

GPC using $CHCl_3$ eluent was performed on an Agilent 390-MDS, comprising of an autosampler and a PLgel 5.0 μm bead-size guard column (50 × 7.5 mm), followed by two 5.0 μm bead-size PLgel Mixed D columns (300 × 7.5 mm) and a differential refractive index detector using $CHCl_3$ as the eluent at 30 ^oC with a flow rate of 1 mL min^{-1}. The GPC system was calibrated using linear poly(methyl methacrylate) EasiVial standards (Agilent Ltd.) range from 200 to 10^5 g mol^{-1} and polystyrene EasiVial standards (Agilent Ltd.) range from 162 to 10^5 g mol^{-1}. Data were collected and analyzed using Cirrus GPC/SEC software (version 3.3).

GPC with THF as eluent was performed on an Agilent 390-MDS, comprising of an autosampler and a PLgel 5.0 μm bead-size guard column (50 × 7.5 mm), followed by two linear 5.0 μm bead-size PLgel Mixed D columns (300 × 7.5 mm) and a differential refractive index detector using THF (2% v/v TEA) as the eluent at 30 ^oC with a flow rate of 1 mL min^{-1}. The GPC system was calibrated using linear poly(methyl methacrylate) EasiVial standards (Agilent Ltd.) range from 200 to 10^5 g mol^{-1} and polystyrene EasiVial standards (Agilent Ltd..) range from 162 to 10^5 g mol^{-1}. Data were collected and analyzed using Cirrus GPC/SEC software (version 3.3).

DMF GPC analyses of the polymers were performed in *N*,*N*-dimethylformamide (DMF, 0.1% w/v LiBr), at 50 ^{o}C (flow rate = 1 mL min^{-1}) using an Agilent 390-MDS system comprised of an autosampler and a PLgel 5.0 μm bead-size guard column (50 × 7.8 mm) followed by two linear 5.0 μm bead-size PLgel Mixed D columns (300 × 7.5 mm) and a differential refractive-index detector. Calibration was achieved with linear poly(methyl methacrylate) EasiVial standards (Agilent Ltd.) range from 200 to 10^5 g mol^{-1}. Data were collected and analyzed using Cirrus GPC/SEC software (version 3.3).

3.3.2. Nuclear magnetic resonance (NMR).

^{1}H NMR spectroscopy was used to determine the molecular weight and structural information for confirmation of thiol-ene click conjugation. NMR spectra were recorded on either a Bruker DPX-300 MHz or a Bruker DPX-400 MHz spectrometer at 298 K on approximately 10% w/v solutions in deuterated NMR solvents from Sigma-Aldrich. All chemical shifts are reported in ppm (δ) relative to tetramethylsilane (TMS), or referenced to the chemical shifts of residual solvent resonances (^{1}H and ^{13}C). The following abbreviations were used to explain the multiplicities: s = singlet, d = doublet, dd = doublet of doublets, t = triplet, m = multiplet.

3.3.3. UV-visible spectroscopy.

UV-visible spectra were recorded using a PerkinElmer Lambda 35 UV-VIS spectrometer equipped with a temperature controller.

3.3.4. Cloud points measurements.

The transmittance of the solution was measured at a wavelength 500 nm through a 10 mm path length cuvettes with a micro stir bar and total volumes of 2 ml referenced against distilled water, using a PerkinElmer Lambda 35 UV-VIS spectrometer. The water-jacketed sample and reference cuvettes holders were coupled with a Peltier PTP 1+1 peltier temperature programmer adjusted at a heating rate of 1 ^{o}C min^{-1}. The cloud points (LCST) were defined as the temperature corresponding to a 50% reduction in the original transmittance of the solution.

3.3.5. Matrix-Assisted Laser Desorption/Ionisation Time-of-Flight Mass Spectrometry (MALDI-ToF MS)

MALDI-ToF MS analysis was performed with a Bruker Daltonics Ultraflex II TOF instrument set in positive reflectron mode with a smartbeam-I, solid state neodymium-doped yttrium aluminium garnet (Nd : YAG) laser. The matrix solution was prepared by dissolving trans-2-[3-(4-*tert*-butylphenyl) -2-methyl-

2-propenylidene]malononitrile (DCTB) in a 1 mL mixture of acetone and water (equal volumes). Sodium iodide was added at 0.1% overall concentration and the polymer dissolved to a concentration of 10 mg cm^{-3}. The matrix solution (0.5 mL) was applied to the stainless steel side and the solvent was allowed to evaporate. The same volume of the polymer sample solution was applied on top of the dried matrix, and the overall mixture was allowed to dry. The sample was irradiated with 300-600 pulsed laser shots at a 1-10% laser power cycling at 50 Hz. Calibration was performed with various linear poly(ethylene glycol) methyl ether standards. Predicted isotopic masses for detected species were generated by Bruker Daltonics Isotope Pattern software. The samples were measured in reflectron ion mode and calibrated against poly (ethylene glycol) methyl ether.

3.4. Results and discussion

Catalytic chain transfer polymerizations (CCTP) of various oligo-(ethylene glycol) methyl ether methacrylates were performed using 2,2'-azobisisobutyronitrile (AIBN) as the initiator, the bis(methanol) complex, $(CH_3OH)_2Co–(dmgBF_2)_2$ (CoBF), as a catalyst and acetonitrile as a solvent at 70 ^oC. The chain transfer constant of catalytic chain transfer polymerization can be calculated using the Mayo equation (3.1). It should be noted that for very short chains (ie. very high concentrations of the transfer agent), the Mayo equation with

standard form can be changed into equation (3.2),[1, 2, 50] provided the monomer conversion is maintained below 10%.

$$\frac{1}{DP_n} = \frac{1}{DP_{n0}} + C_S \frac{[C]}{[M]} \tag{3.1}$$

$$DP_n = 2 + \left(C_S \frac{[C]}{[M]} \right)^{-1} \tag{3.2}$$

Where DP_n is the degree of polymerization, [*C*] is the concentration of the catalyst, and [M] is the initial monomer concentration. The monomers that were used in this study were diethylene glycol methyl ether methacrylate, oligo(ethylene glycol) methyl ether methacrylate (475), and oligo(ethylene glycol) methyl ether methacrylate (1100) as depicted in **Scheme 3.7**.

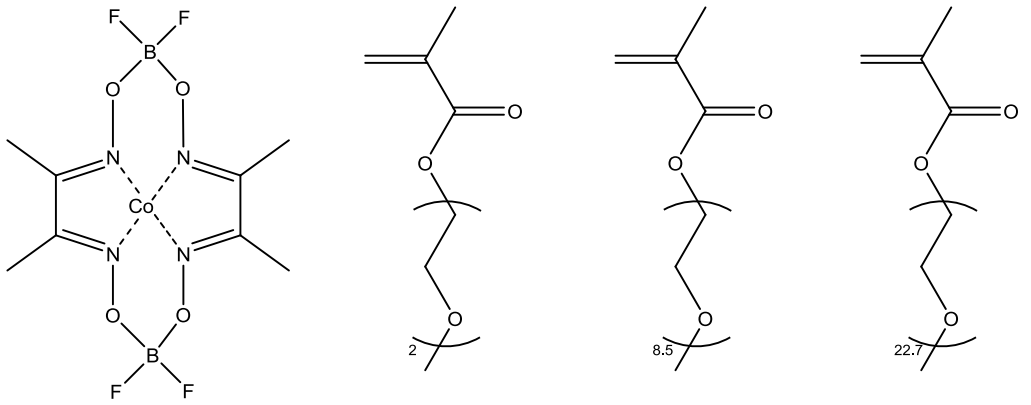

CoBF DEGMEMA $OEGMEMA_{475}$ $OEGMEMA_{1100}$

Scheme 3.7 Representation of CoBF and various oligo(ethylene glycol) monomers used in this study

The polymer molecular weights were analyzed *via* GPC and ^{1}H NMR

spectroscopy. The polymers exhibited unimodal distributions with PDi < 1.5. The polymers, after purification, were analyzed by ^{1}H NMR and by MALDI-ToF (**Figure 3.1**), and the molecular weights were calculated using the signal of the vinyl group at 5.5-6.2 ppm and equation (3.3).

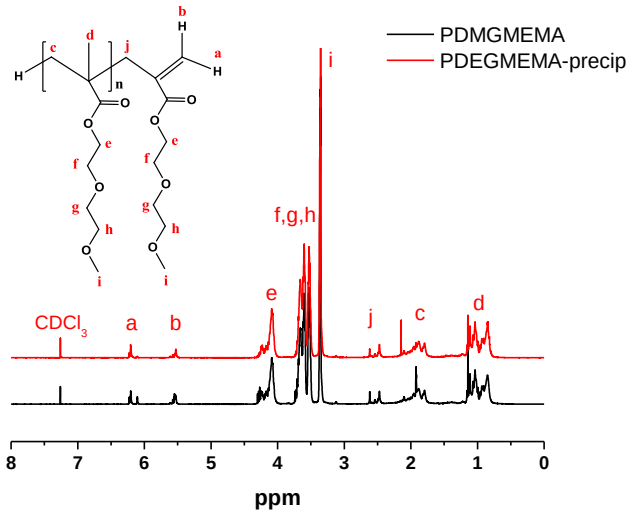

(a)

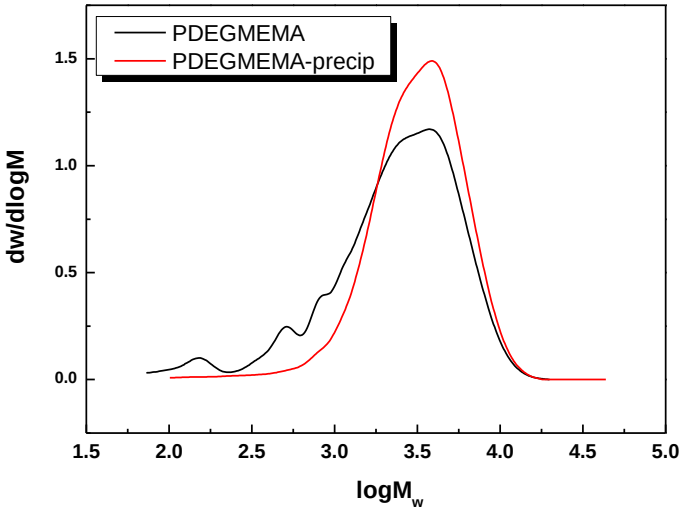

(b)logMW not M_w

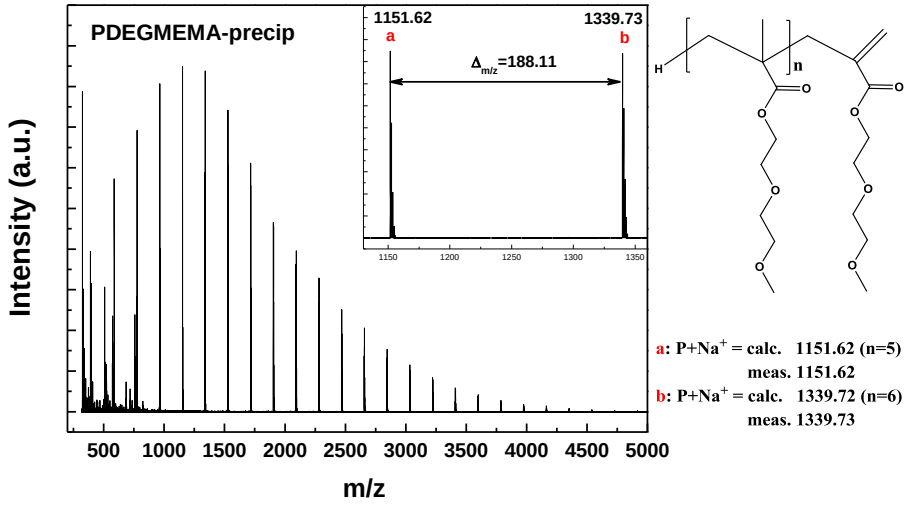

(c)

Figure 3.1 ^{1}H NMR spectrum (a), GPC (b) and MALDI-ToF MS (c) of poly(diethylene glycol) methyl ether methacrylate.

Figure 3.1 (a) shows the ^{1}H NMR spectrum of poly(DEGMEMA) with structural assignments where peak **a** and peak **b** are the vinyl end group in the polymer. Some oligomeric and low molecular weight polymers were observed in THF GPC spectrum (**Figure 3. 1 (b)**). From the MALDI-ToF mass spectrum, we can get a molecular weight distribution of the polymer and determine the end group structure of the polymer (**Figure 3. 1 (c)**). The spectrum shows a peak difference of 188.11 Da denoting the repeat units in the polymer chain, which agree with the molecular weight of DEGMEMA.

It is noteworthy that the signals characteristic of the vinyl bond in the

monomer and in the macromonomer are slightly different, i.e. 5.6-6.1 ppm and 5.5-6.2 ppm for monomer and macromonomer, respectively. This slight shift avoids any error in the molecular weight determination using NMR analyses (from traces of residual monomer).

$$M_{n,\ ^1H\ NMR} = \frac{I^{CH_2OCO}}{I^{CH=CH}} \times M_W^{OEGMEMA} \qquad (3.3)$$

Where $M_w^{OEGMEMA}$, I^{CH2OCO} and $I^{CH=CH}$ correspond to the molar masses of OEGMEMA, integral of the signal at 4.1 ppm (attributed to CH_2 in the adjacent position of ester group) and of vinyl group, respectively. The molecular weights calculated by ^{1}H NMR were in accordance with the molecular weights determined by MALDI-ToF MS. The plot of $1/DP_n$ versus the ratio of [CoBF]/[monomer] gives a linear fit with the gradient = the chain transfer constant of CoBF for each monomer (

Figure 3.2).

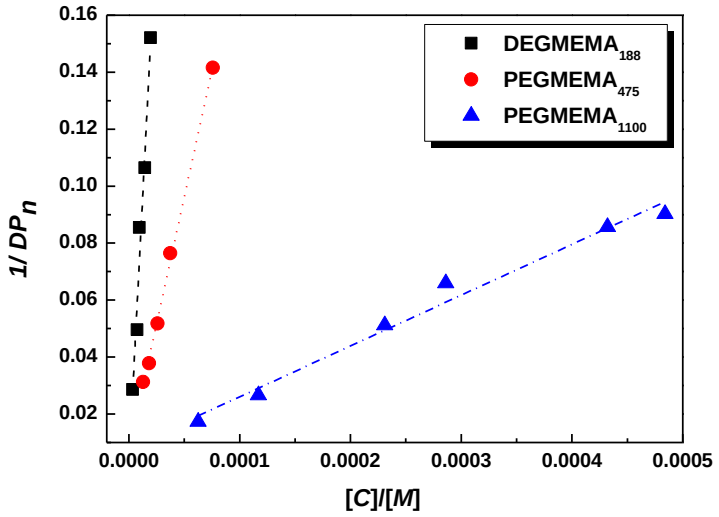

Figure 3.2 Mayo plot for chain transfer coefficient (C_S) of CoBF in CCTP of various oligo(ethylene glycol) methyl ether methacrylates.

3.4.1. CCTP of OEGMEMA

According to the Mayo equation, the chain transfer constants (C_S) of CoBF to DEGMEMA, $POEGMEMA_{475}$, and $POEGMEMA_{1100}$ have been calculated as 7600, 1800, and 180 (**Figure 3.2**), respectively. The chain transfer constants are for polymerization in acetonitrile at 70 ℃, which is important to note that the value is affected by the solvent in the case of catalytic chain transfer polymerization as highlighted by Davis *et.al*.[6, 51] Moreover, the C_S values decrease proportionally with the chain length of the side chain (in this case, oligo(ethylene glycol)). A similar result was obtained by Forster and co-workers[6, 52] for alkyl methacrylate (methyl methacrylate, ethyl methacrylate, and butyl methacrylate). The end-group fidelity of the polymers was well maintained as confirmed by MALDI-ToF for all monomers examined. Further still, the end group fidelity of the polymers are all still well maintained as the NMR peaks were all indicative of the presence of vinyl terminated polymers without any significant impurities (or species). Hence, catalytic chain transfer can be effectively utilized in polymerization of oligo ethylene methacrylate for molecular weight and end group control which will be vinyl termini. By varying the concentration of CoBF, it is possible to synthesize polymer with a DP_n from 7 to 50 in acetonitrile with a PDi less than 1.5.

As OEGMEMA and CoBF are water soluble, it was decided to investigate the

polymerization of these monomers in water at 80 ^{o}C. The addition of methanol (50/100 v/v %), as a co-solvent, was successful for the polymerization of OEGMEMA. **Table 3.1** shows the molecular weights and PDi obtained for the polymerizations of DEGMEMA and $OEGMEMA_{475}$ in methanol or methanol/water.

Table 3.1 CCTP of diethylene glycol methyl ether methacrylate and oligo(ethylene glycol) methyl ether methacrylate using feed and batch techniques

Run	Monomer	[CoBF]/[Monomer]	Technique	$M_{n,\,GPC}$ /g mol^{-1}	PDi
P1[a]	DEGMEMA	1.34×10^{-4}	Batch	1000	1.43
P2[a]	DEGMEMA	4.45×10^{-5}	Batch	1900	1.55
P3[a]	DEGMEMA	2.24×10^{-5}	Batch	2400	1.70
P4[b]	$OEGMEMA_{475}$	4.45×10^{-5}	Feed	3,200	1.68
P5[b]	$OEGMEMA_{475}$	8.90×10^{-5}	Feed	2,600	1.31
P6[b]	$OEGMEMA_{475}$	8.90×10^{-5}	Batch	2,300	1.85
P7[b]	$OEGMEMA_{475}$	4.45×10^{-5}	Batch	4,500	2.03

[a] Polymerization was carried out in methanol

[b] Polymerization was carried out in mixture solvents: methanol/water (50/100 v/v%)

Different concentrations of CoBF were employed for the CCTP of DEGMEMA and $OEGMEMA_{475}$. When the concentration of CoBF was high enough, the polymerization mixture mainly consisted of oligomers such as dimers, trimers, tetramers, and pentamers (P1), **Figure 3.3 (a)**. However, the amount of

oligomers decreased and that of polymers increased during the polymerization process when the concentration of CoBF decreased (P3), **Figure 3. 3 (b)**.

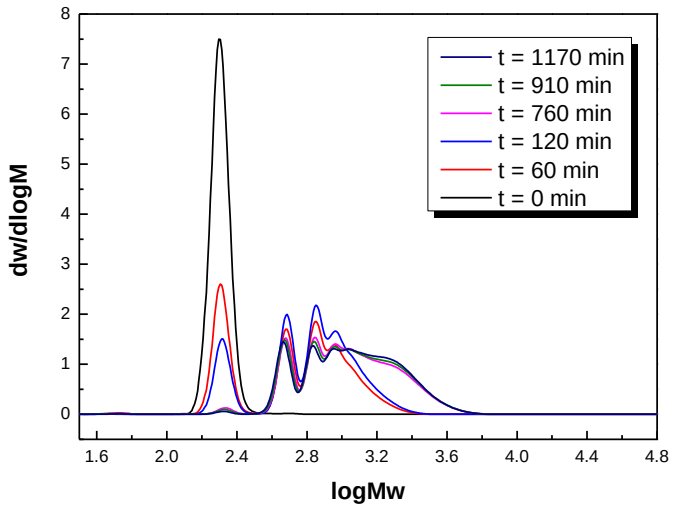

(a)

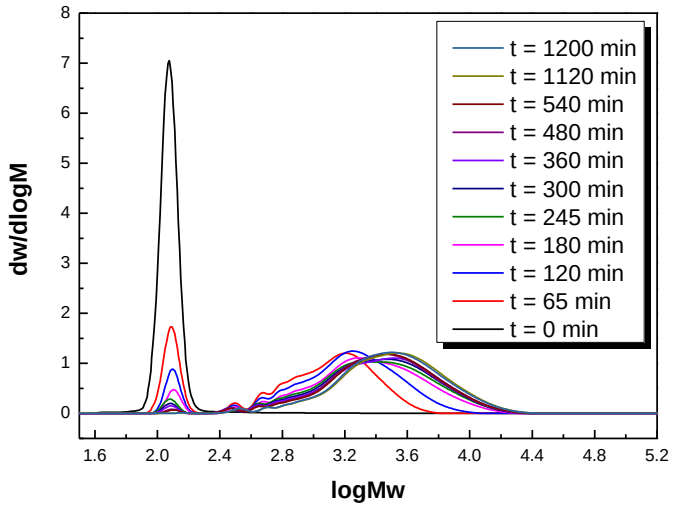

(b)

Figure 3.3 GPC spectra of poly(diethylene glycol) methyl ether methacrylate *via* CCTP at 80 ºC. (a) High ratio of [CoBF]/[Monomer] = 1.34×10^{-4}, P1. (b) Low ratio of [CoBF]/[Monomer] = 2.24×10^{-5}, P3.

These trends of molecular weight distribution during the CCTP of DEGMEMA indicated that the rate of chain transfer to monomer would be equivalent with the rate of propagation as the concentration of CoBF became high enough. Therefore, the ratio of dimers, trimers and other oligomers remained nearly constant during the polymerization if the concentration of CoBF was high enough. In contrast, using low concentration of CoBF, the oligomers generated by the chain transfer process at the beginning of the polymerization could be reinitiated by AIBN or cobalt hydride and then propagate to give polymers of high molecular weight. Therefore the amount of oligomers decreased and that of polymers increased in **Figure 3.3 (b)**.

For polymerization of OEGMEMA in water, poor control of the polymerization was observed as shown by a broadening of the molecular weight distributions. In comparison when acetonitrile was used as a solvent, narrower distributions were obtained. In addition, the molecular weights obtained in acetonitrile were usually lower than the molecular weights obtained in water, showing a better efficiency of transfer. It is possible that this difference in transfer efficiency could be attributed to the slight difference of temperature. However, Davis and Kukulj[53] and Heuts *et al.* [54] show that the efficiency of CoBF (or the transfer constant) is relatively unaffected by temperature. An increase in the temperature causes an increase in propagation rate (k_p) as well as an increase in transfer rate (k_{tr}), resulting in a null effect on the C_S ($C_S = k_{tr}/k_p$). Another possible

explanation is that the differences reported here are attributable to solvent effects. Haddleton and co-workers[9] have previously reported that CoBF can degrade in water at elevated temperatures (~ 70 ^{o}C) and that the kinetics of the degradation process are accelerated at low pH values. The degradation of CoBF causes a decrease in efficiency of the catalyst, inducing significant increases in the PDi during the polymerization. In the case of polymerization with CoBF in water, a semi-batch approach is necessary to keep the concentration of the CoBF constant thereby maintaining lower PDi.[9]

As expected, improved PDis and control of molecular weights were observed for polymers obtained using a feed methodology compared to a bath approach (**Table** 3. 1, P4-P7). In the batch approach, batch approach, the CoBF is degraded during the polymerization, resulting in a change of the [M]/[CoBF] ratio and a subsequent drift in the polymer chain distribution.

3.4.2. Copolymers of OEGMEMA

Inspired by the work of Lutz *et al.*[12, 55] and Ishizone *et al.*,[11] the copolymerization of oligo(ethylene glycol) methyl ether methacrylate ($OEGMEMA_{475}$) with diethylene glycol methyl ether methacrylate (DEGMEMA) using CCTP to yield thermoresponsive macromonomers was investigated. Copolymerizations were performed in acetonitrile at 70 ^{o}C for 14 hours. The feed compositions of these monomers were varied from 50/50 to 90/10 mol% of DEGEMMA/OEGMEMA. The final composition of these copolymers was

calculated from ^{1}H NMR using the ratio between –OCH_2 (ether group of OEG or DEG chains) and OCH_3 (from end-group). **Table 3.2** shows the final composition of each copolymer (F).

Table 3.2 Copolymerization results of diethylene glycol methyl ether methacrylate (DEGEMEMA) with oligo(ethylene glycol) methyl ether methacrylate ($OEGMEMA_{475}$). M_n was calculated by GPC and NMR. Composition of polymer (F) was calculated from ^{1}H NMR

Run	*f* (Initial feed)	F (Final composition)	$M_{n,\,GPC}$/ gmol^{-1}	$M_{n,\,NMR}$/ g mol^{-1}
CP1	50:50	48:52	2800	3000
CP2	70:30	69:31	2600	2700
CP3	80:20	76:24	2600	3200
CP4	90:10	92:8	3000	3400

It is interesting to note that the monomer feed ratio and the final copolymer composition do not differ significantly at low conversion indicative that the reactivity ratios of the monomers are similar, implying that compositional drift is not a major factor in the reactions. The presence of composition drift during copolymerization can result in the synthesis of gradient copolymers, when a living radical polymerization is used,[56] or in the synthesis of heterogeneous copolymers, when a non-living free radical polymerization is employed (such as CCTP).[57]

The copolymer composition of DEGMEMA and OEGMEMA allows tuning of the lower critical solution temperatures (LCSTs) from 16 ^{o}C to 95 ^{o}C as determined by turbidimetry measurements. **Figure 3.4** shows the evolution of

LCST with copolymer composition. An increase of DEGMEMA in the copolymers causes a decrease in the LCST. By varying the composition of the respective monomers, the LCST can be tailored easily to the desired temperature. For all copolymers, a very sharp transition (when heated) was observed (**Figure 3. 4**). A relatively small hysteresis (5 ^{o}C) on heating and cooling was observed, comparable with the hysteresis obtained for copolymers synthesized by ATRP.[12]

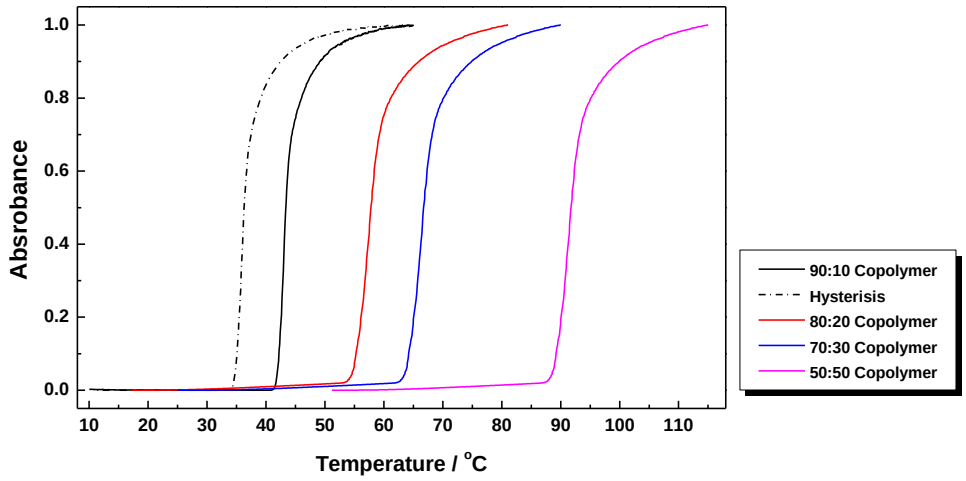

Figure 3.4 UV-Vis plot of various copolymers to show the lower critical solution behavior (LCST) in water

3.4.3. Thiol-ene "click" of OEGMEMA oligomers

Catalytic chain transfer polymerization yields oligomers with terminal vinyl end-groups at high efficiency (almost 100%). This vinyl-functionalization is not possible to achieve by other common radical polymerization techniques, such as ATRP,[58] NMP[59] or RAFT.[60, 61] Since the introduction of the ''click'' concept by

Sharpless *et al.*,[29] there have been a number of efficient conjugation reactions designated as ‘‘click’’ reactions. Recently, Hawker et al.[35] reintroduced an old but very efficient reaction, thiol-ene reactions, as a potential ‘‘click’’ reaction. Thiol-ene reactions embrace two types of mechanism: (i) anti-Markovnikov radical addition and (ii) base or nucleophile catalyzed Michael addition reaction.[29, 31, 35, 41, 45, 62-68]

Thiol-ene reactions can be performed in different solvents and are tolerant of a large range of functionalities. Recent work has been performed on the nature of thiol-ene reaction conditions by Davis and Haddleton and Lowe and co-workers[63, 64] where it was reported that primary amines are more effective catalysts than secondary or tertiary amines, as well as significant reductions in the reactivity of methacrylates attributable to a combination of steric hindrance and inductive effects. The structure of the thiol compound also affects the efficiency of thiol-ene reactions, for example, alkyl thiols are less reactive than functional thiols, such as 2-mercaptoethanol (2-ME) or 1-thioglycerol (TG). However, the previously reported studies were focused mainly on small molecules (monomers) or very short oligomers (dimers, trimers). In this current work it was necessary to optimize the thiol-ene Michael addition, as the “ene” components were methacrylate polymers to ensure high conversion and purity of the final product.

Poly(DEGMEMA) polymer was used to optimize the thiol-ene Michael addition of different kinds of thiols. The efficacy of the catalyst used in these reactions, either phosphine or amine, was then examined. It has been highlighted

previously that phosphine (e.g. dimethyl phenyl phosphine) is an effective catalyst[32, 63, 64] at concentrations less than 0.05 mol% of the ‘‘ene’’ to prevent the side reaction of the conjugation of DMPP to the vinyl bond.[63] In this study, thiol-ene Michael reactions were initially performed and catalyzed by a combination of DMPP and TEA (the concentration of DMPP was maintained at less than 0.1 mol%), in which side reactions of DMPP conjugated to the vinyl end-group of poly(DEGMEMA) were observed (**Figure** 3. 5-**Figure** 3. 10).

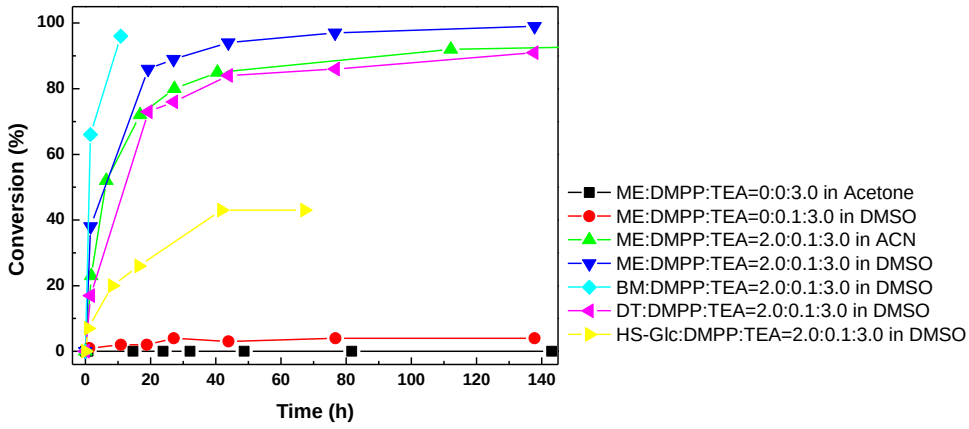

Figure 3.5 Conversion versus time plot for the thiol-Michael addition of poly(DEGMEMA) with different thiols in the presence of DMPP/TEA in different solvents. Conversion values were calculated by ^{1}H NMR following the disappearance of the vinyl group (5.6 ppm - 6.1 ppm)

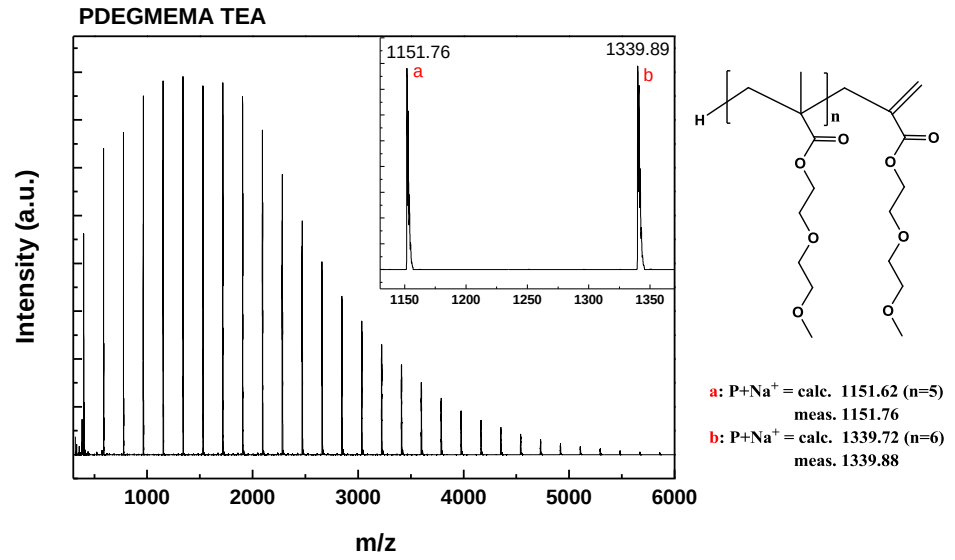

Figure 3.6 MALDI-ToF MS of poly(DEGMEMA) in the presence of TEA. There was no TEA adduct observed in the MALDI-ToF MS.

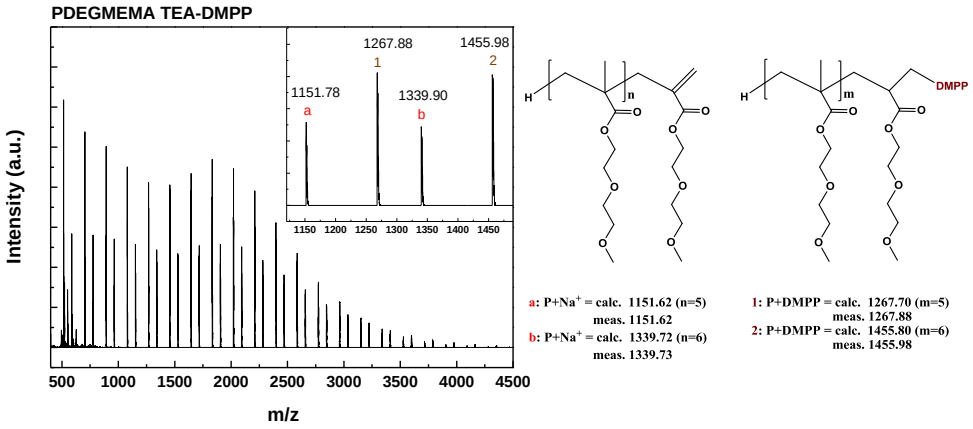

Figure 3.7 MALDI-ToF MS of poly(DEGMEMA) in the presence of TEA and DMPP. There was no TEA adduct detected in the MALDI-ToF MS whereas the DMPP adducts were clearly visible.

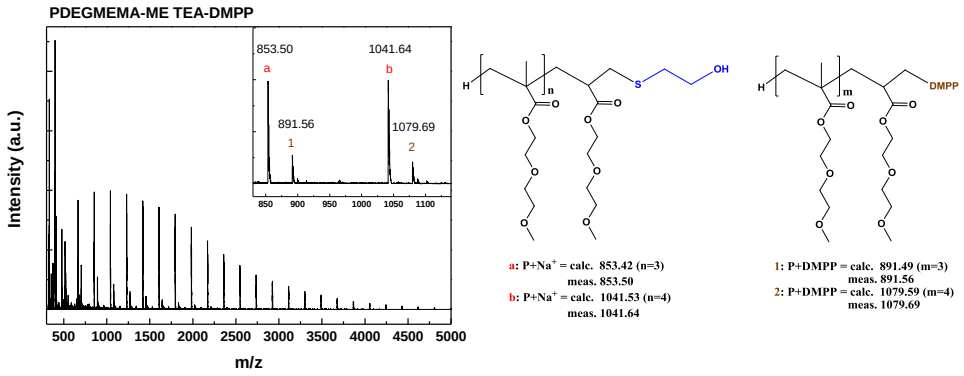

Figure 3.8 MALDI-ToF MS of poly(DEGMEMA) reacted with 2-mercaptoethanol (2-ME) in the presence of TEA and DMPP. The small peak corresponds to the DMPP adduct although it did not give a quantitative comparison with the product.

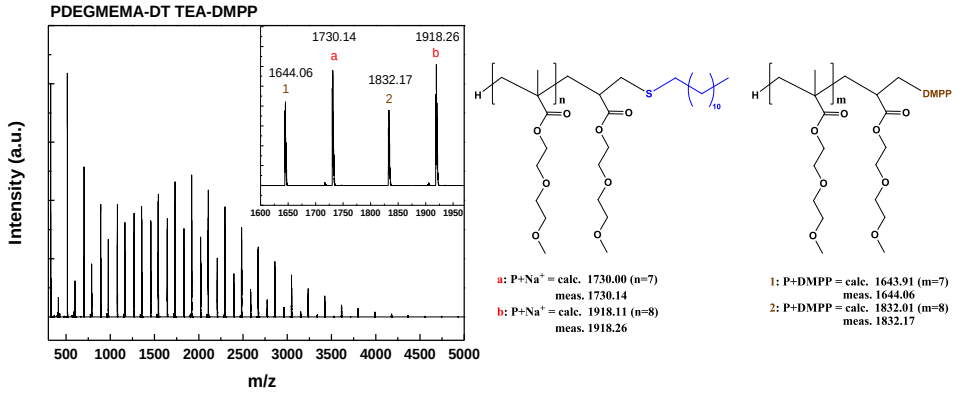

Figure 3.9 MALDI-ToF MS of poly(DEGMEMA) reacted with 1-dodecanthiol (DT) in the presence of TEA and DMPP. The small peak corresponds to the DMPP adduct although it did not give a quantitative comparison.

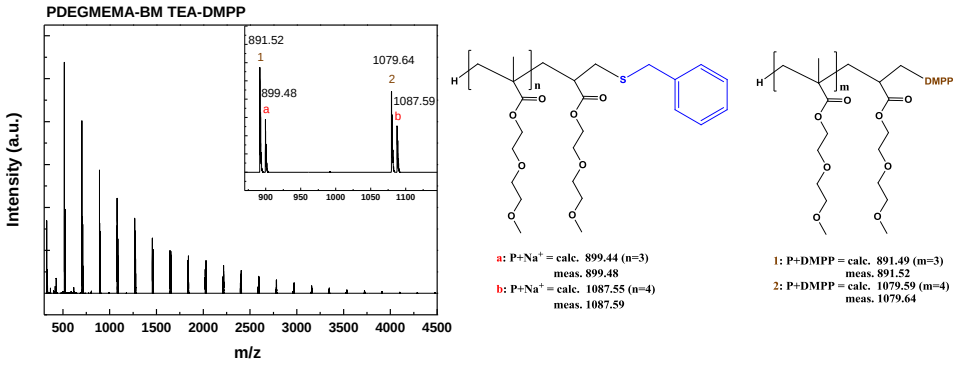

Figure 3.10 MALDI-ToF MS of poly(DEGMEMA) reacted with benzyl mercaptan (BM) in the presence of TEA and DMPP. The large peak corresponds to the DMPP adduct although it did not give a quantitative comparison with the product.

In order to evaluate whether the highly reactive phosphine compound or triethylamine can react with the vinyl group (methacrylate or acrylate) resulting in the formation of side products, we initially performed two blank reactions. One reaction was poly(DEGMEMA) mixed with 3.0 eq. of triethylamine in acetone. Another reaction was poly(DEGMEMA) in the presence of 3.0 eq. of triethylamine and 0.1 eq. of dimethylphenylphosphine (DMPP) in DMSO. After 5 days, the presence of vinyl group was monitored by ^{1}H NMR and it was found that 0% and 4% of vinyl groups were reacted, respectively, **Figure 3.5**. These reactions were then characterized using MALDI-ToF MS. There were no TEA adducts detected in **Figure 3.6** and **Figure 3.7**. However, the DMPP adducts were clearly visible in **Figure 3.7**. According to the **Figure 3.5**, it was also evident that 2-mercaptoethanol (2-ME) and benzyl mercaptan (BM) relatively faster than 1-dodecanthiol (DT) and 1-thiol-β-D-glucose sodium salt (HS-Glc).

The final products of the reaction of poly(DEGMEMA) with different thiols in the presence of TEA and DMPP were characterized using MALDI-ToF MS. Both the thiol-ene Michael products and DMPP conjugated products were observed in **Figure 3. 8**-**Figure 3. 10**. It was important to be noted that MALDI-TOF MS did not provide quantitative information due to potentially different ionization efficiencies of each compound.

Subsequently, to minimize the formation of by-products, it was decided to use amine catalysts. Two different amines were compared: triethylamine (TEA) (tertiary amine) and hexylamine (HA) (primary amine). The TEA catalyst ensured a full conversion of the vinyl end-group of poly(DEGMEMA), without the formation of by-products, when the reaction was performed with 2-mercaptoethanol at ambient temperature. The detailed characterization of the ‘‘clicked’’ polymers was performed using ^{1}H NMR, GPC as well as MALDI-ToF MS. The characterization data are presented in **Figure 3.11**.

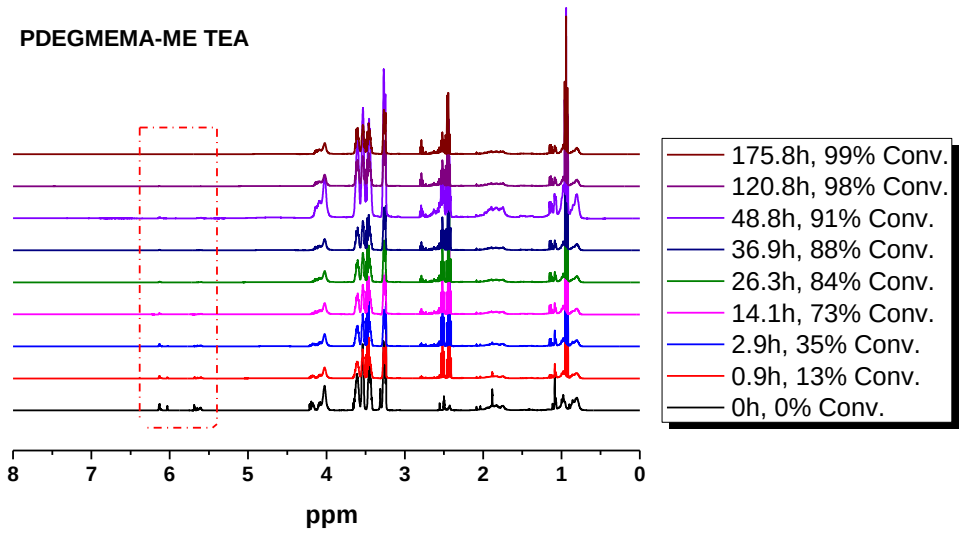

(a)

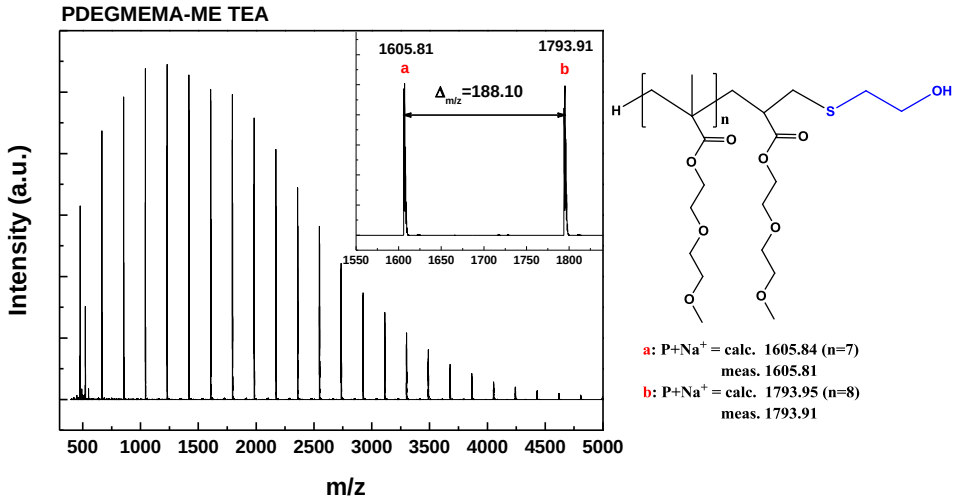

(b)

Figure 3.11 ^{1}H NMR spectrum (a) and MALDI-ToF MS (b) of 2-mercaptoethanol (2-ME) conjugated poly(diethylene glycol) methyl ether methacrylate catalyzed with 1.8 eq. triethylamine in DMSO-d_6.

Figure 3.11 (a) showed the ^{1}H NMR spectra traces collected during polymer functionalization. The concentration of vinyl group (5.6 ppm - 6.1 ppm) decreased over the reaction indicating the Michael addition of a thiol to the polymer. MALDI-TOF analysis (**Figure 3.11 (b)**) confirmed successfully polymer post-functionalized with 2-Mercaptoethanol *via* thiol-ene click chemistry.

In order to establish the best solvent, the thiol-ene reactions were performed in a range of solvents: acetone, acetonitrile, and dimethyl sulfoxide (DMSO). **Figure 3.12** showed the evolution of the vinyl bond conversion versus time in these different solvents for the thiol-ene addition of 2-mercaptoethanol onto vinyl terminated poly(DEGMEMA) at ambient temperature, catalyzed by triethylamine. The following order of reactivity was established: DMSO > acetonitrile > acetone. The reactions carried out in DMSO reached a very high yield 90% after 2 days using 1.8 eq. or 3.0 eq. of TEA and the yields could be also reached above 50-70% in acetonitrile, whereas in acetone, yields > 20% could not be achieved. It was well known that polar solvents, such as DMSO, were good solvents for nucleophilic reactions. This could be explained by the high polarity of DMSO and ACN that allows a better stabilization of thiolate ion, and favors its formation.[62-64]

However, the efficiency of this TEA-catalyzed reaction dropped when an aliphatic or aromatic thiol were used, such as 1-dodecanthiol and benzyl mercaptan. TEA can only drive the reaction to a ca. 70% and 60% after 3 days with benzyl mercaptan and 1-dodecanthiol at ambient temperature, respectively

(**Figure 3.12**). Quantitative conversion could only be attained when the reaction was performed at 40 ^{o}C for 14 hours. In order to accelerate the rate and increase the conversion of the thiol-Michael addition reaction, hexylamine (HA) was used as a catalyst.

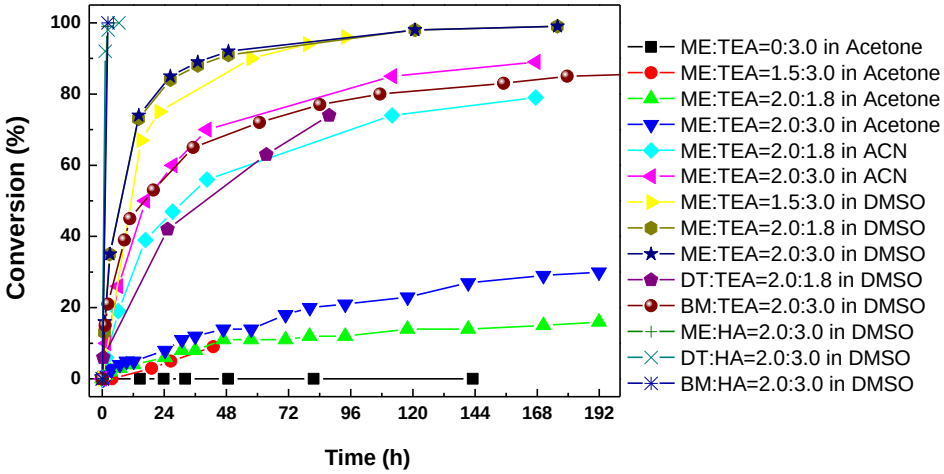

Figure 3.12 Conversion versus time plot for the thiol-Michael addition of poly(diethylene glycol) methyl ether methacrylate with different thiols in the presence of triethylamine or hexylamine in different solvents in order to study the solvents effect. Conversion values were calculated by ^{1}H NMR following the disappearance of the vinyl group (5.6 ppm - 6.1 ppm)

Thus, it was possible to functionalize different homopolymers of DEGMEMA and $OEGMEMA_{475}$ with different functional thiols, such as benzyl mercaptan (BM), 1-dodecanethiol (DT), and 2-mercaptoethanol (2-ME) with a high efficiency. The detailed characterization of the ‘‘clicked’’ polymers was performed using ^{1}H NMR, GPC as well as MALDI-ToF MS. The characterization data are presented in **Figure 3.13**, **Figure 3.14** and **Figure 3.15** for

2-mercaptoethanol (2-ME), 1-dodecanthiol (DT) and benzyl mercaptan (BM), respectively. A range of commercially available thiols were used which demonstrated the versatility of the thiol-ene click reaction.

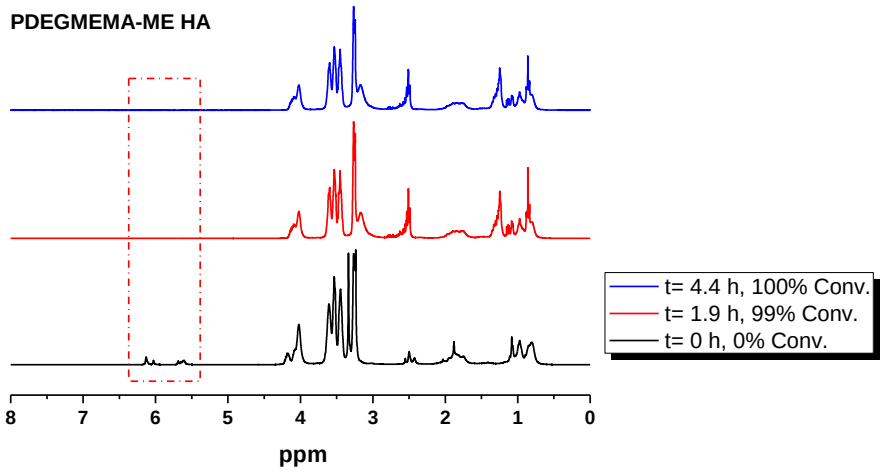

(a)

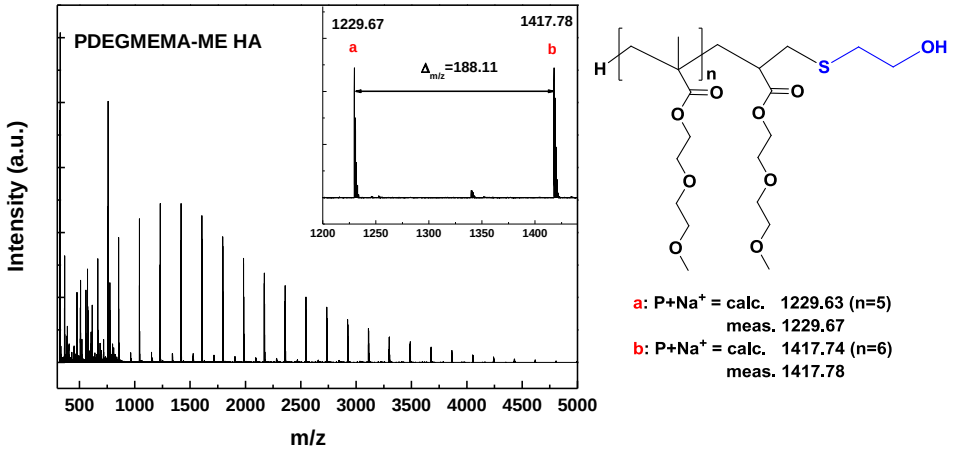

(b)

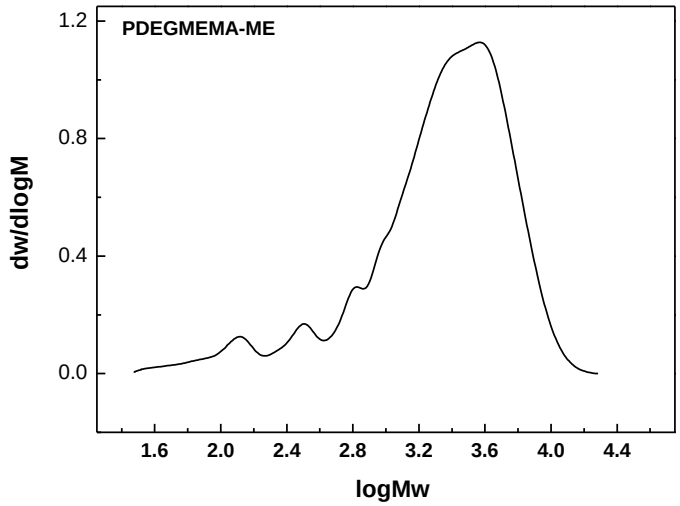

(c)

Figure 3.13 ^{1}H NMR spectrum (a), MALDI-ToF MS (b) and GPC (c) of 2-mercaptoethanol (2-ME) conjugated poly(diethylene glycol) methyl ether methacrylate catalyzed with hexylamine.

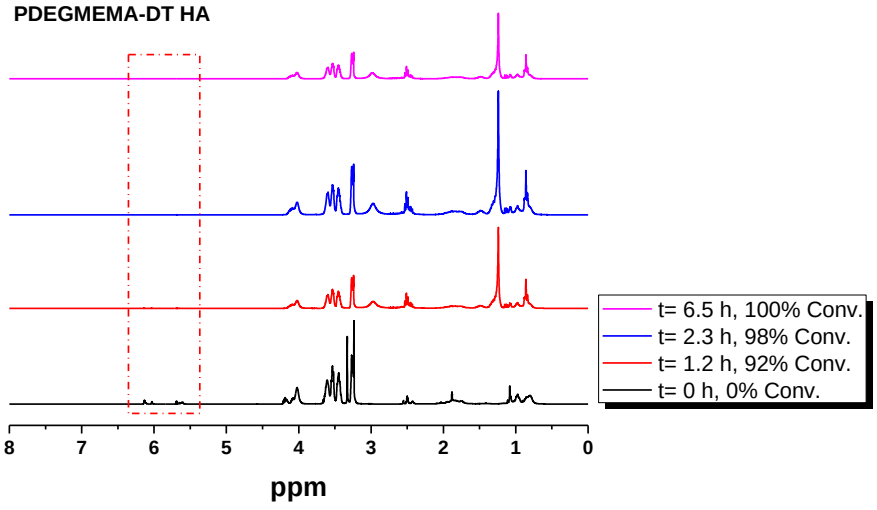

(a)

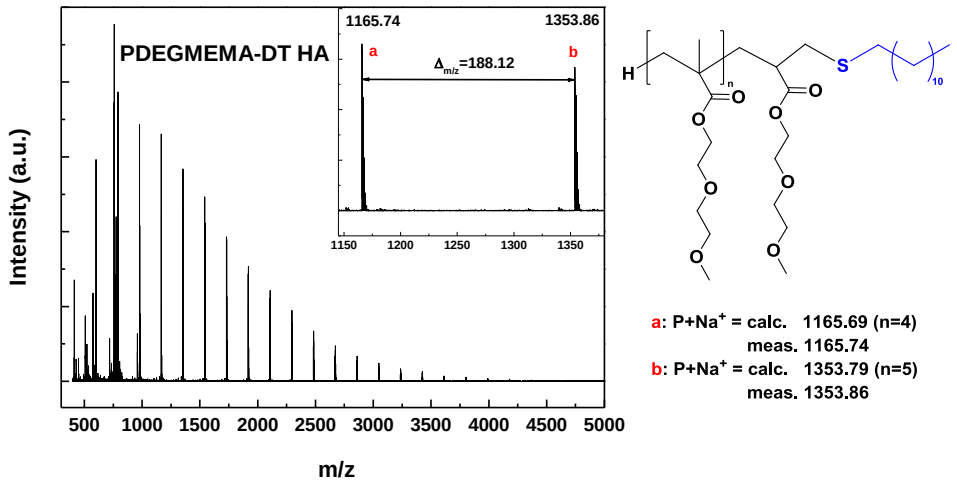

(b)

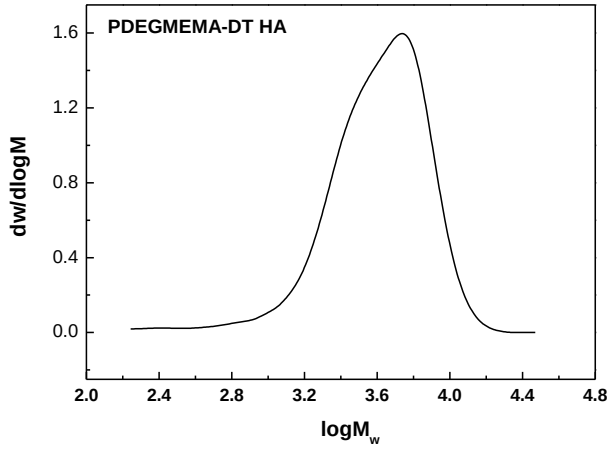

(c)

Figure 3.14 ^{1}H NMR spectrum (a), MALDI-ToF MS (b) and GPC (c) of 1-dodecanethiol (DT) conjugated poly(diethylene glycol) methyl ether methacrylate catalyzed with hexylamine

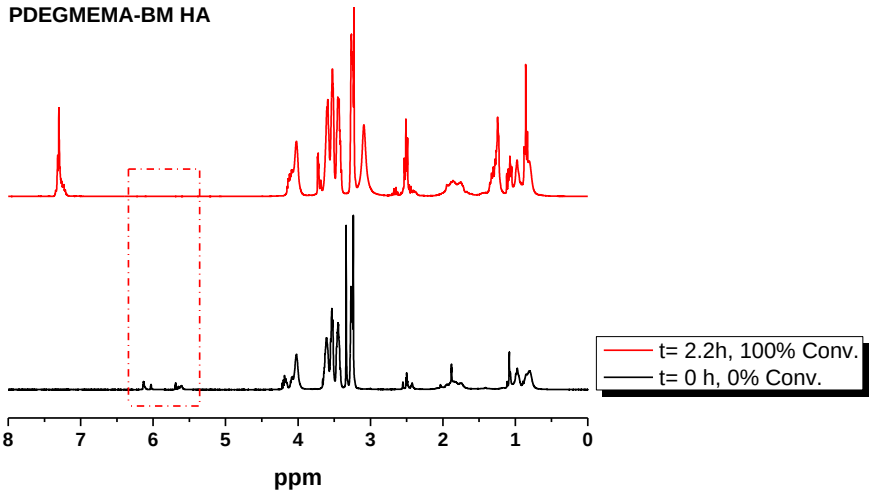
PDEGMEMA-BM HA
t= 2.2h, 100% Conv.
t= 0 h, 0% Conv.
8
7
6
5
4
3
2
1
0
ppm

(a)

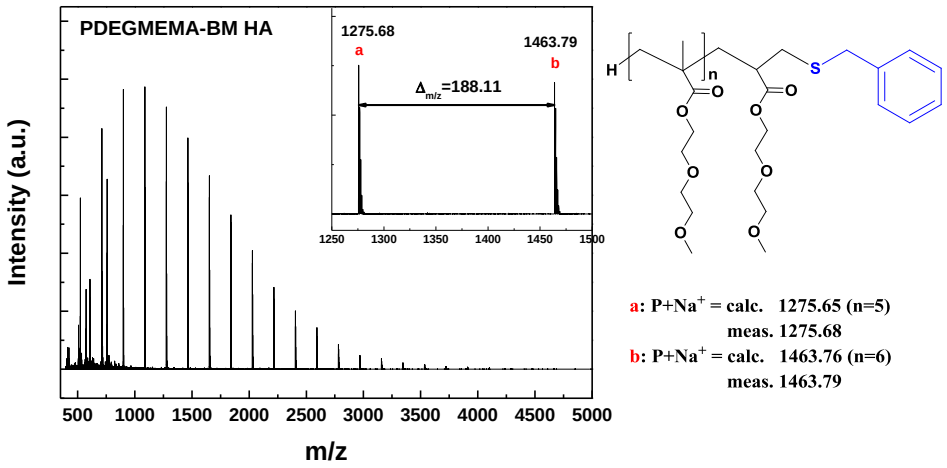
PDEGMEMA-BM HA
1275.68
a
1463.79
b
Δm/z=188.11
1250
1300
1350
1400
1450
1500
Intensity (a.u.)
500
1000
1500
2000
2500
3000
3500
4000
4500
5000
m/z
H
n
S
O
a: P+Na+ = calc. 1275.65 (n=5)
meas. 1275.68
b: P+Na+ = calc. 1463.76 (n=6)
meas. 1463.79

(b)

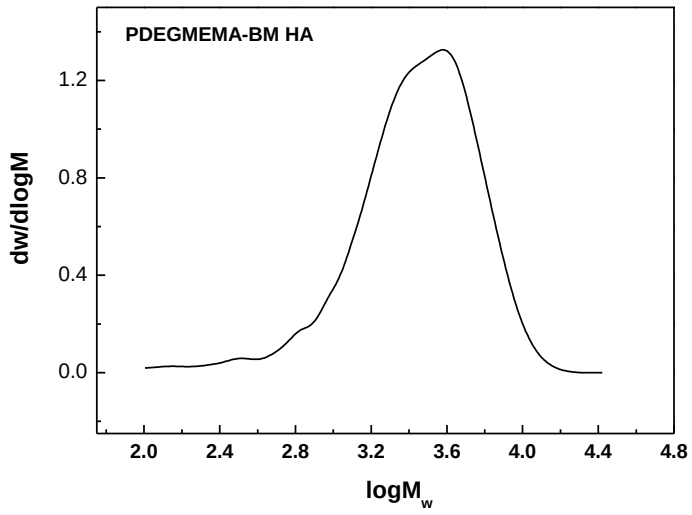

(c)

Figure 3.15 ^{1}H NMR spectrum (a), MALDI-ToF MS (b) and GPC (c) of benzyl mercaptan (BM) conjugated poly(diethylene glycol) methyl ether methacrylate catalyzed with hexylamine.

3.4.4. Catalytic chain transfer copolymerization and thiol-ene modification

Further thiol-ene 'click' chemistry was performed on the homopolymers of DEGMEMA and copolymers of $OEGMEMA_{475}$ to investigate the effect of different end-groups on their thermoresponsive behavior (LCST), **Figure 3.16**.

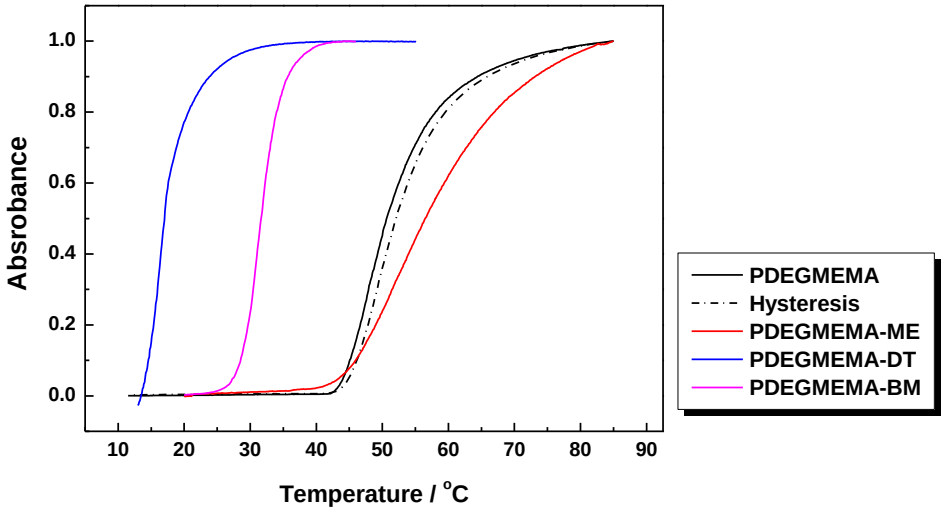

Figure 3.16 UV-Vis plot of poly(DEGMEMA) and various post-functionalization by thiol-Michael addition to show the lower critical solution behavior (LCST) in water

Recently, Theato's group investigated copolymers made with various RAFT agents giving rise to a range of end-group functionalities and they investigated the influence of end-groups on LCST behavior.[69] In this study, homopolymers and copolymers functionalized by 1-dodecanethiol (DT), benzyl mercaptan (BM) and 2-mercaptoethanol (2-ME) gave significantly different LCST temperatures attributable to hydrophobic and hydrophilic effects, **Table 3.3**.

Table 3.3 List of polymers synthesized in this study using CCTP and further modification by thiol-Michael addition to give a LCST library[a]

Run	Structure	$M_{n,GPC}$ g.mol^{-1}	PDi	LCST / ℃
A1	DEGMEMA	2500	1.53	47
A2	DEGMEMA - ME	1100	2.91	52
A3	DEGMEMA - DT	3200	1.50	16
A4	DEGMEMA - BM	2200	1.61	32
A5	PEGMEMA	6000	1.40	>110
CP1	DEGMEMA-PEGMEMA (50:50)	2800	1.55	95
CP2	DEGMEMA-PEGMEMA (70:30)	2600	1.45	65
CP3	DEGMEMA-PEGMEMA (80:20)	2600	1.56	58
CP4	DEGMEMA-PEGMEMA (90:10)	3000	1.52	43
CP5	DEGMEMA-PEGMEMA (90:10) - DT	3100	1.56	35
CP6	DEGMEMA-PEGMEMA (90:10) - ME	3050	1.54	42

[a] A2-A4 were obtained after thiol-ene modification with 2-mercaptoethanol (2-ME), 1-dodecanethiol (DT) and benzyl mercaptan (BM). CP5 and CP6 were obtained after thiol-ene modification with 1-dodecanethiol and 2-mercaptoethanol.

As expected, the thiol-ene ‘‘click’’ reaction of the hydrophobic end-group caused an LCST decreased while ‘‘click’’ reaction of the hydrophilic end-group lead the LCST to increased. Catalytic chain transfer polymerization of oligo (ethylene glycol) methyl ether methacrylate and functionalization with thiol molecules has allowed straight forward synthesis of thermoresponsive polymers

with LCST value which can be easily altered from range 16-95 ℃. The advantage of this technique to other controlled radical polymerization was that CCTP can be easily scale up industrially compare to RAFT and ATRP at the moment. Furthermore, the wide variety of thiol molecules that could be clicked onto the polymer gave massive option depending on the demand and requirement of the materials.

3.5. Conclusions

In conclusion, we reported on the compatibility and kinetic of catalytic chain transfer polymerization of oligo ethylene glycol methyl ether methacrylate using CoBF as catalyst. The chain transfer values were measured to be similar with other (larger) methacrylates and also exhibited the same trends with the ester chain length. Moreover, copolymers of $OEGMEMA_{475}$ and DEGMEMA have been synthesized and characterized in terms of thermal behavior and the lower critical solution temperature (LCST) in water. The terminal vinyl functionality of the oligomers has been exploited in thiol-ene reactions to make a range of functional oligomers. Thus, CCTP coupled thiol-ene click reaction was a successful synthetic approach to several useful kinds of advanced polymeric materials. It should be noted that effects of solvents and types of thiols have a great role on this reaction and should be selected with care based on these optimization reactions.

3.6. References

1. A. Gridnev, *J. Polym. Sci., Part A: Polym. Chem.*, 2000, **38**, 1753-1766.

2. A. A. Gridnev and S. D. Ittel, *Chem. Rev.*, 2001, **101**, 3611-3659.

3. J. P. A. Heuts, G. E. Roberts and J. D. Biasutti, *Aust. J. Chem.*, 2002, **55**, 381-398.

4. T. P. Davis, D. M. Haddleton and S. N. Richards, *J. Macromol. Sci., Rev. Macromol. Chem. Phys.*, 1994, **C34**, 243-324.

5. T. P. Davis, D. Kukulj, D. M. Haddleton and D. R. Maloney, *Trends Polym. Sci.*, 1995, **3**, 365-373.

6. J. P. A. Heuts, D. J. Forster and T. P. Davis, *Macromolecules*, 1999, **32**, 3907-3912.

7. C. Kowollik and T. P. Davis, *J. Polym. Sci., Part A: Polym. Chem.*, 2000, **38**, 3303-3312.

8. A. Debuigne, R. Poli, C. Jerome, R. Jerome and C. Detrembleur, *Prog. Polym. Sci.*, 2009, **34**, 211-239.

9. D. M. Haddleton, E. Depaquis, E. J. Kelly, D. Kukulj, S. R. Morsley, S. A. F. Bon, M. D. Eason and A. G. Steward, *J. Polym. Sci., Part A: Polym. Chem.*, 2001, **39**, 2378-2384.

10. M. E. Thomson, N. M. B. Smeets, J. P. A. Heuts, J. Meuldijk and M. F. Cunningham, *Macromolecules*, 2010, **43**, 5647-5658.

11. S. Han, M. Hagiwara and T. Ishizone, *Macromolecules*, 2003, **36**, 8312-8319.

12. J.-F. Lutz and A. Hoth, *Macromolecules*, 2005, **39**, 893-896.

13. C. Boyer, M. R. Whittaker, M. Luzon and T. P. Davis, *Macromolecules*, 2009, **42**, 6917-6926.

14. C. Boyer, M. R. Whittaker, K. Chuah, J. Q. Liu and T. P. Davis, *Langmuir*, 2010, **26**, 2721-2730.

15. S. A. Meenach, K. W. Anderson and J. Z. Hilt, *J. Polym. Sci., Part A: Polym. Chem.*, 2010, **48**, 3229-3235.

16. M. Chanana, S. Jahn, R. Georgieva, J.-F. o. Lutz, H. Bäumler and D. Wang, *Chem. Mater.*, 2009, **21**, 1906-1914.

17. S. Kessel, S. Schmidt, R. Müller, E. Wischerhoff, A. Laschewsky, J.-F. o. Lutz, K. Uhlig, A. Lankenau, C. Duschl and A. Fery, *Langmuir*, 2009, **26**, 3462-3467.

18. H. M. Zareie, C. Boyer, V. Bulmus, E. Nateghi and T. P. Davis, *ACS Nano*, 2008, **2**, 757-765.

19. E. Wischerhoff, S. Glatzel, K. Uhlig, A. Lankenau, J.-F. o. Lutz and A. Laschewsky, *Langmuir*, 2009, **25**, 5949-5956.

20. E. Wischerhoff, N. Badi, J.-F. Lutz and A. Laschewsky, *Soft Matter*, 2010, **6**, 705-713.

21. Z. Zarafshani, T. Obata and J.-F. o. Lutz, *Biomacromolecules*, 2010, **11**, 2130-2135.

22. C. R. Becer, S. Hahn, M. W. M. Fijten, H. M. L. Thijs, R. Hoogenboom and U. S. Schubert, *J. Polym. Sci., Part A: Polym. Chem.*, 2008, **46**, 7138-7147.

23. T. M. Eggenhuisen, C. R. Becer, M. W. M. Fijten, R. Eckardt, R. Hoogenboom and U. S. Schubert, *Macromolecules*, 2008, **41**, 5132-5140.

24. H. M. L. Thijs, C. R. Becer, C. Guerrero-Sanchez, D. Fournier, R. Hoogenboom and U. S. Schubert, *J. Mater. Chem.*, 2007, **17**, 4864-4871.

25. C. Weber, C. R. Becer, W. Guenther, R. Hoogenboom and U. S. Schubert, *Macromolecules*, 2010, **43**, 160-167.

26. C. Weber, C. R. Becer, R. Hoogenboom and U. S. Schubertt, *Macromolecules*, 2009, **42**, 2965-2971.

27. C. R. Becer, K. Kokado, C. Weber, A. Can, Y. Chujo and U. S. Schubert, *J. Polym. Sci., Part A: Polym. Chem.*, 2010, **48**, 1278-1286.

28. H. Dong and K. Matyjaszewski, *Macromolecules*, 2010, **43**, 4623-4628.

29. H. C. Kolb, M. G. Finn and K. B. Sharpless, *Angew. Chem. Int. Ed.*, 2001, **40**, 2004-2021.

30. R. K. Iha, K. L. Wooley, A. M. Nystrm, D. J. Burke, M. J. Kade and C. J. Hawker, *Chem. Rev.*, 2009, **109**, 5620-5686.

31. C. R. Becer, R. Hoogenboom and U. S. Schubert, *Angew. Chem. Int. Ed.*, 2009, **48**, 4900-4908.

32. J. W. Chan, B. Yu, C. E. Hoyle and A. B. Lowe, *Polymer*, 2009, **50**, 3158-3168.

33. L. Nurmi, J. Lindqvist, R. Randev, J. Syrett and D. M. Haddleton, *Chem. Commun.*, 2009, 2727-2729.

34. B. Yu, J. W. Chan, C. E. Hoyle and A. B. Lowe, *J. Polym. Sci., Part A: Polym. Chem.*, 2009, **47**, 3544-3557.

35. L. M. Campos, K. L. Killops, R. Sakai, J. M. J. Paulusse, D. Damiron, E. Drockenmuller, B. W. Messmore and C. J. Hawker, *Macromolecules*, 2008, **41**, 7063-7070.

36. D. Valade, C. Boyer, T. P. Davis and V. Bulmus, *Aust. J. Chem.*, 2009, **62**, 1344-1350.

37. C. Boyer, A. Granville, T. P. Davis and V. Bulmus, *J. Polym. Sci., Part A Polym. Chem.*, 2009, **47**, 3773-3794.

38. C. Boyer and T. P. Davis, *Chem. Commun.*, 2009, 6029-6031.

39. G. J. Chen, S. Amajjahe and M. H. Stenzel, *Chem. Commun.*, 2009, **10**, 1198-1200.

40. A. B. Lowe, C. E. Hoyle and C. N. Bowman, *J. Mater. Sci.*, 2010, **20**, 4745 - 4750.

41. A. B. Lowe, *Polym. Chem.*, 2010, **1**, 17-36.

42. M. W. Jones, G. Mantovani, S. M. Ryan, X. Wang, D. J. Brayden and D. M. Haddleton, *Chem. Commun.*, 2009, 5272-5274.

43. N. Gupta, B. F. Lin, L. M. Campos, M. D. Dimitriou, S. T. Hikita, N. D.

Treat, M. V. Tirrell, D. O. Clegg, E. J. Kramer and C. J. Hawker, *Nat. Chem.*, 2010, **2**, 138-145.

44. C. J. Hawker and K. L. Wooley, *Science*, 2005, **309**, 1200-1205.

45. M. J. Kade, D. J. Burke and C. J. Hawker, *J. Polym. Sci., Part A: Polym. Chem.*, 2010, **48**, 743-750.

46. K. L. Killops, L. M. Campos and C. J. Hawker, *J. Am. Chem. Soc.*, 2008, **130**, 5062-5064.

47. F. A. Leibfarth, M. Kang, M. Ham, J. Kim, L. M. Campos, N. Gupta, B. Moon and C. J. Hawker, *Nat. Chem.*, 2010, **2**, 207-212.

48. A. Bakac, M. E. Brynildson and J. H. Espenson, *Inorg. Chem.*, 1986, **25**, 4108-4114.

49. A. Bakac and J. H. Espenson, *J. Am. Chem. Soc.*, 1984, **106**, 5197-5202.

50. A. A. Gridnev, *J. Polym. Sci., Part A: Polym. Chem.*, 2002, **40**, 1366-1376.

51. D. J. Forster, J. P. A. Heuts, F. P. Lucien and T. P. Davis, *Macromolecules*, 1999, **32**, 5514-5518.

52. R. A. Sanayei and K. F. Odriscoll, *J. Macromol. Sci., Chem.*, 1989, **A26**, 1137-1149.

53. T. P. Davis and D. Kukuly, *Macromol. Chem. Phys,*, 1998, **199**, 1697-1708.

54. J. P. A. Heuts, L. M. Muratore and T. P. Davis, *Macromol. Chem. Phys.*, 2000, **201**, 2780-2788.

55. J.-F. Lutz, Ö. Akdemir and A. Hoth, *J. Am. Chem. Soc.*, 2006, **128**, 13046-13047.

56. S. Harrison, F. Ercole and B. Muir, *Polym. Chem.*, 2010, **1**, 326 - 332.

57. J. P. A. Heuts, D. Kukulj, D. J. Forster and T. P. Davis, *Macromolecules*, 1998, **31**, 2894-2905.

58. J. F. Lutz and K. Matyjaszewski, *J. Polym. Sci., Part A: Polym. Chem.*, 2005, **43**, 897-910.

59. C. J. Hawker, A. W. Bosman and E. Harth, *Chem. Rev.*, 2001, **101**, 3661-3688.

60. C. Boyer, V. Bulmus, T. P. Davis, V. Ladmiral, J. Q. Liu and S. Perrier, *Chem. Rev.*, 2009, **109**, 5402-5436.

61. C. Boyer, M. H. Stenzel and T. P. Davis, *J. Polym. Sci., Part A: Polym. Chem.*, 2011, **49**, 551-595.

62. G. Z. Li and D. M. Haddleton, *Polym. Prepr. (Am. Chem. Soc., Div. Polym. Chem.)*, 2010, **51**, 555-556.

63. G. Z. Li, R. K. Randev, A. H. Soeriyadi, G. Rees, C. Boyer, Z. Tong, T. P. Davis, C. R. Becer and D. M. Haddleton, *Polym. Chem.*, 2010, **1**, 1196-1204.

64. J. W. Chan, C. E. Hoyle, A. B. Lowe and M. Bowman, *Macromolecules*, 2010, **43**, 6381-6388.

65. C. Boyer, C. Loubat, J. J. Robin and B. Boutevin, *J. Polym. Sci., Part A: Polym. Chem.*, 2004, **42**, 5146-5160.

66. C. Boyer, G. Boutevin, J. J. Robin and B. Boutevin, *Polymer*, 2004, **45**, 7863-7876.

67. B. Boutevin, *J. Polym. Sci., Part A: Polym. Chem.*, 2000, **38**, 3235-3243.

68. C. Boyer, G. Boutevin, J. J. Robin and B. Boutevin, *Macromol. Chem. Phys.*, 2004, **205**, 645-655.

69. P. J. Roth, F. D. Jochum, F. R. Forst, R. Zentel and P. Theato, *Macromolecules*, 2010, **43**, 4638-4645.

Chapter 4. Synthesis of functionalized Glycopolymers homopolymers and copolymers *via* ATRP, ROP and CuAAC click reactions

4.1. Introduction

Natural polysaccharides and synthetic glycopolymers have attracted increasing interest in recently years. This interest originates from carbohydrates involvement in many complex biochemical and physiological process in biological and life sciences. The carbohydrate units not only perform specific biological functions of cells but also have an important role in cell-cell recognition systems, cell-protein interactions, host immune defense and immunoregulation.[1-12] Generally these carbohydrate-binding proteins are termed lectins which are often located on cell surfaces. These recognition processes are specific, weak, noncovalent biological interactions between the carbohydrate and protein, however the interactions can be greatly reinforced by prolonging the multiple copies of monodentate sugar moieties which is known as the cluster glycoside effect.[6, 12-17] Besides the topology, the composition, the position or anomeric configuration (α or β) of the glycoside units, the occurrence of branch points and the branch point density can have a large effect on the recognition

processes.[18] The well-defined, multi-functional glycopolymers, synthetic carbohydrate polymers, can be prepared for different recognition system. The special nature of carbohydrate binging protein has great potential in glycopolymer therapeutics, (pro)drug-delivery, bioactive agents-delivery systems and cell targeting.[19-23] Until recently, the polymerization of different glycoside monomers was achieved by different types of polymerization methods. One of better approaches was to polymerize the monomers with sugar moieties *via* "living"/controlled polymerization,[3, 24, 25] for example, living anionic polymerization,[26, 27] living cationic polymerization,[27, 28] ring-opening polymerization (ROP),[29-32] ring-opening metathesis polymerization (ROMP),[33-35] cyanoxyl(OCN)-mediated free-radical polymerization,[36] nitroxide-mediated radical polymerization (NMP),[37, 38] atom transfer radical polymerization (ATRP)[39-42] and reversible addition fragmentation chain transfer (RAFT) polymerization.[43-45] The "living"/controlled polymerization developed an efficient and flexible synthetic routes to prepare the well-defined glycopolymers with different complicated macromolecular architecture.[37, 39, 41, 46]

Atom transfer radical polymerization (ATRP) was first reported by Sawamoto *et al.*[47] and Matyjaszewski *et al.*[48-50] independently. ATRP is the most explored method amongst the controlled/"living" radical polymerization (CRP) which advantages include versatility and compatibility with a variety of monomers with functional groups, relative high tolerance to solvents and impurities, feasibility in a multitude of reaction conditions. ATRP is based on an

inner sphere electron transfer process, which involves the reduction of propagating radicals through the transformation of a large proportion of these to a dormant species. The dormant species can not initiate the monomer addition. The equilibrium between dominant dormant species and a small proportion, low concentration, of propagating radicals is achieved through a reversible halogen atom transfer between a dormant species and a transition metal complex along with the transition metal complex oxidation-reduction. This process occurs with a rate constant of activation (k_{act}) and deactivation (k_{deact}), respectively.[51-59] ATRP is a rapidly developing area of living radical polymerization and some glycopolymers were synthesized using the protected sugar monomer *via* ARTP.[40-42]

Aliphatic polyesters are an important type of materials due to their excellent biodegradability, biocompatibility, low toxicity, low immunogenicity and relatively low cost which have a range of applications, such as eco-friendly packaging materials, microelectronics, tissue engineering scaffolds, medicine and pharmacy, *etc*.[60-63] The polymerization of cyclic ester monomers, such as ε-caprolactone, glycolide, lactones, lactides and carbonates, *etc*., by ring-opening polymerization (ROP) provides a convenient route for the synthesis of aliphatic polyesters.[63-67]

Recently, click reactions have attracted more and more attention due to its high selectivity, high functional group tolerance, very efficient reaction, almost quantitative yields, mild reaction conditions, without noticeable by-products and

no purification in many cases. Both Sharpless and Meldal independently reported copper-catalyzed Huisgen 1,3-dipolar cycloaddition of azides and alkynes (CuAAC) click reaction, in which organic azide reacted quantitatively with a terminal alkyne in presence of a Cu(I) catalyst.[68-70] CuAAC reactions have been successfully applied for polymer science, which is a popular strategy and powerful tool to creation of well-defined and complex polymers by introducing the functional groups onto the reactive preformed polymer chains.[71-81]

Many studies focus on the cell surfaces glycoproteins, glycolipids, proteoglycans, and mucins over the past several decades. It is the most important development since the critical multi-faceted role of carbohydrates in the process of bio-recognition was discovered.[7, 82-92] In order to understand the molecular mechanism of bio-recognition and realize the potential of diagnosis, therapeutic and biomedical applications, many glycopolymers have been designed, synthesized and used.[3, 4, 10, 21, 23, 24, 46, 56, 93-99]

In this chapter, the ATRP polymerization of TMS-PgMA and TIPS-PgMA and ROP polymerization of aliphatic polyester is reported. A maleimide functional initiator was used in order to achieve post conjugation of nanoparticles for drug delivery. Moreover, the disulfide based bifunctional initiator was introduced into the midpoint of the polymer chain, which could break down to afford the corresponding polymer chain with thiol end group under the reducing condition. The thiol-terminated polymer was also post-functionalized *via* thiol-ene click chemistry. In addition, the aliphatic polycarbonate is a

biocompatible and biodegradable polymer, which is widely used in medical and pharmaceutical applications. The subsequent introduction of sugar moiety to the reactive polymer chain *via* CuAAC click reaction and then the interactions between glycopolymers and lectins were investigated by Surface Plasmon Resonance (SPR) and Quartz Crystal Microbalance with Dissipation (QCM-D).

4.2. Experimental

4.2.1. Materials

Copper(I) bromide (CuBr, Aldrich, 98%) was purified according to the method of Keller *et al.*[100] *N-ethyl*-2-pyridylmethanimine, *N*-(*n*-octyl)-2-pyridylmethanimine[101] and tris(2-(dimethylamino)ethyl)amine (Me_6-TREN)[102, 103] were prepared as described earlier and stored at 0 ℃ under a nitrogen atmosphere prior to use. Triethylamine (TEA, Fischer, 99%) was stored over sodium hydroxide pellets. Methacryloyl chloride (≥ 97%), propargyl alcohol (99%), ethyl magnesium bromide solution 3.0 M in diethyl ether, *N,N,N',N",N"*-pentamethyldiethylenetriamine (PMDETA, 99%), tetrabutyl ammonium fluoride (TBAF) solution 1.0 M in THF, 2-chloro-1,3-dimethylimidazolinium chloride (DMC), sodium azide (≥ 99%), Amberlite® IR120 hydrogen form, 1,8-diazabicyclo[5.4.0]undec-7-ene (DBU, 98%), *N*-hydroxysuccinimide (NHS, 98 %), *N*-(3-dimethylaminopropyl)-*N'*-

ethylcarbodiimide hydrochloride (EDC·HCl), 4-(2-hydroxyethyl)piperazine-1-ethanesulfonic acid (HEPES, ≥ 99.5%), anhydrous tetrahydrofuran (THF, ≥ 99.5%, 0.025% BHT stabilizer, over molecular sieve), anhydrous *N*,*N*-dimethyl-formamide (DMF, 99.8%), D-(+)-glucose (≥ 99.5%), and L-(-)-fucose (≥ 99%), bis(2-hydroxyethyl) disulfide (BHEDS), α-bromoisobutyryl bromide (BiBB, 98%) from Sigma-Aldrich, 3-(trimethylsilyl)propargyl alcohol (98+%), Chlorotriisopropylsilane (97+%), D-(+)-mannose (99%) from Alfa Aesar and D(+)-galactose (99+%) from Acros Organics were used as received. Fluorescein isothiocyanate isomer I (FITC, 90%) from Sigma-Aldrich was used as received and stored at -20 ℃. All other reagents and solvents were obtained from Sigma-Aldrich Company and used as purchased without further purification unless stated otherwise.

4.2.2. Proteins

Soluble recombinant DC-SIGN (dendritic cell-specific ICAM-3 grabbing nonintegrin; CD209) extracellular domain was generated in E. *coli* and purified by affinity chromatography and anion exchange chromatography as described previously.[104] Soluble recombinant HIV envelope glycoprotein gp120 was presented by Dr. Chris Scanlan from Oxford Glycobiology Institute. Concanavalin A (Con A, type IV), peanut agglutinin (PNA) from Sigma-Aldrich was used as received and stored at -20 ℃.

4.2.3. Characterization

^{1}H NMR spectroscopy was used to determine the molecular weight and structural information for confirmation of thiol-ene click conjugation. NMR spectra were recorded on either a Bruker DPX-300 MHz or a Bruker DPX-400 MHz or a Bruker AV III-600 MHz spectrometer at 298 K on approximately 10% w/v solutions in deuterated NMR solvents from Sigma-Aldrich. All chemical shifts were reported in ppm (δ) relative to tetramethylsilane (TMS), or referenced to the chemical shifts of residual solvent resonances (^{1}H and ^{13}C). The following abbreviations were used to explain the multiplicities: s = singlet, d = doublet, dd = doublet of doublets, t = triplet, m = multiplet. The molecular weights of the polymers $M_{n,NMR}$ were calculated by comparing the integrals of the chain-end signals with appropriate peaks related to the polymer backbone.

Gel permeation chromatography (GPC) was used to determine molecular weights and polydispersity ratio (M_w/M_n) of polymer samples.

GPC using $CHCl_3$ eluent was performed on an Agilent 390-MDS, comprising of an autosampler and a PLgel 5.0 μm bead-size guard column (50 × 7.5 mm), followed by two 5.0 μm bead-size PLgel Mixed D columns (300 × 7.5 mm) and a differential refractive index detector using $CHCl_3$ as the eluent at 30 ^{o}C with a flow rate of 1 mL min^{-1}. The GPC system was calibrated using linear poly(methyl methacrylate) EasiVial standards (Agilent Ltd.) range from 200 to 10^5 g mol^{-1} and

polystyrene EasiVial standards (Agilent Ltd.) range from 162 to 10^5 g mol^{-1}. Data were collected and analyzed using Cirrus GPC/SEC software (version 3.3).

GPC with THF as eluent was performed on an Agilent 390-MDS, comprising of an autosampler and a PLgel 5.0 μm bead-size guard column (50 × 7.5 mm), followed by two linear 5.0 μm bead-size PLgel Mixed D columns (300 × 7.5 mm) and a differential refractive index detector using THF (2% v/v TEA) as the eluent at 30 ^oC with a flow rate of 1 mL min^{-1}. The GPC system was calibrated using linear poly(methyl methacrylate) EasiVial standards (Agilent Ltd.) range from 200 to 10^5 g mol^{-1} and polystyrene EasiVial standards (Agilent Ltd.) range from 162 to 10^5 g mol^{-1}. Data were collected and analyzed using Cirrus GPC/SEC software (version 3.3).

DMF GPC analyses of the polymers were performed in *N*,*N*-dimethylformamide (DMF, 0.1% w/v LiBr), at 50 ^oC (flow rate = 1 mL min^{-1}) using an Agilent 390-MDS system comprised of an autosampler and a PLgel 5.0 μm bead-size guard column (50 × 7.8 mm) followed by two linear 5.0 μm bead-size PLgel Mixed D columns (300 × 7.5 mm) and a differential refractive-index detector. Calibration was achieved with linear poly(methyl methacrylate) EasiVial standards (Agilent Ltd.) range from 200 to 10^5 g mol^{-1}. Data were collected and analyzed using Cirrus GPC/SEC software (version 3.3).

The infrared absorption spectra were recorded on a Bruker VECTOR-22 FTIR spectrometer or PerkinElmer Spectrum 100 FT-IR Spectrometers using a Golden Gate diamond attenuated total reflection cell. The following abbreviations

were used to explain the absorption bands: υ, stretching; γ, out-of-plane deformation; δ, in-plane deformation; ρ, rocking; τ, twisting; s, strong; v, very; w, weak; br, broad; m, medium; sh, shoulder. subscripts: a, asymmetric; s, symmetric.

Mass spectra were recorded on a Bruker Esquire 2000 Mass spectrometer using electrospray ionisation (ESI) in positive mode.

TLC performed using pre-coated silica gel 60 F_{254} and developed in the solvent system indicated. Compounds were visualized by use of UV light (254 nm) or a stain solution of potassium permanganate (1.5 g of $KMnO_4$, 10 g K_2CO_3, and 1.25 mL 10% NaOH in 200 mL water). Silica gel (40-63u, 60 A, LC301) from Fluorochem Ltd. was used for column chromatography.

The Surface Plasmon Resonance (SPR) experiments were performed on a Biorad ProteOn XPR36 SPR biosensor (Biorad, Hercules CA). All soluble-phase analytes were prepared in HBS buffer pH 7.4 containing 25 mM HEPES, 150 mM NaCl, 5 mM $CaCl_2$, 0.01% Tween-20 and then flowed over the immobilized materials with a flow rate of 25 μL/min at 25˚C.

The Quartz Crystal Microbalance with Dissipation (QCM-D) measurements were performed by using the Q-sense E4 QCM-D instrument (Q-Sense AB, Västra Frölunda, Sweden) which contains QE 401 Electronics Unit, QCP 401 Chamber Platform and QFM 401 Flow Module with Ismatec IPC-N Pump. The sensor of the QCM consists of a thin disk-shaped, AT-cut piezoelectric quartz plate with two Au-evaporated electrodes (40 nm - 1 μm) on its two faces. The

quartz crystal with a fundamental resonant frequency of 4.95 MHz ± 50 kHz, an active sensor area of diameter of 14 mm and a thickness 0.3 mm were from Q-sense AB, Västra Frölunda, Sweden. The surface roughness of electrode was minimized by using optically polished crystals with the root-mean-square (RMS) roughness less than 3 nm. Prior to use in QCM-D, the sensors were immersed in piranha solution for 10 min, rinsed thoroughly with distilled water. The washed chips were then rinsed with ethanol, dried under nitrogen gas and used within 1 hour after cleaning. The analytes were dissolved in a HBS buffer with 10 mM HEPES, 142 mM NaCl and 1 mM $CaCl_2$, $MgCl_2$, $MnCl_2$ adjusted with HCl and NaOH to pH 7.2 at 25 ^oC or dissolved in a 0.01 M PBS buffer with 0.142 M NaCl and 1 mM $CaCl_2$, $MgCl_2$, $MnCl_2$ adjusted with HCl and NaOH to pH 7.2 at 25 ^oC.

4.2.4. Synthesis of trimethylsilyl-protected propargyl methacrylate (TMS-PgMA) (M_1)

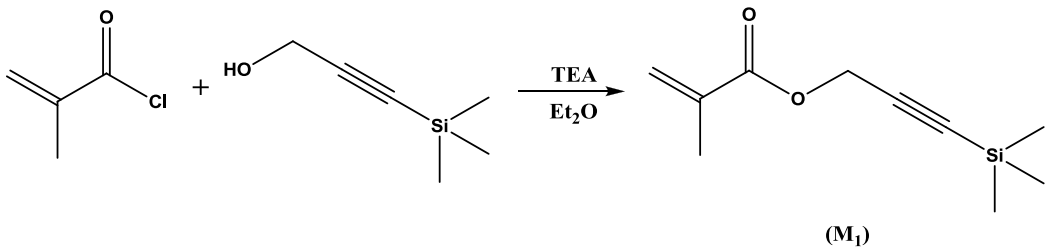

Scheme 4.1 Synthesis of trimethylsilyl-protected propargyl methacrylate (TMS-PgMA)

A solution of 3-(trimethylsilyl)-2-propyn-1-ol (25.0 g) and triethylamine (35.3 mL) in diethyl ether (350 mL) was cooled to 0 ℃ and a solution of methacryloyl chloride (22.9 mL) in diethyl ether (200 mL) was added dropwise over ca. 1 h. The mixture was stirred at this temperature for between 30 min and 1 hour, then at ambient temperature overnight; the ammonium salts were removed by filtration and the volatiles removed under reduced pressure.

^{1}H NMR (400 MHz, $CDCl_3$, 298 K): δ (ppm) = 0.17 (s, 9H, $Si(CH_3)_3$), 1.94 (s, 3H, $CH_2=CCH_3$), 4.74 (s, 2H, OCH_2), 5.59 (s, 1H, 1/2 $CH_2=CCH_3$), 6.15 (s, 1H, 1/2 $CH_2=CCH_3$).

^{13}C NMR (100 MHz, $CDCl_3$, 298 K): δ (ppm) = -0.19 (3C, $Si(CH_3)_3$), 18.39 (1C, $CH_2=CCH_3$), 53.06 (1C, OCH_2), 92.02 (1C, $C\equiv CSi(CH_3)_3$), 99.26 (1C, $C\equiv CSi(CH_3)_3$), 126.46 (1C, $CH_2=CCH_3$), 135.86 (1C, $CH_2=CCH_3$), 166.65 (1C, CO_{ester}).

FIIR (neat): υ (cm^{-1}) = 2961, 2903, 2187, 1723, 1639, 1452, 1367, 1315, 1292, 1251, 1145, 1052, 1035, 1011, 971, 942, 839, 812, 759, 701, 644.

Mass spectrometry: ESI-MS (*m/z*) Calcd. for $C_{10}H_{16}NaO_2Si^+$ ($M+Na^+$) = 219.08, Found 219.08.

4.2.5. Synthesis of 3-(1,1,1-triisopropylsilyl)-2-propyn-1-ol

A round-bottomed flask was equipped with an addition funnel, nitrogen

inlet, a glass stopper, a reflux condenser and a magnetic stirring bar. The apparatus was flushed with nitrogen and then charged with 100 mL of dry THF and ethylmagnesium bromide (100 mL, 3 M in diethyl ether, 0.3 mol). A solution of propargyl alcohol (5.61 g) in dry THF 100 mL was cautiously added dropwise over 2 hours at ambient temperature. After complete addition, the reaction mixture was heated at reflux for 24 hours. The resulting solution was cooled to ambient temperature, and then a solution of triisopropylsilyl chloride (27.57 g) in 100 mL of anhydrous THF was added dropwise to the stirred solution over 1 hour at room temperature. Subsequently the resulting brown suspension was refluxed for 8 days. The suspension was cooled to ambient temperature and then 200-mL of 10% HCl solution was cautiously added dropwise over 1 hour. The aqueous layer was separated and extracted with diethyl ether, and the combined organic phases were washed with saturated sodium chloride solution, dried over anhydrous magnesium sulfate, filtered, and concentrated under reduced pressure to get a brown oily crude product. The brown oily residue was dissolved in methanol and SiO_2 (20 g) was added. The solvent was removed using a rotary evaporator and the silica-supported reaction mixture was loaded onto a column previously filled with SiO_2 and pre-eluted with petroleum ether/Et_2O (20/1 vol/vol). After elution with the same solvent mixture, appropriate fractions were collected and then the solvents were removed by rotary evaporation to afford 3-(1,1,1-triisopropylsilyl) -2-propyn-1-ol as a yellow liquid.

^{1}H NMR (400 MHz, $CDCl_3$, 298 K): δ (ppm) = 1.04-1.05 (m, 21H,

(CH_3)$_2$-C*H*)$_3$-Si), 2.78 (br. s., 1H, CH_2-O*H*), 4.26 (s, 2H, C*H*$_2$-OH).

^{13}C NMR (100 MHz, $CDCl_3$, 298 K): δ (ppm) = 11.22 (3C, ((CH_3)$_2$*C*H)$_3$-Si), 18.59 (6C, ((*C*H$_3$)$_2$CH)$_3$-Si), 51.48 (1C, CH_2-OH), 86.45 (1C, Si-*C*≡C-CH_2), 105.94 (1C, Si-C≡*C*-CH_2).

FIIR (neat): υ (cm^{-1}) = 3318 (υ_{O-H}), 2943, 2892, 2865, 2174 ($\upsilon_{C\equiv C}$), 1463, 1383, 1367, 1039, 997, 981, 919, 883, 664, 632, 564.

Mass spectrometry: ESI-MS (*m/z*) Calcd. for $C_{12}H_{26}NaOSi^+$ ($M+Na^+$) = 237.16, Found 237.16.

4.2.6. Synthesis of triisopropylsilyl-protected propargyl methacrylate (TIPS-PgMA) (M_2)

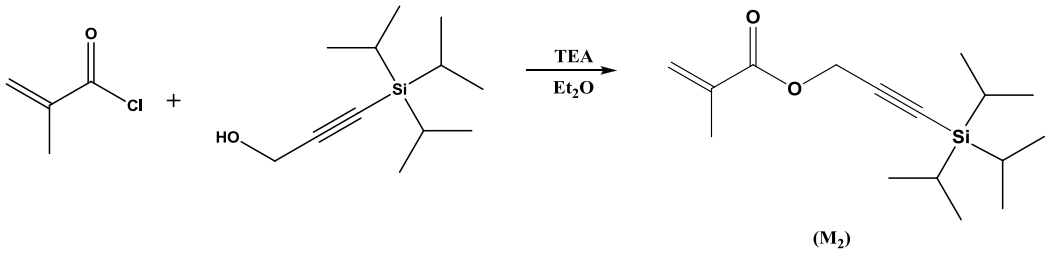

Scheme 4.2 Synthesis of triisopropylsilyl-protected propargyl methacrylate (TIPS-PgMA)

A solution of 3-(1,1,1-triisopropylsilyl)-2-propyn-1-ol (2.5 g) and triethyl-amine (2.13 mL) in diethyl ether (35 mL) was cooled to 0 ℃ and a solution of methacryloyl chloride (1.38 mL) in diethyl ether (15 mL) was added dropwise over ca. 30 mins to 1hour. The mixture was stirred at this temperature for 30mins

or 1 hour, then at ambient temperature overnight; the ammonium salts were removed by filtration and the volatiles removed under reduced pressure. The brown oily residue was dissolved in methanol and SiO_2 (5 g) was added. The solvent was removed using a rotary evaporator and the silica-supported reaction mixture was loaded onto a column previously filled with SiO_2 and pre-eluted with petroleum ether/Et_2O (200/1 vol/vol). After elution with the same solvent mixture, appropriate fractions were collected and then the solvents were removed by rotary evaporation to afford triisopropylsilyl-protected propargyl acrylate as a pale yellow liquid.

^{1}H NMR (400 MHz, $CDCl_3$, 298 K): δ (ppm) = 1.06 (s, 21H, $(CH_3)_2$-$CH)_3$-Si), 1.95 (s, 3H, CH_2=CCH_3), 4.77 (s, 2H, OCH_2), 5.59 (t, *J*=1.51 Hz, 1H, 1/2 CH_2=CCH_3), 6.15 (s, 1H, 1/2 CH_2=CCH_3).

^{13}C NMR (100 MHz, $CDCl_3$, 298 K): δ (ppm) = 11.21 (3C, $(CH_3)_2CH)_3$-Si), 18.37 (1C, CH_2=CCH_3), 18.61 (6C, $((CH_3)_2CH)_3$-Si), 53.21 (1C, OCH_2), 88.44 (1C, Si-C≡C-CH_2), 101.21 (1C, Si-C≡C-CH_2), 126.20 (1C, CH_2=CCH_3), 135.99 (1C, CH_2=CCH_3)), 166.64 (1C, CO_{ester}).

FIIR (neat): υ (cm^{-1}) = 2943, 2893, 2866, 2184, 1726, 1639, 1463, 1403, 1383, 1366, 1314, 1291, 1145, 1032, 996, 970, 941, 920, 882, 812, 677, 663, 638, 599, 565, 530

Mass spectrometry: ESI-MS (*m/z*) Calcd. for $C_{16}H_{28}NaO_2Si^+$ ($M+Na^+$) = 303.18, Found 303.18.

4.2.7. Synthesis of maleimide protected initiator (3)

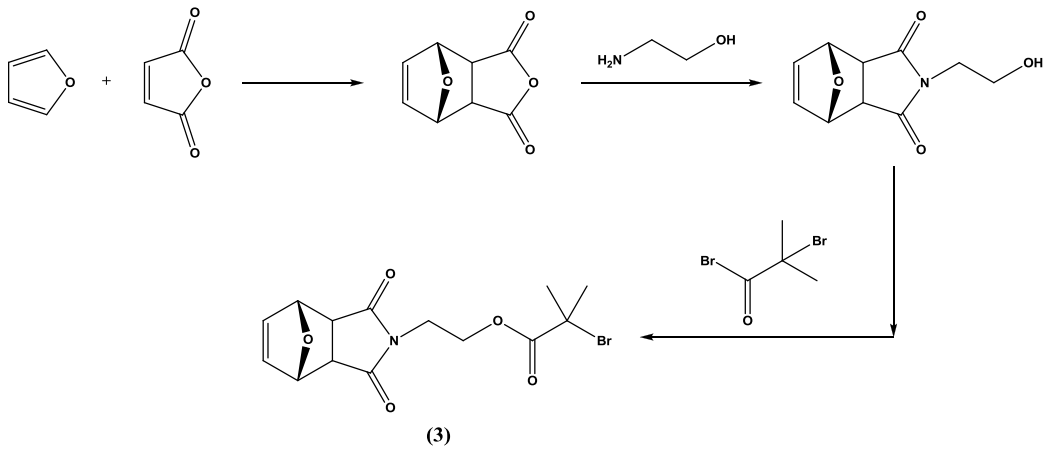

(3)

Scheme 4.3 Synthesis of maleimide protected initiator (3)

Maleimide protected initiator was prepared as described earlier.[4]

^{1}H NMR (400 MHz, $CDCl_3$, 298 K): δ (ppm) = 1.90 (s, 6H, CH_3), 2.87 (s, 2H, CH), 3.82 (t, *J* = 5.3 Hz, 2H, NCH_2), 4.33 (t, *J* = 5.3 Hz, 2H, OCH_2), 5.26 (t, *J* = 1.0 Hz, 2H, CHO), 6.51 (t, J = 1.0 Hz, 2H, CH_{vinyl}).

^{13}C NMR (100 MHz, $CDCl_3$, 298 K): δ (ppm) = 30.73 (2C, CH_3), 37.75 (1C, NCH_2), 47.64 (2C, CH), 55.82 (1C, $C(CH_3)_2Br$), 62.34 (1C, OCH_2), 80.99 (2C, CHO), 136.70 (2C, CH_{vinyl}), 171.57 (1C, CO_{ester}), 176.01 (2C, CO_{imide}).

FIIR (neat): υ (cm^{-1}) = 2978, 2959, 1773, 1734, 1696, 1462, 1421, 1395, 1374, 1359, 1336, 1277, 1190, 1157, 1107, 1096, 1016, 989, 968, 953, 938, 926, 917, 910, 875, 852, 824, 799, 782, 724, 706, 655, 603, 594.

Mass spectrometry: ESI-MS (*m/z*) Calcd. for $C_{14}H_{16}BrNNaO_5^+$ ($M+Na^+$) = 380.01, Found 380.01.

M_p: 83-85 ℃.

4.2.8. Synthesis of *N*-ethyl-2-pyridylmethanimine

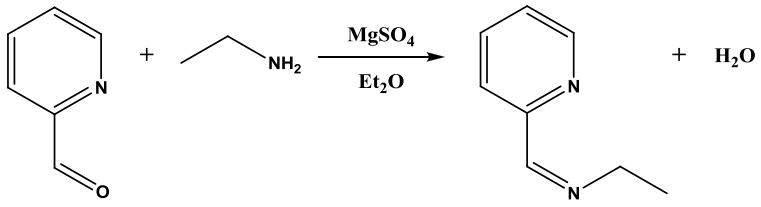

Scheme 4.4 Synthesis of *N*-ethyl-2-pyridylmethanimine

2-Pyridinecarboxaldehyde (20 mL, 0.21 mol) and diethyl ether (20 mL) were added to a flask containing dried magnesium sulphate (15 g). The flask was cooled to 0^{o}C in an ice bath and an excess of ethylamine solution (70 wt. % in H_2O) (20 mL, 0.25 mol) was added drop wise to the stirring slurry. After complete addition of the amine, the flask was removed from the ice bath and kept stirring for 2 hours at ambient temperature. The mixture was then filtered and the solvent was removed by rotary evaporation yielding a yellow oil. In order to remove any unreacted amine, the crude product was purified by vacuum distillation to afford a straw-colored oil (25 g, 89%) (Bp: 60 ℃ at 0.4 Torr). The oil was freeze-pump-thawed several times in an ampoule until all dissolved gasses were removed. The ampoule was then stored in the refrigerator.

^{1}H NMR (400 MHz, $CDCl_3$, 298 K): δ (ppm) = 1.32 (t, *J*=7.28 Hz, 3H, CH_3), 3.71 (qd, *J*=7.32, 1.38 Hz, 2H, CH_2N), 7.29 (ddd, *J*=7.47, 4.83, 1.00 Hz, 1H,

H_{pyr}), 7.72 (td, *J*=7.72, 1.63 Hz, 1H, H_{pyr}), 7.98 (dd, *J*=7.91, 0.88 Hz, 1H, H_{pyr}), 8.39 (s, 1H, CH=N), 8.63 (dd, *J*=4.89, 0.88 Hz, 1H, H_{pyr}).

^{13}C NMR (100 MHz, $CDCl_3$, 298 K): δ (ppm) = 15.97 (1C, CH_3), 55.56 (1C, CH_2N), 121.12 (1C, C_{pry}), 124.52 (1C, C_{pry}), 136.45 (1C, C_{pry}), 149.32 (1C, C_{pry}), 154.58 (1C, C_{pry}-CH=N), 161.25 (1C, *C*H=N)

FIIR (neat): υ (cm^{-1}) = 3055, 2971, 2847, 1649 ($\upsilon_{C=N}$), 1587, 1567, 1468, 1436, 1374, 1356, 1329, 1292, 1228, 1138, 1100, 1088, 1043, 992, 971, 955, 905, 857, 771, 742, 656, 616.

Mass spectrometry: ESI-MS (*m/z*) Calcd. for $C_8H_{10}N_2Na^+$ ($M+Na^+$) = 157.07, Found 157.07.

4.2.9. Synthesis of Sugar azides (9)

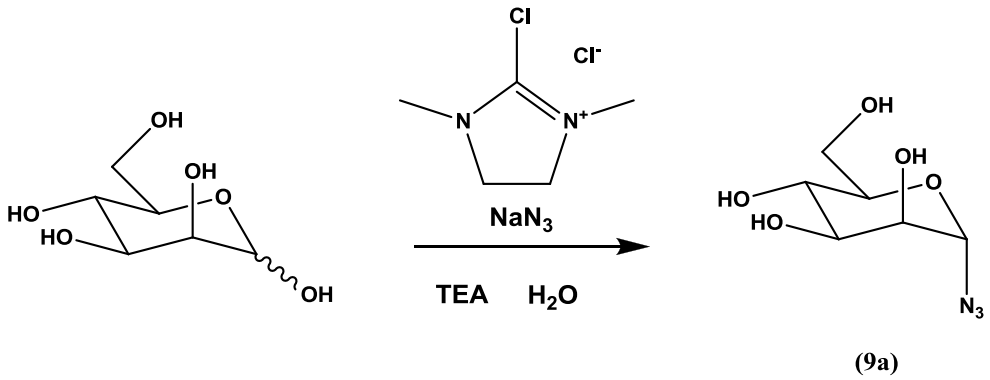

(9a)

Scheme 4.5 Synthesis of α-D-mannopyranosyl azide

Sodium azide (7.26 g, 111 mmol), D-(+)-mannose (2.00 g, 11.1 mmol) and

triethylamine (15.5 mL, 111 mmol) were dissolved in water (40 mL) and cooled to 0 ℃. 2-Chloro-1,3-dimethylimidazolinium chloride (5.61 g, 33.3 mmol) was added and the mixture was stirred for 1 hour at 0 ℃. The solvent was removed under reduced pressure and ethanol was added. The solids were removed by filtration and the solution was purified on Amberlite IR-120 column. The mixture was checked with FTIR to confirm the removal of all sodium azide (ν = 2022 cm^{-1}). The solvent was removed under reduced pressure, water was added and the mixture was washed with dichloromethane. The solvent was removed under reduced pressure, water (10 mL) was added and the solution was freeze-dried overnight to give α-D-mannopyranosyl azide as an off-white solid.

α-D-Mannopyranosyl azide:

^{1}H NMR (400 MHz, D_2O, 298 K), δ (ppm) = 3.57 - 3.66 (m, 1H, H^5), 3.68 - 3.77 (m, 3H), 3.84 (dd, J = 3.01, 2.01 Hz, 1H, H^2), 3.88 (d, J = 10.04 Hz, 1H), 5.43 (d, J = 2.01 Hz, 1H, H^1).

^{13}C NMR (100 MHz, D_2O, 298 K), δ (ppm) = 60.81 (1C, C^6), 66.38 (1C, C^4), 69.75 (1C, C^3), 69.83 (1C, C^2), 74.62 (1C, C^5), 89.71 (1C, C^1).

FIIR (neat): υ (cm^{-1}) = 3331 (υ(O-H)), 2933, 2110 ($\upsilon_{as}(-N_3)$), 1407, 1294, 1237, 1092, 1060, 933, 803, 667, 566.

Mass spectrometry: ESI-MS (*m/z*) Calcd. for $C_6H_{11}N_3NaO_5^+$ ($M+Na^+$) = 228.06, Found 228.06.

Besides D-(+)-mannose, other sugars were used to prepare different kinds of glycosyl azides following a similar procedure, **Scheme 4.6**.

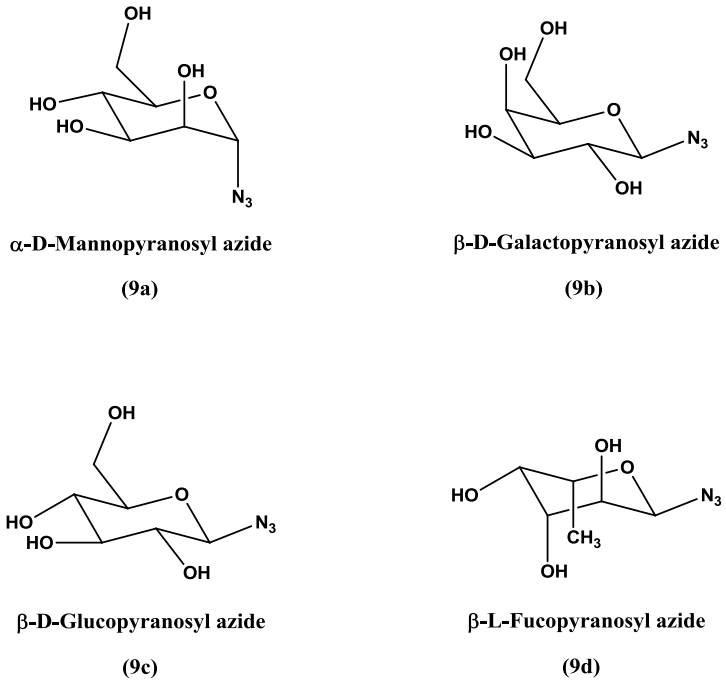

Scheme 4.6 Various sugar azides prepared in this study

β-D-Galactopyranosyl azide:

^{1}H NMR (400 MHz, D_2O, 298 K), δ (ppm) = 3.48 (dd, *J*=9.79, 8.78 Hz, 1H, H^2), 3.65 (dd, *J*=9.79, 3.26 Hz, 1H, H^3), 3.69 - 3.79 (m, 3H, H^{6a}, H^{6b}, H^5), 3.93 (d, *J*=3.26 Hz, 1H, H^4), 4.63 (d, *J*=8.78 Hz, 1H, H^1)

^{13}C NMR (100 MHz, D_2O, 298 K), δ (ppm) = 60.92 (1C, C^6), 68.48 (1C, C^4), 70.29 (1C, C^2), 72.61 (1C, C^3), 77.17 (1C, C^5), 90.51 (1C, C^1)

FIIR (neat): υ (cm^{-1}) = 3315 (υ(O-H)), 2900, 2116 ($\upsilon_{as}(-N_3)$), 1406, 1243, 1034, 892, 869, 780, 691, 661.

Mass spectrometry: ESI-MS (*m/z*) Calcd. for $C_6H_{11}N_3NaO_5^+$ ($M+Na^+$) = 228.06, Found 228.06.

β-D-Glucopyranosyl azide:

^{1}H NMR (400 MHz, D_2O, 298 K), δ (ppm) = 3.25 (t, *J* = 8.98, 8.98 Hz, 1H, H^2), 3.41 (t, *J* = 9.51, 9.51 Hz, 1H, H^4), 3.51 (t, *J* = 9.01, 9.01 Hz, 1H, H^3), 3.54 (m, 1H, H^5), 3.74 (dd, *J* = 5.59, 12.42 Hz, 1H, H^{6b}), 3.92 (dd, *J* = 1.95 Hz, 12.42 Hz, 1H, H^{6a}), 4.74 (d, *J* = 8.78 Hz, 1H, H^1).

^{13}C NMR (100 MHz, D_2O, 298 K), δ (ppm) = 60.5 (1C, C^6), 69.1 (1C, C^4), 72.8 (1C, C^2), 75.7 (1C, C^3), 77.9 (1C, C^5), 90.1 (1C, C^1).

FIIR (neat): υ (cm^{-1}) = 3442 (υ(O-H)), 2917, 2119 ($\upsilon_{as}(-N_3)$), 1250.

Mass spectrometry: ESI-MS (*m/z*) Calcd. for $C_6H_{11}N_3NaO_5^+$ ($M+Na^+$) = 228.06, Found 228.06.

β-L-Fucopyranosyl azide:

^{1}H NMR (400 MHz, D_2O, 298 K), δ (ppm) = 1.25 (d, *J* = 6.51 Hz, 3H, H^6), 3.44 (dd, *J* = 8.72, 9.79Hz, 1H, H^2), 3.65 (dd, *J* = 9.83, 3.43 Hz, 1H, H^3), 3.76 (dd, *J* = 3.47, 0.77 Hz, 1H, H^4), 3.86 (dd, *J* = 6.49, 0.91 Hz, 1H, H^5), 4.61 (d, *J* = 8.69 Hz, 1H, H^1).

^{13}C NMR (100 MHz, D_2O, 298 K), δ (ppm) = 15.4 (C^6), 70.0, 71.1, 72.8, 73.1, 90.5 (C^1).

FIIR (neat): υ (cm^{-1}) = 3277 (υ(O-H)), 2893, 2113 ($\upsilon_{as}(-N_3)$), 1642, 1373, 1247, 1164, 1030, 995, 898, 750, 662.

Mass spectrometry: ESI-MS (*m/z*) Calcd. for $C_6H_{11}N_3NaO_4^+$ ($M+Na^+$) =

212.06, Found 212.06.

4.2.10. Typical procedure for the synthesis of clickable homopolymers *via* ATRP

N-ethyl-2-pyridylmethanimine ligand (0.058 mL, 0.412 mmol), TMS-PgMA (2.02 g, 10.289 mmol), maleimide protected initiator (0.074 g, 0.206 mmol) and mesitylene (internal NMR standard, 1.0 mL) were charged into a dry Schlenk tube along with toluene as solvent. The tube was sealed with a rubber septum and subjected to five freeze-pump-thaw cycles. This solution was then transferred *via* cannula under nitrogen into a second Schlenk tube, previously evacuated and filled with nitrogen, containing Cu(I)Br (0.030 g, 0.206 mmol) and a magnetic stir bar. The temperature was adjusted at 30 ℃ or 70 ℃ with constant stirring (t = 0). Samples were removed periodically using a degassed syringe for molecular weight and conversion analysis. At the end of the polymerization the mixture was diluted with THF and air was bubbled through for 4 h. The reaction mixture was passed through a short neutral alumina column and subsequently washed with THF. The volatiles were removed under reduced pressure and the residues dissolved in THF prior to precipitation into 10:2 vol/vol methanol/water mixture. The white solid was isolated by vacuum filtration, washed with some additional methanol/water mixture. The residue was dissolved in THF, dried over anhydrous $MgSO_4$, filtered, and the solvent removed under reduced pressure.

4.2.11. Typical procedure for the synthesis of clickable copolymers *via* ATRP

N-ethyl-2-pyridylmethanimine ligand (0.058 mL, 0.412 mmol), TMS-PgMA (2.02 g, 10.289 mmol), TIPS-PgMA (2.886g, 10.289 mmol), Maleimide-protected initiator (0.074 g, 0.206 mmol) and mesitylene (internal NMR standard, 1.0 mL) were charged into a dry Schlenk tube along with toluene as solvent. The tube was sealed with a rubber septum and subjected to five freeze-pump-thaw cycles. This solution was then transferred *via* cannula under nitrogen into a second Schlenk tube, previously evacuated and filled with nitrogen, containing Cu(I)Br (0.030 g, 0.206 mmol) and a magnetic stir bar. The temperature was adjusted at 70 ℃ with constant stirring (t = 0). Samples were removed periodically using a degassed syringe for molecular weight and conversion analysis. At the end of the polymerization the mixture was diluted with THF and air was bubbled through for 4 h. The reaction mixture was passed through a short neutral alumina column and subsequently washed with THF. The volatiles were removed under reduced pressure and the residues dissolved in THF, prior to precipitation into 10:3 vol/vol methanol/water cold mixture. The white solid was isolated by vacuum filtration, washed with some additional methanol/water mixture. The residue was dissolved in THF, dried over anhydrous $MgSO_4$, filtered, and the solvent removed under reduced pressure.

4.2.12. Typical procedure of removal of $Si(CH_3)_3$ protecting group

The trimethylsilyl protected polymer (2 g) and acetic acid (2 equiv. mol/mol with respect to the alkyne-trimethylsilyl groups) were dissolved in THF (50 mL). The pale yellow solution was cooled to 0 ℃. A 0.20 M solution of TBAF in THF (2 equiv. mol/mol with respect to the alkyne-trimethylsilyl groups) was added slowly *via* pressure equalizing dropping funnel. The resulting turbid mixture was stirred at this temperature for 30 min and then warmed to ambient temperature and the deprotection was complete in approximately 3 h. The reaction solution was passed through a silica pad in order to remove the excess of TBAF and the pad was subsequently washed with additional THF. The resulting solution was then concentrated under reduced pressure and the polymer was precipitated in petroleum ether 40 - 60 ℃. The off-white solid was isolated by vacuum filtration, washed with some additional petroleum ether 40 - 60 ℃. The residue was transferred to a vacuum oven and dried to constant weight at ambient temperature.

4.2.13. Post-functionalization of polymer *via* CuAAC click reaction

A solution containing propargyl polymer (240 mg, 1.93 mmol propargyl groups), mannose azide (476 mg, 2.32 mmol) and CuBr (277 mg, 1.93 mmol) in DMSO (24 mL) was bubbled with nitrogen for 30 minutes. Ethyl ligand (519 mg, 3.87 mmol) was bubbled with nitrogen for 12 min and then was injected into the solution. The solution was continued to be bubble with nitrogen for 15 minutes. The solution was subsequently stirred at 25 ^{o}C for two days. The mixture was purified by dialysis (MWCO: 1,000) against distilled water/methanol (1/1 vol/vol) for two days, while changing the water at least four times. It was then concentrated under reduced pressure and freeze-dried overnight.

4.2.14. Typical procedure for polymer deprotection (Retro Diel-Alder maleimide deprotection)

A dry round bottom flask, fitted with a reflux condenser and magnetic stirrer, was charged with glycopolymer (0.2 g) and DMSO (20 mL). The reaction was subsequently stirred at 120 ^{o}C for overnight and then cooled to ambient temperature. The solution was purified by dialysis (MWCO: 1,000) against distilled water/ethanol (1/1 vol/vol) and water for two days. It was then concentrated under reduced pressure and freeze-dried overnight. The product was obtained as a white powder.

4.2.15. General Procedure for FITC Labeling of glycopolymers

In an oven-dried, round-bottom flask, the glycopolymer (140.6 mg, 0.01 mmol) was weighed in and dried for 1 h under vacuum. The flask was then sealed with a rubber septum and filled with Nitrogen. Anhydrous DMF (8 mL) was added. When the glycopolymer was dissolved in DMF, fluorescein isothiocyanate (FITC, 3.9 mg, 0.01 mmol) was added. The sealed mixture was stirred for 24 h under nitrogen. The reaction was quenched and the polymer was purified by dialysis (MWCO: 1,000) against distilled water for two days. It was then concentrated under reduced pressure and freeze-dried overnight.

4.2.16. General Procedure for Surface Plasmon Resonance (SPR)

SPR sensorgrams were recorded in a Biorad ProteOn XPR36 SPR biosensor (Biorad, Hercules CA). All soluble-phase analytes were prepared in HBS buffer pH 7.4 containing 25 mM HEPES, 150 mM NaCl, 5 mM $CaCl_2$, 0.01% Tween-20 and then flowed over the immobilized materials at a rate of 25 μL/min at 25˚C, except that the DC-SIGN, a novel cell-surface C-type lectin expressed on dendritic cells, was prepared in acetate buffer pH 5.0 for optimal

immobilization effect. Soluble DC-SIGN and gp120 envelope glycoprotein of human immunodeficiency virus-1were immobilized to 6000 response units (RU) on discrete channels within Biorad GMC sensor chips *via* amine coupling reaction. The surface of chips was attached by carboxylic acid and then modified by *N*-hydroxysuccinimide (NHS) in presence of *N*-ethyl-*N*'-(3-dimethylaminopropyl) carbodiimide hydrochloride (EDC · HCl) which reacts with amine groups in DC-SIGN and Con A. Regeneration of the sensor chip surfaces was performed using the solution of 10 Mm glycine hydrochloride pH 2.5 at a flow rate of 100 μL/min at 25˚C and contact time of 27s. Datasets were exported to BIAcore BIA evaluation software for kinetic calculations or evaluated using Matlab software and Origin software. Kinetic parameters were obtained by fitting curves to a 1:1 Langmuir mode with correction for baseline drift where necessary. Competition assays were evaluated using Origin software.

4.2.17. Conjugation method for nanosponge drug delivery system

A small vial equipped with a stir bar was added 5% allyl PAVL-co-VL nanosponge, glycopolymer and dry DMSO. The vial was sealed and purged with argon. The mixture stirred at room temperature, shielded from light, for 24 hours. The reaction mixtures were purified by dialyzing with SnakeSkin Pleated

Dialysis Tubing (MWCO: 1 000) against distilled water. The final product was freeze-dried to yield an off-white and light solid.

4.2.18. Synthesis of disulfide-based bifunctional initiator (DSDBr)

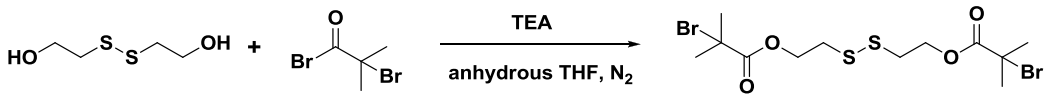

Scheme 4.7 Synthesis of disulfide-based bifunctional initiator (DSDBr)

Bis(2-hydroxyethyl) disulfide (6.0 mL, 49.05 mmol) and triethylamine (15.0 mL, 107.91 mmol) was added to a 500 mL round bottom flask along with a magnetic stirring bar, and was purged with nitrogen for 20 minutes in an ice bath. Anhydrous THF (180 mL) was cannulated into the system, and allowed to cool to 0 ℃. A solution of α-bromoisobutyryl bromide (12.7 mL, 103.01 mmol) in anhydrous THF (50 mL) was added dropwise over ca. 30 mins to 1 hour using a pressure equalizing addition funnel under a nitrogen atmosphere. The solution was stirred at this temperature for 30 mins or 1 hour and subsequently allowed to reach ambient temperature for 6 hours. The resulting triethylammonium bromide salts were removed by filtration, and volatiles removed using rotary evaporation. The resulting pale yellow residue was stirred with 0.10 M aqueous Na_2CO_3 so as to hydrolyze any residual 2-bromoisobutyryl bromide. The crude product was

then extracted three times with dichloromethane using the separating funnel. The combined dichloromethane phases were dried with over anhydrous magnesium sulfate, filtered, and concentrated under reduced pressure to afford bis[2-(2'-bromoisobutyryloxy)ethyl]disulfide as a yellow liquid (17.9 g, 80.7 %). The product was then stored in a refrigerator.

^{1}H NMR (400 MHz, $CDCl_3$, 298 K), δ (ppm) = 1.91 (s, 12H, 2*$C(CH_3)_2$), 2.96 (t, *J*=6.65 Hz, 4H, 2*SCH_2), 4.41 (t, *J*=6.53 Hz, 4H, 2*OCH_2).

^{13}C NMR (100 MHz, $CDCl_3$, 298 K), δ (ppm) = 30.79 (4C, 2*$C(CH_3)_2$), 36.82 (2C, 2*SCH_2), 55.58 (2C, 2*$C(CH_3)_2$), 63.57 (2C, 2*OCH_2), 171.47 (2C, 2*CO_{ester})

FIIR (neat): υ (cm^{-1}) = 3004, 2977, 2931, 1732, 1463, 1389, 1370, 1268, 1152, 1105, 1049, 1010, 975, 917, 761, 642.

Mass spectrometry: ESI-MS (*m/z*) Calcd. for $C_{12}H_{20}Br_2NaO_4S_2^+$ ($M+Na^+$) = 472.91, Found 472.91.

4.2.19. Synthesis of 2-(2-azidoethoxy)ethanol (AzEE)

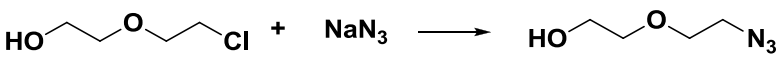

Scheme 4.8 Synthesis of 2-(2-azidoethoxy)ethanol (AzEE)

In a round-bottom flask fitted with a reflux column, a solution of 20 g of 2-(2-chloroethoxy)ethanol in 80 mL of water was added to 26.09 g of sodium

azide. The solution was kept under reflux for 24 h behind a safety shield, After cooling to ambient temperature, the resulting solution was treated with 5% NaOH solution and then extracted with diethyl ether. The combined organic layers were washed with saturated $NaHCO_3$ solution, dried with over anhydrous $MgSO_4$, filtered and concentrated under reduced pressure to give a pale yellow viscous liquid. Yield: 80%.

CAUTION: The organic azide is very sensitive explosive compounds and it should be handled with great care !!!

^{1}H NMR (400 MHz, $CDCl_3$, 298 K), δ (ppm) = 2.63 (t, *J*=5.90 Hz, 1H, CH_2-O*H*), 3.36 (t, *J*=5.02 Hz, 2H, N_3-CH_2), 3.52 - 3.58 (m, 2H, O-C*H*$_2$-CH_2-OH), 3.60 - 3.66 (m, 2H, N_3-CH_2-C*H*$_2$-O), 3.66 - 3.72 (m, 2H, C*H*$_2$-OH)

^{13}C NMR (100 MHz, $CDCl_3$, 298 K), δ (ppm) = 50.68 (1C, N_3-CH_2), 61.64 (1C, CH_2-OH), 69.94 (1C, N_3-CH_2-*C*H_2-O), 72.45 (1C, O-*C*H_2-CH_2-OH).

^{1}H NMR (400 MHz, D_2O, 298 K), δ (ppm) = 3.54 (t, *J*=4.64 Hz, 2H, N_3-CH_2), 3.64 - 3.71 (m, 2H, O-C*H*$_2$-CH_2-OH), 3.72-3.78 (m, 4H, N_3-CH_2-C*H*$_2$-O, C*H*$_2$-OH)

^{13}C NMR (100 MHz, D_2O, 298 K), δ (ppm) = 50.23 (1C, N_3-CH_2), 60.39 (1C, CH_2-OH), 69.14 (1C, N_3-CH_2-*C*H_2-O), 71.65 (1C, O-*C*H_2-CH_2-OH)

FIIR (neat): υ (cm^{-1}) = 3411 (υ(O-H)), 2924, 2869, 2091 (υ_{as}(-N_3)), 1442, 1346, 1283, 1124, 1060, 921, 887, 847, 811, 639, 580, 556

Mass spectrometry: ESI-MS (*m/z*) Calcd. for $C_4H_9N_3NaO_2^+$ ($M+Na^+$) = 154.06, Found 154.06.

4.2.20. General Procedure for glycopolymers with different functional group density

General procedure for preparation of glycopolymers (**19**): A solution containing propargyl functional polymer (180 mg, 1.45 mmol propargyl groups), mannose azide (268 mg, 1.31mmol), 2-(2-azidoethoxy)ethanol (57 mg, 0.435 mmol), triethylamine (0.081 ml, 0.581 mmol) and CuBr (42 mg, 0.29 mmol) in DMSO (15 mL) was bubbled with nitrogen for 30 minutes. Ethyl ligand (78 mg, 0.581 mmol) was bubbled with nitrogen for 15 min and then was injected into the solution. The solution was continued to bubble with nitrogen for 15 minutes. The solution was subsequently stirred at 25 ^{o}C for two days. The mixture was purified by dialysis (MWCO: 1,000) against distilled water/methanol (1/1 v/v) for two days, while changing the water at least four times. It was then concentrated under reduced pressure and freeze-dried overnight to give the product.

4.2.21. General measurement Procedure for Quartz Crystal Microbalance with Dissipation (QCM-D)

The measurements were performed as follows: 5 ml of degassed HBS buffer (10 mM, pH 7.4) was introduced into the chamber of QCM-D system at a flow

rate of 0.1 ml/min until the flat and stable baselines of frequency and dissipation were obtained. Subsequently, the disulfide initiated glycopolymers in HBS buffer solution (1mg/mL) was loaded into the QCM-D at a flow rate of 0.1 ml/min and the frequency shift (Δf) and dissipation shift (ΔD) were recorded simultaneously. After the interaction of the glycopolymers with the chip for 10 hours, the curves of Δf and ΔD reached a plateau and then HBS buffer was passed over the chip to remove any unbound glycopolymers on the gold surface. Subsequently, the ConA in HBS solution (0.1 mg/ml) was injected into the chamber at a 0.1 ml/min flow rate for 13 hours until a flat line frequency and dissipation were achieved. Finally, the ConA layer was flushed with degassed HBS buffer until all unadsorbed lectin was removed.

4.2.22. General Procedure for synthesis of glycopolymers with different binding epitope density

General synthetic procedure for glycopolymers (**24**): A solution containing propargyl polymer (60 mg, 0.29 mmol propargyl groups), mannose azide (53 mg, 0.261 mmol), galactose azide (18 mg, 0.087 mmol), triethylamine (0.016 ml, 0.116 mmol) and CuBr (8 mg, 0.058 mmol) in DMSO (6 mL) was bubbled with nitrogen for 30 minutes. Ethyl ligand (16 mg, 0.116 mmol) was bubbled with nitrogen for 15 min and then was injected into the solution. The solution was continued to be

bubbled with nitrogen for 15 minutes. The solution was subsequently stirred at 25 ^{o}C for two days. The mixture was purified by dialysis (MWCO: 1,000) against distilled water/methanol (1/1 v/v) for two days, while changing the water at least four times. It was then concentrated under reduced pressure and freeze-dried overnight to give the product.

4.3. Results and Discussion

4.3.1. Synthesis of the "clickable" alkyne homopolymers (6)

The trimethylsilyl-protected propargyl methacrylate monomer (M_1) was synthesized from commercially available 3-trimethylsilypropyn-1-ol and methacryloyl chloride *via* a one step reaction. Maleimide-protected initiator was chosen since the furan protecting units' protons can be used as ^{1}H NMR internal standards for the calculation of the number average molecular weight ($M_{n, NMR}$) of the corresponding polymers and the α-maleimide functional terminal after deprotection can be conjugated with some thiol-containing protein, **Scheme 4.9**.

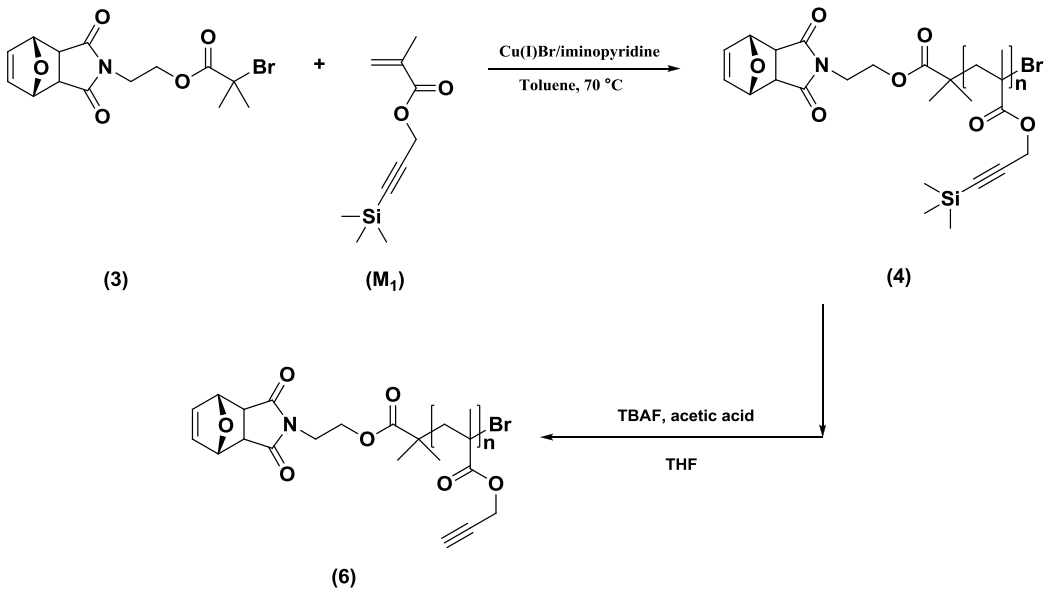

Scheme 4.9 Synthesis approach towards to "clickable" alkyne homopolymers

The first step involves synthesis of TMS-PgMA homopolymers which were prepared by a general synthetic strategy based on atom transfer radical polymerization (ATRP) in presence of a CuBr/alkylpyridylmethanimine type ligands catalytic system in toluene solvent. Secondly, the trimethylsilyl protecting groups in polymer were removed by the addition of TBAF in THF solution in the presence of acetic acid as a buffering agent.

The results of ATRP polymerization of TMS-PgMA are shown in **Table 4.1**, **Figure 4.1**, **Figure 4.2**. A series of polymers with different number average molecular weights were synthesis by varying the molar ratios of [Monomer]/[Initiator]. The first-order kinetic plots of TM1-6 show a good linear relationship during the polymerization and the linear increase in M_n with monomer conversion and the narrow polydispersity index (PDi) of product

indicating good control over the molecular weight and molecular weight distribution, **Table 4.1**, **Figure 4.1**, **Figure 4.2**.

Table 4.1 Kinetic investigation of the polymerization of TMS-PgMA

Run	[M]/[I][a]	W_M/ $W_{Solv.}$	React. Time, mins	Conv. (%)	M_n(GPC) (g mol^{-1})	PDi	Temp. (^oC)
TM1	50/1	1/6	18420	93	9600	1.32	30
TM2	50/1	1/6	360	54	6200	1.28	70
TM3[b]	110/1	1/2	360	65	12300	1.18	50
TM4[c]	110/1	1/2	2500	50	9700	1.20	50
TM5[b]	80/1	1/2	1440	83	11100	1.34	50
TM6	18/1	1/2.4	240	94	7200	1.22	70
TM7	15/1	1/2.5	120	82	5900	1.27	70
TM8	2/1	1/6	120	95	2200	1.24	70

Obtained by GPC analysis using $CHCl_3$ as the mobile phase and DRI detection.

All polymerizations were carried out in presence of a 1 eq. of CuBr and 2 eq. of *N*-ethyl-2-pryidylmethanimine as catalyst in toluene.

[a] [M]/[I] = monomer/ initiator

[b] 2.5 eq. of *N*-ethyl-2-pryidylmethanimine

[c] 2.5 eq. of *N*-(*n*-octyl)-2-pryidylmethanimine

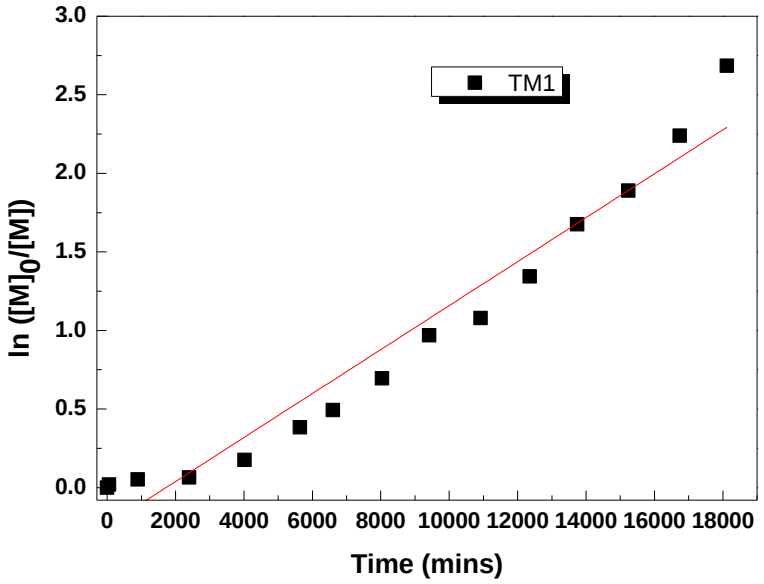
TM1
ln ([M]0/[M])
Time (mins)
0.0
0.5
1.0
1.5
2.0
2.5
3.0
0
2000
4000
6000
8000
10000
12000
14000
16000
18000

(a)

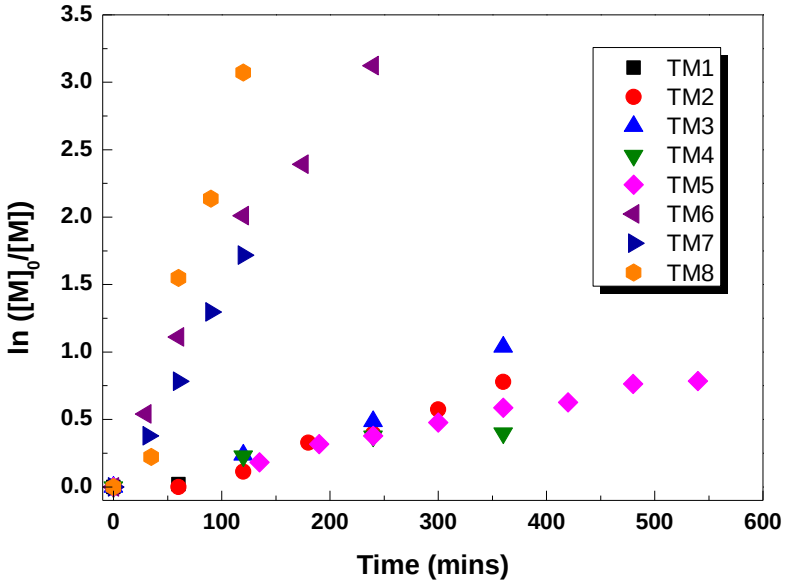
TM1
TM2
TM3
TM4
TM5
TM6
TM7
TM8
ln ([M]0/[M])
Time (mins)
0.0
0.5
1.0
1.5
2.0
2.5
3.0
3.5
0
100
200
300
400
500
600

(b)

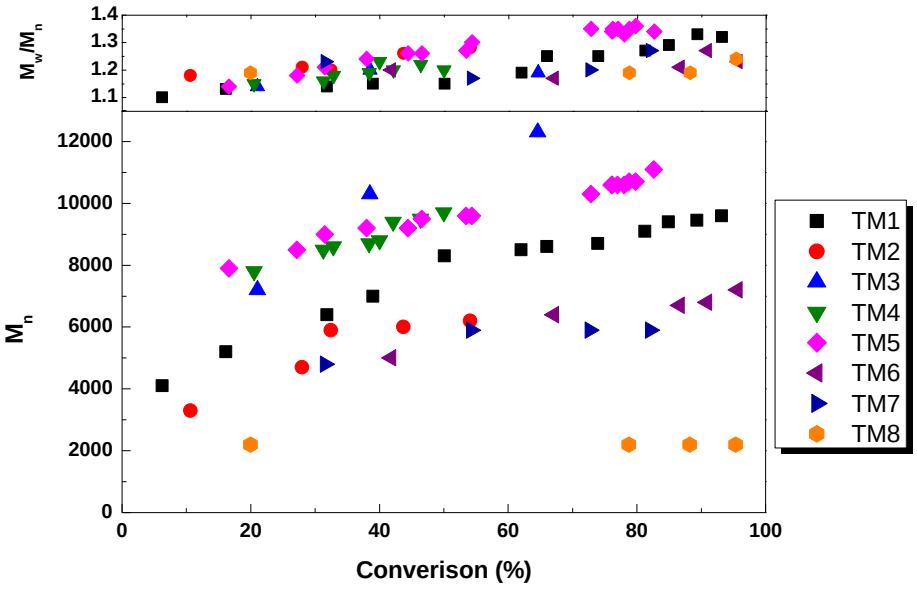

(c)

Figure 4.1 (a) Kinetic plots of polymerization of TMS-PgMA, TM1; (b) kinetic plots of polymerization of TMS-PgMA under different reaction conditions, TM1-TM8; (c) dependence of molecular weights and molecular weight distributions on the monomer conversions.

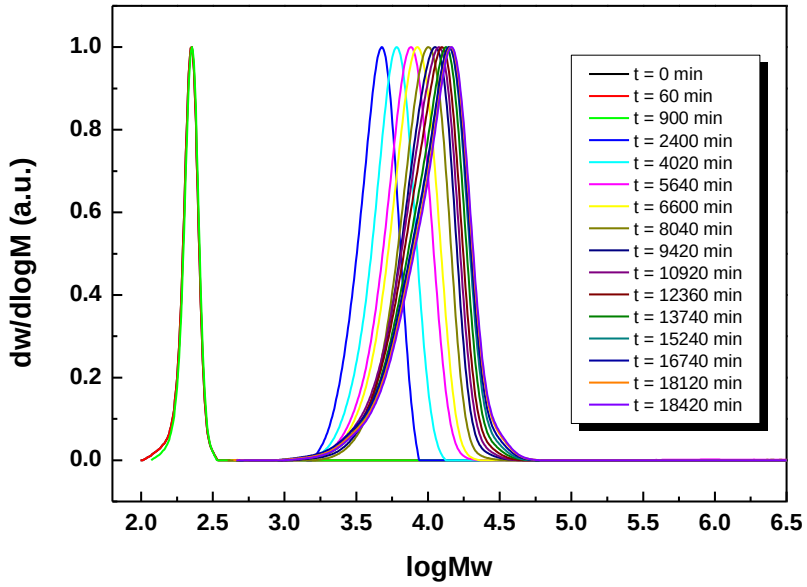

(a)

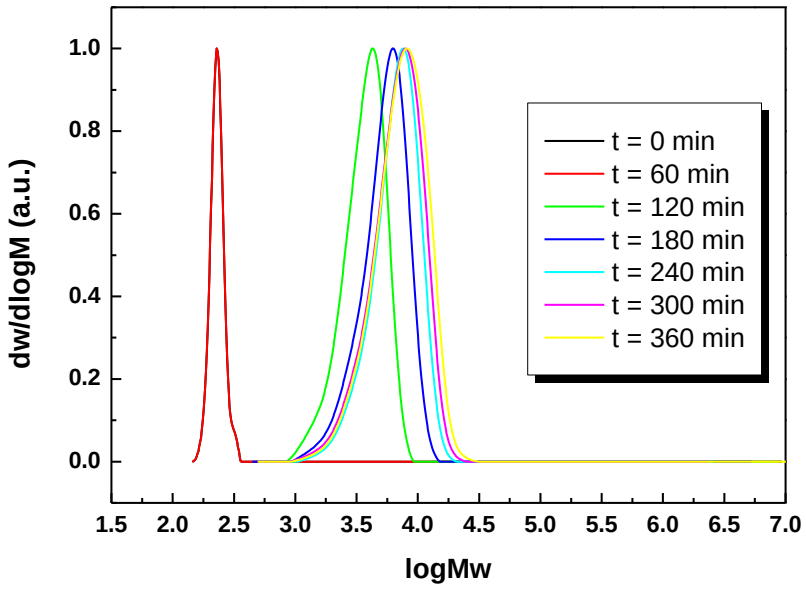
dw/dlogM (a.u.)
logMw
t = 0 min
t = 60 min
t = 120 min
t = 180 min
t = 240 min
t = 300 min
t = 360 min

(b)

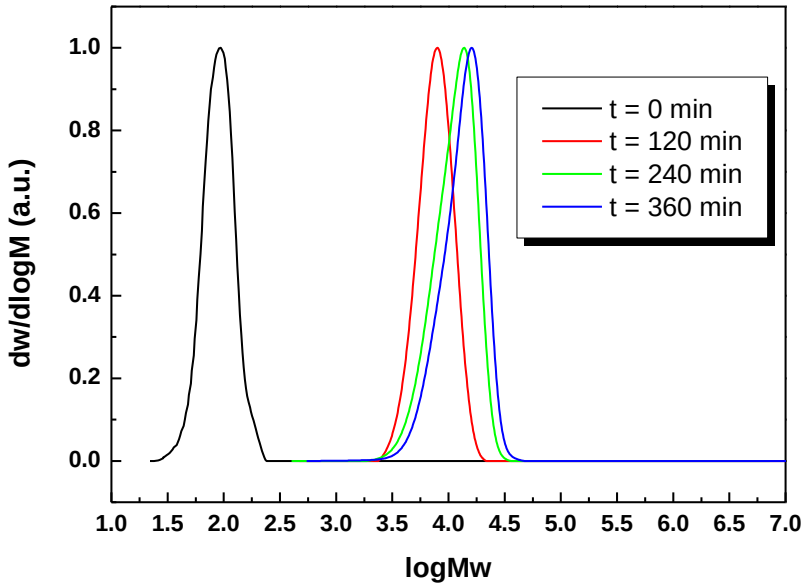
dw/dlogM (a.u.)
logMw
t = 0 min
t = 120 min
t = 240 min
t = 360 min

(c)

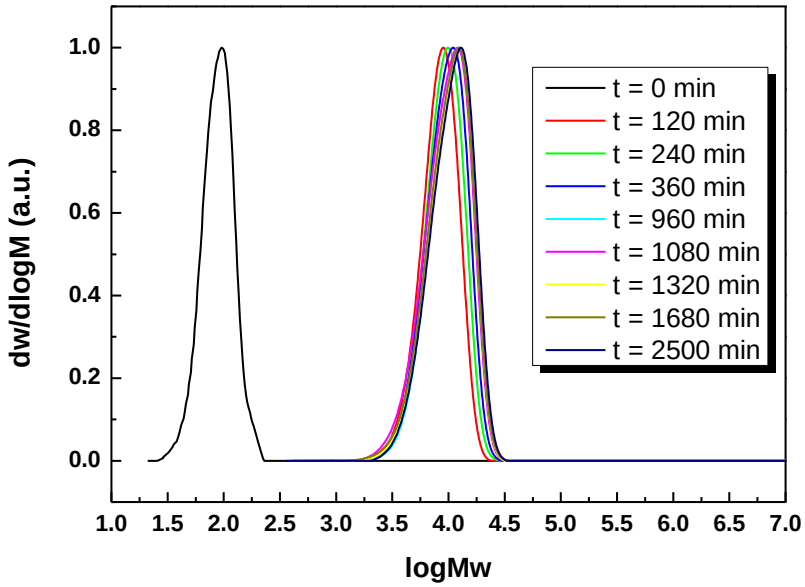

(d)

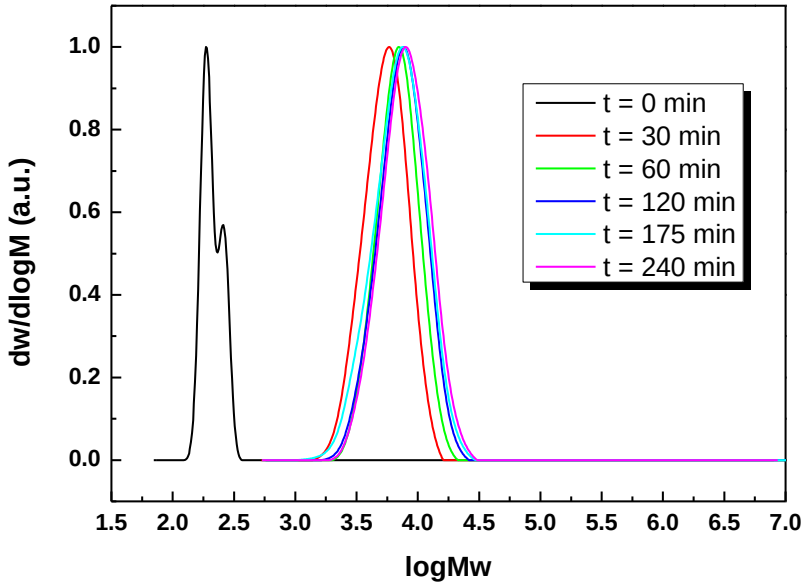

(e)

Figure 4.2 GPC traces (normalized to peak height) of P(TMS-PgMA) *via* ATRP polymerization, (a) TM1; (b) TM2; (c) TM3; (d) TM4; (e)TM6.

Firstly, the polymerization was performed at relatively low temperature, 30

^{o}C, in order to avoid retro-Diels-Alder deprotection of the initiator (**3**) . However, the rate of polymerization was slow. The polymerization reached 93% conversion after 12 days of reaction, TM1. As expected, when the temperature was increased to 70 ^{o}C, the polymerization rate increases (54% conversion in 6 hours) and the protected-maleimide moiety of initiator still remained stable over the reaction time, TM2.

The ligand type has a great effect on the rates of polymerization and resulting molecular weights. The rate of polymerization in presence of *N*-(*n*-octyl)-2-pryidylmethanimine ligand (Octyl-L) (TM4) was found to be slower than the polymerization in presence of *N*-ethyl-2-pryidylmethanimine (Ethyl-L) (TM3). This is ascribed to the length of the alkyl group effecting the solubility of the catalyst.[101] When the length of the alkyl group was increased, the copper complexes became more soluble in nonpolar media. At present it is not fully understood why the rate of polymerization is faster for the heterogeneous polymerization, which needs to be further investigated. In the two reactions, both of M_n increased with conversion and the molecular weight distributions remained narrow.

In order to prepare low DP of polymer, the polymerizations were performed in presence of high concentration of initiator, TM6, TM7, TM8. The first-order kinetic plots of the polymerization of TM6, TM7 and TM8 showed good linear relations, yet the dependence of M_n with monomer conversion showed some deviation from the linearity, but the polydispersity index (PDi) were low at 1.22,

1.27 and 1.24, respectively, **Table 4.1**, **Figure 4.1**, **Figure 4.2**.

The formation of trimethylsilyl protected polymer was shown by ^{1}H NMR with the disappearance of the two vinyl peaks of the TMS-PgMA monomers at 5.59 ppm and 6.15 ppm. The ratio of the corresponding integration values of the **3** peaks (δ = 4.59 ppm) to the **4** peak (δ = 0.19 ppm) was 2:9 which demonstrated that the pendant trimethylsilyl groups kept unchanged. It could further be seen the small signal of maleimide-protected units (**a, b**) of the initiator (δ = 6.54 ppm and 5.27 ppm) after the polymerization in the **Figure 4.3**.

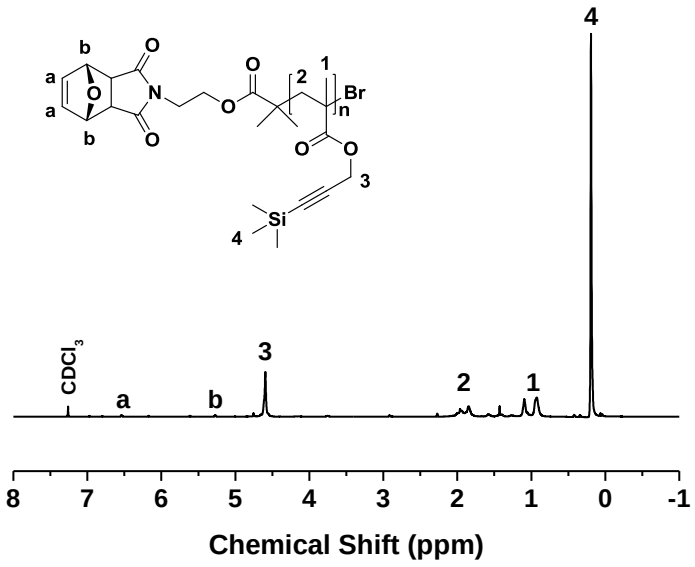

Figure 4.3 ^{1}H NMR spectrum of the PTMS-PgMA prepared by ATRP, TM2. Reaction conditions: [M]:[I]:[Cu(I)]:[Ethyl L] = 50:1:1:2 in toluene at 30 ^{o}C.

The clickable polymer with pendent alkyne functional groups then can be obtained by deprotection reaction to remove the trimethylsilyl protecting group.

The deprotection reaction was performed by addition of tetrabutyl ammonium fluoride (TBAF) solution in presence of acetic acid buffering agent at ambient temperature.

The successful removal of the trimethylsilyl group was demonstrated by ^{1}H NMR with the disappearance of the trimethylsilyl signal at 0.19 ppm along with the appearance of an alkyne signal at 2.50 ppm. The ratio of the corresponding integration values of the **3** peaks (δ = 4.62 ppm) to the **4** peak (δ = 2.50 ppm) was 2:1 which suggested that the pendant acetylene groups remained intact. It could further be seen the peaks of maleimide-protected terminals (**a, b**) of the initiator (δ = 6.54 ppm and 5.27 ppm) after the deprotection reaction in the **Figure 4.4**.

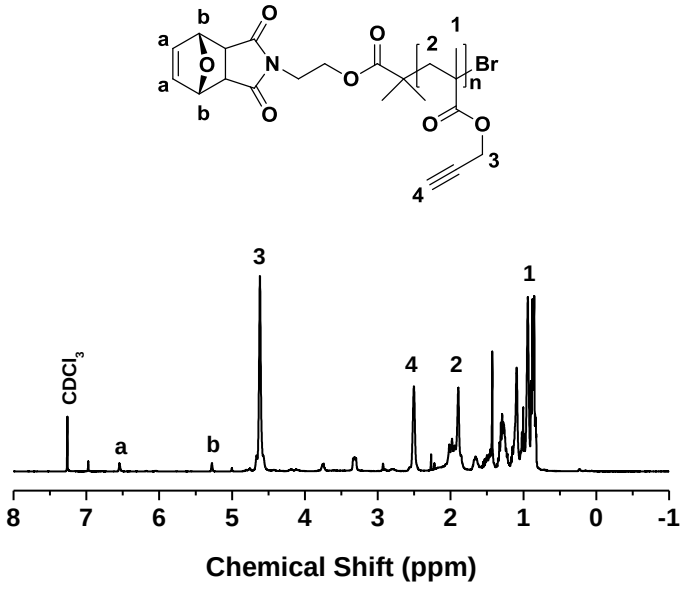

Figure 4.4 ^{1}H NMR spectrum of the polymer after deprotection reaction, PA2

The removal of the trimethylsilyl group was further be confirmed by FT-IR

spectra and GPC spectra. For example, the major difference between the two FT-IR spectra was appearance of one new absorption band at 3293 cm^{-1} attributed to alkyne C-H stretching vibration (υ (≡C-H)) after deprotection reaction. In addition, the original characteristic absorption peaks of the CH_3 symmetric deformation of Si-CH_3 (δ_s (Si(C-H_3))) at 1250 cm^{-1} and the CH_3 rocking mode of Si-CH_3 (ρ (Si(C-H_3))) at 840 cm^{-1} also disappeared after removal of the trimethylsilyl group. Moreover, the absorption bands of the alkyne C≡C stretching vibration (υ (C≡C)) shifted from 2189 cm^{-1} to 2128 cm^{-1} after the deprotection reaction, **Figure 4.5**.[1, 6, 13] Moreover, The GPC analysis also revealed that, as expected, the number average molecular weight of the polymer deceased from 6200 Da to 4200 Da after protection reaction while the PDi of the polymer remained constant, **Figure 4.6**.

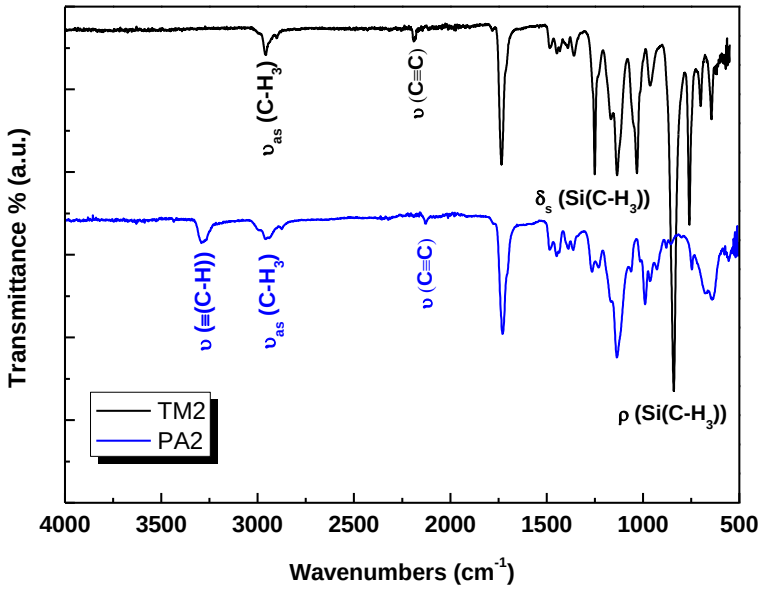

Figure 4.5 FT-IR spectra of the polymer before (TM2) and after (PA2) deprotection

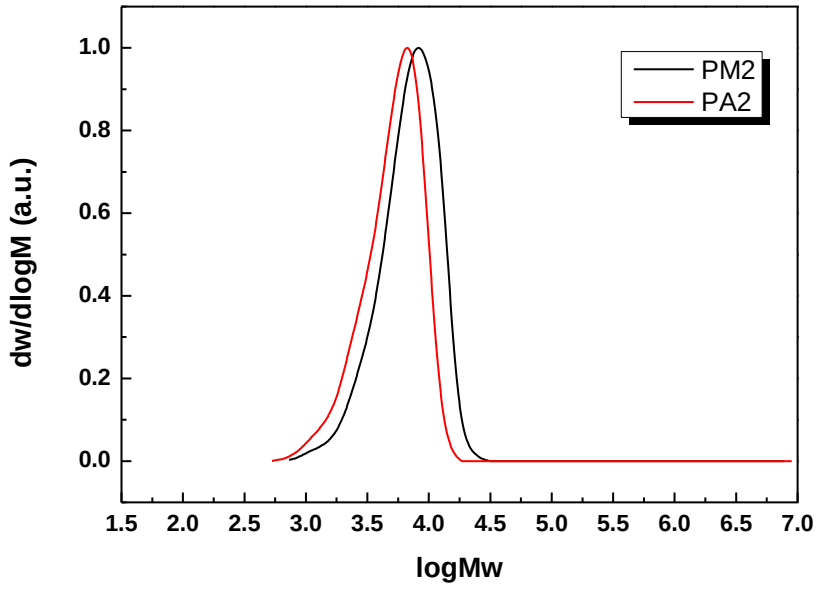

Figure 4.6 GPC spectra of the polymer before (TM2) and after (PA2) deprotection

4.3.2. Synthesis of the "clickable" alkyne copolymers (7,13)

Both the monomers trimethylsilyl-protected propargyl methacrylate (M_1) and triisopropylsilyl-protected propargyl methacrylate (M_2) were synthesized using methacryloyl chloride reaction with 3-(trimethylsilyl)-2-propyn-1-ol or 3-(1,1,1-triisopropylsilyl)-2-propyn-1-ol, respectively. Maleimide-protected initiator was chosen as the furan protecting units' protons can be used as ^{1}H NMR internal standards for the calculation of the $M_{n,\,NMR}$ of the corresponding

copolymers and the α-maleimide functional terminal after deprotection can be conjugated with some thiol-containing protein, **Scheme 4.10**

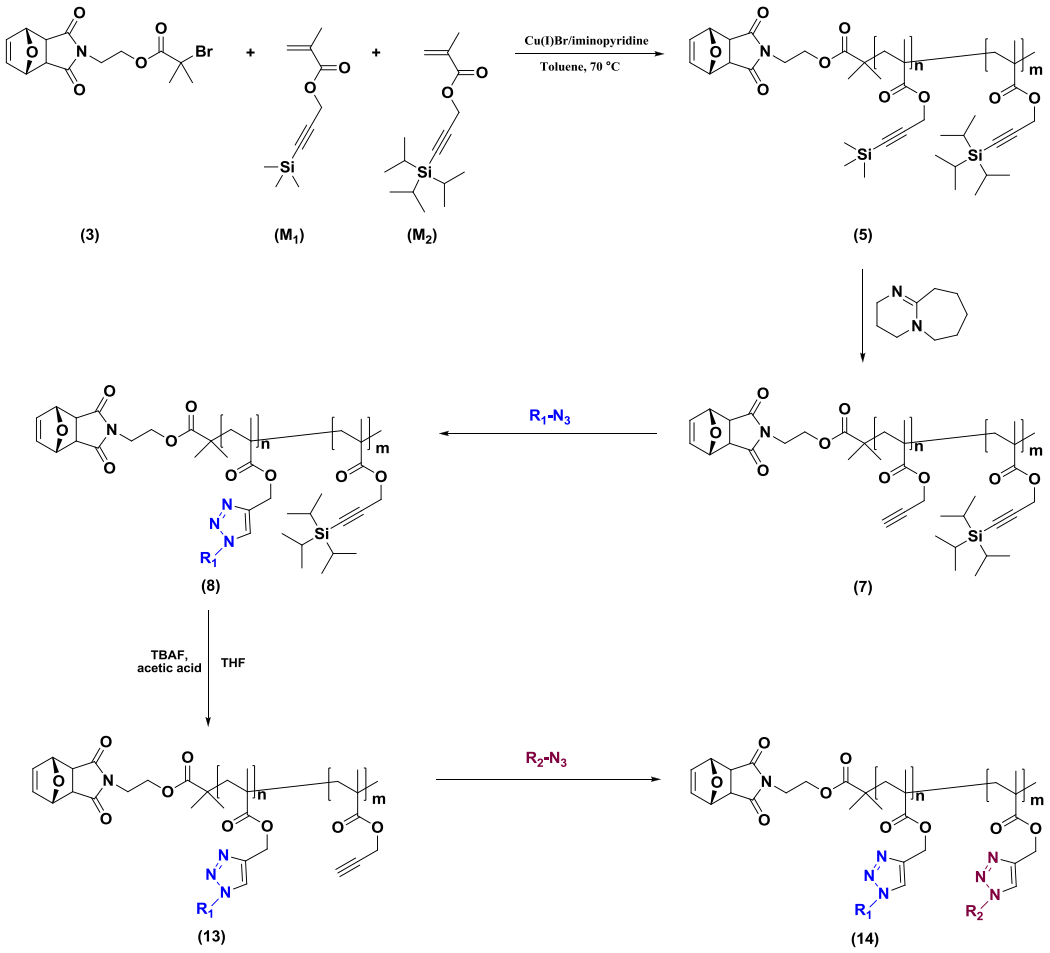

Scheme 4.10 Synthesis approach towards to "clickable" alkyne copolymers

The first step involved synthesis of PTMSPgMA-*co*-PTIPSPgMA copolymers which were prepared by a general polymerization strategy in presence of a CuBr/alkylpyridylmethanimine type ligands in toluene as solvent. Secondly, the trimethylsilyl protecting groups in the polymer were removed by treatment with DBU solution in isopropyl alcohol whilst the triisopropylsilyl group remained unchanged, and then reaction with organic azide compounds *via*

CuAAC click reaction. Finally, the triisopropylsilyl protecting units in copolymers were removed by the addition of TBAF in THF solution in the presence of acetic acid as buffering agent and following CuAAC click reaction with different organic azides. Therefore, a series of copolymers with different functional groups could be synthesized by this strategy.

The results of the statistical copolymerization of PTMSPgMA-*co*-PTIPSPgMA are shown in **Figure 4.7**, **Figure 4.8**. The first-order kinetic plots showed a good linear relationship during the polymerization yet the dependence of M_n on the monomer conversion displayed some deviation from the linear mode along with the narrow PDi of product, which suggests that the polymerization had processed in a controlled fashion.

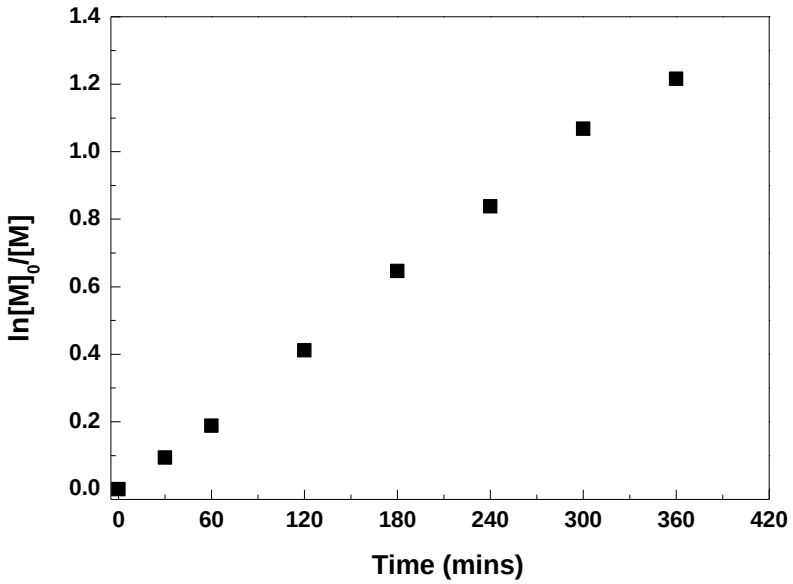

(a)

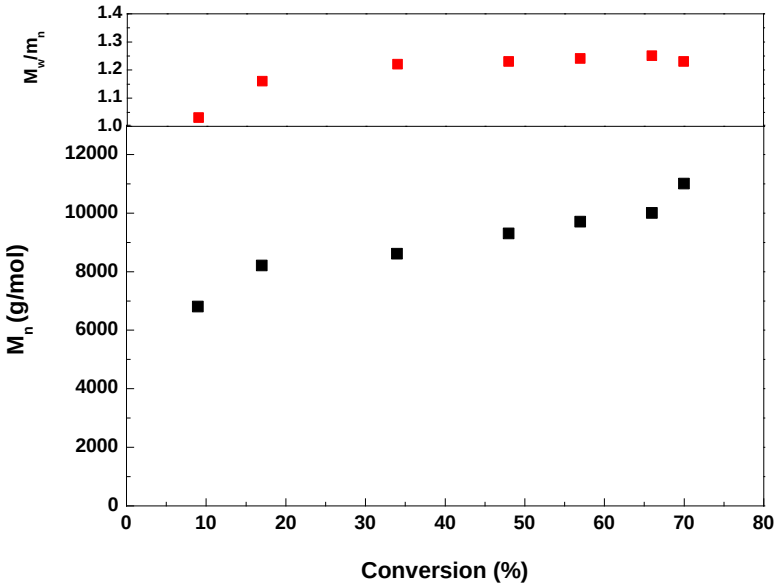

(b)

Figure 4.7 (a) Kinetic plots of copolymerization of P(TMSPgMA-*co*-TIPSPgMA); (b) dependence of M_n and MWDs on the monomer conversions. Reaction conditions: $[M_1]:[M_2]:[I]:[Cu(I)]:[Ethyl\ L] = 25:25:1:1:2$, $W_M:W_{Solv.} = 1:2$, T = 70 °C.

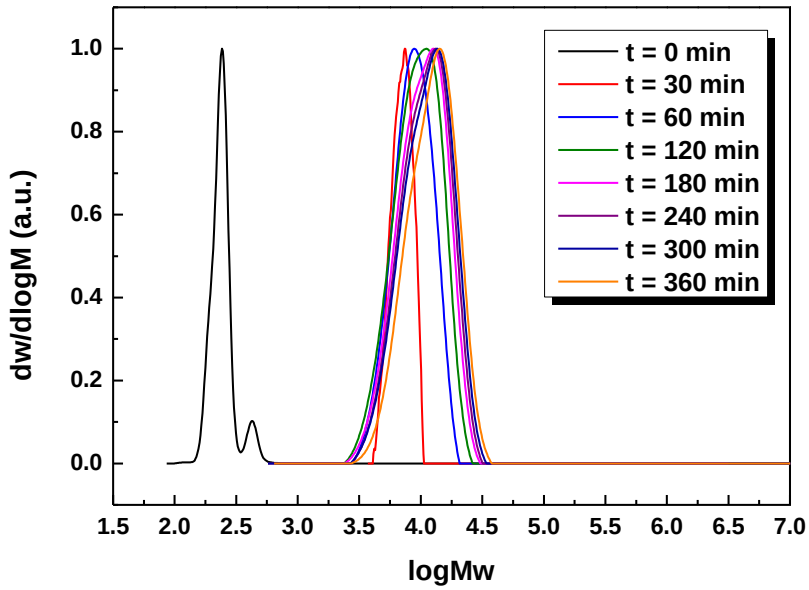

Figure 4.8 GPC traces (normalized to peak height) of P(TMSPgMA-*co*-TIPSPgMA).

The evolution of P(TMSPgMA-*co*-TIPSPgMA) copolymer was monitored by ^{1}H NMR with the disappearance of four vinyl peaks of TMS-PgMA monomers (5.59 ppm, 6.15 ppm) and TIPS-PgMA monomers (5.58 ppm, 6.13 ppm), **Figure 4.9 (a)**. The peak of **4** (δ = 0.19 ppm) attributed to the trimethylsilyl groups and the **4'** peaks (δ = 1.09 ppm) attributed to the triisopropylsilyl groups were shown in the **Figure 4.9 (b).** It could further be seen the small signal of maleimide-protected units (**a, b**) of the initiator (δ = 6.54 ppm and 5.27 ppm) after the polymerization in the **Figure 4.9 (b)**.

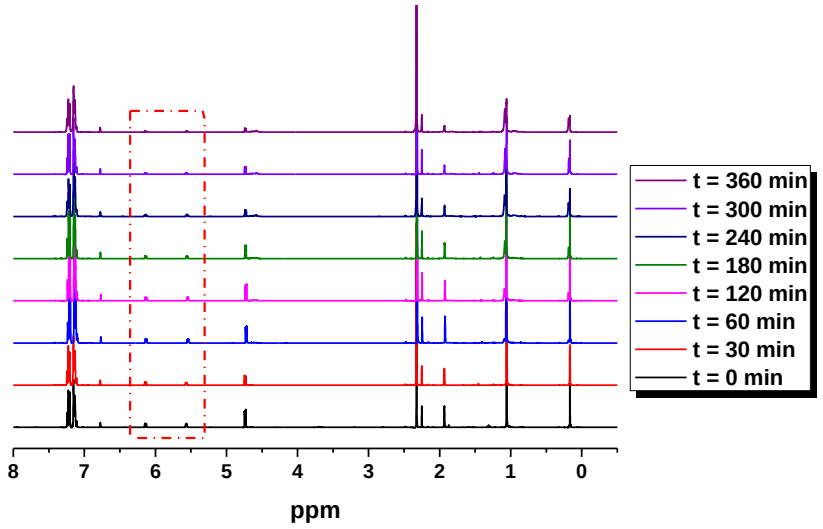

(a)

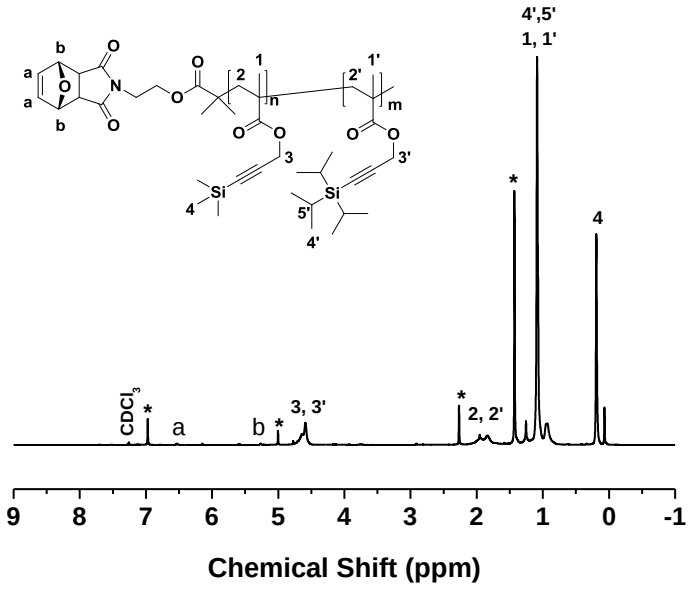

(b)

Figure 4.9 (a): Copolymerization of PTMSPgMA-*co*-PTIPSPgMA followed by ^{1}H NMR. (b): ^{1}H NMR spectrum of the PTMSPgMA-*co*-PTIPSPgMA copolymer. * The characteristic signals of 2,6-bis(1,1-dimethylethyl)-4-methyl phenol (BHT).

4.3.3. Synthesis of sugar azides (9)

A novel one-step and highly stereoselective synthesis method for various glycosyl azide, *via* an intermolecular nucleophilic attack of the azide ion to the anomeric carbon atom of unprotected sugars in presence of 2-chloro-1,3-dimethylimidazolinium chloride (DMC) and triethylamine in water, were described by S. Shoda *et al.*[105] The reaction conditions require the sugar without protection of hydroxyl group and preformed smoothly in aqueous solvent

at ambient temperature which leads to the synthesis method of glycosyl azide without complicating sugar protection and deprotection chemistry.

Based on these results, the reaction mechanism for DMC-mediated formation of sugar azides was proposed, **Scheme 4.11**. One plausible mechanism involves the nucleophilic attack of hemiacetal-type hydroxyl group of *β*-D-glucose (**1β**) to the 2 position of DMC, generating a reactive intermediate **2β** with *β* configuration promoted by triethylamine or *N*,*N*-diisopropylethylamine. The 2-hydroxy group of **2β** then attacks the anomeric carbon atom, affording an 1,2-anhydro intermediate **3** and 1,3-dimethyl-2-imidazolidinone (DMI) in presence of triethylamine or *N*,*N*-diisopropylethylamine. The third step is the attack of sodium azide to the anomeric carbon of **3** from the *β* side, giving rise to *β*-D-glucopyranosyl azide (**4β**). Conversely, the *α*-D-glucose (**1α**) is in equilibrium with *β*-D-glucose which also can react with DMC to form the corresponding *α*-glycosyl adduct **2α**. Nevertheless, the resulting intermediate **2α** is hydrolyzed by the attack of water *via* S_N2 or S_N1 nucleophilic substitution reaction, regenerating the *β*-D-glucose (**1β**). The formation of other glycosyl azides can be explained in the similar mode, **Scheme 4.11** (a).

Another plausible mechanism involves the initial formation of the a reactive intermediate **2β** with *β* configuration as a result of a nucleophilic attack of hemiacetal-type hydroxyl group of *β*-D-glucose (**1β**) to the 2 position of DMC promoted by triethylamine or *N*,*N*-diisopropylethylamine as a general base. The resulting intermediate **2β** is then converted to the 1,2-anhydro intermediate **3** by

the adjacent group reaction between the 2-hydroxy group and the anomeric carbon in presence of triethylamine or *N*,*N*-diisopropylethylamine, along with forming 3-dimethyl-2-imidazolidinone (DMI). After this stage, sodium azide attacks to the anomeric carbon from *β* side to afford *β*-D-glucopyranosyl azide (**4β**). Besides the *α*-D-glucose (**1α**), being in equilibrium with *β*-D-glucose it can also react with DMC to form a corresponding *α*-glycosyl adduct **2α**, which is attacked by sodium azide to generate *β*-D-glucopyranosyl azide (**4β**) and DMI. This route can be used to explain the formation of other sugar azides, **Scheme 4.11** (b).[105-108]

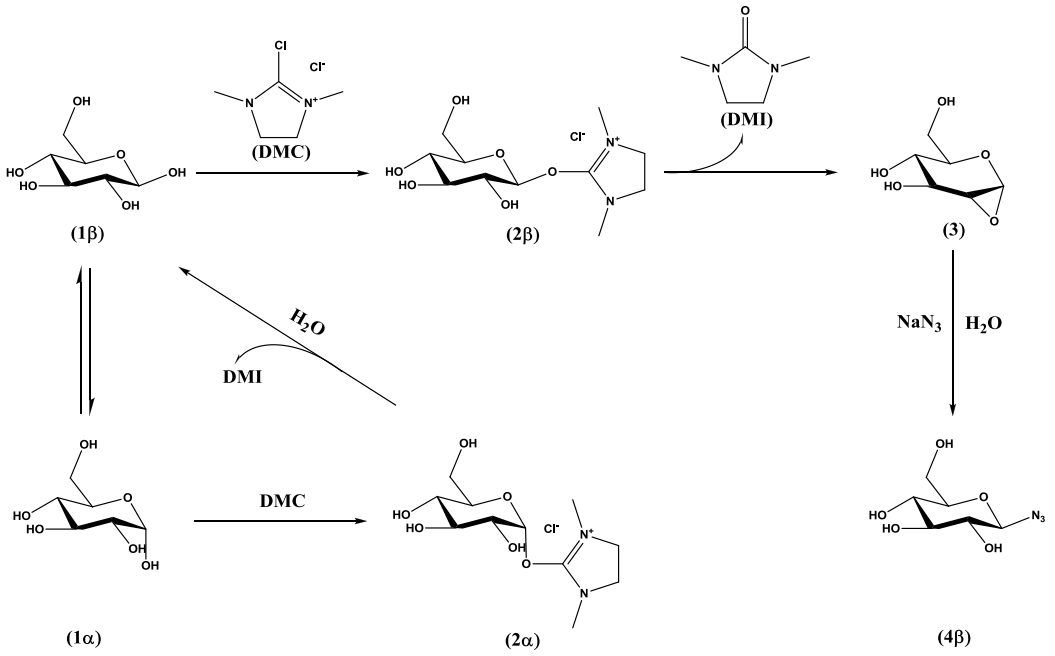

(a)

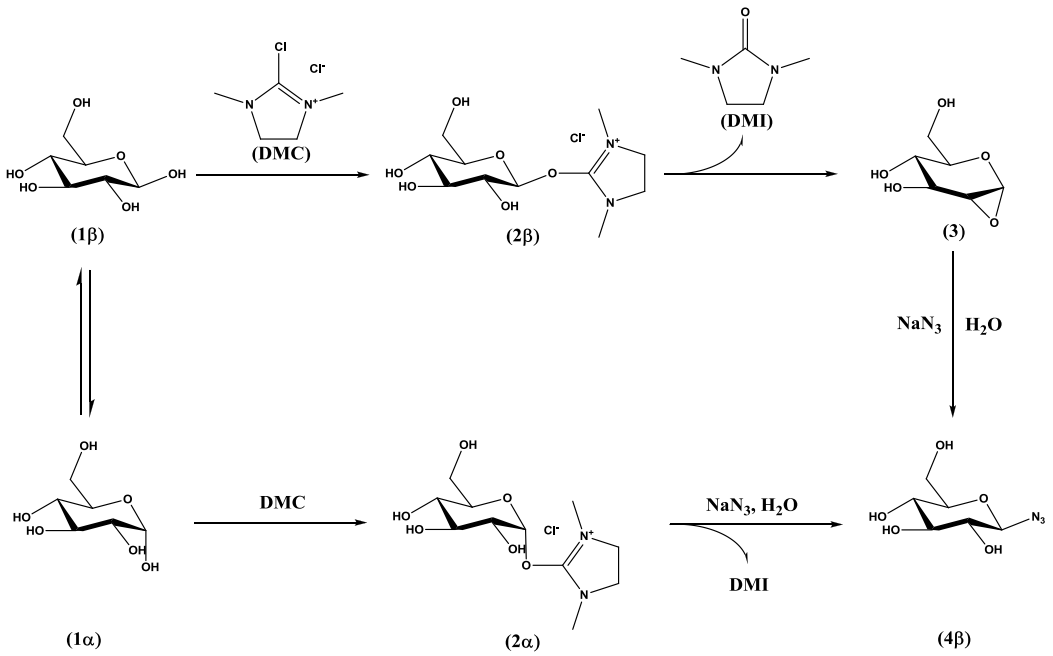

(b)

Scheme 4.11 Plausible mechanisms for sugar azides formation *via* one-step reaction in aqueous media

The synthesis of sugar azides in this work were performed according to the similar method of S. Shoda *et al*. but the purification process was changed from an HPLC protocol to precipitation in ethanol and use of a strongly acidic cation exchange resin column and extraction. The desired sugar azides were isolated as off-white solids with yields of approximately 90%. Compared with the FTIR spectra following to the α-D-mannopyranosyl azide purification process, there was a single absorbance band of the azide group (υ_{as}(-N_3) asymmetric stretching vibration) at 2110 cm^{-1} and the characteristic absorbance peak of the NaN_3 at 2022 cm^{-1} disappeared completely after the Amberlite IR-120 column, **Figure 4.10** (a). It has the similar results from the FTIR spectra following the

preparation process of β-D-galactopyranosyl azide, **Figure 4.10** (b). There was also one single absorbance peak at 2116 cm^{-1} attribute to the azide group ($\upsilon_{as}(-N_3)$ asymmetric stretching vibration) of β-D-galactopyranosyl azide.

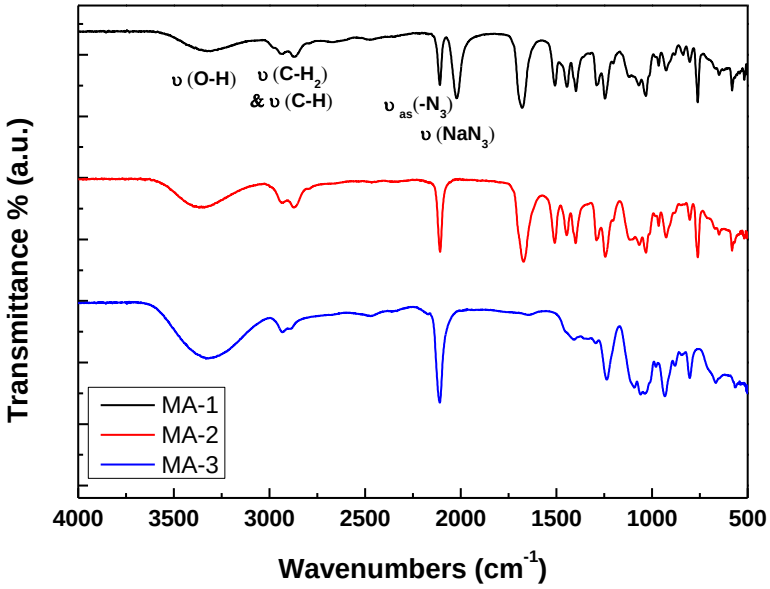

(a)

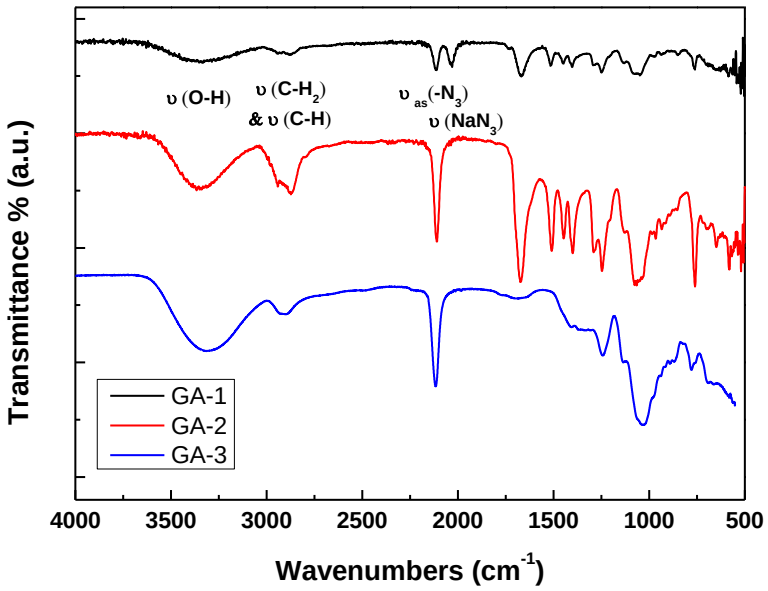

(b)

Figure 4.10 (a) FT-IR spectra of *α*-D-mannopyranosyl azide, MA-1: before the Amberlite IR-120 column; MA-2: after the Amberlite IR-120 column; MA-3: extraction and freeze-drying; (b) FT-IR spectra of β-D-galactopyranosyl azide, GA-1: before the Amberlite IR-120 column; GA-2: after the Amberlite IR-120 column; GA-3: extraction and freeze-drying

The desired sugar azides were prepared *via* a one-step reaction which was confirmed by ^{1}H NMR and ^{13}C NMR spectra, **Figure 4.11**. The anomeric azide with axial configuration (α) or equatorial configuration (β) can be determined by the ^{1}H NMR. The α-glycosides have higher chemical shifts (> 5 ppm) and smaller coupling constants (J) than the corresponding β-isomers. Most of the glycosyl azides were converted to β-anomers except of mannose azide with axial configuration. The concentrations of the β-glycosyl azides were up to 80%, indicating the reaction with high stereoselectivity, which were confirmed by the

^{1}H NMR spectra where two different strength signs of anomeric proton and the ^{13}C NMR spectra where a single signal of anomeric carbon appeared between 89 ppm and 100 ppm. These results supported the reaction mechanism for sugar azides formation *via* 1,2-anhydro intermediate as a result of neighboring group participation reaction.[108] Compared to the previous glycosylation synthesis of Koenigs-Knorr reaction requiring the protection, deprotection, catalysts, dry organic solvent, additional purification and long reaction period, this method is more simple and efficient.[109-114]

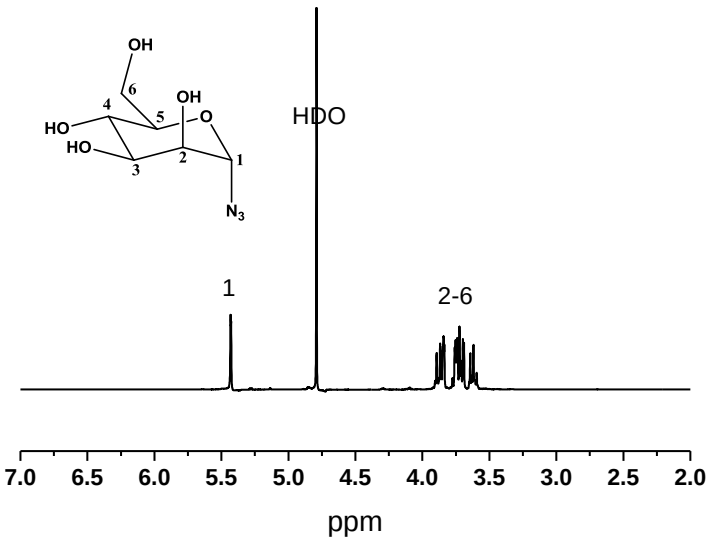

(a)

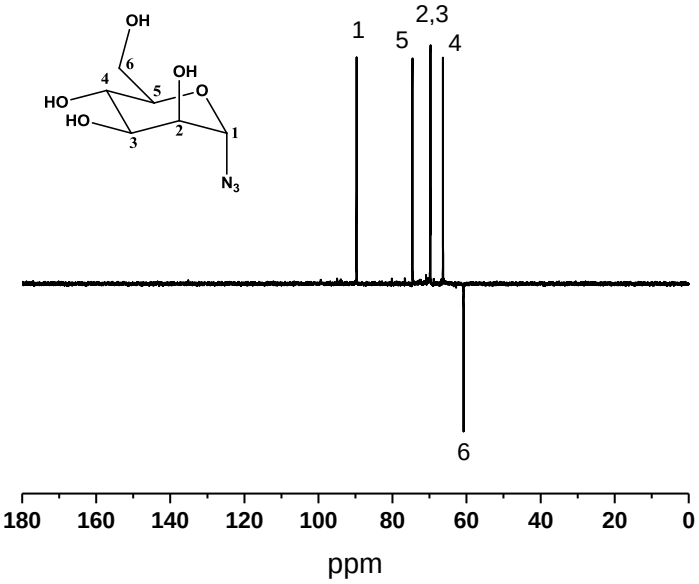

(b)

Figure 4.11 (a) ^{1}H NMR spectrum of α-D-mannopyranosyl azide in D_2O; (b) ^{13}C NMR spectrum of α-D-mannopyranosyl azide in D_2O.

4.3.4. Synthesis of glycopolymers (10) *via* CuAAC click chemistry

The polymers with pendant alkyne functional groups (**6**), (**7**) and (**13**) were used as one of the starting materials for the synthesis of various glycopolymers, obtained by CuAAC click reaction with a series of different of glycosyl azides. In this study, α-D-mannopyranosyl azide and β-D-galactopyranosyl azide were used as model of sugar-based azides for the click reaction. The CuAAC reaction conditions performed in presence of CuBr/*N*-ethyl-2-pyridylmethanimine/

triethylamine catalyst system in DMSO to ensure the complete solubility of all reagents and the product was purified by dialyzing against water/methanol and then freeze-drying, which was described by Haddleton *et al*, **Scheme 4.12**.[114-117]

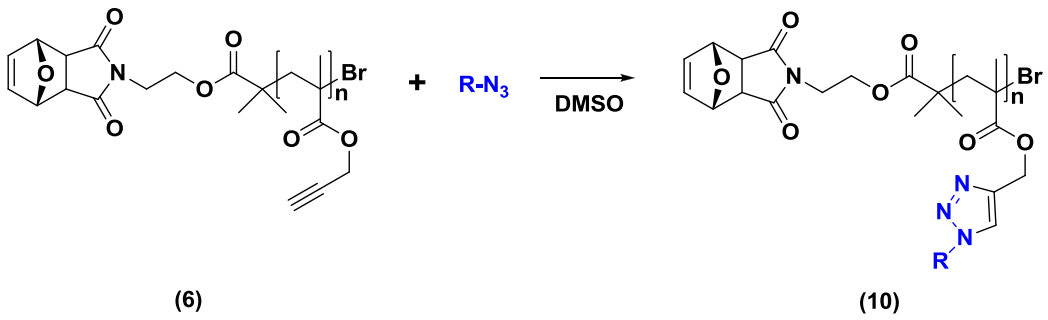

(6) (10)

Scheme 4.12 Synthesis approach towards to glycopolymers *via* CuAAC click reaction. Reagents: R = α-D-mannopyranosyl azide, β-D-galactopyranosyl azide, β-D-glucopyranosyl azide or β-L-fucopyranosyl azide. Reaction conditions: RN_3, CuBr, *N-ethyl*-2-pyridyl-methanimine, triethylamine, DMSO, 25 ^{o}C

Table 4.2 summarized the versatility of glycopolymers with different molecular weights and different sugar groups. The number average molecular weight and polydispersity index of all glycopolymers were obtained by GPC using DMF as the mobile phase.

Table 4.2 Maleimide-protected glycopolymers with different sugar groups

Run	Pendant Sugar units	M_n(GPC) g mol^{-1}	DP (GPC)	PDi
GP1	Mannose	9600	28	1.27
GP2	Galactose	10200	30	1.27

GP3	Mannose	18000	54	1.18
GP4	Galactose	14500	43	1.32
GP5	Mannose	18800	56	1.28
GP6	Galactose	20800	62	1.32

Obtained by GPC analysis using DMF as the mobile phase and DRI detection

The successful CuAAC click reaction was confirmed by the ^{1}H NMR spectra of glycopolymers with the appearance of the new triazole peak **i** at 8.3 ppm and several typical peaks (δ = 3.3-6.0 ppm) from the mannose units (**Figure 4.12** (a)) or the new triazole peak **i** at 8.3 ppm and several typical peaks (δ = 3.3-6.2 ppm) from the galactose group (**Figure 4.12** (b)). The ratio of the corresponding integration values of the **g** peak to **i** peak was 3:1, which suggested that the conversion of CuAAC click reaction had reached close to 100%. It could further be seen the small signal of maleimide-protected units (**a, a'**) in the glycopolymers, **Figure 4.12**.

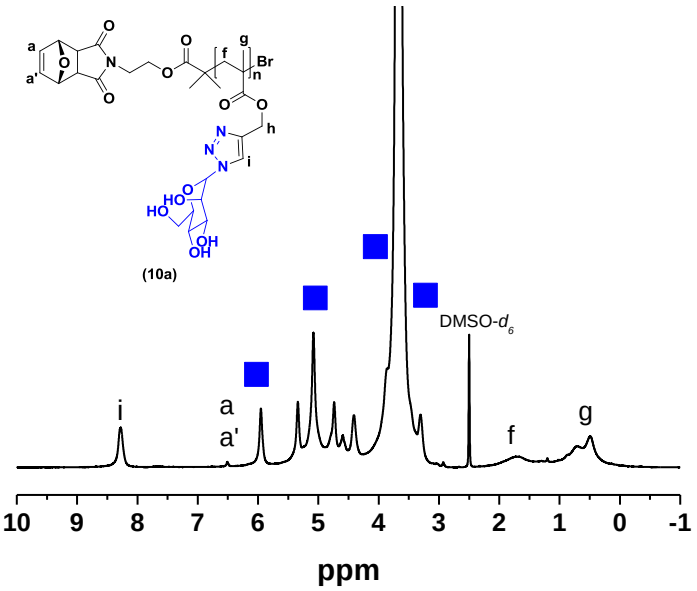

(a)

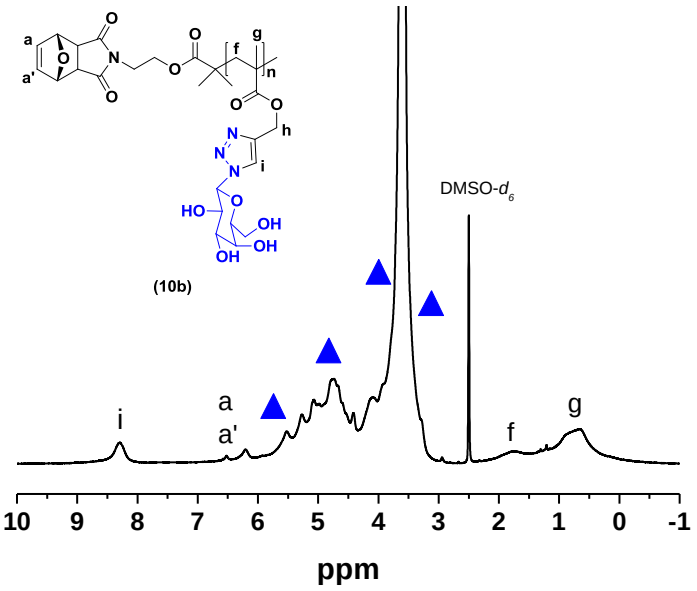

(b)

Figure 4.12 ^{1}H NMR spectra of the glycopolymer prepared by CuAAC click reaction in DMSO-d_6. (a) GP5, ■: The characteristic peaks of mannose units. (b) GP6, ▲: The characteristic peaks of galactose units.

Moreover, both GPC and FTIR data further indicated that the glycopolymers were successfully prepared. For example, the M_n of the polymer increased from 8000 Da (clickable polymer, PA6) to 18000 Da and 14500 Da, respectively (after CuAAC click reaction, GP3 and GP4), **Figure 4.13**. Meanwhile, the MWD of the polymer remained unchanged.

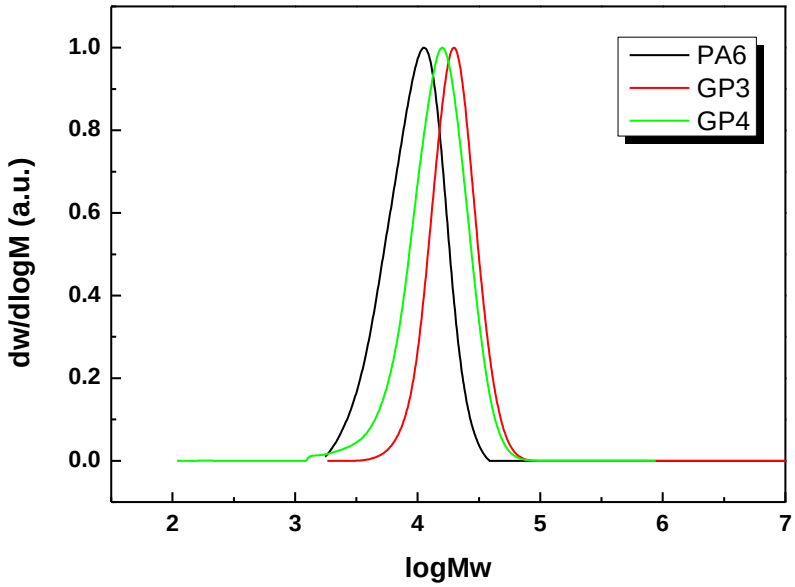

Figure 4.13 GPC spectra of the polymers before and after CuAAC click reaction

Furthermore, compared with the FTIR spectra of the polymer before and after CuAAC click reaction, the original characteristic absorption band of the alkyne group ($\upsilon_{(C\equiv C)}$ stretching vibration) at 2128 cm^{-1} disappeared after the click reaction with sugar azide. One new large board peaks at 3345 cm^{-1} or 3350 cm^{-1} assigned to $\upsilon_{(O-H)}$ stretching vibration appeared and the triazole groups $\upsilon_{(N=N)}$ stretching

vibration frequencies appeared at 1642 cm^{-1} or 1639 cm^{-1} region after the CuAAC click reaction, **Figure 4.14**.

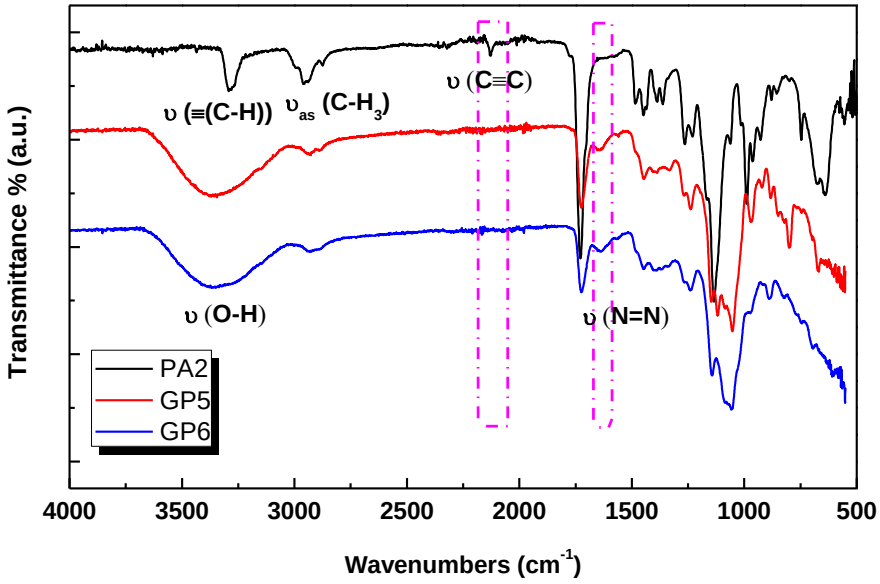

Figure 4.14 FTIR spectra of the polymers before and after click reactions

4.3.5. Polymer deprotection (Retro Diels-Alder reactions) and Preparation of FITC-labeled glycopolymers

The α-maleimide functional glycopolymers were obtained following a retro Diels-Alder reaction. One of deprotection condition was the glycopolymer was dissolved in DMSO and stirred at 80 ^{o}C or suspended in toluene and refluxed for 24 hours to remove the furan protecting group, resulting in the desired products with an α-maleimide moiety. A further reaction condition that was used heating

in a vacuum oven at 80 °C, under vacuum for 24 hours, leading to the α-functional maleimide glycopolymers without the use of the organic solvent and omitting an additional purification process, **Scheme 4.13**.

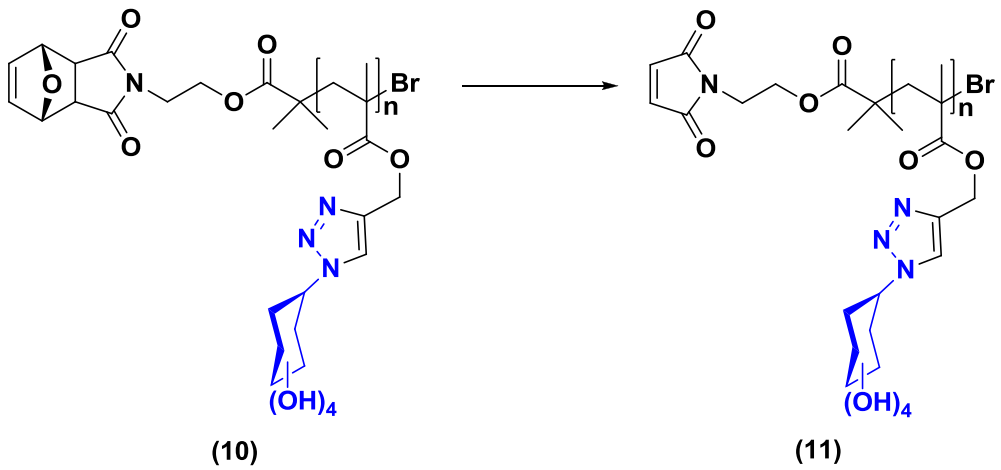

Scheme 4.13 Deprotection of α-maleimide functional group *via* retro Diels-Alder reaction

The complete removal of the furan protecting group was monitored by ^{1}H NMR spectroscopy, along with appearance of the maleimide olefinic signals at 6.95 ppm or 7.02 ppm and the disappearance of oxatricyclo vinyl peaks at 6.63 ppm or 6.54 ppm. Moreover, the triazole peak **i** at 8.32 ppm or 8.31 ppm and several typical peaks from sugar moieties remained the same as before protection, suggesting the backbones of polymers were stable in this procedure, **Figure 4.15** (a-d).

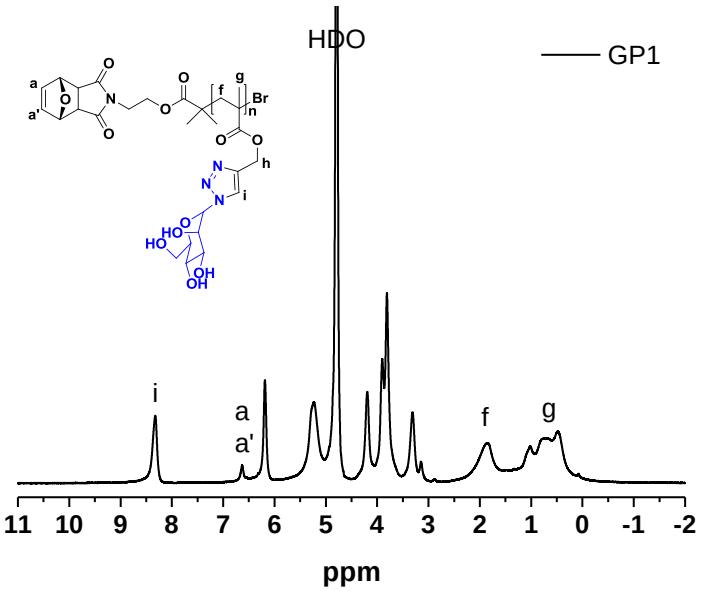
HDO
GP1
i
a
a'
f
g
11 10 9 8 7 6 5 4 3 2 1 0 -1 -2
ppm

(a)

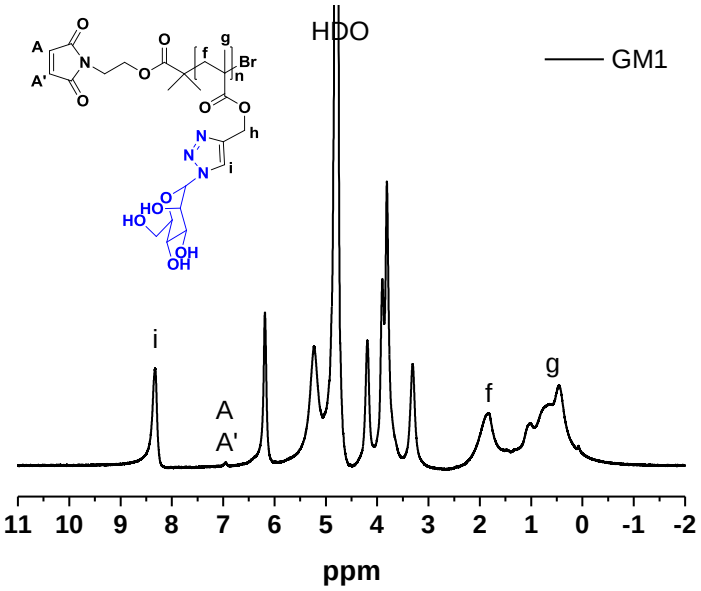
HDO
GM1
i
A
A'
f
g
11 10 9 8 7 6 5 4 3 2 1 0 -1 -2
ppm

(b)

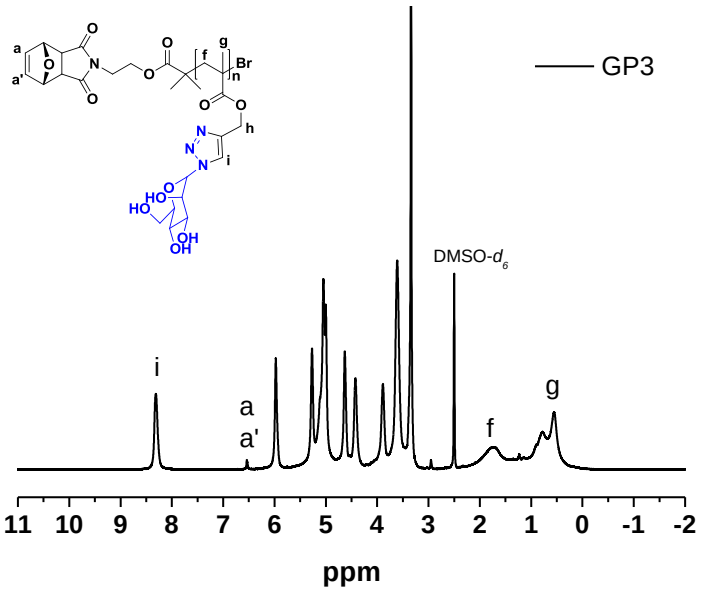

(c)

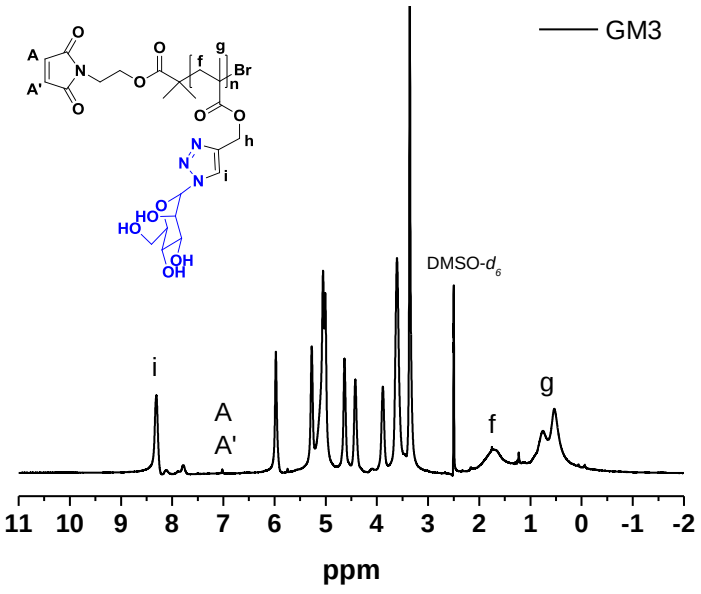

(d)

Figure 4.15 ^{1}H NMR spectra of the polymers before and after retro Diels-Alder reaction (a) GP1 in D_2O; (b) GM1 in D_2O; (c) GP3 in DMSO-d_6; (d) GM3 in DMSO-d_6.

Table 4.3 summarized the versatility of glycopolymers with different molecular weights and different sugar groups after the deprotection of α-maleimide functional group *via* Retro Diels-Alder reaction. The M_n and PDi of all glycopolymers were obtained by GPC using DMF as the mobile phase. The hydrodynamic volume and molecular distribution of the polymer essentially unchanged before and after the retro Diels-Alder deprotection reaction, which demonstrated the backbone of the glycopolymers were stable and there was not degradation and coupling side reactions in this process (**Table 4.2** and **Table 4.3**).

Table 4.3 Maleimide-terminated glycopolymers with different sugar groups

Run	Pendant Sugar units	M_n(GPC) g mol^{-1}	DP (GPC)	PDi
GM1	Mannose	9500	28	1.28
GM2	Galactose	10200	30	1.28
GM3	Mannose	18000	54	1.23
GM4	Galactose	16300	49	1.36
GM5	Mannose	18800	56	1.29
GM6	Galactose	20900	63	1.32

Obtained by GPC analysis using DMF as the mobile phase and DRI detection

About fluorescence labeling glycopolymers, the fluorescein isothiocyanate (FITC) and glycopolymers were vacuum-dried and then dissolved in anhydrous

DMF. After stirring for 24 hours under nitrogen, the polymer was purified by dialysis against distilled water and freeze-dried to afford yellow powder product, **Scheme 4.14**.

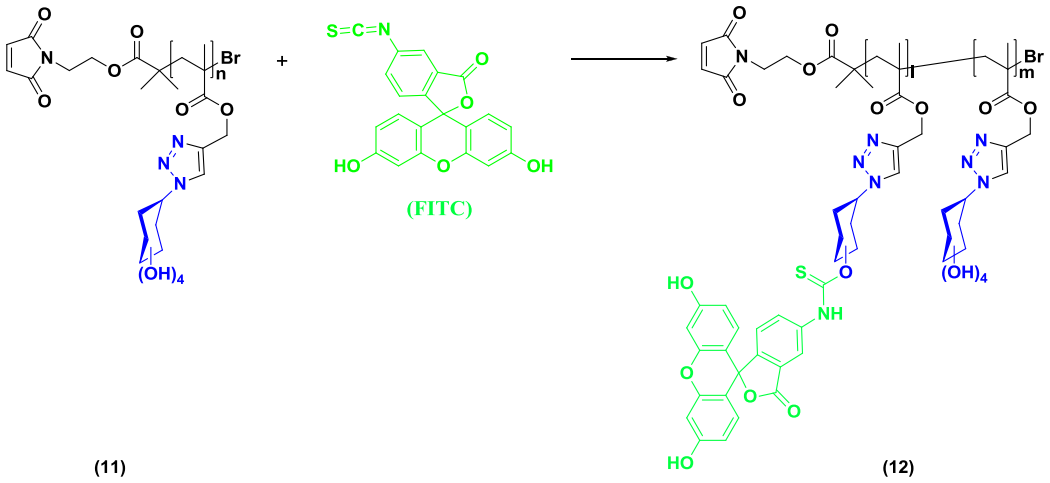

Scheme 4.14 Preparation of FITC-labeled glycopolymers **(12)**

The ^{1}H NMR spectra showed some new peaks belong to the FITC appearing from 10.05 ppm to 10.17 ppm and from 6.53 ppm to 6.67 ppm, which signified that the FITC labeling glycopolymers were successfully prepared.

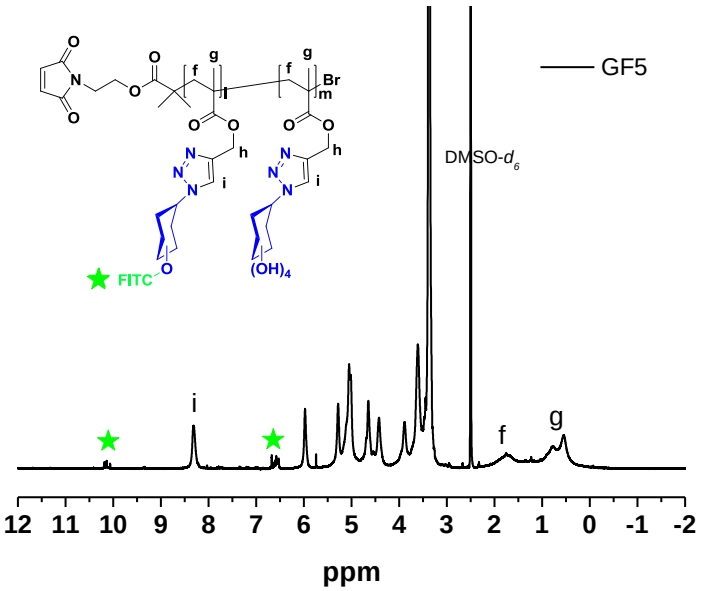

(a)

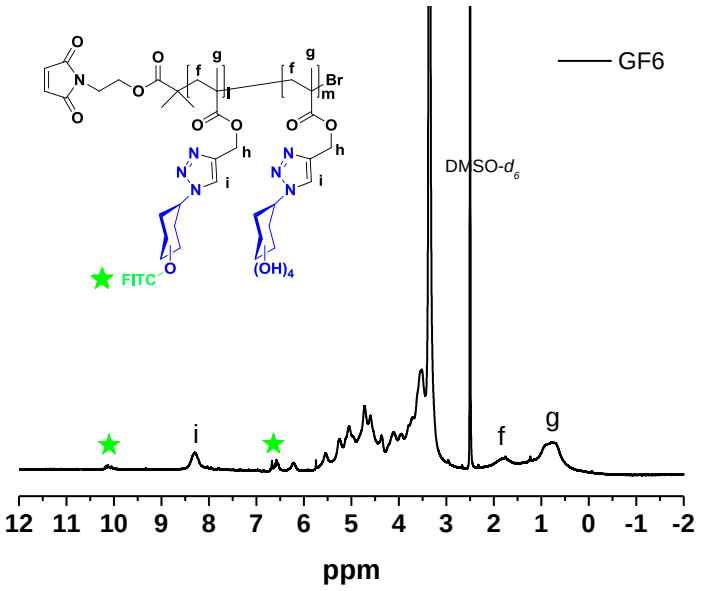

(b)

Figure 4.16 ^{1}H NMR spectra of the FITC-labeled glycopolymers (a) GF5 in DMSO-d_6; (b) GF6 in DMSO-d_6

4.3.6. Multichannel Surface Plasmon Resonance (MC-SPR)

Surface Plasmon Resonance (SPR) were observed by Wood in 1902, which was a label-free, real time, optical sensitive detection, fast, cost-effective, capable of detecting the refractive index of surface bound layer method.[118, 119] SPR was a physic optical phenomenon which occurred as a result of total internal reflection of light at metal interfaces.[120] SPR is an important new technique which has very wide range of application in many types of interface analysis, biological interaction investigation.[121-123]

As the SPR is a continuous, real-time detection, the kinetics studies can be investigated by SPR.[124-133] In the first association phase of an SPR biosensor run, the analyte (A) solution flowed over the sensor surface bound immobilized interactants (ligand, B). The association phase can be assumed to according to the simple reversible interaction model:

$$\mathbf{A + B} \underset{k_d}{\overset{k_a}{\rightleftharpoons}} \mathbf{AB} \qquad (4.1)$$

The rate of formation of AB complexes fit in the pseudo-first order process. These following equations described these relations in the association phase.

$$d[AB]/dt = k_a[A][B] - k_d[AB] \qquad (4.2)$$

$$d[AB]/dt = k_a[A]([B]_0-[AB]) - k_d[AB] \qquad \mathbf{(4.3)}$$

$$dR/dt = k_aC(R_{max}-R) - k_dR \qquad (4.4)$$

$$dR/dt = k_aCR_{max} - (k_aC + k_d)R \quad (4.5)$$

$$k_s = k_aC + k_d \quad (4.6)$$

$$R_t = (1 - \frac{k_d}{k_s})R_{\max}(1 - e^{-k_s(t-t_0)}) + R_i \quad (4.7)$$

Where *dR/dt* is the rate of formation of AB complexes; k_a is the association rate constant or on-rate ($M^{-1}s^{-1}$); k_d is the disassociation rate constant or off-rate (s^{-1}); k_s is the observed rate constant; $[B]_0$ is the concentration of B at the starting time; *C* is the molar concentration of the analyte in solution; *R* is the amount of bound analyte in resonance units; R_{max} is the capacity of the immobilized ligand in resonance units; R_i is an fitting parameter equivalent to the signal at the start of the association; t_0 is the starting time of the association and *t* is the interaction time in seconds. The observed rate constant is determined by fitting the kinetic time for a series of analyte concentrations against the corresponding amount of bound analyte in resonance units, **Eq. (4.7)**. Then the association rate constant (k_a) can be obtained from the slope of a secondary plot of observed rate constant versus the molar concentration of the analyte.

Then in the second dissociation phase, the buffer solution replaced the analyte solution and flow over the surface of the chip. The AB complexes on the sensor surface start to dissociate and release free analyte and free bound ligand. Under this condition, the dissociation relationships of the formed complexes, AB, were described by these equations:

$$d[AB]/dt = -k_d[AB] \quad (4.8)$$

$$dR/dt = -k_dR \quad (4.9)$$

$$R_t = R_a e^{-k_d (t-t_1)} + R_{(t\to\infty)} \quad (4.10)$$

$$K_A = k_a/k_d \quad (4.11)$$

$$K_D = k_d/k_a \quad (4.12)$$

Where R_a denotes the signal at the starting time of the dissociation phase; t_1 denotes the start time of the dissociation experiments; the fitting parameter $R_{(t\to\infty)}$ denotes the response value after infinite time; K_A denotes association constant and K_D denotes dissociation constant. The data obtained during the association phase can be calculated the quantitation of the dissociation rate constant (k_d) according to **Eq. (4.10)**. The significance of the kinetic studies of both the association and the dissociation will be discussed below.

Multi channel surface plasmon resonance was used to investigate the binding affinity of the glycopolymers with recombinant human DC-SIGN immobilized on the sensor chip. The interactions between glycopolymers and DC-SIGN depending on the glycopolymers concentrations were confirmed by **Figure 4.17**. The SPR response rose exponentially with an increase in the concentration of glycopolymers. The sensorgrams demonstrated that both glycopolymers and gp120 bind to the immobilized DC-SIGN with high affinity, in a dose-dependent fashion. Moreover, the maximum SPR response in the association phase changed with different glycopolymers. The RU_{max} of both glycopolymers with mannose group bigger than that of glycopolymers with galactose glycopolymers, which suggested that the amount of mannose glycopolymers attached on the surface of DC-SIGN was more than the

glycopolymers containing galactose.

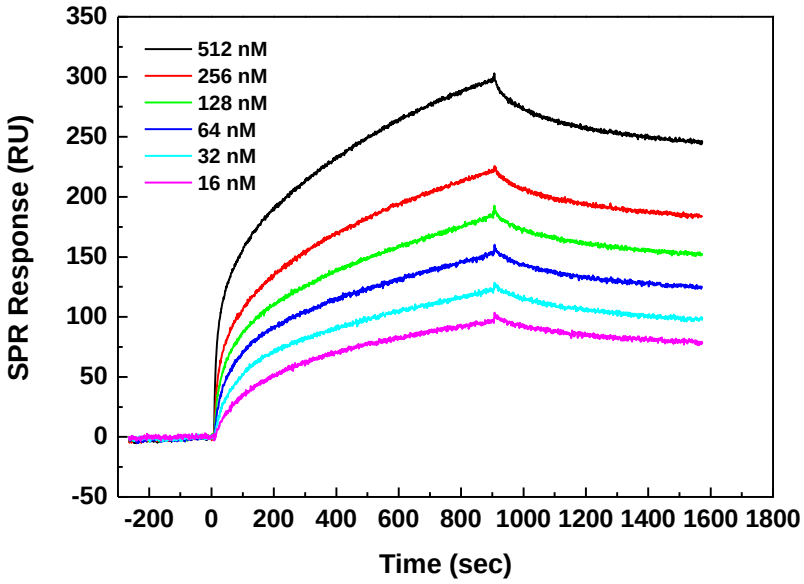

(a)

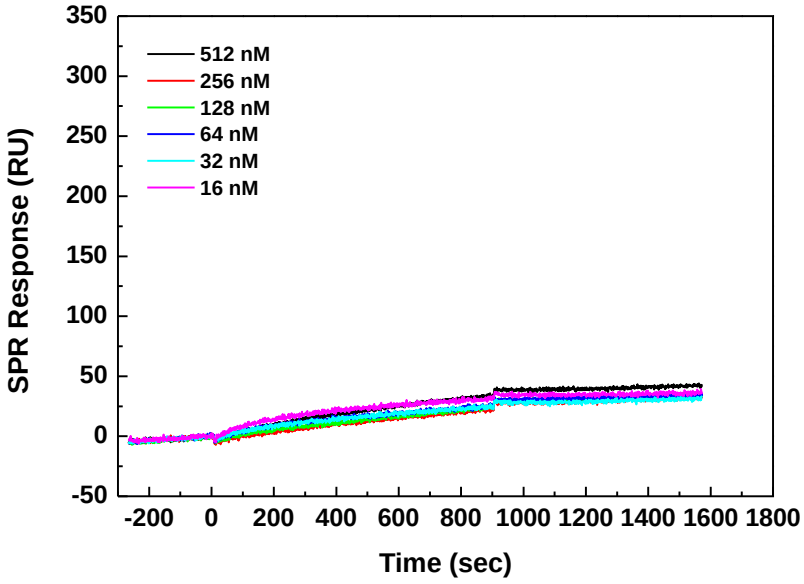

(b)

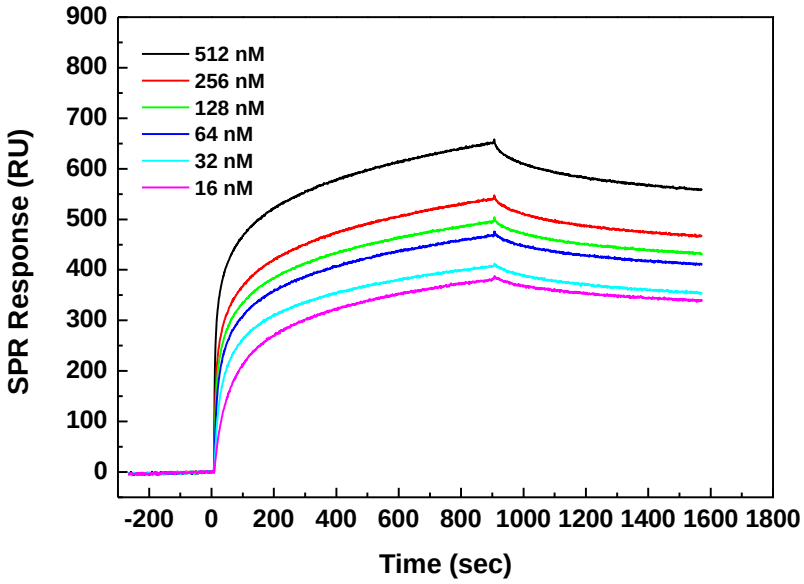
512 nM
256 nM
128 nM
64 nM
32 nM
16 nM
SPR Response (RU)
Time (sec)
900
800
700
600
500
400
300
200
100
0
-200
0
200
400
600
800
1000
1200
1400
1600
1800

(c)

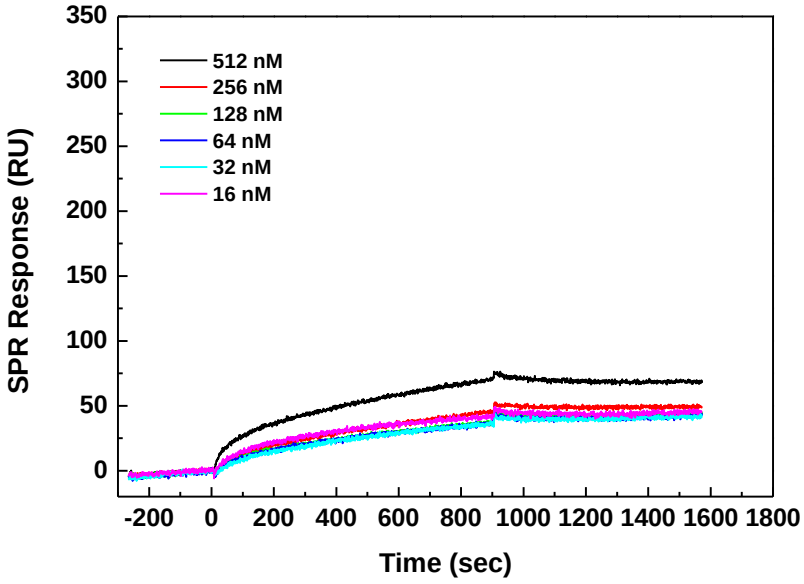
512 nM
256 nM
128 nM
64 nM
32 nM
16 nM
SPR Response (RU)
Time (sec)
350
300
250
200
150
100
50
0
-200
0
200
400
600
800
1000
1200
1400
1600
1800

(d)

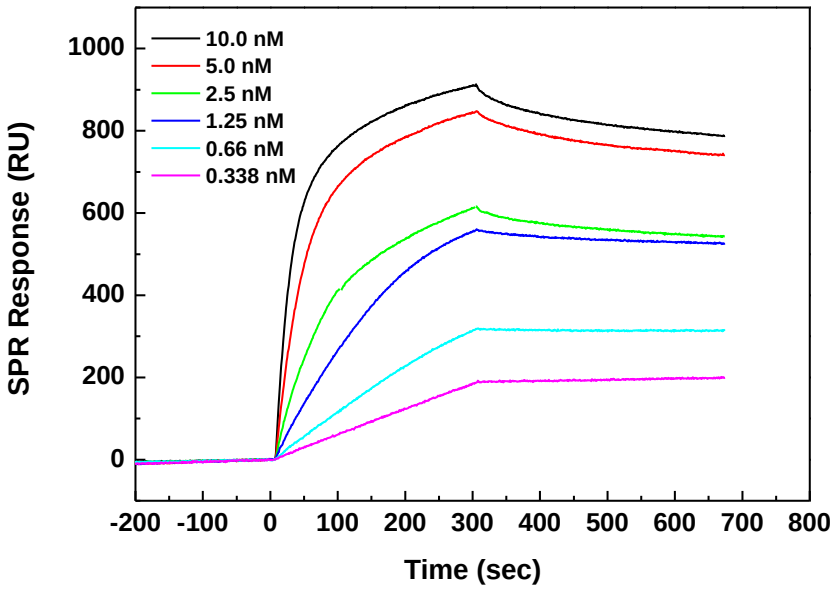

(e)

Figure 4.17 SPR sensorgrams for the interactions of glycopolymers and gp120 with DC-SIGN functionalized surface at different concentrations. The concentration ranges for glycopolymers and gp120 were from 16 nM to 512 nM and from 0.338 nM to 10.0 nM, respectively. (a) GM1; (b) GM2; (c)GM5; (d) GM6; (e) gp120.

The data was fitted by the kinetic model (**Eq. (4.1) - (4.7)**(4.7)) and the results shown in **Figure 4.17** and **Table 4.4**. As expected, the kinetic parameters are in good agreement with those results in **Figure 4.17**. The glycopolymers containing pendant mannose functional groups (GM1 and GM5) have an affinity binding with K_D of 9.86×10^{-7} and 2.09×10^{-7}, respectively. Compared to galactose glycopolymers (GM2 and GM6) which have no significant binding observed, highlighting the importance of binding site relevant to the glycoside stereochemistry with equatorial hydroxyl groups at C3 and C4 positions of the

pyranoside ring, **Table 4.4**.[134-136] Furthermore, it was shown that the chain length of the backbone of mannose glycopolymers correlated positively with binding affinity to immobilized DC-SIGN. For example, the dissociation constant K_D of glycopolymers GM1 is larger than that of glycopolymers GM5, which determined that the binding affinity of GM1 is weak than that of GM5. The lower K_D value indicated the strong binding effect provided by the high mannose density in GM5, which can be explained by the glycoside cluster effect attributed to the longer chain of mannose glycopolymers GM5.

Table 4.4 Kinetic parameters for glycopolymers and gp120 binding to the immobilized DC-SIGN obtained form the SPR measurements.

Run	Pendant Sugar units	k_a ($M^{-1}s^{-1}$)	k_d (s^{-1})	K_D (M)
GM1	Mannose	4.22×10^3	4.16×10^{-3}	9.86×10^{-7}
GM2[a]	Galactose	--	--	--
GM5	Mannose	1.74×10^4	3.65×10^{-3}	2.09×10^{-7}
GM6	Galactose	2.90×10^3	2.15×10^{-2}	7.42×10^{-6}
gp120	--	2.18×10^6	7.69×10^{-3}	3.53×10^{-9}

Note: The resulting data were analyzed by the curve fitting program of Matlab and Origin software. [a] The signals of SPR were too weak to calculated the k_a, k_d and K_D.

4.3.7. Preparation of glycopolymers-nanosponge drug delivery system

This study has involved the collaboration with Professor Eva M. Harth's research group at Vanderbilt University. Nanosponge is one new type of nanoparticles which is a three-dimensional polyester scaffold with cavities where drug can be absorbed and loaded. The linear polyester precursors with pendant functional group were synthesized by ring-opening copolymerization of *δ*-valerolactone with *α*-allyl-*δ*-valerolactone, *α*-propargyl-*δ*-valerolactone and 2-oxepane-1,5-dione, respectively and then react with bifunctional linker to form the controlled cross-linking 3-D polyester networks.[137-140] The nanoparticles formation and nanoscopic scale are primarily controlled by the alkyne, allyl moiety density in the precursor and the amount of diamine, bisazide and dithiol cross-linking reagents. The size of nanoparticles is relevant to the effectiveness of these drug delivery systems. One kind of nanosponge formation is shown in **Scheme 4.15**.

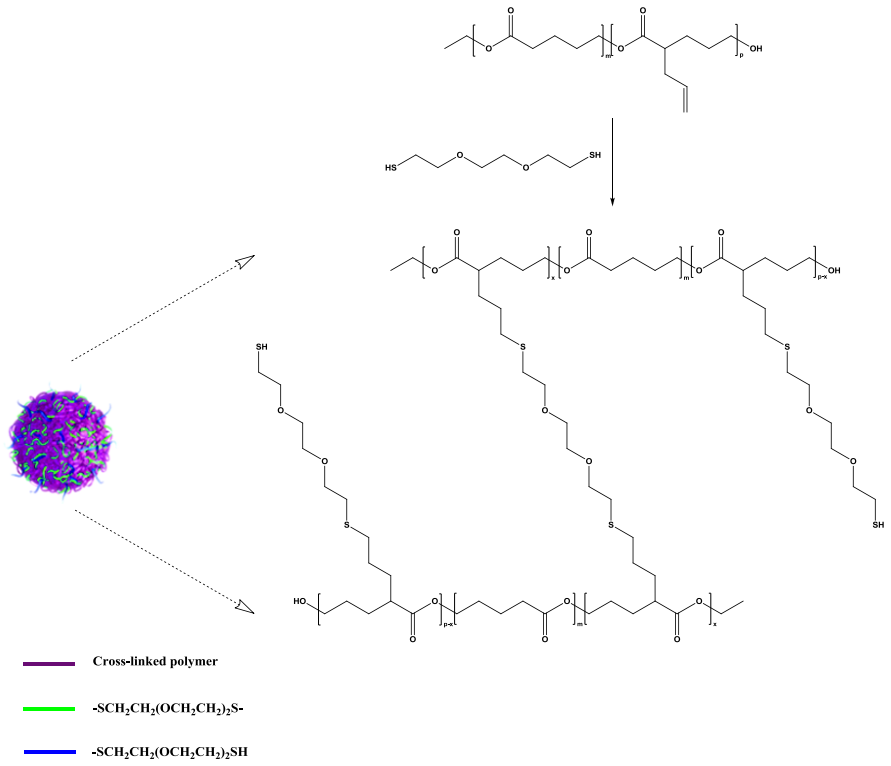

Scheme 4.15 Nanosponge formation *via* thiol-ene click cross-linking

The polyester is designed to be biodegradable and it decomposes gradually and released the carried drug in a controllable and predictable fashion. The nanoparticles surfaces were then modified by the glycopolymers *via* thiol-ene click chemistry, **Scheme 4.16**. The different kind of glycopolymers can selectively target a protein conjugate to cancer cells in the presence of normal cells and release large amounts of a drug in the cancer cell. The nanoparticles functionalized with glycopolymers can be a high efficient and specific identifiable drug delivery system.

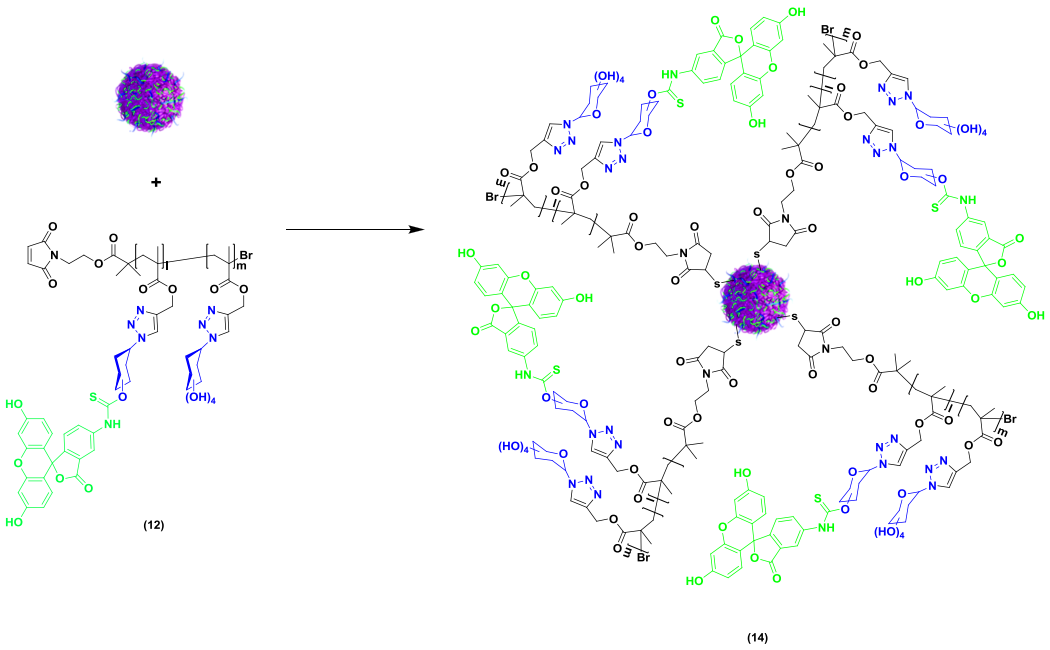

Scheme 4.16 Glycopolymer/nanosponge conjugate *via* a thiol-ene click reaction

4.3.8. Synthesis of the "clickable" alkyne homopolymers (18)

The disulfide based bifunctional initiator was chosen as the methylene's protons can be used as ^{1}H NMR internal standards for the calculation of the $M_{n,\ NMR}$ of the corresponding polymers and the cleavable disulfide functionality was introduced into the midpoint of the polymer chain. The internal disulfide bond could break down to afford the corresponding polymer with thiol end group by the reducing agent. The polymer containing thiol end group could react with (meth)acrylates or vinyl terminated polymers by thiol-ene click reaction in presence of phosphine or amine. Moreover, the thiol-containing polymer can

interact with metal ions and metal substrate (gold, platinum, silver, etc) to form coordinate covalent bonds.[141-146] In addition, the terminal thiol group could also efficiently coupled back to the internal disulfide bridge to yield the starting disulfide-containing polymer under oxidizing environment, **Scheme 4.17**. [146-149]

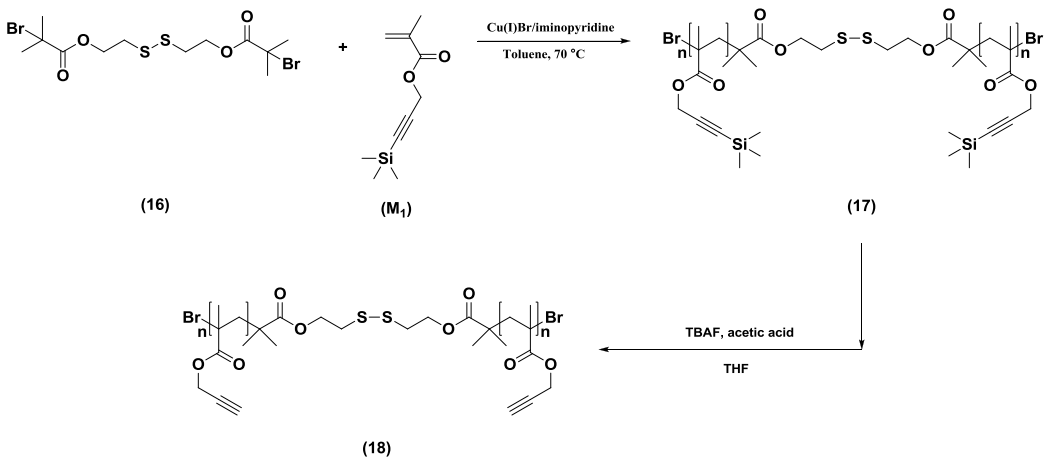

Scheme 4.17 Synthesis of the "clickable" alkyne homopolymers (18) using disulfide initiator

The first step involves synthesis of TMS-PgMA homopolymers using a CuBr/alkylpyridylmethanimine type ligands in toluene solvent. Secondly, the trimethylsilyl protecting groups in polymer were fully deprotected by employing TBAF in THF solution with acetic acid as buffering agent.

The polymerization results for TMS-PgMA are shown in **Figure 4.18**. The first-order kinetic plots of P(TMS-PgMA) (**17**) shows a good linear relationship during the polymerization and the M_n increasing in linear fashion with respect to monomer conversion and producing polymers with a PDi which demonstrate a good control of the polymerization, **Figure 4.18**, **Figure 4.19**.

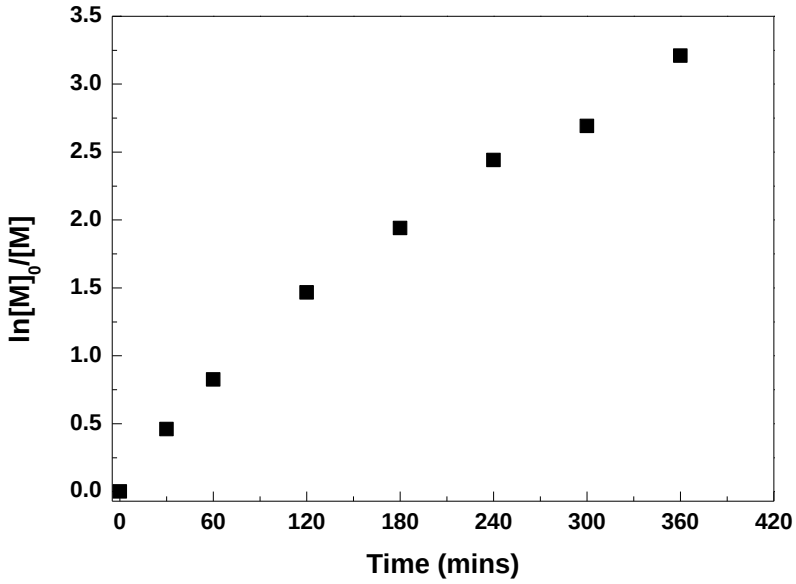
3.5
3.0
2.5
2.0
1.5
1.0
0.5
0.0
ln[M]0/[M]
0
60
120
180
240
300
360
420
Time (mins)

(a)

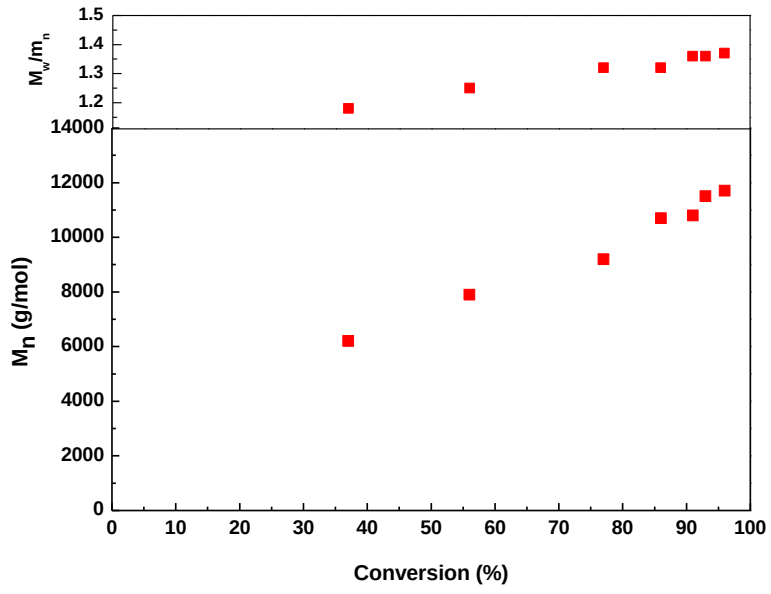
1.5
1.4
1.3
1.2
Mw/mn
14000
12000
10000
8000
6000
4000
2000
0
Mn (g/mol)
0
10
20
30
40
50
60
70
80
90
100
Conversion (%)

(b)

Figure 4.18 (a) Kinetic plots of polymerization of TMS-PgMA; (b) dependence of M_n and PDi on the monomer conversions. Reaction conditions: [M]:[I]:[Cu(I)]:[L]=80:1:2:4 in toluene at 70 ^{o}C.

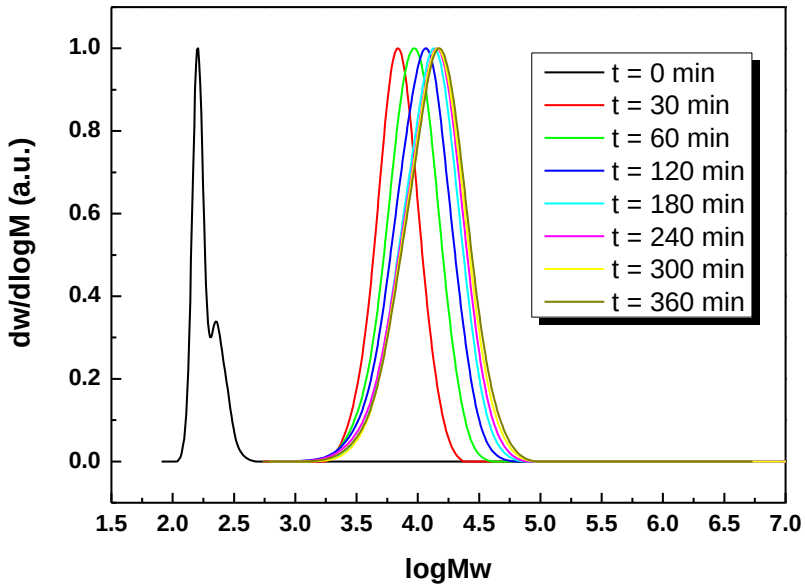

Figure 4.19 GPC traces (normalized to peak height) of P(TMS-PgMA) **(17**)

The trimethylsilyl protected polymer (**17**) was confirmed by ^{1}H NMR with the disappearance of the two vinyl peaks of the TMS-PgMA monomers at 5.55 ppm and 6.15 ppm. The ratio of the corresponding integration values of the **3** peak (δ = 4.59 ppm, C(O)OCH$_2$) to the **4** peak (δ = 0.19 ppm, (CH$_3$)$_3$Si) was 2:9 which demonstrated that the presence of the pendant trimethylsilyl groups. It could further be seen the small signal of methylene group (**a, b**) of the initiator (δ = 2.87-2.96 ppm and 4.21-4.33 ppm) after the polymerization, **Figure 4.20**.

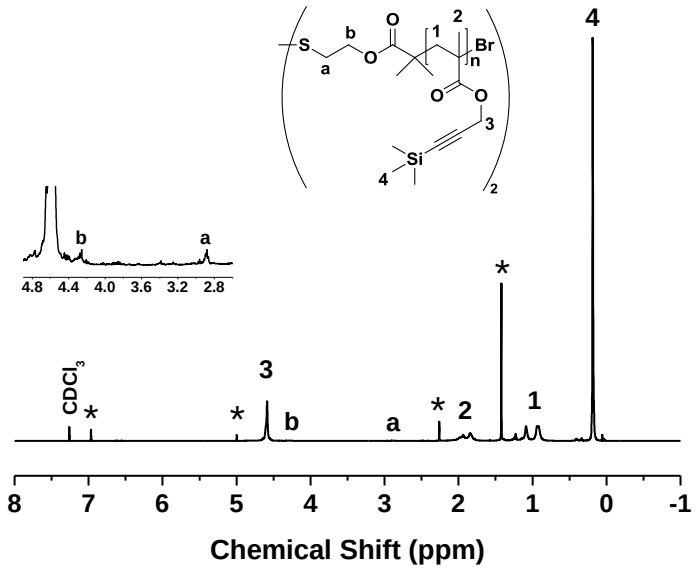

Figure 4.20 ^{1}H NMR spectrum of the polymer **(17).** * Characteristic peaks of 2,6-bis(1,1-dimethylethyl)-4-methyl phenol (BHT).

The clickable polymer containing pendent alkyne functional groups (**18**) was obtained by deprotection to remove the trimethylsilyl group. The deprotection reaction was performed by addition of TBAF solution in presence of acetic acid buffering agent at ambient temperature.

The successful removal of the trimethylsilyl group was demonstrated by ^{1}H NMR with the disappearance of the trimethylsilyl signal at 0.19 ppm along with the appearance of the alkyne signal at 2.49 ppm. The ratio of the corresponding integration values of the **3** peaks (δ = 4.60 ppm) to the **4** peak (δ = 2.49 ppm) was 2:1 which suggested that the pendant acetylene groups remained intact. It could further be seen the peaks of internal methylene (**a, b**) of the initiator (δ = 2.88-2.96 ppm and 4.24-4.32 ppm) after the deprotection reaction in the **Figure**

4.21.

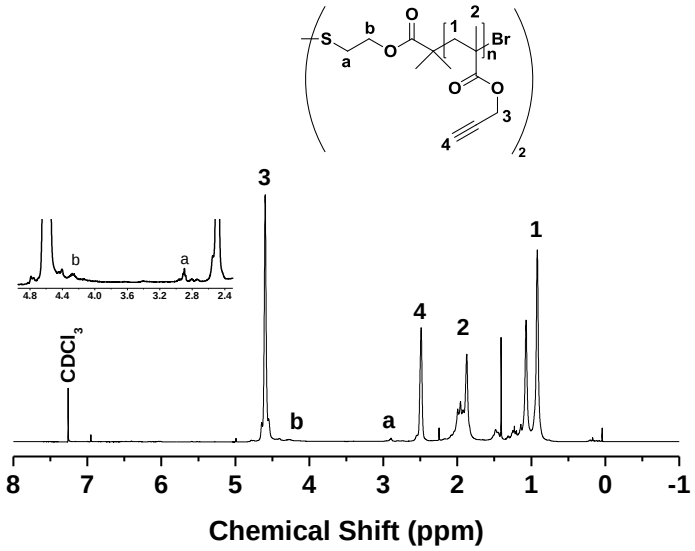

Figure 4.21 ^{1}H NMR spectrum of the polymer **(18)** after deprotection reaction

The removal of the trimethylsilyl group was further be confirmed by FT-IR spectra and GPC spectra. For example, the major difference between the two FT-IR spectra was appearance of one new absorption band at 3293 cm^{-1} attributed to alkyne C-H stretching vibration (υ (≡C-H)) after deprotection reaction. In addition, the original characteristic absorption peaks of the CH_3 symmetric deformation of Si-CH_3 (δ_s (Si(C-H_3))) at 1250 cm^{-1} and the CH_3 rocking mode of Si-CH_3 (ρ (Si(C-H_3))) at 840 cm^{-1} also disappeared after removal of the trimethylsilyl group. Moreover, the absorption bands of the alkyne C≡C stretching vibration (υ (C≡C)) shifted from 2188 cm^{-1} to 2131 cm^{-1} after deprotection, **Figure 4.22**.[1, 6, 13]

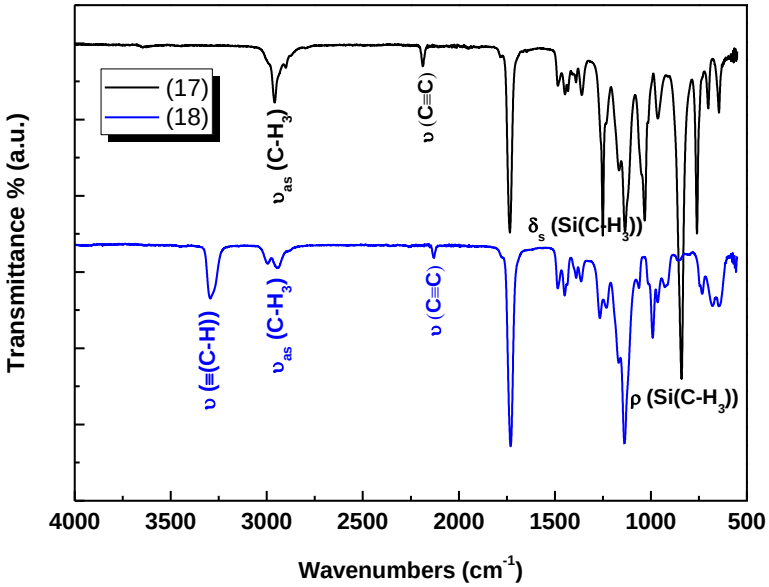

Figure 4.22 FT-IR spectra of the polymer before **(17)** and after **(18)** deprotection

Moreover, The GPC analysis also revealed that, as expected, the M_n of the polymer deceased from 12900 Da to 8100 Da after deprotection whilst the PDi remained constant, **Figure 4.23**.

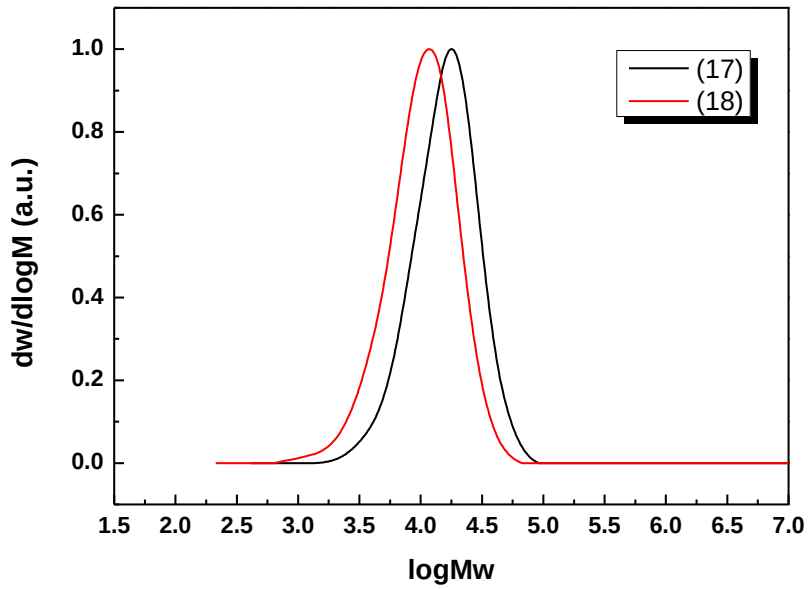

Figure 4.23 GPC spectra of the polymer before **(17)** and after **(18)** deprotection

4.3.9. Synthesis of glycopolymers (19) with different functional group density utilizing a CuAAC "co-click" strategy

Polymers containing pendant alkyne functional group **(18)** were used as one of the starting materials for the multiple parallel synthesis of a diverse library of glycopolymers. This involved the CuAAC click reaction with a range of different of glycosyl azides (ie. mannose azide, glucose azide, galactose azide, etc) and small organic azide, typically in DMSO solvent at ambient temperature. In this study, α-D-mannopyranosyl azide and 2-(2-azidoethoxy) ethanol (AzEE) were used as a model of water-soluble organic azides for the click reaction. The

CuAAC reaction conditions performed in presence of CuBr/*N*-ethyl-2-pyridyl-methanimine/triethylamine catalyst system in DMSO to ensure the complete solubility of all reagents and the product was purified by dialyzing against water/methanol and then freeze-drying, as reported by Haddleton *et al*, **Scheme 4.18**.[114-117]

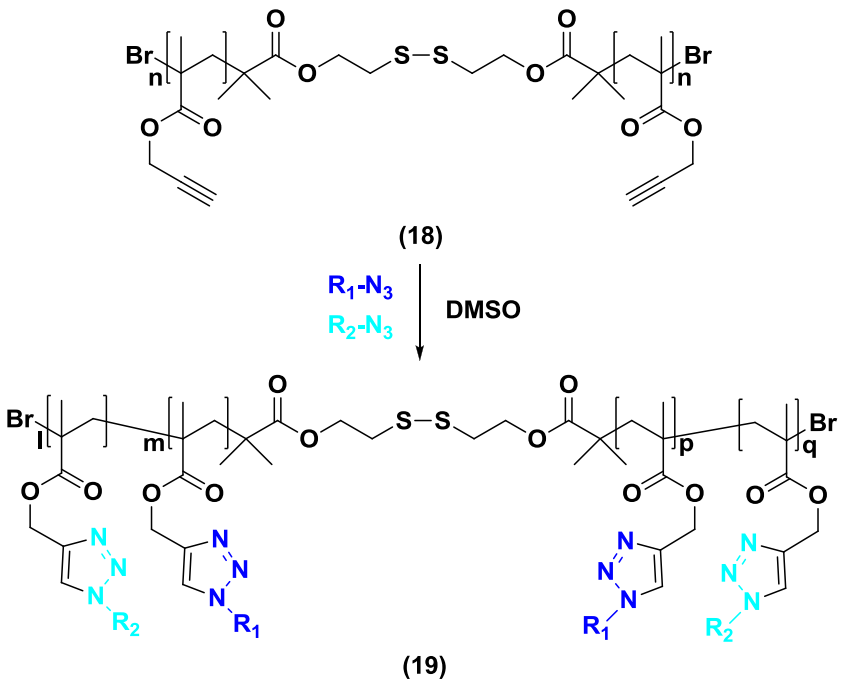

Scheme 4.18 Synthesis approach towards to glycopolymers *via* CuAAC click reaction. Reagents: R_1, R_2 = *α*-D-mannopyranosyl azide, *β*-D-galactopyranosyl azide, 2-(2-azidoethoxy)ethanol. Reaction conditions: R_1N_3, R_2N_3, CuBr, *N*-ethyl-2-pyridyl-methanimine, triethylamine, DMSO, 25 ^{o}C.

Table 4.5 summarized the versatility of glycopolymers with different sugar moiety density. The M_n and PDi of all glycopolymers were obtained by GPC using DMF as the mobile phase. The "co-click" strategy is an attractive way to

create a series of polymers with identical native macromolecular properties (polymer skeleton, average molecular weight, molecular weight distribution, polarity) and the only difference in their carbohydrate-binding epitope density.

Table 4.5 Synthetic glycopolymers with different azide density

Run	Mannoside (%)	AzEE (%)	M_n (GPC) [a] g mol^{-1}	PDi [a]
GS1	100	0	25600	1.51
GS2	75	25	22800	1.21
GS3	50	50	20700	1.38
GS4	25	75	19100	1.33
GS5	0	100	17700	1.39

[a] Obtained by GPC analysis using DMF as the mobile phase with DRI detection

The successful CuAAC click reaction was confirmed by the ^{1}H NMR spectra of glycopolymers with the appearance of the new triazole peak **i** at 8.3 ppm and several typical peaks (δ = 3.0-6.2 ppm) from the mannose units (**Figure 4.24** (a)) or the new triazole peak **i** at 8.2 ppm and several typical peaks (δ = 3.56 - 4.65 ppm) from the 2-(2-azidoethoxy)ethanol group (**Figure 4.24** (b)). The ratio of the corresponding integration values of the **g** peak to **i** peak was 3:1, which suggested that the conversion of CuAAC click reaction reached 100%. It could further be seen the characteristic signal of $C(O)OCH_2$ group (**h**) in polymers,

Figure 4.24.

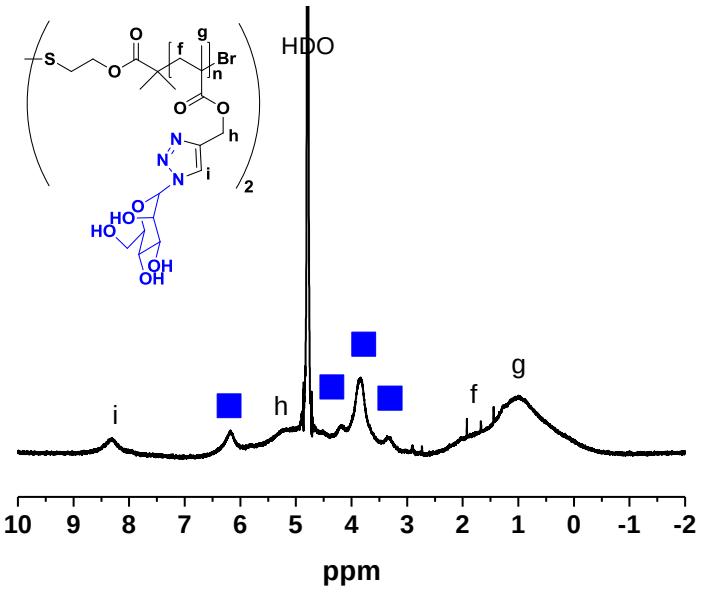

(a)

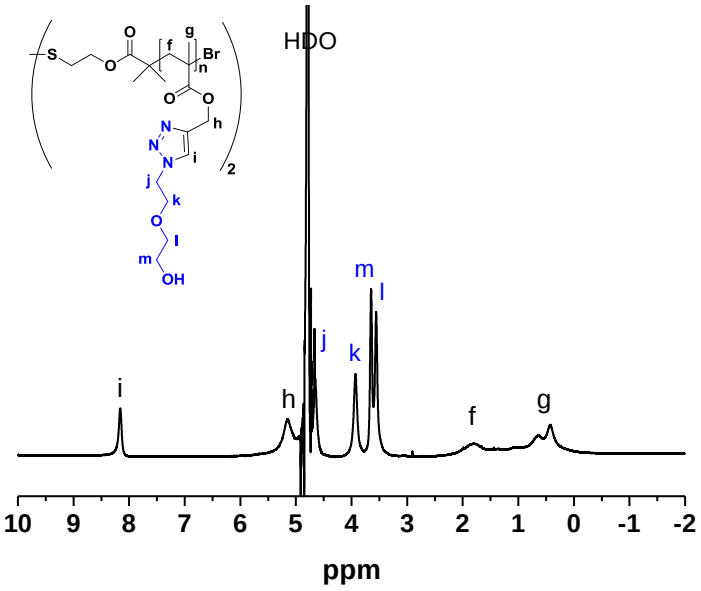

(b)

Figure 4.24 ^{1}H NMR spectra of the polymer prepared by CuAAC click reaction in D_2O. (a) GS1, ■: The characteristic peaks of mannose units; (b) GS5, j-l: The characteristic peaks of 2-(2-azidoethoxy)ethanol units.

Moreover, both GPC and FTIR data further indicated that the glycopolymers were prepared successfully. For example, the M_n of the polymer increased from 8100 Da (clickable polymer, **18**) to 25600 Da and 17700 Da, respectively (after CuAAC click reaction, GS1 and GS5), **Figure 4.25**. Meanwhile, the PDi of the polymer stayed very similar.

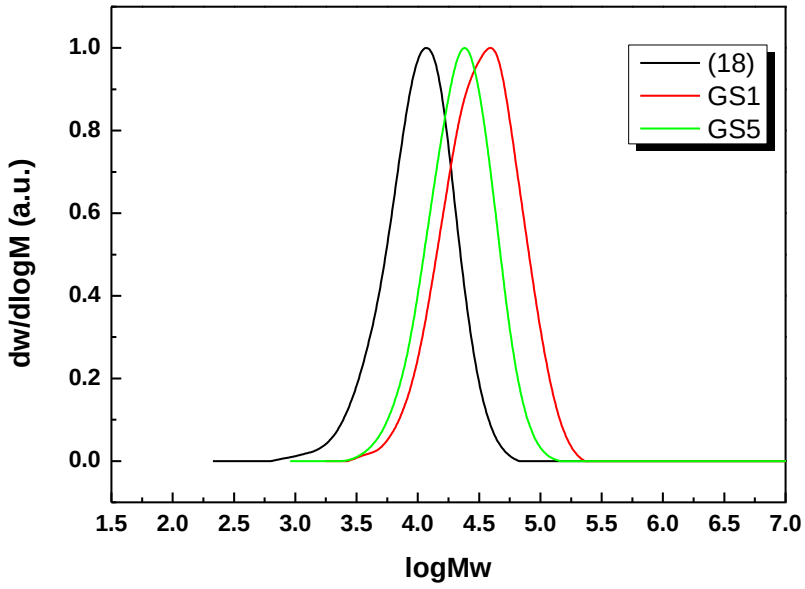

Figure 4.25 GPC spectra of the polymers before **(18)** and after (GS1, GS2) CuAAC click reaction

Furthermore, compared with the FTIR spectra of the polymer before and after CuAAC click reaction, the original characteristic absorption band of the alkyne

group ($\upsilon_{(C\equiv C)}$ stretching vibration) at 2131 cm^{-1} disappeared after the click reaction with sugar azide. One new large broad peaks at 3362 cm^{-1} or 3377 cm^{-1} assigned to $\upsilon_{(O-H)}$ stretching vibration appeared and the triazole groups $\upsilon_{(N=N)}$ stretching vibration frequencies appeared at 1639 cm^{-1} or 1648 cm^{-1} region after the CuAAC click reaction, **Figure 4.26**.

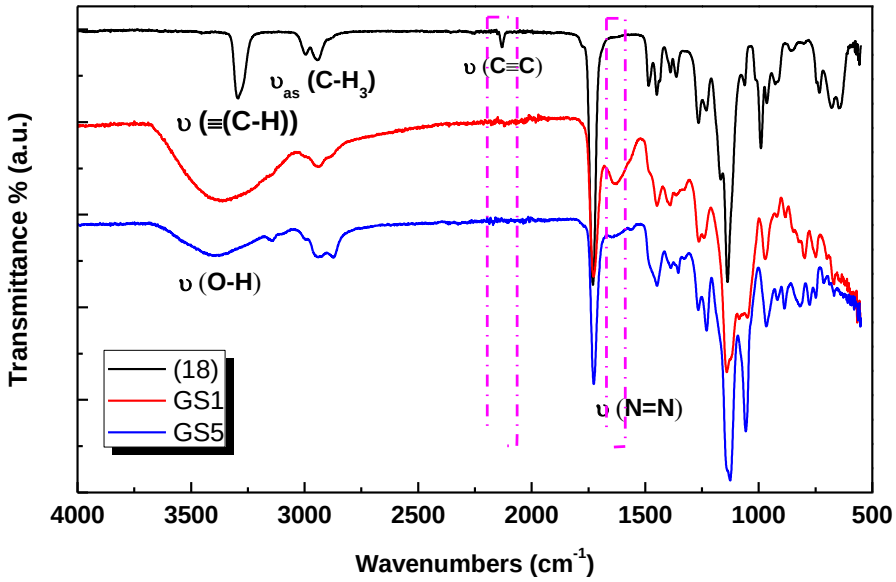

Figure 4.26 FTIR spectra of the polymers before and after click reaction

4.3.10. Quartz Crystal Microbalance with Dissipation (QCM-D)

The QCM-D is a sensitive tool to investigate the time-resolved adsorption kinetics, conformation and interactions of polymer or protein onto a surface in aqueous solutions. In a QCM-D system, when an AC voltage is pulsed across the

electrode of the sensors, the excited oscillation of the quartz crystal can occur in the shear mode at its resonant frequency. The resonant frequency and dissipation of the quartz crystal is recorded in real time and relies on the total mass and the intrinsic properties of the piezoelectric quartz crystal. An increase of the adsorbed mass on the chip will induce a decrease in resonant frequency along with a rise of corresponding dissipation.

When the crystal is coated with a thin rigid layer with non-slip condition in vacuum of air, the relationship of the change in total mass (Δm) and the change in the resonant frequency (Δf) is described by the Sauerbrey equation:[150-152]

$$\Delta m = -\frac{\rho_q v_q}{2 f_0^{\,2}} \frac{\Delta f}{n} = -\frac{\rho_q h_q}{f_0} \frac{\Delta f}{n} = -C \frac{\Delta f}{n} \qquad (4.13)$$

Where ρ_q, v_q and h_q are the specific density, the shear wave velocity and the thickness of the quartz crystal, respectively; f_0 is the fundamental frequency; n is overtone number (n = 1, 3, 5, …). C is a physical constant based on the physical properties of the quartz crystal, which is 17.7 $ng \cdot cm^{-2} \cdot Hz^{-1}$ at 5 MHz for the quartz crystal used.

The dissipation shit (ΔD) is defined as:[153, 154]

$$\Delta D = \Delta(\frac{1}{Q}) = \Delta(\frac{E_d}{2\pi E_S}) \qquad (4.14)$$

Where Q is a dimensionless Q-factor; E_d is the energy dissipated during each oscillation cycle; E_s is the total energy stored in the system.

The thickness of the films, h_f, is defined by dividing the total absorbed mass of the film on the surface by the effective density of the film.[152]

$$h_f = \frac{\Delta m}{\rho_{eff}} \tag{4.15}$$

Where the h_f is the thickness of the film; ρ_{eff} is the effective density.

When the crystal is exposed in a bulk Newtonian liquid, the frequency response of quartz crystal can be described by the Kanazawa-Gordon equation:[155-158]

$$\Delta f = -\sqrt{n f_0^3}\sqrt{\frac{\eta_l \rho_l}{\pi \mu_q \rho_q}} \tag{4.16}$$

Where f_0 is the fundamental frequency, n is the overtone number; η_l and ρ_l are the viscosity and density of the adjacent liquid, respectively; μ_q and ρ_q are the shear modulus and density of quartz crystal, respectively.

The dissipation response is defined by, [159]

$$\Delta D = 2\sqrt{\frac{f_0}{n}}\sqrt{\frac{\eta_l \rho_l}{\pi \mu_q \rho_q}} \tag{4.17}$$

When the QCM-D is absorbed with a viscoelastic soft film and is oscillating in a liquid which can exhibit additional energy dissipation and a frequency (overtone)-dependent response, the equation **(4.13)** is not necessarily valid. The Voigt-Voinova model represents visoelastic film which is homogeneous and has uniform thickness and density in Newtonian liquid and no-slip conditions.

$$G^* = G' + iG'' = \mu_f + i2\pi f\eta_f = \mu_f(1 + i2\pi f\tau_f) \tag{4.18}$$

Where G^* is complex shear modulus, G' is the elastic (storage) modulus, G'' is the loss modulus, μ_f is the elastic (storage) modulus of the film, η_f is the shear viscosity of the film. f is the oscillation frequency, τ_f is the characteristic relaxation time of the film. In this case, the resonant frequency shit, Δf, and the

dissipation shit, ΔD, in presence of the viscoelastic film are obtained from the imaginary and real parts of the β-function[151, 160-162]

$$\Delta f = \frac{\mathrm{Im}(\beta)}{2\pi\rho_q h_q} \tag{4.19}$$

$$\Delta D = -\frac{\mathrm{Re}(\beta)}{\pi f\rho_q h_q} \tag{4.20}$$

Where

$$\beta = \xi_1 \frac{2\pi f\eta_f - i\mu_f}{2\pi f}\frac{1-\alpha\exp(2\xi_1 h_f)}{1+\alpha\exp(2\xi_1 h_f)} \tag{4.21}$$

$$\alpha = \frac{\frac{\xi_1}{\xi_2}\frac{2\pi f\eta_f - i\mu_f}{2\pi f\eta_l}+1}{\frac{\xi_1}{\xi_2}\frac{2\pi f\eta_f - i\mu_f}{2\pi f\eta_l}-1} \tag{4.22}$$

$$\xi_1 = \sqrt{-\frac{(2\pi f)^2\rho_f}{\mu_f + i2\pi\eta_f}} \tag{4.23}$$

$$\xi_2 = \sqrt{i\frac{2\pi f\rho_l}{\eta_l}} \tag{4.24}$$

and where ρ_q and h_q are the density and thickness of quartz crystal, respectively; ρ_f, h_f and η_f are the density, thickness and viscosity of the viscoelastic film respectively; ρ_l, h_l and η_l are the density, thickness and viscosity of bulk-liquid respectively; μ_f is the elastic (storage) modulus of the viscoelastic film.

In **Figure 4.27** (a), the shift in frequency (Δf) and dissipation (ΔD) were measured when 1 mg/mL disulfide initiated glycopolymers were pumped into the chamber followed by an injection of ConA in HBS buffer solution. The initial baseline showed the pure HBS buffer passed through the chamber of QCM-D

system. When the glycopolymer solution was loaded ito the chamber at a flow rate of 0.1 ml/min, the frequency shift immediately went down about 177 Hz along with the dissipation shift ascend about 25 $\times 10^{-6}$ simultaneously which suggested that the glycopolymers was quickly grafted on the gold surface. After 9.5 hours, both Δf and ΔD reached a constant indicating the saturation absorption of glycopolymer on the gold surface. A small proportion of unbound glycopolymers was removed from the surface corresponding to a slight increased in frequency after the buffer rinse the surface which revealed the overall change in frequency for glycopolymers adsorbed on the gold surface was ca. 173 Hz. The next step was to investigate the conjugation of ConA to the glycopolymers layer. When the ConA buffer solution was passed over the glycopolymers and then buffer was inject to remove any non-adsorbed ConA, the change in frequency for the lectin adsorption showed a gradual decrease with time and then a litter increase in frequency and the overall change in frequency showed ca. 90 Hz indicating the ConA formed films on the glycopolymers surface, **Figure 4.27** (b).

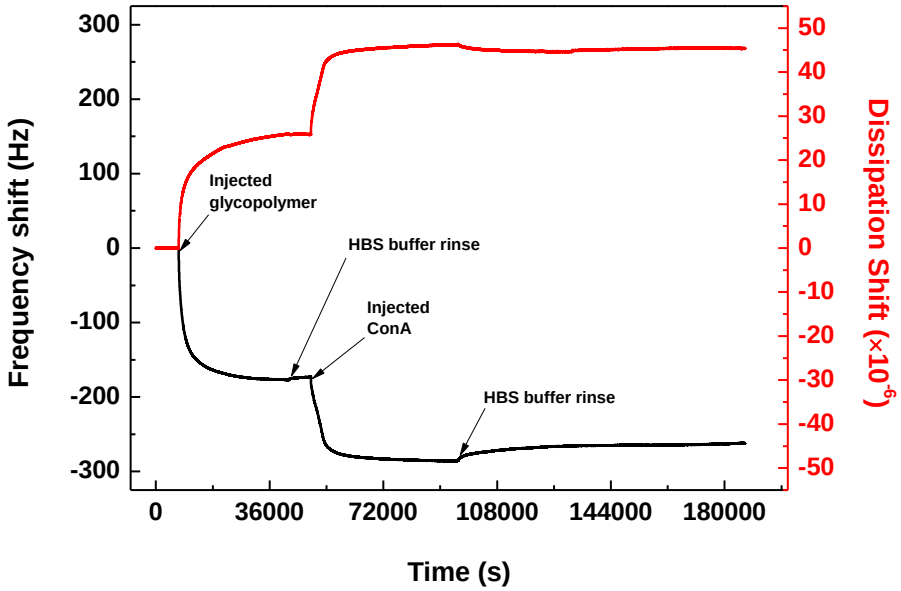

(a)

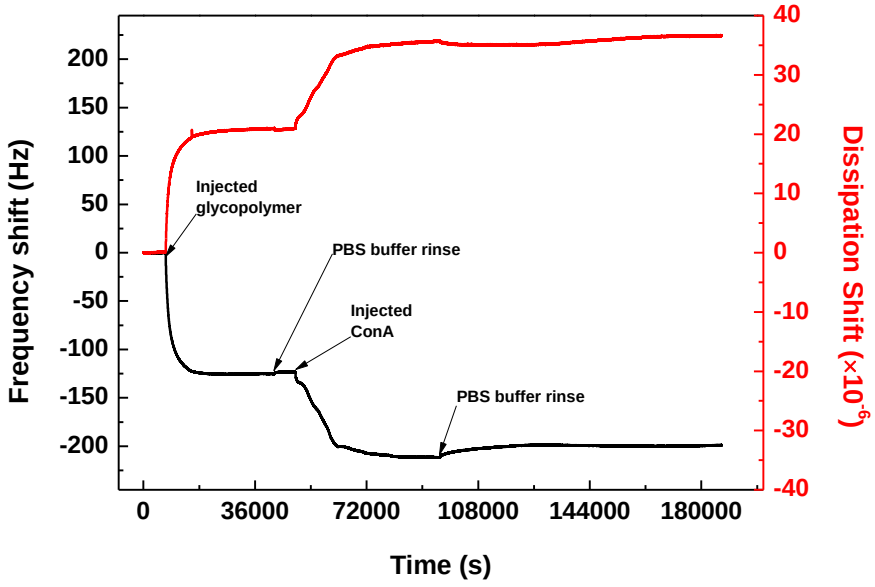

(b)

Figure 4.27 QCM-D curves showing the frequency shift and dissipation shift vs. time for glycopolymers and ConA. (a) analyte solutions were prepared in HBS buffer pH 7.2 (b) analyte solutions were prepared in PBS buffer pH 7.2.

A trace of *f* against *D* shows the relationship between mass adsorbed on the chip surface and changes in rigidity. If the plot of *f vs. D* shows a linear relationship, it suggests that there are not conformational changes during the interaction process.[163-166] Both glycopolymers and ConA show approximate linear *f-D* relations, indicating both of them form relatively more rigid structures on the chips, **Figure 4.28**.

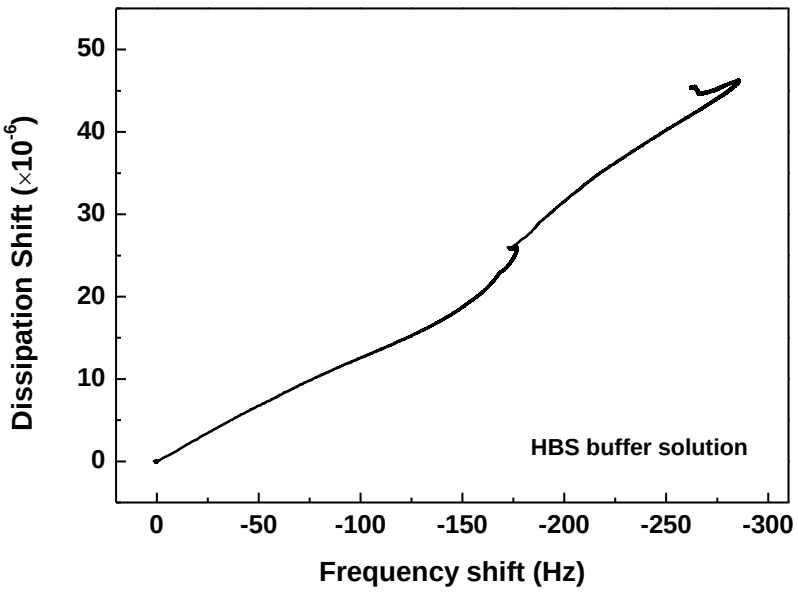

(a)

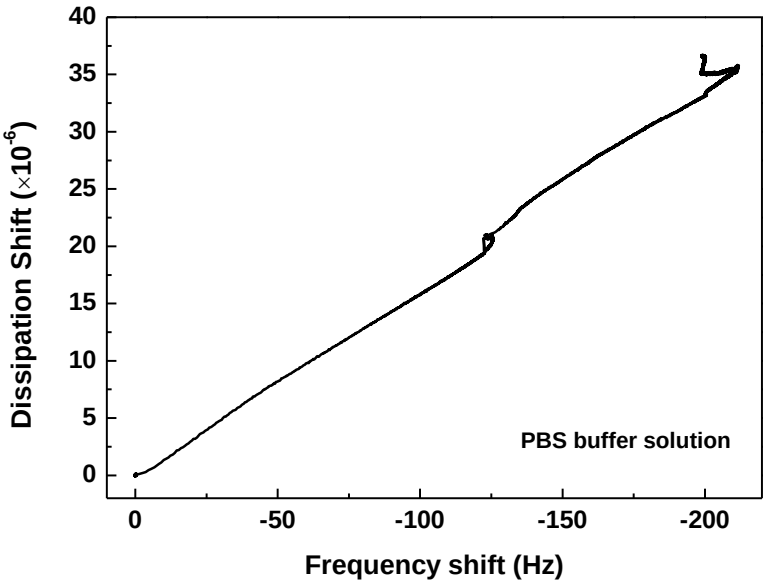

(b)

Figure 4.28 The corresponding frequency *vs.* dissipation trace showing the overall adsorption profile of polymer and lectin. (a) analyte solutions were prepared in HBS buffer pH 7.2 (b) analyte solutions were prepared in PBS buffer pH 7.2.

Each process of the mass deposited on the modified gold chip was calculated by the Sauerbrey relation, **Eq.** (4.13). In both HBS buffer solutions and PBS buffer solution, the mass has been adsorbed onto the chip surface, **Figure 4.29**.

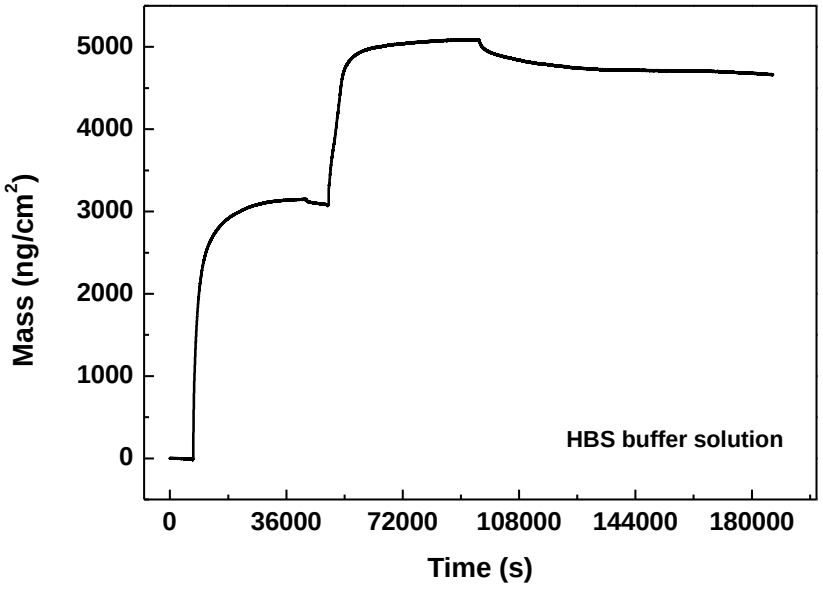

(a)

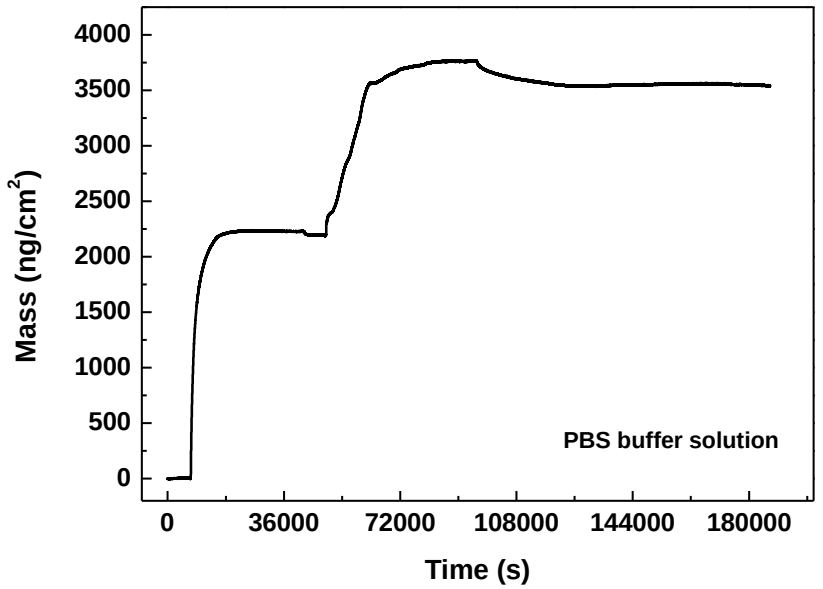

(b)

Figure 4.29 Estimate adsorbed mass on the modified gold chip calculated *via* Sauerbrey equation (a) analyte solutions were prepared in HBS buffer pH 7.2 (b) analyte solutions were prepared in PBS buffer pH 7.2.

4.3.11. Synthesis of "clickable" alkyne homopolymers (23) *via* ring-opening polymerization (ROP)

This study has involved the collaboration with Andrew P. Dove's research group. The 5-methyl-5-propargyloxycarbonyl-1,3-dioxane-2-one (MPC) monomer with propargyl functional group was synthesized from commercially available 2,2-bis(hydroxymethyl)propionic acid (bis-MPA) *via* two-step procedure as previously reported, **Scheme 4.19** (a).[31]

Dove reported that thiourea-tertiary amine compounds are highly effective catalysts for the ROP of lactide, such as 1-(3,5-bis(trifluoromethyl)phenyl)-3-cyclohexylthiourea (bis-TPTU).[167] The stronger base can facilitate the ROP of cyclic esters. 1,5,7-Triazabicyclo[4.4.0]dec-5-ene (TBD), *N*-methyl-TBD (MTBD), and 1,8-diazabicyclo[5.4.0]-undec-7-ene (DBU) were shown high catalyst effect on the ROP.[168] The homopolymers PMPC was prepared by ring-opening polymerization (ROP) of MPC in presence of benzyl alcohol as the initiator with DUB, bis-TPTU as catalyst in DCM solvent as shown in **Scheme 4.19** (b). After the desired time, the polymerization was quenched by the addition of Amberlyst® A21, and then isolated by filtration, precipitated in hexane. The homopolymer (DP = 10) was further purified by column chromatography on silica gel in hexane/ethyl acetate (4/1, v/v).

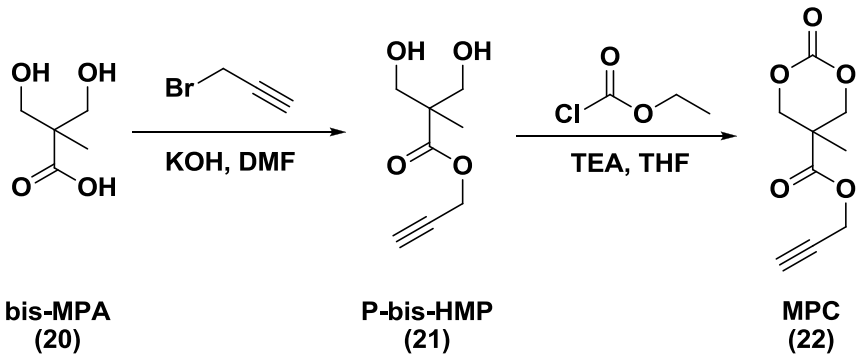

bis-MPA (20) P-bis-HMP (21) MPC (22)

(a)

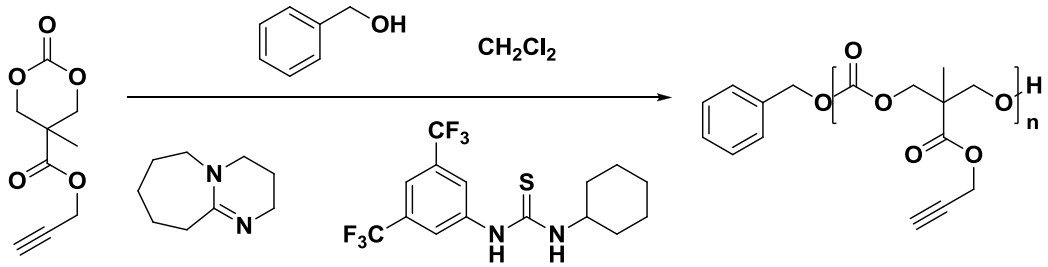

MPC (22) PMPC (23)

(b)

Scheme 4.19 (a) Synthesis and (b) ring-opening polymerization of 5-methyl-5-propargyloxycarbonyl-1,3-dioxane-2-one (MPC). Conditions: (i) propargy bromide, KOH, DMF, 100 ^{o}C for 2h and then 70 ^{o}C for 72h; (ii) ethyl chloroformate, TEA, THF, 0 ^{o}C for 2.5h and then 25 ^{o}C for 24h; (iii) ROH, DBU, bis-TPTU, dry DCM, RT.

The polymer with the alkyne functional group was confirmed by ^{1}H NMR spectrum and GPC. The degree of polymerization was obtained by comparison of the corresponding integration values of the **b** peak (δ = 5.12 ppm) and the **g** peaks (δ = 2.51-2.52 ppm) originating from the benzyl alcohol initiator moiety and alkyne functionality in the polymer, respectively (**Figure 4.30**). Furthermore, GPC analysis also revealed the M_n = 2200 g·mol^{-1}, whilst the PDi = 1.41, **Figure**

4.31.

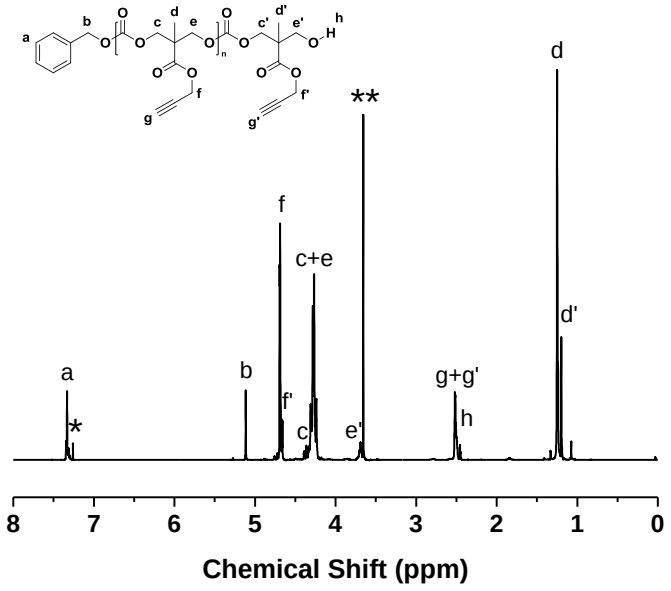

Figure 4.30 ^{1}H NMR spectrum of the $PMPC_{10}$ (23) initiated from benzyl alcohol using DBU (5 mol% to monomer) and bis-TPTU(10 mol% to monomer) *via* ROP polymerization. * The characteristic peaks of residual $CDCl_3$. ** The characteristic peak of CH_2Cl_2 solvent.

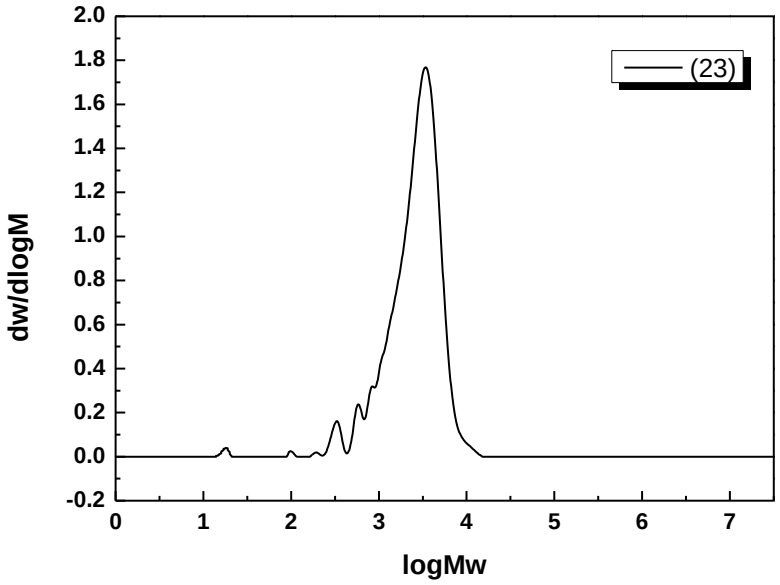

Figure 4.31 GPC spectrum of the polymer (**23**) *via* ROP polymerization

4.3.12. Synthesis of glycopolymers (24) with different binding epitope density utilizing CuAAC "co-click" strategy

The polymers containing pendant alkyne functional group (**24**) were used as one of the starting materials for the multiple parallel synthesis of diverse libraries of glycopolymers. It involved the CuAAC click reaction with a range of different of glycosyl azides (ie. mannose azide, glucose azide, galactose azide, etc) typically in DMSO solvent at room temperature. In this study, α-D-mannopyranosyl azide and β-D-galactopyranosyl azide were used as a model of sugar azides for the CuAAC click reaction. The CuAAC reaction conditions performed in presence of CuBr/*N*-ethyl-2-pyridyl-methanimine/triethylamine in DMSO to ensure the complete solubility of all reagents and the product was purified by dialyzing against water/methanol and then freeze-drying from those previously reported by Haddleton *et al*, **Scheme 4.20**.[114-117]

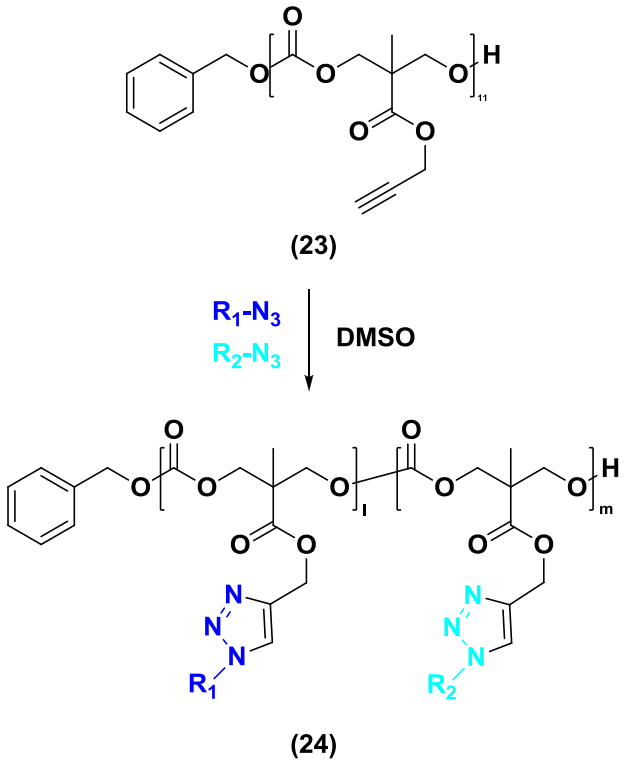

Scheme 4.20 Synthesis approach towards to glycopolymers (24) *via* CuAAC click reaction. Reagents: R_1, R_2 = α-D-mannopyranosyl azide, β-D-galactopyranosyl azide. Reaction conditions: R_1N_3, R_2N_3, CuBr, *N*-ethyl-2-pyridylmethanimine, triethylamine, DMSO, 25 ^{o}C.

Table 4.6 summarized the versatility of glycopolymers with different sugar moiety density. The M_n and PDi of all glycopolymers were obtained by GPC using DMF as the mobile phase.

Table 4.6 Synthetic glycopolymers with different sugar azide density

Run	Mannoside (%)	Galactoside (%)	M_n (GPC) [a] g mol^{-1}	PDi [a]
GBP1	100	0	8600	1.26
GBP2	75	25	9900	1.24

GBP3	50	50	9200	1.28
GBP4	25	75	10400	1.29
GBP5	0	100	10500	1.33

[a] Obtained by GPC analysis using DMF as the mobile phase and DRI detection

The successful CuAAC click reaction was confirmed by the ^{1}H NMR spectra of glycopolymers with the appearance of the new triazole peak **i** at 8.2 ppm and several typical peaks (δ = 3.1 - 6.1 ppm) from the mannose units or the new triazole peak **i'** at 8.3 ppm and several typical peaks (δ = 3.5 - 5.7 ppm) from the galactose groups. The change in integration areas of **i** peak and **i'** peak indicated the density of two different kind of sugar moiety in polymer scaffolds. It could further be seen the characteristic peaks of benzyl group (**a**) assigned to the initiator (δ = 7.3 ppm) in polymers after the CuAAC click reaction, **Figure 4.32**.

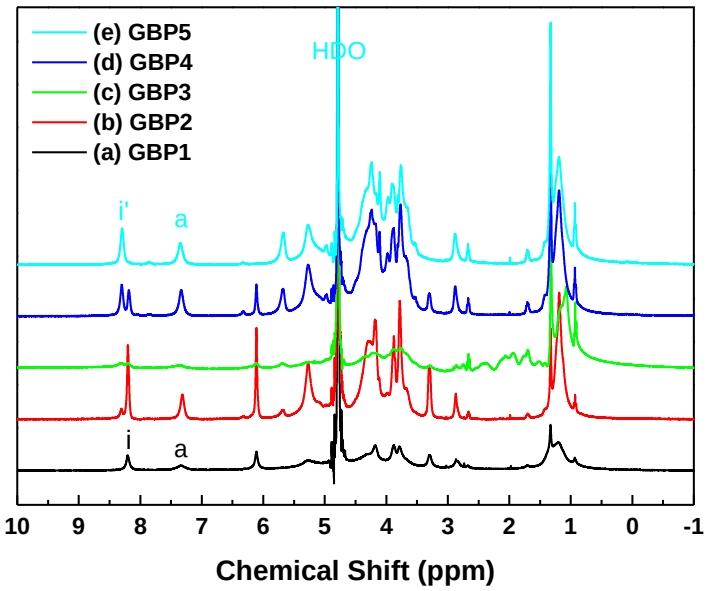

Figure 4.32 ^{1}H NMR spectra of the glycopolymer prepared by CuAAC click reaction in DMSO-d_6. (a): GBP1; (b): GBP2; (c): GBP3; (d): GBP4; (e): GBP5.

Moreover, GPC data further indicated that these glycopolymers were successfully prepared. The M_n of the polymer increased from 2200 Da (clickable polymer, 23) to 8600 Da, 9900 Da, 9200 Da, 10400 Da, 10500 Da, respectively (after CuAAC click reaction, GBP1-5), **Figure 4.33**. Meanwhile, the PDi of these glycopolymers remained narrow, **Table 4.6**.

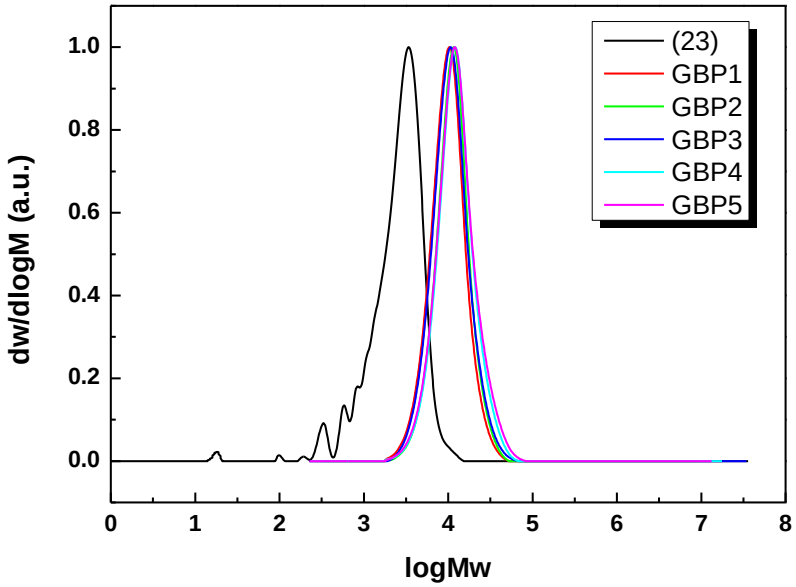

Figure 4.33 GPC spectra of the polymers before (**23**) and after (GBP1-5) CuAAC click reaction

4.4. Conclusions

Three different kinds of alkyne polymer were synthesized by different preparation methods. One controlled polymerization of trimethylsilyl-protected propargyl methacrylate (TMS-PgMA) initiated from maleimide protected initiator *via* copper catalyzed living radical polymerization was prepared. Another kind of P(TMS-PgMA) polymer was synthesized polymerization using a disulfide-based bifunctional initiator. Meanwhile, the third kind of polymers containing alkyne functional group were prepared by ROP polymerization of 5-methyl-5-propargyloxycarbonyl-1,3-dioxane-2-one (MPC). The synthesis of a

library of sugar azides were achieved by a simple and efficient one-step reaction. Moreover, a novel series of glycopolymer with different sugar units (eg. mannose, galactose, glucose and fucose) were then successfully prepared by employing the CuAAC "co-click" strategy. The PDi of polymers remained narrow before and after being functionalized by a range of monosaccharides. In addition, glycopolymer conjugated nanosponges as potential in drug delivery system was prepared successfully by thiol-ene click chemistry.

The binding affinity of the glycopolymers with recombinant human DC-SIGN was investigated by SPR. Kinetic parameters were obtained by fitting curves to a 1:1 Langmuir mode using Matlab software and Origin software. Besides, the disulfide-based glycopolymer adsorption on the gold chip and then interaction with the ConA lectin were followed by QCM-D experiments.

4.5. References

1. F. D. Tropper, A. Romanowska and R. Roy, *Methods Enzymol.*, 1994, **242**, 257-271.
2. M. A. Findeis, C. H. Wu and G. Y. Wu, *Methods Enzymol.*, 1994, **247**, 341-351.
3. V. Ladmiral, E. Melia and D. M. Haddleton, *Eur. Polym. J.*, 2004, **40**,

431-449.

4. S. R. S. Ting, G. J. Chen and M. H. Stenzel, *Polym. Chem.*, 2010, **1**, 1392-1412.

5. M. Ambrosi, N. R. Cameron, B. G. Davis and S. Stolnik, *Org Biomol Chem*, 2005, **3**, 1476-1480.

6. M. Ambrosi, N. R. Cameron and B. G. Davis, *Org Biomol Chem*, 2005, **3**, 1593-1608.

7. R. A. Dwek, *Chem. Rev.*, 1996, **96**, 683-720.

8. D. A. Tirrell, *Nature*, 2004, **430**, 837-837.

9. S. L. Flitsch and R. V. Ulijn, *Nature*, 2003, **421**, 219-220.

10. D. B. Werz and P. H. Seeberger, *Chem. Eur. J.*, 2005, **11**, 3194-3206.

11. P. M. Rudd, T. Elliott, P. Cresswell, I. A. Wilson and R. A. Dwek, *Science*, 2001, **291**, 2370-2376.

12. J. E. Gestwicki, C. W. Cairo, L. E. Strong, K. A. Oetjen and L. L. Kiessling, *J. Am. Chem. Soc.*, 2002, **124**, 14922-14933.

13. J. J. Lundquist and E. J. Toone, *Chem. Rev.*, 2002, **102**, 555-578.

14. E. A. Smith, W. D. Thomas, L. L. Kiessling and R. M. Corn, *J Am Chem Soc*, 2003, **125**, 6140-6148.

15. L. L. Kiessling, J. E. Gestwicki and L. E. Strong, *Angew. Chem. Int. Ed.*, 2006, **45**, 2348-2368.

16. A. V. Pukin, H. M. Branderhorst, C. Sisu, C. A. G. M. Weijers, M. Gilbert, R. M. J. Liskamp, G. M. Visser, H. Zuilhof and R. J. Pieters,

Chembiochem, 2007, **8**, 1500-1503.

17. G. T. Noble, S. L. Flitsch, K. P. Liem and S. J. Webb, *Org Biomol Chem*, 2009, **7**, 5245-5254.
18. B. Voit and D. Appelhans, *Macromol. Chem. Phys.*, 2010, **211**, 727-735.
19. B. Twaites, C. D. Alarcon and C. Alexander, *J. Mater. Chem.*, 2005, **15**, 441-455.
20. P. K. Dhal, S. R. Holmes-Farley, C. C. Huval and T. H. Jozefiak, *Adv Polym Sci*, 2006, **192**, 9-58.
21. R. Duncan, *Nature Reviews Drug Discovery*, 2003, **2**, 347-360.
22. R. Satchi-Fainaro, R. Duncan and C. M. Barnes, *Adv Polym Sci*, 2006, **193**, 1-65.
23. J. Khandare and T. Minko, *Prog. Polym. Sci.*, 2006, **31**, 359-397.
24. S. G. Spain, M. I. Gibson and N. R. Cameron, *J. Polym. Sci., Part A: Polym. Chem.*, 2007, **45**, 2059-2072.
25. A. Narumi and T. Kakuchi, *Polym. J.*, 2008, **40**, 383-397.
26. W. J. Ye, S. Wells and J. M. DeSimone, *J. Polym. Sci., Part A: Polym. Chem.*, 2001, **39**, 3841-3849.
27. J. Bernard, M. Schappacher, A. Deffieux, P. Viville, R. Lazzaroni, M. H. Charles, M. T. Charreyre and T. Delair, *Bioconjug Chem*, 2006, **17**, 6-14.
28. K. Yamada, M. Minoda and T. Miyamoto, *J. Polym. Sci., Part A: Polym. Chem.*, 1997, **35**, 751-757.
29. K. Aoi, K. Tsutsumiuchi, E. Aoki and M. Okada, *Macromolecules*, 1996,

29, 4456-4458.

30. K. Aoi, K. Tsutsumiuchi and M. Okada, *Macromolecules*, 1994, **27**, 875-877.

31. C. H. Lu, Q. Shi, X. S. Chen, T. C. Lu, Z. G. Xie, X. L. Hu, J. Ma and X. B. Jing, *J. Polym. Sci., Part A: Polym. Chem.*, 2007, **45**, 3204-3217.

32. K. Tsutsumiuchi, K. Aoi and M. Okada, *Macromolecules*, 1997, **30**, 4013-4017.

33. K. Nomura and R. R. Schrock, *Macromolecules*, 1996, **29**, 540-545.

34. C. Fraser and R. H. Grubbs, *Macromolecules*, 1995, **28**, 7248-7255.

35. K. H. Mortell, M. Gingras and L. L. Kiessling, *J. Am. Chem. Soc.*, 1994, **116**, 12053-12054.

36. S. J. Hou, X. L. Sun, C. M. Dong and E. L. Chaikof, *Bioconjug Chem*, 2004, **15**, 954-959.

37. K. Ohno, Y. Tsujii, T. Miyamoto, T. Fukuda, M. Goto, K. Kobayashi and T. Akaike, *Macromolecules*, 1998, **31**, 1064-1069.

38. H. Gotz, E. Harth, S. M. Schiller, C. W. Frank, W. Knoll and C. J. Hawker, *J. Polym. Sci., Part A: Polym. Chem.*, 2002, **40**, 3379-3391.

39. K. Ohno, Y. Tsujii and T. Fukuda, *J. Polym. Sci., Part A: Polym. Chem.*, 1998, **36**, 2473-2481.

40. M. Ejaz, K. Ohno, Y. Tsujii and T. Fukuda, *Macromolecules*, 2000, **33**, 2870-2874.

41. Z. C. Li, Y. Z. Liang, G. Q. Chen and F. M. Li, *Macromol Rapid Commun*,

2000, **21**, 375-380.

42. R. Narain and S. P. Armes, *Chem. Commun.*, 2002, 2776-2777.

43. O. Abdelkader, S. Moebs-Sanchez, Y. Queneau, J. Bernard and E. Fleury, *J. Polym. Sci., Part A: Polym. Chem.*, 2011, **49**, 1309-1318.

44. M. Ahmed and R. Narain, *Biomaterials*, 2011, **32**, 5279-5290.

45. J. Bernard, X. J. Hao, T. P. Davis, C. Barner-Kowollik and M. H. Stenzel, *Biomacromolecules*, 2006, **7**, 232-238.

46. M. Okada, *Prog. Polym. Sci.*, 2001, **26**, 67-104.

47. M. Kato, M. Kamigaito, M. Sawamoto and T. Higashimura, *Macromolecules*, 1995, **28**, 1721-1723.

48. J.-S. Wang and K. Matyjaszewski, *J. Am. Chem. Soc.*, 1995, **117**, 5614-5615.

49. J. S. Wang and K. Matyjaszewski, *Macromolecules*, 1995, **28**, 7572-7573.

50. J.-S. Wang and K. Matyjaszewski, *Macromolecules*, 1995, **28**, 7901-7910.

51. K. Matyjaszewski and J. H. Xia, *Chem. Rev.*, 2001, **101**, 2921-2990.

52. M. Kamigaito, T. Ando and M. Sawamoto, *Chem. Rev.*, 2001, **101**, 3689-3746.

53. T. E. Patten and K. Matyjaszewski, *Adv. Mater.*, 1998, **10**, 901-+.

54. M. Kamigaito, T. Ando and M. Sawamoto, *Chemical Record*, 2004, **4**, 159-175.

55. K. Min and K. Matyjaszewski, *Cent. Eur. J. Chem.*, 2009, **7**, 657-674.

56. D. J. Siegwart, J. K. Oh and K. Matyjaszewski, *Prog. Polym. Sci.*, 2012, **37**, 18-37.

57. M. Kamigaito, *Polym. J.*, 2011, **43**, 105-120.

58. V. Coessens, T. Pintauer and K. Matyjaszewski, *Prog. Polym. Sci.*, 2001, **26**, 337-377.

59. W. Tang and K. Matyjaszewski, *Macromol. Theory Simul.*, 2008, **17**, 359-375.

60. K. E. Uhrich, S. M. Cannizzaro, R. S. Langer and K. M. Shakesheff, *Chem. Rev.*, 1999, **99**, 3181-3198.

61. E. Leo, A. Scatturin, E. Vighi and A. Dalpiaz, *J. Nanosci. Nanotechno.*, 2006, **6**, 3070-3079.

62. R. Langer, *Acc. Chem. Res.*, 2000, **33**, 94-101.

63. H. Y. Tian, Z. H. Tang, X. L. Zhuang, X. S. Chen and X. B. Jing, *Prog. Polym. Sci.*, 2012, **37**, 237-280.

64. K. M. Stridsberg, M. Ryner and A. C. Albertsson, *Adv Polym Sci*, 2002, **157**, 41-65.

65. O. Coulembier, P. Degee, J. L. Hedrick and P. Dubois, *Prog. Polym. Sci.*, 2006, **31**, 723-747.

66. C. M. Thomas, *Chem. Soc. Rev.*, 2010, **39**, 165-173.

67. T. Biela, A. Kowalski, J. Libiszowski, A. Duda and S. Penczek, *Macromolecular Symposia*, 2006, **240**, 47-55.

68. H. C. Kolb, M. G. Finn and K. B. Sharpless, *Angew. Chem. Int. Ed.*, 2001,

40, 2004-2021.

69. C. W. Tornoe, C. Christensen and M. Meldal, *J. Org. Chem.*, 2002, **67**, 3057-3064.

70. V. V. Rostovtsev, L. G. Green, V. V. Fokin and K. B. Sharpless, *Angew. Chem. Int. Ed.*, 2002, **41**, 2596-2599.

71. A. Carlmark, C. J. Hawker, A. Hult and M. Malkoch, *Chem. Soc. Rev.*, 2009, **38**, 352-362.

72. D. Fournier, R. Hoogenboom and U. S. Schubert, *Chem. Soc. Rev.*, 2007, **36**, 1369-1380.

73. C. J. Hawker and K. L. Wooley, *Science*, 2005, **309**, 1200-1205.

74. R. K. Iha, K. L. Wooley, A. M. Nystrom, D. J. Burke, M. J. Kade and C. J. Hawker, *Chem. Rev.*, 2009, **109**, 5620-5686.

75. G. Tillet, B. Boutevin and B. Ameduri, *Prog. Polym. Sci.*, 2011, **36**, 191-217.

76. C. R. Becer, R. Hoogenboom and U. S. Schubert, *Angew. Chem. Int. Ed.*, 2009, **48**, 4900-4908.

77. M. A. Gauthier and H. A. Klok, *Chem. Commun.*, 2008, 2591-2611.

78. R. Fu and G. D. Fu, *Polym. Chem.*, 2011, **2**, 465-475.

79. M. A. Gauthier, M. I. Gibson and H. A. Klok, *Angew. Chem. Int. Ed.*, 2009, **48**, 48-58.

80. M. A. Tasdelen, M. U. Kahveci and Y. Yagci, *Prog. Polym. Sci.*, 2011, **36**, 455-567.

81. A. J. Qin, J. W. Y. Lam and B. Z. Tang, *Chem. Soc. Rev.*, 2010, **39**, 2522-2544.

82. V. P. Bhavanandan, *Glycobiology*, 1991, **1**, 493-503.

83. S. I. Hakomori, *Adv. Cancer Res.*, 1989, **52**, 257-331.

84. J. Schlepperschafer, D. Hulsmann, A. Djovkar, H. E. Meyer, L. Herbertz, H. Kolb and V. Kolbbachofen, *Exp. Cell Res.*, 1986, **165**, 494-506.

85. A. Varki, *Glycobiology*, 1993, **3**, 97-130.

86. K. A. Karlsson, *Current Opinion in Structural Biology*, 1995, **5**, 622-635.

87. H. J. Gabius, H. C. Siebert, S. Andre, J. Jimenez-Barbero and H. Rudiger, *Chembiochem*, 2004, **5**, 740-764.

88. S. Hakomori, *Proc. Natl. Acad. Sci. USA*, 2002, **99**, 10231-10233.

89. M. Ono and S. Hakomori, *Glycoconjugate J.*, 2003, **20**, 71-78.

90. I. Garcia, M. Marradi and S. Penades, *Nanomedicine*, 2010, **5**, 777-792.

91. J. M. De la Fuente and S. Penades, *Biochim. Biophys. Acta Gen. Subj.*, 2006, **1760**, 636-651.

92. Y. C. Lee and R. T. Lee, *Acc. Chem. Res.*, 1995, **28**, 321-327.

93. L. L. Kiessling and N. L. Pohl, *Chemistry & Biology*, 1996, **3**, 71-77.

94. R. Roy, *Current Opinion in Structural Biology*, 1996, **6**, 692-702.

95. C. R. Bertozzi and L. L. Kiessling, *Science*, 2001, **291**, 2357-2364.

96. S. G. Spain and N. R. Cameron, *Polym. Chem.*, 2011, **2**, 60-68.

97. J. Nicolas, G. Mantovani and D. M. Haddleton, *Macromol Rapid Commun*, 2007, **28**, 1083-1111.

98. B. Le Droumaguet and J. Nicolas, *Polym. Chem.*, 2010, **1**, 563-598.

99. S. Slavin, J. Burns, D. M. Haddleton and C. R. Becer, *Eur. Polym. J.*, 2011, **47**, 435-446.

100. R. N. Keller, H. D. Wrcoff and L. E. Marchi, *Inorg. Synth.*, 1946, **2**, 1-4.

101. D. M. Haddleton, M. C. Crossman, B. H. Dana, D. J. Duncalf, A. M. Heming, D. Kukulj and A. J. Shooter, *Macromolecules*, 1999, **32**, 2110-2119.

102. M. Ciampolini and N. Nardi, *Inorg. Chem.*, 1966, **5**, 41-44.

103. J. Queffelec, S. G. Gaynor and K. Matyjaszewski, *Macromolecules*, 2000, **33**, 8629-8639.

104. D. A. Mitchell, A. J. Fadden and K. Drickamer, *J. Biol. Chem.*, 2001, **276**, 28939-28945.

105. T. Tanaka, H. Nagai, M. Noguchi, A. Kobayashi and S. Shoda, *Chem. Commun.*, 2009, 3378-3379.

106. T. Tanaka, W. C. Huang, M. Noguchi, A. Kobayashi and S. Shoda, *Tetrahedron Lett.*, 2009, **50**, 2154-2157.

107. M. Noguchi, T. Tanaka, H. Gyakushi, A. Kobayashi and S. Shoda, *J. Org. Chem.*, 2009, **74**, 2210-2212.

108. T. Tanaka, T. Matsumoto, M. Noguchi, A. Kobayashi and S. Shoda, *Chem. Lett.*, 2009, **38**, 458-459.

109. J. A. Watt and S. J. Williams, *Org. Biomol. Chem.*, 2005, **3**, 1982-1992.

110. J. Dahmen, T. Frejd, G. Gronberg, T. Lave, G. Magnusson and G. Noori,

Carbohydr. Res., 1983, **116**, 303-307.

111. A. Y. Chernyak, G. V. M. Sharma, L. O. Kononov, P. R. Krishna, A. B. Levinsky, N. K. Kochetkov and A. V. R. Rao, *Carbohydr. Res.*, 1992, **223**, 303-309.

112. M. Kleinert, N. Rockendorf and T. K. Lindhorst, *Eur. J. Org. Chem.*, 2004, 3931-3940.

113. J. Geng, G. Mantovani and D. H. Haddleton, *Abstracts of Papers of the American Chemical Society*, 2007, **234**.

114. V. Ladmiral, G. Mantovani, G. J. Clarkson, S. Cauet, J. L. Irwin and D. M. Haddleton, *J. Am. Chem. Soc.*, 2006, **128**, 4823-4830.

115. J. Geng, G. Mantovani, L. Tao, J. Nicolas, G. J. Chen, R. Wallis, D. A. Mitchell, B. R. G. Johnson, S. D. Evans and D. M. Haddleton, *J Am Chem Soc*, 2007, **129**, 15156-15163.

116. J. Geng, J. Lindqvist, G. Mantovani and D. M. Haddleton, *Angew. Chem. Int. Ed.*, 2008, **47**, 4180-4183.

117. L. Nurmi, J. Lindqvist, R. Randev, J. Syrett and D. M. Haddleton, *Chem. Commun.*, 2009, 2727-2729.

118. R. W. Wood, *Philosophical Magazine Series 6*, 1902, **4**, 396-402.

119. R. W. Wood, *Proc. Phys. Soc. Lond.*, 1902, **18**, 269.

120. B. Liedberg, I. Lundstrom and E. Stenberg, *Sens. Actuators B: Chem.*, 1993, **11**, 63-72.

121. X. D. Hoa, A. G. Kirk and M. Tabrizian, *Biosens. Bioelectron.*, 2007, **23**,

151-160.

122. J. Homola, S. S. Yee and G. Gauglitz, *Sens. Actuators B: Chem.*, 1999, **54**, 3-15.

123. C. Boozer, G. Kim, S. X. Cong, H. W. Guan and T. Londergan, *Curr. Opin. Biotechnol.*, 2006, **17**, 400-405.

124. D. G. Myszka and T. A. Morton, *Trends Biochem. Sci*, 1998, **23**, 149-150.

125. T. A. Morton and D. G. Myszka, *Methods Enzymol.*, 1998, **295**, 268-294.

126. D. G. Myszka, *Curr. Opin. Biotechnol.*, 1997, **8**, 50-57.

127. R. Karlsson and A. Falt, *J. Immunol. Methods*, 1997, **200**, 121-133.

128. B. Nguyen, F. A. Tanious and W. D. Wilson, *Methods*, 2007, **42**, 150-161.

129. P. Schuck and A. P. Minton, *Trends Biochem. Sci*, 1996, **21**, 458-460.

130. L. P. Lin, L. S. Huang, C. W. Lin, C. K. Lee, J. L. Chen, S. M. Hsu and S. Lin, *Curr Drug Targets Immune Endocr Metabol Disord*, 2005, **5**, 61-72.

131. P. Bjorquist and S. Bostrom, *Thromb. Res.*, 1997, **85**, 225-236.

132. D. J. Oshannessy, M. Brighamburke, K. K. Soneson, P. Hensley and I. Brooks, *Anal. Biochem.*, 1993, **212**, 457-468.

133. E. Bouffartigues, H. Leh, M. Anger-Leroy, S. Rimsky and M. Buckle, *Nucleic Acids Res.*, 2007, **35**, e39.

134. W. I. Weis, K. Drickamer and W. A. Hendrickson, *Nature*, 1992, **360**, 127-134.

135. H. Feinberg, D. A. Mitchell, K. Drickamer and W. I. Weis, *Science*, 2001, **294**, 2163-2166.

136. R. Ilyas, R. Wallis, E. J. Soilleux, P. Townsend, D. Zehnder, B. K. Tan, R. B. Sim, H. Lehnert, H. S. Randeva and D. A. Mitchell, *Immunobiology*, 2011, **216**, 126-131.

137. A. E. van der Ende, J. Harrell, V. Sathiyakumar, M. Meschievitz, J. Katz, K. Adcock and E. Harth, *Macromolecules*, 2010, **43**, 5665-5671.

138. A. E. van der Ende, E. J. Kravitz and E. Harth, *J. Am. Chem. Soc.*, 2008, **130**, 8706-8713.

139. A. E. van der Ende, V. Sathiyakumar, R. Diaz, D. E. Hallahan and E. Harth, *Polym. Chem.*, 2010, **1**, 93-96.

140. R. J. Passarella, D. E. Spratt, A. E. van der Ende, J. G. Phillips, H. M. Wu, V. Sathiyakumar, L. Zhou, D. E. Hallahan, E. Harth and R. Diaz, *Cancer Res.*, 2010, **70**, 4550-4559.

141. R. G. Nuzzo and D. L. Allara, *J. Am. Chem. Soc.*, 1983, **105**, 4481-4483.

142. E. B. Troughton, C. D. Bain, G. M. Whitesides, R. G. Nuzzo, D. L. Allara and M. D. Porter, *Langmuir*, 1988, **4**, 365-385.

143. A. Ihs, K. Uvdal and B. Liedberg, *Langmuir*, 1993, **9**, 733-739.

144. M. G. Samant, C. A. Brown and J. G. Gordon, *Langmuir*, 1992, **8**, 1615-1618.

145. A. J. Arduengo, J. R. Moran, J. Rodriguezparada and M. D. Ward, *J. Am. Chem. Soc.*, 1990, **112**, 6153-6154.

146. R. A. Sperling and W. J. Parak, *Philos Transact A Math Phys Eng Sci*, 2010, **368**, 1333-1383.

147. N. V. Tsarevsky and K. Matyjaszewski, *Macromolecules*, 2002, **35**, 9009-9014.

148. N. V. Tsarevsky and K. Matyjaszewski, *Macromolecules*, 2005, **38**, 3087-3092.

149. J. A. Syrett, M. W. Jones and D. M. Haddleton, *Chem. Commun.*, 2010, **46**, 7181-7183.

150. G. Sauerbrey, *Z. Phys. A: Hadrons Nucl.*, 1959, **155**, 206-222.

151. M. Rodahl, F. Hook, C. Fredriksson, C. A. Keller, A. Krozer, P. Brzezinski, M. Voinova and B. Kasemo, *Faraday Discuss.*, 1997, **107**, 229-246.

152. E. F. Irwin, J. E. Ho, S. R. Kane and K. E. Healy, *Langmuir*, 2005, **21**, 5529-5536.

153. B. Borovsky, J. Krim, S. A. Syed Asif and K. J. Wahl, *J. Appl. Phys.*, 2001, **90**, 6391-6396.

154. A. Dolatshahi-Pirouz, K. Rechendorff, M. B. Hovgaard, M. Foss, J. Chevallier and F. Besenbacher, *Colloids Surf., B*, 2008, **66**, 53-59.

155. K. K. Kanazawa and J. G. Gordon, *Anal. Chem.*, 1985, **57**, 1770-1771.

156. G. Z. Zhang and C. Wu, *Macromol. Rapid Commun.*, 2009, **30**, 328-335.

157. C. M. Marxer, M. C. Coen, T. Greber, U. F. Greber and L. Schlapbach, *Anal. Bioanal. Chem.*, 2003, **377**, 578-586.

158. J. C. Munro and C. W. Frank, *Polymer*, 2003, **44**, 6335-6344.

159. M. Rodahl and B. Kasemo, *Sens. Actuators A: Phys.*, 1996, **54**, 448-456.

160. F. Hook, B. Kasemo, T. Nylander, C. Fant, K. Sott and H. Elwing, *Anal. Chem.*, 2001, **73**, 5796-5804.

161. M. V. Voinova, M. Rodahl, M. Jonson and B. Kasemo, *Phys. Scr.*, 1999, **59**, 391-396.

162. N. J. Chot, K. K. Kanazawa, J. S. Glenn and C. W. Frank, *Anal. Chem.*, 2007, **79**, 7027-7035.

163. F. Hook, M. Rodahl, P. Brzezinski and B. Kasemo, *Langmuir*, 1998, **14**, 729-734.

164. A. Monkawa, T. Ikoma, S. Yunoki, T. Yoshioka, J. Tanaka, D. Chakarov and B. Kasemo, *Biomaterials*, 2006, **27**, 5748-5754.

165. J. T. Kim, N. Weber, G. H. Shin, Q. Huang and S. X. Liu, *J. Food Sci.*, 2007, **72**, E214-E221.

166. W. Y. X. Peh, E. Reimhult, H. F. Teh, J. S. Thomsen and X. D. Su, *Biophys. J.*, 2007, **92**, 4415-4423.

167. A. P. Dove, R. C. Pratt, B. G. G. Lohmeijer, R. M. Waymouth and J. L. Hedrick, *J. Am. Chem. Soc.*, 2005, **127**, 13798-13799.

168. B. G. G. Lohmeijer, R. C. Pratt, F. Leibfarth, J. W. Logan, D. A. Long, A. P. Dove, F. Nederberg, J. Choi, C. Wade, R. M. Waymouth and J. L. Hedrick, *Macromolecules*, 2006, **39**, 8574-8583.

Chapter 5. Synthesis of glycopolymers *via* SET and SET-RAFT polymerization and CuAAc click chemistry for bioconjugation

5.1. Introduction

Recently both naturally occurring polysaccharides and synthetic glycopolymers have attracted increasing attention due to their involvement in many biochemical and physiological processes. They have potential biocompatibility and can have strong interactions with proteins and peptides.[1-5] Synthetic glycopolymers, with multiple copies of monodentate sugar moieties, can exhibit an increased bio-recognition effect compared to the individual carbohydrate unimers due to the *cluster glycoside effect*.[6-12] Glycopolymers have been investigated in many applications including cell-cell recognition,[13, 14] cell-protein interactions[15], biocatalytic hydrogels,[16] biosensitive hydrogels,[17] therapeutics,[18-20] and gene/drug delivery systems,[21-25] chiral molecularly imprinted materials,[26] model biomembranes,[27] or synthetic biology.[28]

A larger number of well-defined glycopolymers with different complex macromolecular architectures have been prepared by different kinds of "living"/controlled polymerization methodology,[3, 29, 30] for example, living anionic polymerization,[31, 32] living cationic polymerization,[32, 33] ring-opening

polymerization (ROP), [34-37] ring-opening metathesis polymerization (ROMP),[38-40] cyanoxyl(OCN)-mediated free-radical polymerization,[41] nitroxide-mediated radical polymerization (NMP),[42, 43] atom transfer radical polymerization (ATRP)[44-46] and reversible addition fragmentation chain transfer (RAFT) polymerization.[47, 48]

Amongst the "living"/controlled radical polymerization, single-electron transfer living radical polymerization (SET-LRP), as reported by Percec *et al*,[49] has been shown to have distinct advantages over ATRP, including mild reaction conditions (ambient and sub-ambient temperature), small quantities and facile removal of catalyst, "*ultra-fast*" rate of polymerization, excellent control of molecular weight and narrow polydispersity index with almost perfect end group fidelity.[50-52] SET-LRP could be considered a specific mechanism-outer-sphere single electron transfer process. This process was not activated by a Cu(I)X complex but by the electron-donor catalysis Cu(0), Cu_2Se, Cu_2Te, Cu_2S, or Cu_2O species, while the reversible deactivation of propagating macro-radicals was mediated by Cu(II)X_2/*N*-containing ligands species. Critical for the SET-LRP process to be effective is an appropriate balance of Cu(0) and Cu(II)X_2/L species *via* disproportionation of Cu(I)X. The spontaneous disproportionation of Cu(I)X/L compounds generated *in situ* result in both an active Cu(0) and deactivating Cu(II)X_2/L species in the presence of appropriate polar/coordinating solvents and ligands, providing a pathway to minimize biradical termination, leading to excellent living polymerization.[49, 53, 54] Dhamodharan has reported a

single-electron transfer initiation followed by reversible addition fragmentation chain transfer (SET-RAFT) polymerization.[55] This could improve the living character of polymerization and was found to be suitable for controlled polymerization at ambient temperature, leading to thermal self-initiation; irreversible chain transfer, thermal crossing-linking, irreversible chain termination and other side reactions were suppressed/eliminated owing to the presence of chain transfer agent (CTA) along with Cu(II) generated in situ. SET-RAFT can be considered as a combination of SET-LRP and RAFT polymerization. The method was a relatively simple and alternative controlled polymerization system.[56, 57]

More recently, the exploitation of click chemistry has opened new avenues for the design and creation of novel polymers with different complex structure for many applications in chemistry and materials.[58-68] Copper catalyzed azide-alkyne cycloadditions (CuAAC) click reaction, in which organic azide reacted quantitatively with a terminal acetylene and then triazole was formed, was independently reported by Sharpless and Meldal.[58, 69, 70] This has been shown to be robust, quite general, orthogonal, insensitive to many functional groups, rapid and highly efficient in presence of catalyst under mild conditions and leads to the synthesis of the desired products in high yield and purity. CuAAC reactions have been widely applied to the modification of living and controlled radical polymerization and post-polymerization modification, affording a simple alternative effective route to functional polymer materials through the reaction of appropriately functionalized substrates onto the activated preformed polymer

backbones.[71-76]

Although synthesis of glycopolymers have been described in the last decade, very few examples of glycopolymers prepared through SET-LRP/SET-RAFT and CuAAC click chemistry have been reported to date. To the best of our knowledge, there was no published research on the glycopolymers prepared by the use of SET-LRP/SET-RAFT and CuAAC click reaction.

In this present work, the controlled SET-LRP polymerization of TMS-PgMA and SET-RAFT polymerization PgMA with the intact alkyne at ambient temperature is reported. A maleimide functional initiator and CPDB, as the chain transfer agent have been employed. The introduction of maleimide moiety was to allow for post polymerization conjugation to peptides *via* reaction with cysteines. The subsequent introduction of sugar azides to click with the reactive polymer containing alkyne group and the glycopolymers through CuAAC was also investigated. This is the first report that the glycopolymer has been successfully prepared combining the SET-LRP/SET-RAFT and CuAAc click chemistry at ambient temperature. The summary of the work is presented in **Scheme 5.1**.

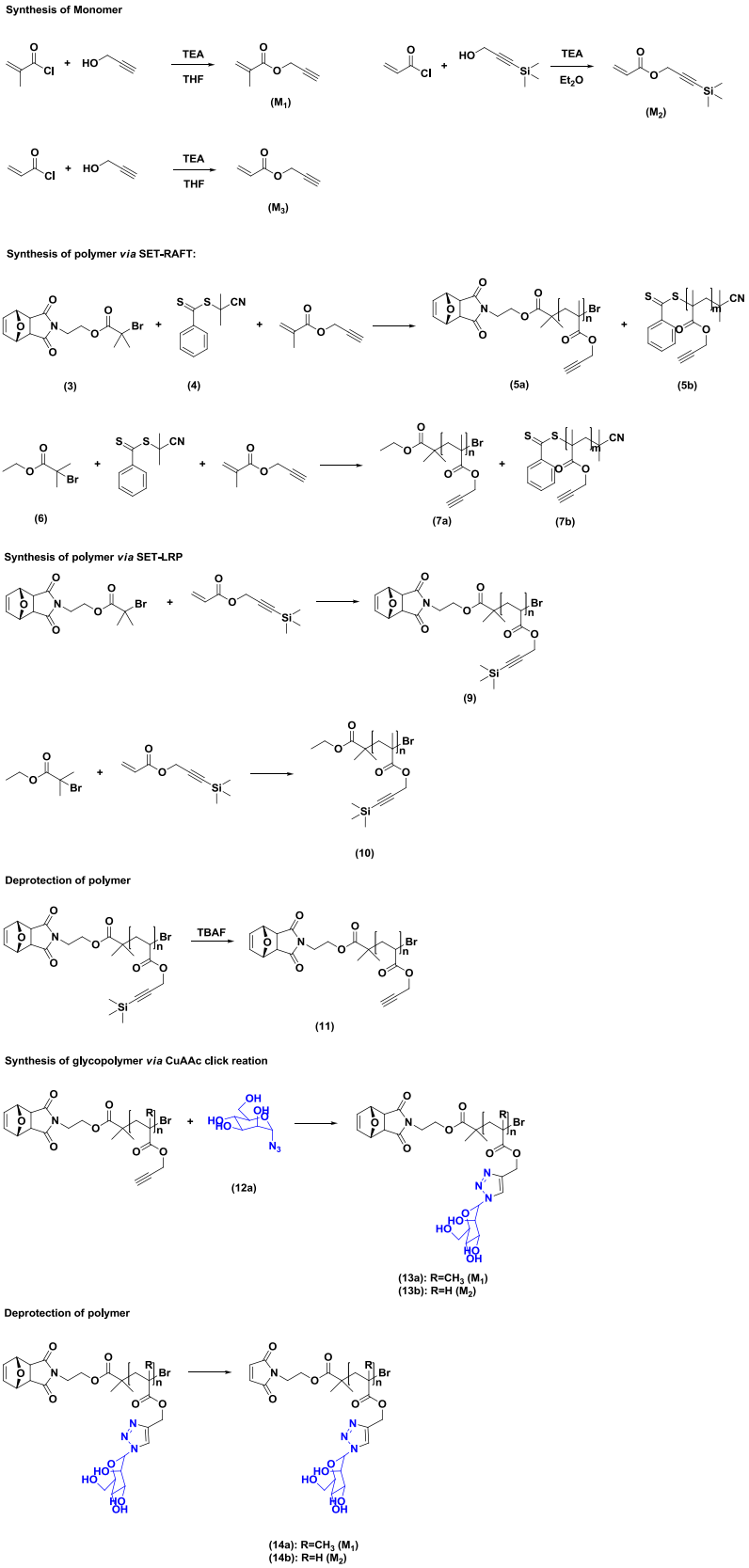

Scheme 5.1 Summary of the general synthesis approach from monomer synthesis to the preparation of final glycopolymer in this study

5.2. Experimental

5.2.1. Materials

Copper(I) bromide (CuBr, Aldrich, 98%) was purified according to the method of Keller *et al.*[77]. *N*-Ethyl-2-pyridylmethanimine[78] and tris(2-(dimethylamino)ethyl)amine (Me_6-TREN)[79, 80] were prepared as described earlier and stored at 0 ℃ under a nitrogen atmosphere prior to use. Triethylamine (TEA, Fischer, 99%) was stored over sodium hydroxide pellets. Cu(0) wire (Φ = 0.25 mm, 500 $g.m^{-3}$) from Comax Engineered wires company was activated by washing with 37% HCl for 10 min and then rinsed with distilled water and acetone. Cu(0) powder (99%, +45 μm particle size (2% max)), copper(II) bromide ($CuBr_2$, 99%), methyl 2-bromopropionate (BMP, 98%), ethyl α-bromoisobutyrate (EBiB, 98%), 3-(trimethylsilyl)propargyl alcohol (99%), 2-(dodecylthiocarbonothioylthio)-2-methylpropionic acid (TTCA, 98%), propargyl alcohol (99%), methacryloyl chloride (≥ 97%), acryloyl chloride (≥ 97%), *N,N,N',N'',N''*- pentamethyldiethylenetriamine (PMDETA, 99%), tetrabutyl ammonium fluoride (TBAF) solution 1.0 M in THF, 2-chloro-1,3-dimethylimidazolinium chloride (DMC), sodium azide (≥ 99%), Amberlite® IR120 hydrogen form, anhydrous tetrahydrofuran (THF, ≥ 99.5%, 0.025% BHT stabilizer, over molecular sieve), anhydrous

N,*N*-dimethylformamide (DMF, 99.8%), D-(+)-glucose (≥ 99.5%), and L-(-)-fucose (≥ 99%) from Sigma-Aldrich, D-(+)-mannose (99%) from Alfa Aesar and D(+)-galactose (99+%) from Acros Organics were used as received. Phenol (≥ 99%) from VWR International Ltd. was used as received. Bovine Serum Albumin (BSA, ≥ 95%) from Sigma-Aldrich was used as received and stored at 4 ℃. Fluorescein isothiocyanate isomer I (FITC, 90%) from Sigma-Aldrich was used as received and stored at -20 ℃. All other reagents and solvents were obtained from Sigma-Aldrich Company and used as purchased without further purification unless stated otherwise.

5.2.2. Characterization

^{1}H NMR spectroscopy was used to determine the number average molecular weight and structural information for confirmation of thiol-ene click conjugation. NMR spectra were recorded on either a Bruker DPX-300 MHz or a Bruker DPX-400 MHz or a Bruker AV III-600 MHz spectrometer at 298 K with approximately 10% w/v solutions in deuterated NMR solvents from Sigma-Aldrich. All chemical shifts were reported in ppm (δ) relative to tetramethylsilane (TMS), or referenced to the chemical shifts of residual solvent resonances (^{1}H and ^{13}C). The following abbreviations were used to explain the multiplicities: s = singlet, d = doublet, dd = doublet of doublets, t = triplet, m = multiplet. The molecular weight of the polymers $M_{n,NMR}$ were calculated by

comparing the integrals of the chain-end signals with appropriate peaks related to the polymer backbone.

Gel permeation chromatography (GPC) was used to determine molecular weights and polydispersity ratio (M_w/M_n) of polymer samples.

GPC using $CHCl_3$ eluent was performed on an Agilent 390-MDS, comprising of an autosampler and a PLgel 5.0 μm guard column (50 × 7.5 mm), followed by two 5.0 μm PLgel Mixed D columns (300 × 7.5 mm) and a differential refractive index detector using $CHCl_3$ as the eluent at 30 ^oC with a flow rate of 1 mL min^{-1}. The GPC system was calibrated using linear poly(methyl methacrylate) EasiVial standards (Agilent Ltd.) range from 200 to 10^5 g mol^{-1} and polystyrene EasiVial standards (Agilent Ltd.) range from 162 to 10^5 g mol^{-1}. Data were collected and analyzed using Cirrus GPC/SEC software (version 3.3).

GPC with THF as eluent was performed on an Agilent 390-MDS, comprising of an autosampler and a PLgel 5.0 μm guard column (50 × 7.5 mm), followed by two linear 5.0 μm PLgel Mixed D columns (300 × 7.5 mm) and a differential refractive index detector using THF (2% v/v TEA) as the eluent at 30 ^oC with a flow rate of 1 mL min^{-1}. The GPC system was calibrated using linear poly(methyl methacrylate) EasiVial standards (Agilent Ltd.) range from 200 to 10^5 g mol^{-1} and polystyrene EasiVial standards (Agilent Ltd..) range from 162 to 10^5 g mol^{-1}. Data were collected and analyzed using Cirrus GPC/SEC software (version 3.3).

DMF GPC analyses of the polymers were performed in *N*,*N*-dimethylformamide (DMF, 0.1% w/v LiBr), at 50 ^oC (flow rate = 1 mL min^{-1})

using an Agilent 390-MDS system comprised of an autosampler and a PLgel 5.0 μm guard column (50 × 7.8 mm) followed by two linear 5.0 μm PLgel Mixed D columns (300 × 7.5 mm) and a differential refractive-index detector. Calibration was achieved with linear poly(methyl methacrylate) EasiVial standards (Agilent Ltd.) range from 200 to 10^5 g mol^{-1}. Data were collected and analyzed using Cirrus GPC/SEC software (version 3.3).

The infrared absorption spectra were recorded on a Bruker VECTOR-22 FTIR spectrometer or PerkinElmer Spectrum 100 FT-IR Spectrometers using a Golden Gate diamond attenuated total reflection cell. The following abbreviations were used to explain the absorption bands: υ, stretching; γ, out-of-plane deformation; δ, in-plane deformation; ρ, rocking; τ, twisting; s, strong; v, very; w, weak; br, broad; m, medium; sh, shoulder. subscripts: a, asymmetric; s, symmetric.

Mass spectra were recorded on a Bruker Esquire 2000 Mass spectrometer using electrospray ionisation (ESI) in positive mode.

TLC performed using pre-coated silica gel 60 F_{254} and developed in the solvent system indicated. Compounds were visualized by use of UV light (254 nm) or a stain solution of potassium permanganate (1.5 g of $KMnO_4$, 10 g K_2CO_3, and 1.25 mL 10% NaOH in 200 mL water). Silica gel (40-63u, 60 A, LC301) from Fluorochem Ltd. was used for column chromatography.

5.2.3. Synthesis of Monomers

5.2.3.1. Synthesis of propargyl methacrylate (PgMA (M_1))

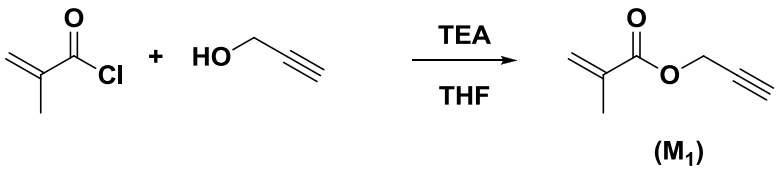

Scheme 5.2 Synthesis of propargyl methacrylate (PgMA (M_1))

A solution of propargyl alcohol (23.7 g, 419.19 mmol) and Et_3N (105 mL, 754.55 mmol) in THF (260 mL) was cooled to 0 ℃ and a solution of methacryloyl chloride (61.4 mL, 629 mmol) in THF (122 mL) was added dropwise over ca. 1 h. The mixture was stirred at this temperature for 30 min or 1 hour, then at ambient temperature overnight or in some instances 24 hours; the ammonium salts were removed by filtration and the volatiles removed under reduced pressure. PgMA was further purified by reduced distillation.

^{1}H NMR (400 MHz, $CDCl_3$, 298 K): δ (ppm) = 1.92-1.93 (m, 3H, CH_3C=C), 2.46 (t, *J*=2.51 Hz, 1H, *H*C≡C), 4.72 (d, *J*=2.51 Hz, 2H, OCH_2), 5.59 (t, *J*=1.38 Hz, 1H, 1/2 C*H*$_2$=CCH_3), 6.14 (s, 1 H, 1/2 C*H*$_2$=CCH_3).

^{13}C NMR (100 MHz, $CDCl_3$, 298 K): δ (ppm) = 18.27 (1C, *C*H_3C=C), 52.23 (1C, OCH_2), 74.87 (1C, HC≡*C*), 77.82 (1C, H*C*≡C), 126.58 (1C, *C*H_2=CCH_3), 135.69 (1C, CH_2=*C*CH_3), 166.55 (1C, CO_{ester}).

FIIR (neat): υ (cm^{-1}) = 3294, 2958, 2133, 1720, 1638, 1452, 1437, 1369, 1317, 1293, 1148, 1013, 990, 943, 813, 634, 538.

Mass spectrometry: ESI-MS (*m/z*) Calcd. for $C_7H_8NaO_2^+$ ($M+Na^+$) = 147.04, Found 147.04.

5.2.3.2. Synthesis of trimethylsilyl-protected propargyl acrylate (TMS-PgA (M_2))

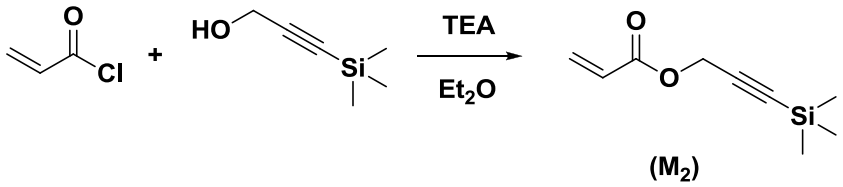

Scheme 5.3 Synthesis of trimethylsilyl-protected propargyl acrylate (TMS-PgA (M_2))

A solution of trimethylsilyl propyn-1-ol (25.0 g, 194.9 mmol) and Et_3N (35.3 mL, 253.4 mmol) in Et_2O (350 mL) was cooled to 0 ℃ and a solution of acryloyl chloride (mL, 233.9 mmol) in Et_2O (200 mL) was added dropwise over ca. 1 h. The mixture was stirred at this temperature for between 30 min and 1 hour, then at ambient temperature overnight; the ammonium salts were removed by filtration and the volatiles removed under reduced pressure.

^{1}H NMR (400 MHz, $CDCl_3$, 298 K): δ (ppm) = 0.15 (s, 9H, $Si(CH_3)_3$), 4.74 (s, 2H, OCH_2), 5.85 (dd, *J*=10.42, 1.38 Hz, 1H, 1/2 C*H*$_2$=CH), 6.13 (dd, *J*=17.32, 10.54 Hz, 1H, CH_2=C*H*), 6.43 (dd, *J*=17.32, 1.51 Hz, 1H, 1/2 C*H*$_2$=CH).

^{13}C NMR (100 MHz, $CDCl_3$, 298 K): δ (ppm) = -0.23 (3C, $Si(CH_3)_3$), 52.90 (1C, OCH_2), 92.24 (1C, C≡*C*Si$(CH_3)_3$), 98.96 (1C, *C*≡CSi$(CH_3)_3$), 127.85 (1C, CH_2=*C*H), 131.73 (1C, *C*H_2=CH), 165.35 (1C, CO_{ester}).

FIIR (neat): υ (cm^{-1}) = 2962, 2900, 2187, 1731, 1635, 1406, 1363, 1294, 1250, 1171, 1050, 984, 967, 838, 808, 760, 701, 644.

Mass spectrometry: ESI-MS (*m/z*) Calcd. for $C_9H_{14}NaO_2Si^+$ ($M+Na^+$) = 205.07, Found 205.07.

5.2.3.3. Synthesis of propargyl acrylate (PgA (M_3))

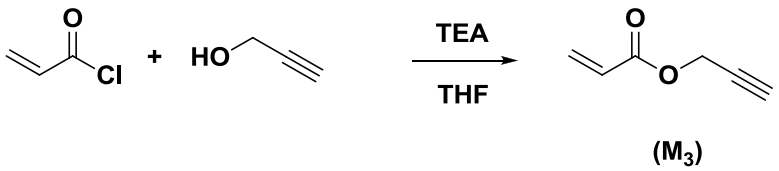

Scheme 5.4 Synthesis of propargyl acrylate (PgA (M_3))

A solution of propargyl alcohol (10 g, 178.38 mmol) and Et_3N (45 mL, 321.09 mmol) in THF (110 mL) was cooled to 0 ℃ and a solution of acryloyl chloride (22 mL, 267.57 mmol) in THF (43 mL) was added dropwise over ca. 1 h. The mixture was stirred at this temperature for between 30 min and 1 hour, then at ambient temperature overnight or in some cases for 24 hours; the ammonium salts were removed by filtration and the volatiles removed under reduced pressure. PgA was further purified by reduced distillation.

^{1}H NMR (400 MHz, $CDCl_3$, 298 K): δ (ppm) = 2.47 (t, *J*=2.38 Hz, 1H, *H*C≡C), 4.72 (d, *J*=2.26 Hz, 2H, OCH_2), 5.86 (dd, *J*=10.54, 1.00 Hz, 1H, 1/2 C*H*$_2$=CH), 6.11 (dd, *J*=17.32, 10.54 Hz, 1H, CH_2=C*H*), 6.43 (dd, *J*=17.32, 1.00 Hz, 1H, 1/2 C*H*$_2$=CH).

^{13}C NMR (100 MHz, $CDCl_3$, 298 K): δ (ppm) = 52.10 (1C, OCH_2), 75.06 (1C, HC≡*C*), 77.62 (1C, H*C*≡C), 127.66 (1C, CH_2=*C*H), 131.95 (1C, 1C, *C*H_2=CH), 165.29 (1C, CO_{ester}).

FIIR (neat): υ (cm^{-1}) = 3295, 2951, 2131, 1725, 1635, 1620, 1437, 1407, 1365, 1293, 1257, 1170, 1054, 983, 934, 808, 671, 639.

Mass spectrometry: ESI-MS (*m/z*) Calcd. for $C_6H_6NaO_2^+$ ($M+Na^+$) = 133.03, Found 133.03.

5.2.4. Synthesis of Maleimide protected initiator

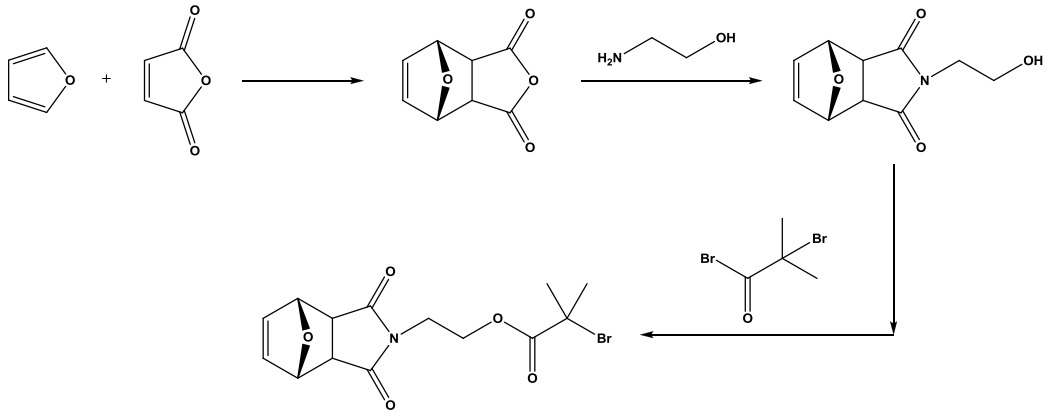

Scheme 5.5 Synthesis of maleimide protected initiator

Maleimide protected initiator was prepared as described earlier.[81]

^{1}H NMR (400 MHz, $CDCl_3$, 298 K): δ (ppm) = 1.90 (s, 6H, CH_3), 2.87 (s, 2H, CH), 3.82 (t, *J* = 5.3 Hz, 2H, NCH_2), 4.33 (t, *J* = 5.3 Hz, 2H, OCH_2), 5.26 (t, *J* = 1.0 Hz, 2H, CHO), 6.51 (t, J = 1.0 Hz, 2H, CH_{vinyl}).

^{13}C NMR (100 MHz, $CDCl_3$, 298 K): δ (ppm) = 30.73 (2C, CH_3), 37.75 (1C, NCH_2), 47.64 (2C, CH), 55.82 (1C, $C(CH_3)_2Br$), 62.34 (1C, OCH_2), 80.99 (2C, CHO), 136.70 (2C, CH_{vinyl}), 171.57 (1C, CO_{ester}), 176.01 (2C, CO_{imide}).

FIIR (neat): υ (cm^{-1}) = 2978, 2959, 1773, 1734, 1696, 1462, 1421, 1395, 1374, 1359, 1336, 1277, 1190, 1157, 1107, 1096, 1016, 989, 968, 953, 938, 926, 917, 910, 875, 852, 824, 799, 782, 724, 706, 655, 603, 594

Mass spectrometry: ESI-MS (*m/z*) Calcd. for $C_{14}H_{16}BrNNaO_5^+$ ($M+Na^+$) = 380.01, Found 380.01.

M_p: 83-85 ℃.

5.2.5. Synthesis of 2-cyanopropan-2-yl benzodithioate (CPDB) transfer agent

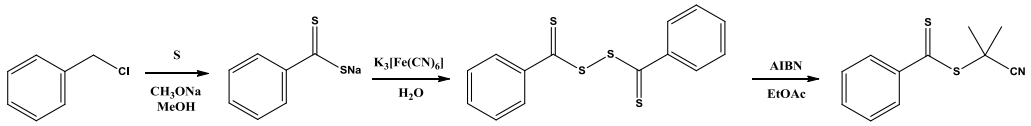

Scheme 5.6 Synthesis of 2-cyanopropan-2-yl benzodithioate (CPDB)

CPDB transfer agent was prepared according to a standard procedure described in the literature.[82]

^{1}H NMR (400 MHz, $CDCl_3$, 298 K), δ (ppm) = 1.94 (s, 6H, -2*CH_3), 7.39 (t, 2H, *J* = 8.3 Hz, *meta*-ArH), 7.56 (t, 1H, *J* = 7.8 Hz, *para*-ArH), 7.91 (d, 2H, *J* = 8.0 Hz, *ortho*-ArH).

^{13}C NMR (150 MHz, $CDCl_3$, 298 K), δ (ppm) = 26.56 (2C, C(CN)(CH_3)$_2$), 41.82 (1C, *C*(CN)(CH_3)$_2$), 120.06 (1C, CN), 126.73 (2C, *ortho*-ArC), 128.64 (1C, *meta*-ArC), 133.00 (2C, *para*-ArC), 144.64 (1C, *ipso*-Ar*C*), 223.25 (1C, C=S)

Mass spectrometry: ESI-MS (*m/z*) Calcd. for $C_{11}H_{11}NNaS_2^+$(M+Na^+) = 244.02, Found 244.02.

5.2.6. Synthesis of Sugar azides

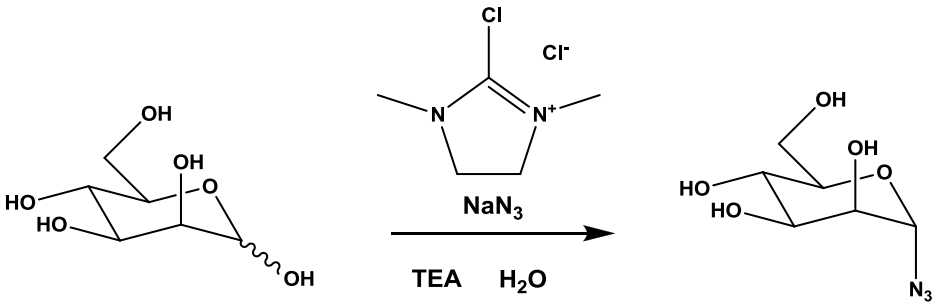

Scheme 5.7 Synthesis of α-D-mannopyranosyl azide

Sodium azide (7.26 g, 111 mmol), D-(+)-mannose (2.00 g, 11.1 mmol) and triethylamine (15.5 mL, 111 mmol) were dissolved in water (40 mL) and cooled to 0 ℃. 2-Chloro-1,3-dimethylimidazolinium chloride (5.61 g, 33.3 mmol) was added and the mixture was stirred for 1 hour at 0 ℃. The solvent was removed under reduced pressure and ethanol was added. The solids were removed by

filtration and the solution was purified on Amberlite IR-120 column. The mixture was checked with FTIR to confirm the removal of all sodium azide (ν = 2022 cm^{-1}). The solvent was removed under reduced pressure, water was added and the mixture was washed with dichloromethane. The solvent was removed under reduced pressure, water (10 mL) was added and the solution was freeze-dried overnight to give α-D-Mannopyranosyl azide as an off-white solid.

^{1}H NMR (400 MHz, D_2O, 298 K), δ (ppm) = 3.57 – 3.66 (m, 1H), 3.68 - 3.77 (m, 3H), 3.84 (dd, *J* = 3.01, 2.01 Hz, 1H), 3.88 (d, *J* = 10.04 Hz, 1H), 5.43 (d, *J* = 2.01 Hz, 1H).

^{13}C NMR (100 MHz, D_2O, 298 K), δ (ppm) = 60.81, 66.38, 69.75, 69.83, 74.62, 89.71.

FIIR (neat): υ (cm^{-1}) = 3331, 2933, 2110, 1407, 1294, 1237, 1092, 1060, 933, 803, 667, 566.

Mass spectrometry: ESI-MS (*m/z*) Calcd. for $C_6H_{11}N_3NaO_5^+$ ($M+Na^+$) = 228.06, Found 228.06.

Besides D-(+)-mannose, other sugars were used to prepare different kinds of sugar azides following the similar procedure, **Scheme 4.6**.

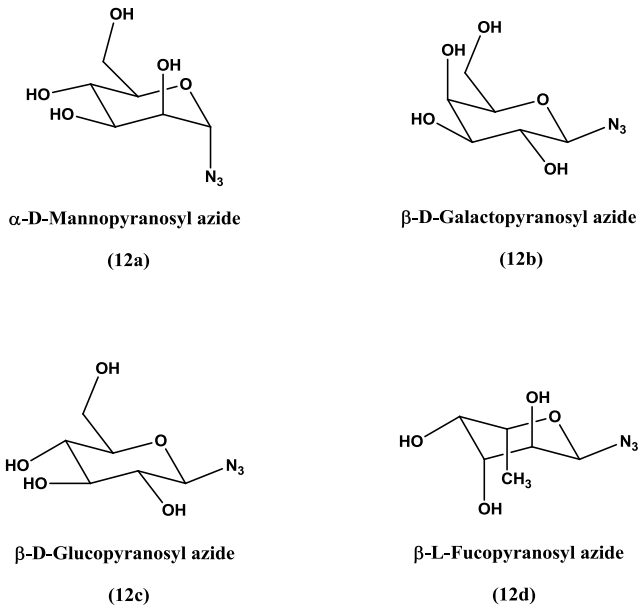

Scheme 5.8 Representation of various sugar azides prepared in this study

5.2.7. Typical procedure of SET-LRP polymerizations

TMS-PgA (50 eq., 10.972 mmol, 2 g), EBiB inititor (1 eq., 0.219 mmol, 0.0428 mL), Me_6Tren (1 eq., 0.219 mmol, 0.0506 g), phenol (20 eq., 4.389 mmol, 0.413 g), toluene (3 mL, 2/5 solids) and mesitylene (internal NMR standard) were added to a clean, dried Schlenk tube, along with a magnetic stir bar. The Schlenk tube was sealed with a suba-seal and three freeze-pump-thaw degassing cycles were then carried out in liquid nitrogen to remove oxygen. A positive pressure of nitrogen was passed into the Schlenk tube and then transferred *via* cannula under nitrogen into a second Schlenk tube, previously evacuated and filled with nitrogen, containing Cu(0) powder (1 eq., 0.219 mmol, 0.0139 g), Cu(II)Br_2 (0.1 eq., 0.022 mmol, 0.0049 g) and a magnetic stir bar. The temperature was adjusted at 25 ℃

with constant stirring (t = 0). (Temperatures were recorded using a thermocouple.) Samples were taken periodically *via* a degassed syringe for ^{1}H NMR and GPC analysis. When approximately 90% conversion had been reached, THF was added to the Schlenk tube and the solution bubbled with air for 1 hour.

The solution was then passed through a neutral alumina to remove unreacted Cu(0) catalyst and Cu(II) compounds and subsequently washed with THF. The volatiles were removed on a rotary evaporator and the resulting crude polymer redissolved in a minimum THF. The solution was precipitated in cold 10:3 vol/vol methanol/water mixture with stirring. The off-white solid was isolated by vacuum filtration, washed with some additional methanol/water mixture. The final polymer was dried in a vacuum oven until constant weight was reached.

5.2.8. Typical procedure of removal of $Si(CH_3)_3$ protecting group

The trimethyl silyl protected polymer (2 g) and acetic acid (2 equiv. mol/mol with respect to the alkyne-trimethylsilyl groups) were dissolved in 50 mL THF. The pale yellow solution was cooled to 0 ℃. A 0.20 M solution of TBAF in THF (2 equiv. mol/mol with respect to the alkyne-trimethylsilyl groups) was added slowly *via* pressure equalising dropping funnel and then the funnel was rinsed with THF. The resulting turbid mixture was stirred at this temperature for 30 min and then warmed to ambient temperature. The polymer deprotection was complete in

about 3 h . The reaction solution was passed through a silica pad in order to remove the excess of TBAF and the pad was subsequently washed with additional THF. The resulting solution was then concentrated under reduced pressure and the polymer was precipitated in petroleum ether 40 - 60 ℃. The off-white solid was isolated by vacuum filtration, washed with some additional petroleum ether. The residue was transferred to a vacuum oven and dried to constant weight.

5.2.9. Typical procedure of SET-RAFT polymerizations

A typical procedure for the SET-RAFT polymerization was as follows: PgMA (1.04 g, 8.37 mmol), EBiB (8.10 mg, 0.0418 mmol), Cu(0) powder (8.0 mg, 0.125 mmol), CPDN (11.4 mg, 0.0418 mmol) and solvent DMSO (1.0 mL) were added to a dry glass ampoule with a magnetic bar. The reaction mixture was bubbled with nitrogen for approximately 10 min, and then PMDETA (26.0 μL, 0.125 mmol) was added to the mixture. The solution was bubbled with argon for approximately 10 min to eliminate the oxygen, and then the ampoule was sealed under nitrogen atmosphere and placed in the oil bath at 25 ^{o}C. At the designed time, the ampoule was immersed into liquid nitrogen and then opened, and then the contents were diluted with THF prior to addition of BHT (0.2 wt%). The reaction mixture was passed through a short neutral alumina column and subsequently washed with THF. The volatiles were removed under reduced pressure and the residues were diluted with THF prior to precipitation into cold 10:3 vol/vol methanol/water

mixture. The samples were obtained by filtration, washed with some additional methanol/water mixture. The residue was dissolved in THF and then dried over anhydrous $MgSO_4$, filtrated, and the solvent removed reduced pressure. After that, the pink sample was again precipitated into petroleum ether 40 - 60 ℃, isolated by vacuum filtration, washed with some additional petroleum ether. The residue was transferred to a vacuum oven and dried to constant weight.

5.2.10. Post-functionalization of polymer *via* CuAAC click reation

A solution containing propargyl polymer (240 mg, 1.0 eq, 1.93 mmol propargyl groups), mannose azide (476 mg, 1.2 eq, 2.32 mmol) and CuBr (277 mg, 1.0 eq, 1.93 mmol) in DMSO (24 mL) was bubbled with nitrogen for 30 minutes. *N*-Ethyl-2-pyridylmethanimine ligand (519 mg, 2.0 eq, 3.87 mmol) was bubbled with nitrogen for 12 min and then injected into the solution. The solution was continued to be bubbled with nitrogen for 15 minutes. The solution was subsequently stirred at 25 ^{o}C for two days. The mixture was purified by dialysis (MWCO: 1,000) against distilled water/methanol (1/1 vol/vol) for two days, while changing the water at least four times a day. It was then concentrated under reduced pressure and freeze-dried overnight.

5.2.11. Typical procedure for Polymer deprotection (Retro Diel-Alder maleimide deprotection)

A dried round bottom flask, fitted with a reflux condenser and magnetic stirrer, was charged with glycopolymer (0.2 g) and toluene (20 mL). The reaction was subsequently refluxed for overnight and then cooled to ambient temperature. The volatiles were removed under reduced pressure and the off-white solid dissolved in water. The solution was purified by dialysis (MWCO: 1,000) against distilled water/ethanol (1/1 vol/vol) and water for two days, while changing the water at least four times a day. It was then concentrated under reduced pressure and freeze-dried overnight. The product was obtained as a white powder.

5.2.12. Surface Plasmon Resonance (SPR) analysis

SPR Sensorgrams were recorded in a Biorad ProteOn XPR36 SPR biosensor (Biorad, Hercules CA). Soluble DC-SIGN and gp120 were immobilized to 6000 response units (RU) on discrete channels within Biorad GMC sensor chips *via* amine coupling. Soluble-phase analytes were prepared in 25 mM HEPES pH 7.4, 150 mM NaCl, 5 mM CaCl2, 0.01% Tween-20 and flowed over the immobilized materials at a rate of 25 μL/min at 25˚C. Regeneration of the sensor chip surfaces was performed using 10 mM glycine pH 2.5. Datasets were exported

to BIAcore BIAevaluation software for kinetic calculations. Kinetic parameters were obtained by fitting curves to a 1:1 Langmuir model with correction for baseline drift where necessary. Competition assays were evaluated using Origin software.

5.3. Results and Discussion

5.3.1. Synthesis of the glycopolymers *via* SET-LRP and CuAAC click reaction

The glycopolymers were prepared following four sequential synthetic steps. A fluorescent dye derivative of FITC was introduced into the polymer in order to facilitate characterization of the protein conjugates and promote the bioconjugation traceability during the in vitro tests.

The first step was polymerization of TMS-PgA in toluene and methanol mixtures using either EBiB (**6**) or the maleimide protected initiator (**3**) in present of copper powder, $CuBr_2$ and Me_6-TREN. Secondly, the trimethylsilyl protecting groups in polymers were removed with TBAF and acetic acid. Thirdly the polymer click reaction was carried out with a sugar azide in DMSO and fourthly the deprotection of the maleimide moiety *via* a retro-Diels-Alder reaction generate the glycopolymer with a maleimide α terminal end group (**14b**). Finally the glycopolymer was labeled by FITC in DMF solution.

The results of SET-LRP polymerization of TMS-PgMA were shown in **Table 5.1**. The first-order kinetic plots of polymerization using EBiB **(6)** or maleimide protected initiator **(3)** and the dependence of the M_n and monomer conversions showed the linear relation, indicating good control over the polymer molecular weight and PDi, **Figure 5.1**.

The removal of the trimethylsilyl protecting group afforded polymers with pendent alkyne functional group by the addition of TBAF solution in the present of acetic acid as buffering agent.[83, 84] The complete removal of the trimethylsilyl groups was confirmed by both ^{1}H NMR, with the appearance of the C≡C*H* signal at 2.5 ppm along with the disappearance of the Si(C*H*$_3$)$_3$ signal at 0.2 ppm, and by FTIR analysis with the alkyne C-H stretch peak being visible at 3291 cm^{-1}. The SEC analysis also revealed that, as expected, the hydrodynamic volume of the deprotection polymers decreased while the molecular weight distribution remained the same with the trimethylsilyl protected polymers.

Table 5.1 SET-LRP Polymerization of TMS-PgA

Run	Initiator	Solv.	React. Time (mins)	Conv. (%)	Mn (GPC) (g mol-1)	PDi
TP1	EBiB (6)	toluene	240	44	9900	1.27
TP2	Maleimide (3)	toluene	120	41	5800	1.27
TP3	Maleimide (3)	toluene /MeOH	480	36	6000	1.15

Obtained by GPC analysis using $CHCl_3$ as the mobile phase and DRI detection

Reaction conditions: TP1 and TP2: [M]:[I]:[Cu(0)]:[Cu(II)]:[Me_6-TREN]:[Phenol] = 50:1:1:0.1:1:20 in toluene solution at 25 ^oC, [M]/Solvent =2/3 w/v. TP3: [M]:[I]:[Cu(0)]:[Cu(II)]:[Me_6-TREN] = 50:1:1:0.15:1.15 in toluene/MeOH (14/1 v/v) at 25 ^oC, [M]/Solvent =2/3 w/v.

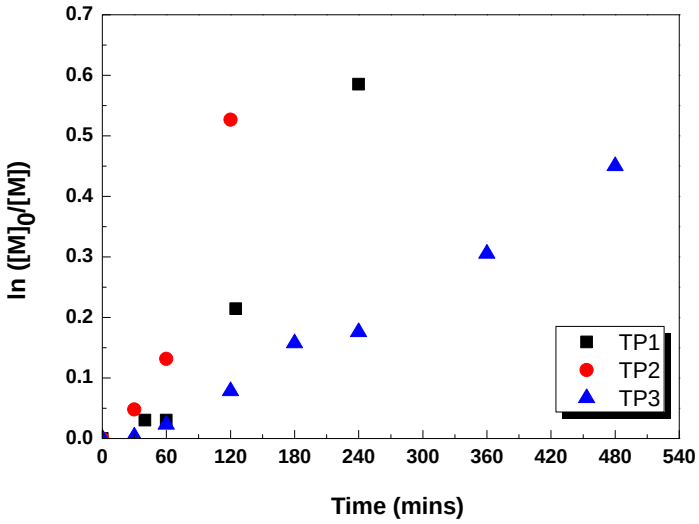

(a)

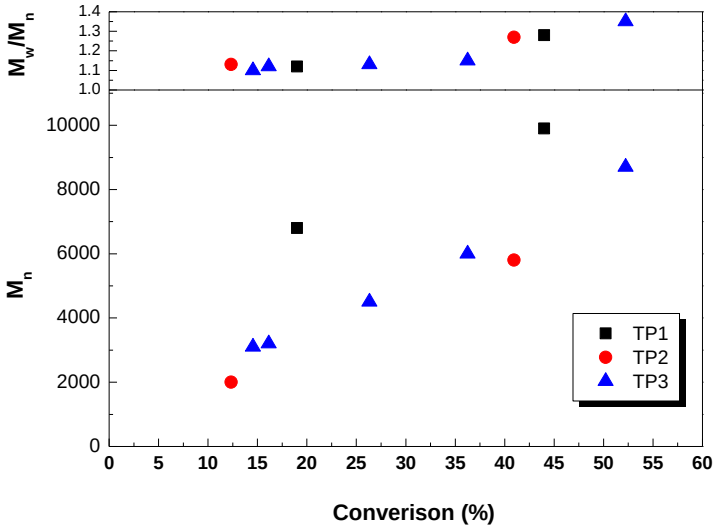

(b)

Figure 5.1 (a) Kinetic plots of polymerization of PgMA with different reaction conditions at 25 ^{o}C; (b) dependence of M_n and molecular weight distributions on the monomer conversions.

5.3.2. Synthesis of the glycopolymers *via* SET-RAFT and CuAAC click reaction

The first step was polymerization of PgMA in DMSO solvent using EBiB (**6**) or a maleimide protected initiator (**3**) and CPDB RAFT agent (**4**) in presence of Cu(I)Br and *N*-ethyl-2-pyridylmethanimine ligand. Secondly the click reaction was carried out using with sugar azide (**12**) in DMSO solution and thirdly the deprotection of the maleimide moiety *via* a retro-Diels-Alder reaction to generate the glycopolymer with a maleimide α-terminal end group (**14a**). Finally the glycopolymer was labeled by FITC in DMF solution.

The direct preparation of well-defined polymer with intact alkyne groups remains a challenge due to potential side reactions. Quemener *et. al.* reported that the attempted controlled polymerization of propargyl methacrylate (PgMA) *via* ATRP, RAFT and SET-LRP showed uncontrolled behavior leading to crosslinking of polymer. [73, 85, 86] Thus there was a general method that protected monomer was employed to avoid the undesired side reactions and then deprotection procedure was carried out. However, Zhang also reported the SET-RAFT propargyl methacrylate (PgMA) and could show good control in some conditions.[86] It has significant advantages for the synthesis of well-defined polymers containing

alkyne group by one step reaction.

SET-RAFT was a relatively new method for the controlled polymerization of vinyl monomers.[55-57] The results of SET-RAFT polymerization of PgMA were shown in **Table 5.2**, **Figure 5.2** and **Figure 5.3**. The final polymers prepared *via* SET-RAFT polymerization were confirmed by ^{1}H NMR spectrum (**Figure 5.4**). The ratio of the corresponding integration values of the **h** peak (δ = 4.62 ppm, $C(O)OCH_2$) to the **i** peak (δ = 2.51 ppm, CH_{alkyne}) was 2:1 which demonstrated that the pendant acetylene groups remained intact. It could further be seen the small signals of maleimide-protected units (**a, b**) of the initiator (δ = 6.51, 5.26 ppm) and small peaks of the aromatic group (**c, d, e**) of RAFT agent (δ = 7.36-7.96 ppm) after this reaction in the **Figure 5.4**.

Table 5.2 SET-RAFT polymerization of PgMA

Run	Initiator	$W_M/W_{Solv.}$	React. Time, mins	Conv. (%)	M_n(GPC) (g mol^{-1})	PDi	k_p^{app}, min^{-1}
PM1[a]	EBiB (**6**)	1/1	320	60	24200	1.47	0.0023
PM2[b]	Maleimide (**3**)	1/1	60	58	11400	1.74	0.0150
PM3[a]	Maleimide (**3**)	1/3	120	42	12500	1.39	0.0088
PM4[c]	Maleimide (**3**)	1/3	240	59	8000	1.43	0.0056

PM5[a]	Maleimide (**3**)	1/4.5	180	53	13600	1.40	0.0048
PM6[a]	Maleimide (**3**)	1/5	180	42	9500	1.44	0.0046
PM7[a]	Maleimide (**3**)	1/5	210	47	10400	1.44	0.0031
PM8[d]	Maleimide (**3**)	1/5	300	49	13200	1.45	0.0025
PM9[e]	Maleimide (**3**)	1/5	600	49	31300	1.46	0.0012
PM10[a]	Maleimide (**3**)	1/7	480	30	7400	1.37	0.0016

Obtained by GPC analysis using $CHCl_3$ as the mobile phase and DRI detection

Polymerization was carried out in DMSO at 25 ^{o}C.

Reaction conditions:

[a] [M]:[I]:[Cu(0)]:[PMDETA]:[CPDB] = 200:1:3:3:1;

[b] [M]:[I]:[Cu(0) wire]:[PMDETA]:[CPDB] = 200:1:-:3:1 @ Cu(0) wire (Φ = 0.25 mm, L = 16 cm);

[c] [M]:[I]:[Cu(0)]:[PMDETA]:[CPDB] = 200:1:3:3:2;

[d] [M]:[I]:[Cu(0)]:[PMDETA]:[CPDB] = 320:1:3:3:1;

[e] [M]:[I]:[Cu(0)]:[PMDETA]:[CPDB] = 680:1:3:3:1;

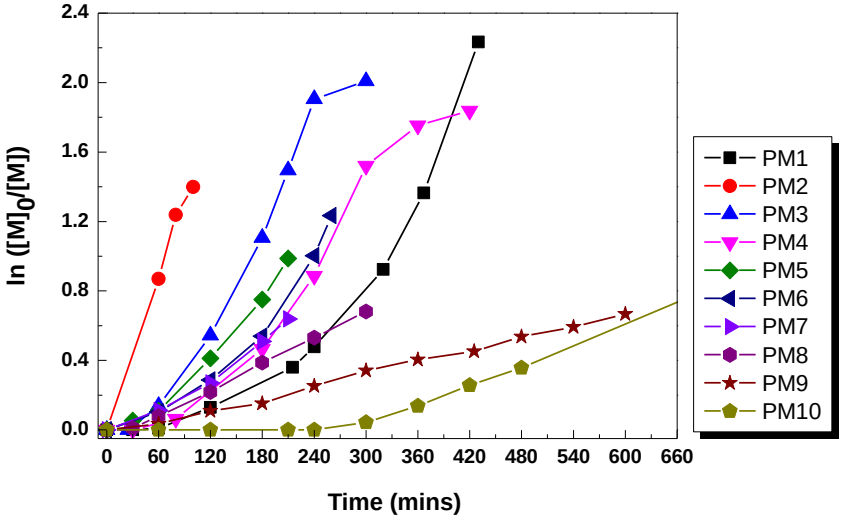

(a)

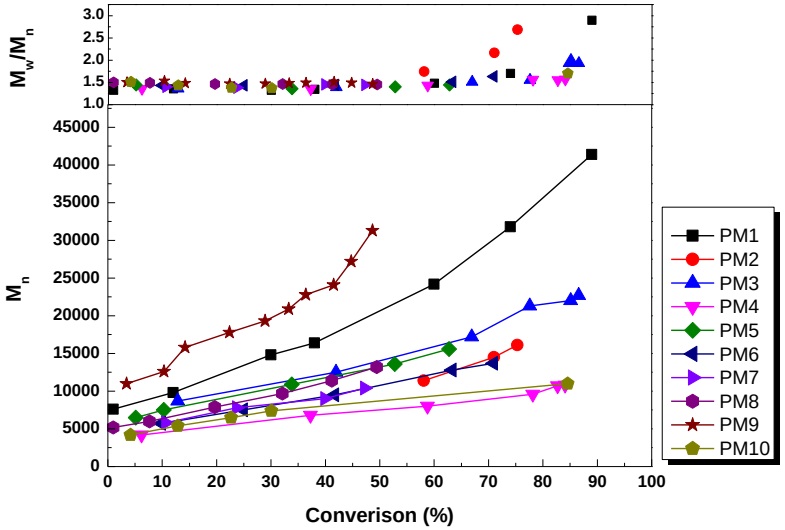

(b)

Figure 5.2 (a) Kinetic plots of polymerization of PgMA with different reaction conditions at 25 ^{o}C; (b) dependence of molecular weights and PDi on the monomer conversions

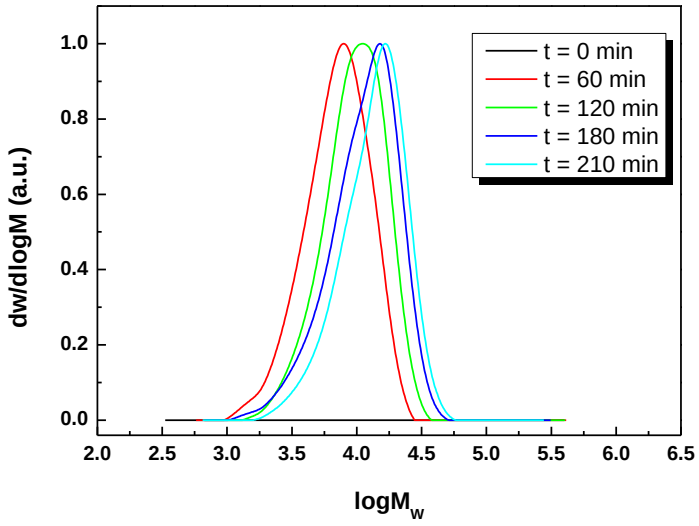
t = 0 min
t = 60 min
t = 120 min
t = 180 min
t = 210 min
dw/dlogM (a.u.)
logM$_w$
1.0
0.8
0.6
0.4
0.2
0.0
2.0
2.5
3.0
3.5
4.0
4.5
5.0
5.5
6.0
6.5

(a)

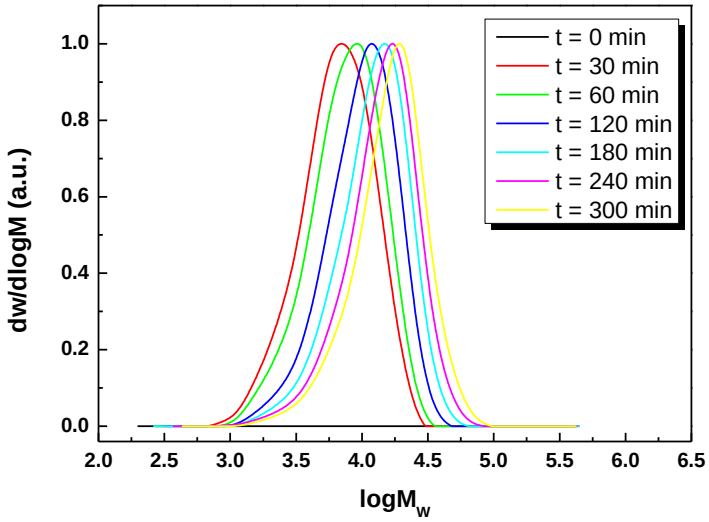
t = 0 min
t = 30 min
t = 60 min
t = 120 min
t = 180 min
t = 240 min
t = 300 min
dw/dlogM (a.u.)
logM$_w$
1.0
0.8
0.6
0.4
0.2
0.0
2.0
2.5
3.0
3.5
4.0
4.5
5.0
5.5
6.0
6.5

(b)

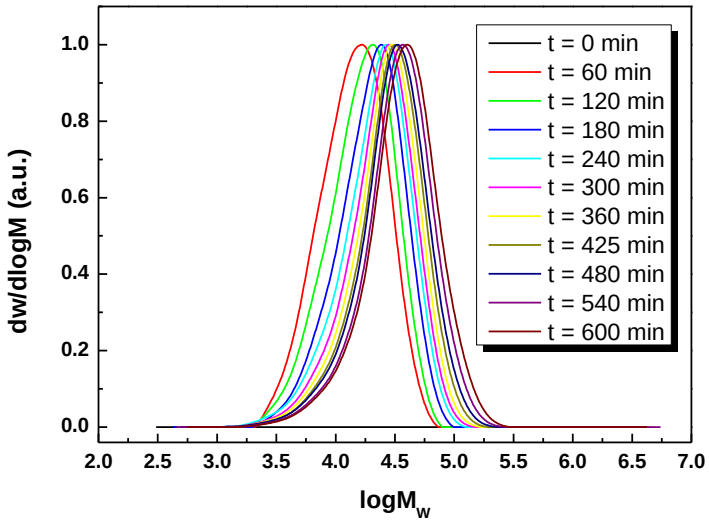

(c)

Figure 5.3 GPC traces (normalized to peak height) of PPgMA *via* SET-RAFT polymerization in DMSO at 25 ^{o}C (a) [M]:[I] = 200:1, PM7; (b) [M]:[I] = 320:1, PM8; (c) [M]:[I] = 680:1, PM9.

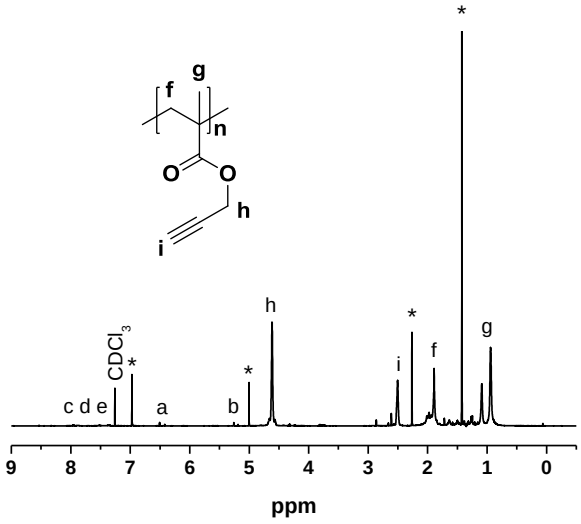

Figure 5.4 ^{1}H NMR spectrum of the PPgMA prepared by SET-RAFT polymerization, PM7. Reaction conditions: [M]:[I]:[Cu(0)]:[PMDETA]:[CPDB] = 200:1:3:3:1, W_M:$W_{Solv.}$ = 1:5, T = 25 ^{o}C. * The characteristic peaks of butylated hydroxytoluene (BHT).

The first-order kinetic plots of the polymerization using either EBiB **(6)** or a maleimide protected initiator **(3)** and CPDB **(4)** as RAFT agent and the dependence of the M_n and monomer conversions showed relatively good linear relationship during the middle period of polymerization and deviation at the late period of polymerization, **Figure 5.2**. Furthermore, the PDi was < 1.35 at an appropriate conversion and < 1.45 with ca. 50% conversion which demonstrates an acceptable control of polymerization. However, the PDi increased at relatively high monomer conversion (PM3, 78% conv., PDi = 1.55), indicating some side reactions also seen as a steep rise in viscosity. Thus, within certain constraints, SET-RAFT is an acceptable technique for the controlled polymerization of PgMA without the need for protecting group chemistry.

The [I]:[CPDB] molar ratios have a great effect on the rates of polymerization and resulting molecular weights. The polymerization rates and molecular weights deceased sharply with an increase in CPDB concentration. (PM3, PM4 in **Figure 5.2**). These results were in accordance with the theoretical molecular weight equation of SET-RAFT ($M_n = [M]_0/([I]_0+[CTA]_0) \times M_o \times$Conversion, where $[M]_0$, $[CTA]_0$ and $[I]_0$ represent the initial concentration of monomer and the initial concentration of chain transfer agent and initiator, respectively. M_o is the molecular weight of monomer and conversion was the monomer conversion).

Moreover, the molecular weight distribution also depended on the molar ratios of [I]:[CPDB]. For example, PDi did not exceed 1.57 after 84% conversion in the presence of [I]: [CPDB] = 1:2 (PM4) in comparison to PM3, which the PDi reached 1.95 after 85% conversion in the presence of [I]: [CPDB] = 1:1. It was noted that the transfer agent concentration should be confined in a proper amount in order to synthesis high molecular weight polymer.

The [M]:[I] molar ratios also effect the rates of polymerization and molecular weights. The polymerization rates deceased and molecular weights increased as the [M]:[I] molar ratios increased. (PM7, PM8 and PM9 in **Figure 5.2**). As the molar ratio of PgMA to initiator gave rise from 200:1 to 320:1 and 680:1, the apparent rate constant of propagation k_p^{app} deceased from 0.0031 min^{-1} to 0.0025 min^{-1} and 0.0012 min^{-1} (**Table 5.2**). GPC traces of PM7, PM8 and PM9 were shown in **Figure 5.3** (a), (b), (c), respectively.

In order to prepare the PgMA with a low PDi and relatively high conversion, the polymerization is terminated at an appropriate reaction time. If the polymerization rate was too fast, it was difficult to terminate the polymerization at optimal time. **Table 5.2** and **Figure 5.2** summarized the kinetic data for the SET-RAFT of PgMA in different of monomer/solvent mass ratio (W_M/ W_{DMSO}). The mass ratio of monomer to solvent ranged from 1 g monomer : 1 g DMSO solvent to 1 g monomer : 7 g DMSO solvent in presence of [M]:[I]: [PMDETA]:[CPDB] = 200:1:3:1 (PM2, PM3, PM5-7 and PM10). As expect, the polymerization rate and the apparent rate constant of propagation k_p^{app} changed

with different monomer/solvent mass ratio. For the higher monomer/solvent mass ratios such as 1 g monomer : 1 g solvent, the rate of polymerization was very fast and the reaction mixture became very viscous and stir difficultly (PM2). However, for the lower ratios such as 1 g monomer : 7 g solvent, the polymerization was very slow and polymerization time was long (PM10). Simultaneously, the apparent propagation rate constant k_p^{app} was 0.015 min^{-1}, as compared to 0.0016 min^{-1}. Among these monomer/solvent mass ratios, 1 g monomer : 5 g solvent was found to be most suitable for the PgMA polymerization in DMSO for producing high molecular weight polymers with the low PDi and relatively higher conversion at the appropriate reaction time (PM6 and PM7). Conversely, the apparent propagation rate constant k_p^{app} depended on the ratio of monomer to solvent in SET-LRP. The rise of solvent concentration led to a faster rate of polymerization while keeping well-controlled molecular weight and molecular weigh distribution, which was opposite to that observed for ATRP potentially indicating different mechanisms of SET-LRP and ATRP.[49] In this work, the effects of the monomer/solvent ratio were different from the common SET-LRP but in accordance with the common RAFT. These results suggested the SET-RAFT may have the a mixture of characteristics of both SET-LRP and RAFT. It was noted that low levels of BHT must be added into the reaction mixture after the polymerization was terminated, otherwise the side reaction could occur during the post-treatment procedure leading to very high PDi polymer or gel formation.

Various molecular weights of polymer with alkyne side group were prepared,

Table 5.2, **Figure 5.2**, **Figure 5.3** and **Figure 5.4**. It was concluded that SET-RAFT polymerization provided a convenient one-step method to synthesis high molecular weight with acceptable PDi of polymers with pendant alkyne groups.

5.3.3. Synthesis of PPgA *via* SET-LRP or SET-RAFT

In this study, both SET-LRP and SET-RAFT polymerization were employed to investigate another monomer propargyl acrylate (PgA) as opposed to propargyl methacrylate. From **Table 5.3**, it can be seen that PgA polymerization did not occur using EBiB initiator under usual SET-LRP reaction conditions (P2). While the polymerization conditions were changed, SET of PgA showed uncontrolled behavior. The first-order kinetic plots of the SET-LRP and the dependence of the M_n's and monomer conversions deviated from a linear relationship, **Figure 5.5**. The molecular weight distributions were very board (**Figure 5.5** P3, P4 and **Figure 5.6** (a), (b)), which indicate that side reaction are present in this SET-LRP polymerization.

Table 5.3 also summarized kinetic data for the SET-RAFT of PgA under different polymerization conditions. SET-RAFT of PgA showed uncontrolled behavior which may be due to some of the side reactions. The first-order kinetic plots of the SET-RAFT and the dependence of the M_n's and monomer conversions

showed in a nonlinear relationship during the polymerization (**Figure 5.5**). The PDi were very high (P5 and P6), **Figure 5.6** (c) and (d).

Table 5.3 SET-LRP or SET-RAFT polymerization of PgA

Run	Init.	Solv.	V_M/ $V_{Solv.}$	Reac. Time, mins	Conv. (%)	M_n (GPC)	PDi	Technique
P1[a]	MBP	DMSO	2/1	970	0			SET-LRP
P2[b]	EBiB	DMSO	2/1	370	0			SET-LRP
P3[c]	EBiB	Toluene	2/3	810	58	17700	2.11	SET-LRP
P4[d]	EBiB	Toluene	3/4	240	30	6300	1.98	SET-LRP
P5[e]	EBiB	DMSO	1/1	540	42	15100	1.97	SET-RAFT
P6[f]	EBiB	DMSO	1/1	480	57	13300	2.11	SET-RAFT

Obtained by GPC analysis using $CHCl_3$ as the mobile phase and DRI detection

Reaction conditions:

[a] [M]:[I]:[Cu(0)]:[Me_6-TREN] = 222:1:0.1:0.1;

[b] [M]:[I]:[Cu(0)]:[Me_6-TREN] = 100:1:1:1;

[c] [M]:[I]:[Cu(0)]:[Cu(II)]:[Me_6-TREN]:[Phenol] = 50:1:1:0.1:1:20;

[d] [M]:[I]:[Cu(0)]:[Cu(II)]:[Me_6-TREN]:[Phenol] = 100:1:1:0.1:1:20;

[e] [M]:[I]:[Cu(0)]:[PMDETA]:[TTCA] = 200:1:3:3:1;

[f] [M]:[I]:[Cu(0) wire]:[Cu(II)]:[PMDETA]: [TTCA] = 200:1:-0.1:1.5:1 @ Cu(0) wire (Φ = 0.25 mm, L = 5cm).

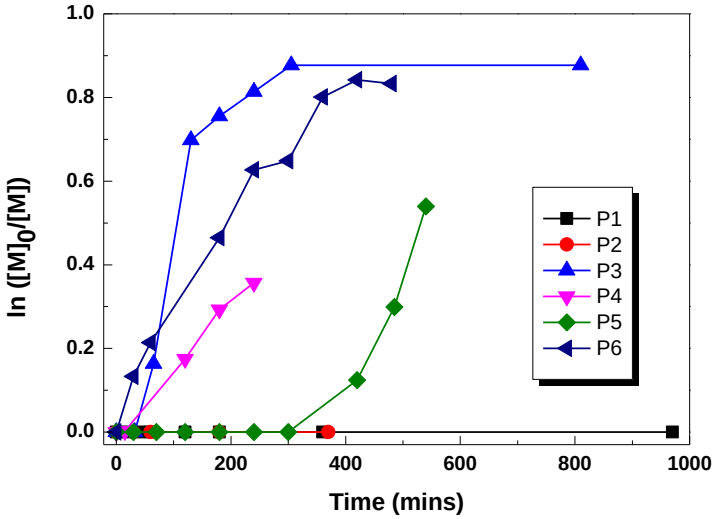

(a)

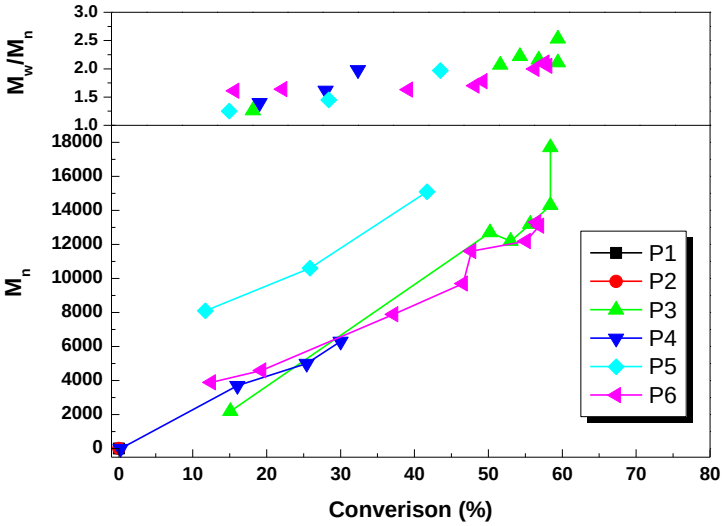

(b)

Figure 5.5 (a) Kinetic plots of polymerization of PgA with different reaction conditions at 25 ^{o}C; (b) dependence of molecular weights and molecular weight distributions on the monomer conversions

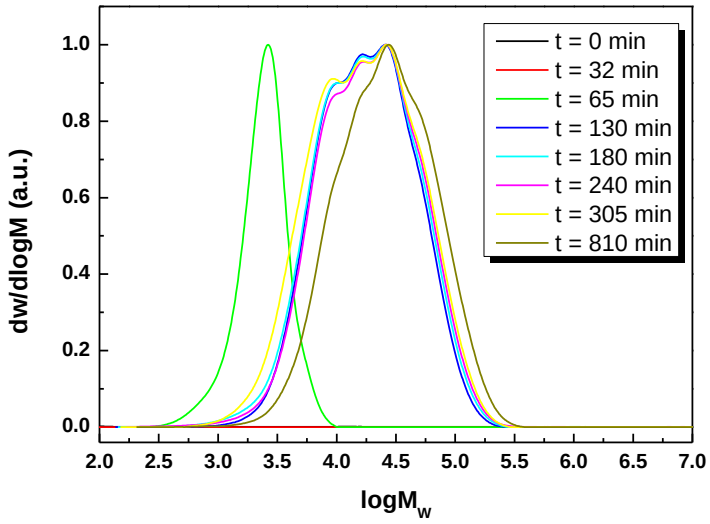
t = 0 min
t = 32 min
t = 65 min
t = 130 min
t = 180 min
t = 240 min
t = 305 min
t = 810 min
dw/dlogM (a.u.)
logM$_w$
1.0
0.8
0.6
0.4
0.2
0.0
2.0
2.5
3.0
3.5
4.0
4.5
5.0
5.5
6.0
6.5
7.0

(a)

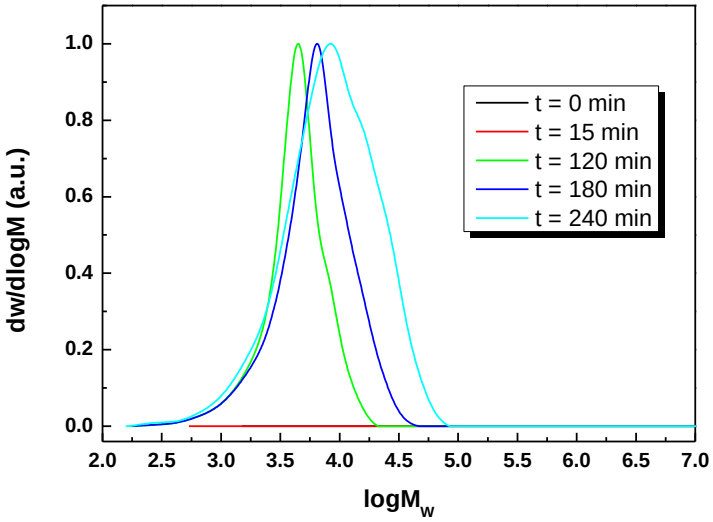
t = 0 min
t = 15 min
t = 120 min
t = 180 min
t = 240 min
dw/dlogM (a.u.)
logM$_w$
1.0
0.8
0.6
0.4
0.2
0.0
2.0
2.5
3.0
3.5
4.0
4.5
5.0
5.5
6.0
6.5
7.0

(b)

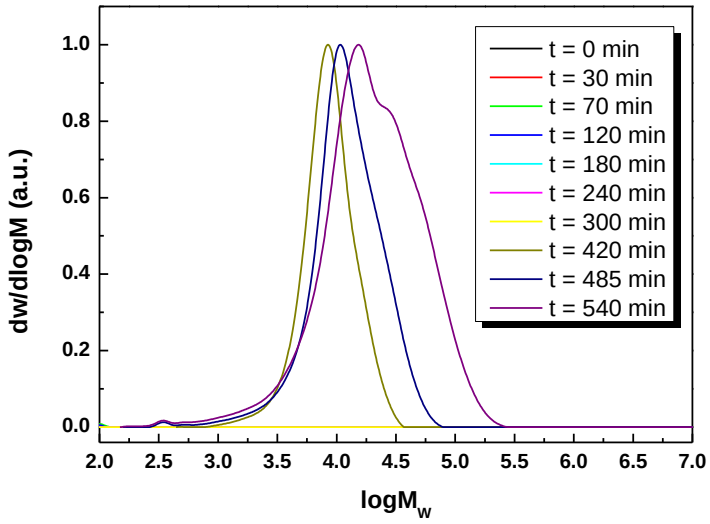

(c)

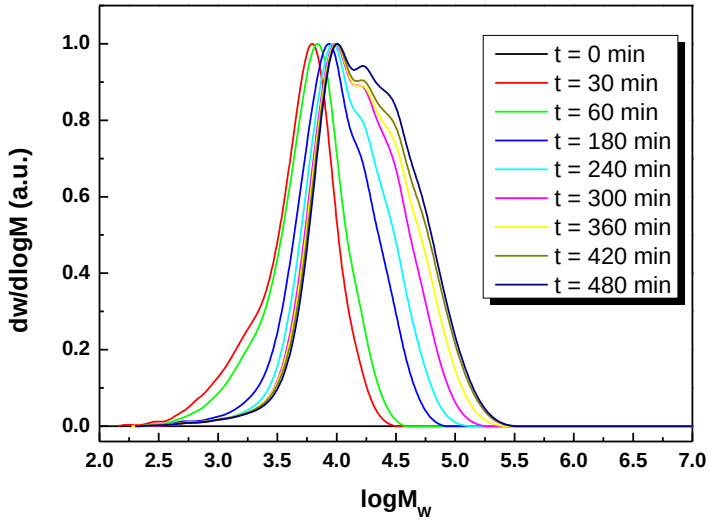

(d)

Figure 5.6 GPC traces (normalized to peak height) of PPgA *via* SET-LRP or SET-RAFT polymerization at 25 ^{o}C (a) [M]:[I]:[Cu(0)]:[Cu(II)]: [Me_6-TREN]:[Phenol] = 50:1:1:0.1:1:20, P3; (b) [M]:[I]:[Cu(0)]:[Cu(II)]:[Me_6-TREN]: [Phenol] = 100:1:1:0.1:1:20, P4; (c) [M]:[I]:[Cu(0)]:[PMDETA]:[TTCA] = 200:1:3:3:1, P5; (d) [M]:[I]:[Cu(0) wire]:[Cu(II)]: [PMDETA]:[TTCA] = 200:1:5 cm:0.1:1.5:1, P6

5.3.4. Synthesis of glycopolymers *via* CuAAC click chemistry

The homopolymers with functional alkyne groups (**5**) or (**11**) were used as one of starting materials for the synthesis of a library of glycopolymer, obtained by CuAAC click reactions of mannose, galactose, glucose and fucose-based azides. In this study, α-D-mannopyranosyl azide and β-D-galactopyranosyl azide were used as model sugar-based azides for the click reaction. The CuAAC click reaction conditions chosen form those reported by Haddleton *et al.* with CuBr/*N*-ethyl-2-pyridylmethanimine as catalyst system in the presence of triethylamine in DMSO to ensure the complete solubility of all reactants.[71, 87-89] **Table 5.4** summarized the various glycopolymers with different molecular weights and different sugar units. Molecular weight and molecular weight distribution of all glycopolymers were obtained from GPC using DMF as the mobile phase.

Table 5.4 Maleimide-terminated glycopolymers with different sugars

Run	Pendant Sugar units	M_n(GPC) g mol^{-1}	DP (GPC)	PDi
G1	Mannose	27800	84	1.39
G2	Galactose	32900	100	1.41

G3	Mannose	49800	151	1.44
G4	Galactose	53000	161	1.46
G5	Mannose	87000	264	1.56
G6	Galactose	89300	271	1.58

Obtained by GPC analysis using DMF as the mobile phase and DRI detection

The successful CuAAC click reaction was confirmed by the ^{1}H NMR spectrum of glycopolymers by the appearance of the new triazole peak **i** at 8.3 ppm and several typical peaks (δ = 3.3-6.2 ppm) from the sugar units (**Figure 5.7** (a)) or the new triazole peak **i** at 8.4 ppm and several typical peaks (δ = 3.5-5.7 ppm) from the galactose group (**Figure 5.7** (b)).

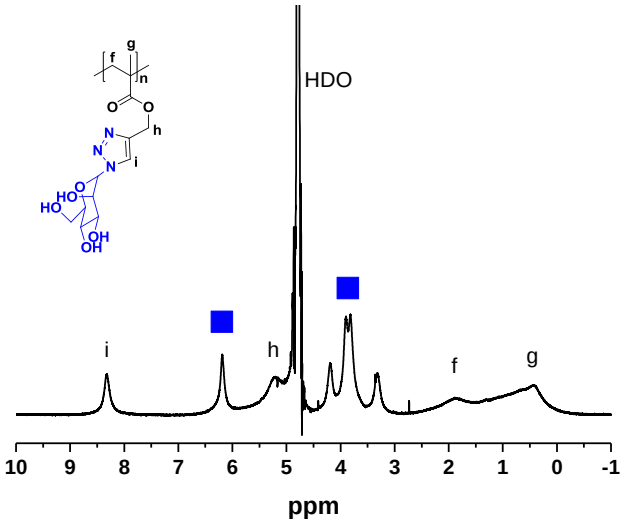

(a)

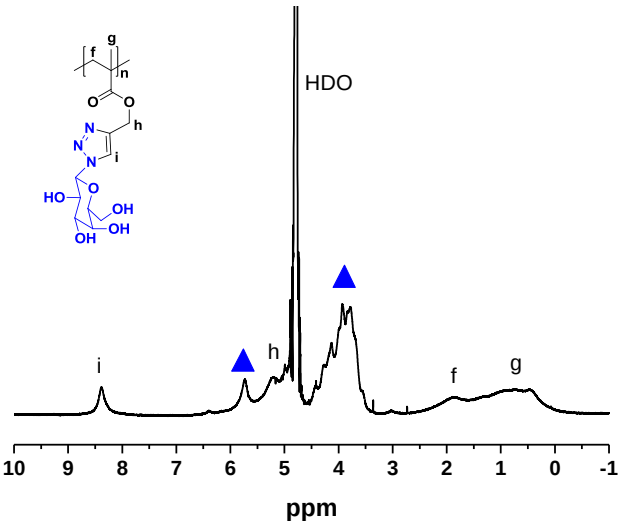

(b)

Figure 5.7 ^{1}H NMR spectrum of the glycopolymer prepared by CuAAC click reaction in D_2O. (a) G1, ■: The characteristic peaks of mannose units. (b) G2, ▲: The characteristic peaks of galactose units.

Furthermore, both GPC and FTIR data further indicated that the glycopolymers were obtained. For example, the number average molecular weight (M_n) of the polymer increased from 10400 Da (clickable polymer, PM7) to 27800 Da and 32900 Da, respectively (after CuAAC click reaction, G1 and G2), **Figure 5.8**. Meanwhile, the PDi of the glycopolymers stayed constant. Moreover, compared with the FTIR spectra of the polymer before and after CuAAC click reaction, the original characteristic absorption peak of the alkyne group ($\upsilon_{(C\equiv C)}$ stretching vibration) at 2129 cm^{-1} disappeared after the click reaction with sugar azide. One new large board peaks at 3360 cm^{-1} attributed to $\upsilon_{(O-H)}$ stretching vibration appeared and the triazole groups $\upsilon_{(N=N)}$ stretching vibration frequencies

appeared at 1638 cm^{-1} region after the CuAAC click reaction, **Figure 5.9**.

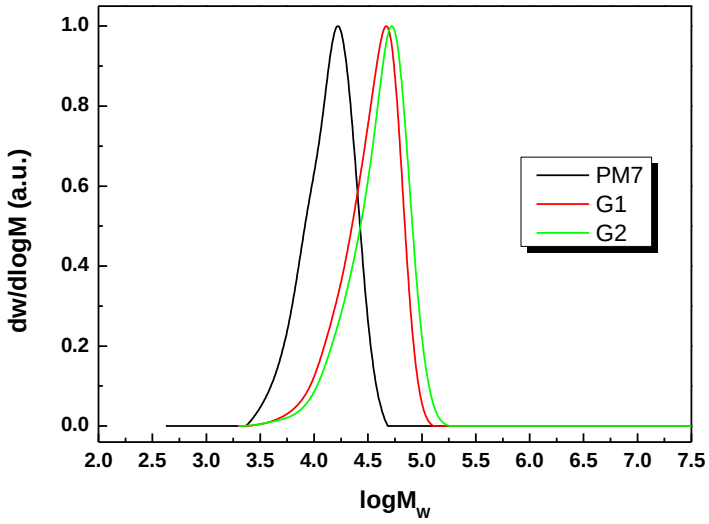

Figure 5.8 GPC spectra of the polymers before and after click reaction

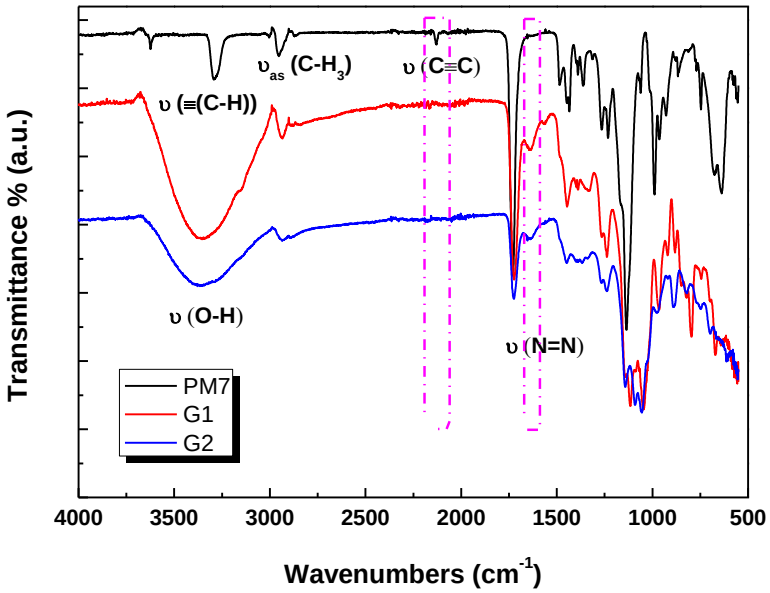

Figure 5.9 FTIR spectra of the polymers before and after click reaction

5.4. Conclusion

Two kinds of alkyne polymer were synthesized by different polymerization methods. One controlled polymerization of propargyl methacrylate (PgMA) *via* SET-RAFT was prepared without the need of protection and deprotection procedures. SET-RAFT technique was a simple tool to prepare well-controlled polymer with pendant alkyne group. The other controlled polymerization of trimethylsilyl protected propargyl acrylate (TMS-PgA) was prepared by SET-LRP polymerization. A novel series of glycopolymer with different epitope units (eg. mannose, galactose, glucose and fucose) were then successfully prepared by CuAAC click chemistry. The molecular weight distribution of polymers remained constant before and after being functionalized by carbohydrates.

5.5. Further Work

5.5.1. Lectin conjugation studies

The potential of glycopolymers as multivalent ligands are known to undergo numerous recognition events when interacting with appropriate corresponding lectins. The ability of glycopolymers to interact with lectins or cells strongly depended on their size, shape, composition, structure and binding epitope density.

For the mannose-based glycopolymers, the lection Concanavalin A (Con A) will be used as it selectively interacts with α-D-mannose units. Simultaneously, the Peanut agglutinin (PNA, Arachis hypogaea) will be chosen for the binding studies as it has a β-D-galactose selectivity.

The interactions between lectin and glycopolymers will be monitored by the turbidimetric assay using a UV-Vis spectrophotometer. The rate of the lectin-ligand binding is a critical factor in biological science, where the time scale could change from seconds to hours. The rates of the binding of lectins to sugar-containing glycopolymers will be investigated by turbidimetry. When the lectin conjugated to the glycopolymers, the formation of precipitating clusters will change the absorbance in the solution.[90] By measuring absorbance changes at 420 nm over time in a solution of Con A and glycopolymers with pendant mannose units in HEPES buffer at pH 7.4, the rate of the ligand-lectin cluster formation could be obtained.

5.5.2. Multichannel Surface Plasmon Resonance (MC-SPR)

The binding affinity of glycopolymers with bacterially expressed soluble recombinant human DC-SIGN tetramers will be investigated by the use of multichannel Surface Plasmon resonance (MC-SPR).

5.5.3. Preparation of sCT-glycopeptide

Salmon calcitonin (sCT) was a commercially available 32-amino acid linear polypeptide hormone which was produced in humans primarily by the parafollicular cells (also called as C-cells) of the thyroid and in many other animals by the ultimobranchial gland. Salmon calcitonin was used for the treatment of postmenopausal osteoporosis, Paget's disease of bone, hypercalcaemia, bone metastases, phantom limb pain, etc.[91] sCT contains a disulfide bridge (Cys^1-Cys^7) that can be reduced to give two thiol functional groups which are available for thiol-maleimide click reaction. Want *et al*. reported that this Cys^1-Cys^7 disulfide bond of sCT was reduced and functionalized without losing bioactivity.[92]

Glycopeptide will be prepared in the present study by reaction of glycopolymer with maleimide end group with sCT prior to being reduced in the presence of tris(2-caboxyethyl) phosphine (TECP), **Scheme 5.9**.

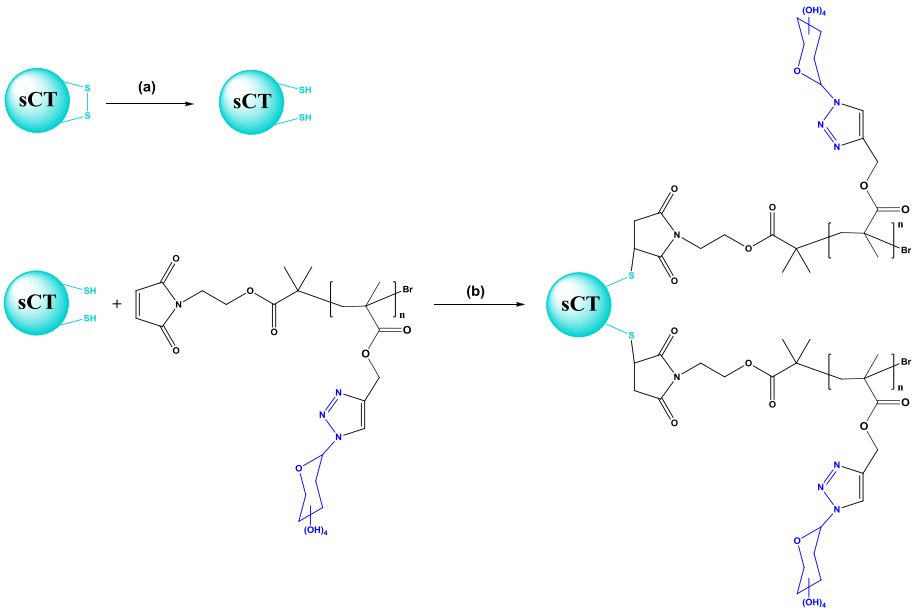

Scheme 5.9 Synthesis of the glycopeptide *via* thiol–maleimide click reaction

5.5.4. Preparation of BSA-glycoprotein

Bovine serum albumin (BSA) was a commercially available 66 kDa protein containing a single thiol at the surface. The Cys34 residue was used as the attachment site for BSA site-specific conjugation. As illustrated by the publications of both Haddleton and Maynard who describe the preparation the BSA conjugated functional polymer *via* living radical polymerization. The functional polymer chain end group can react with the free thiol residue of the protein.[87, 93, 94]

Glycoproteins will be prepared in the present study by reaction of

glycopolymer with maleimide end group with BSA in DMSO/PBS (50 mM, pH 7.0) (1/1 v/v) (**Scheme 5.10**).

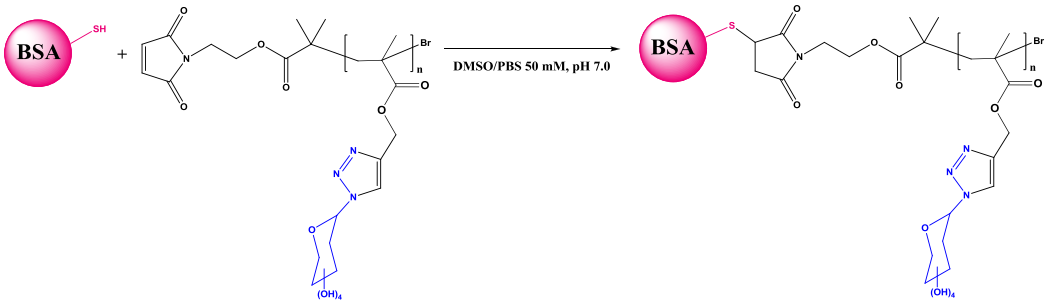

Scheme 5.10 Synthesis of the glycoprotein *via* thiol–maleimide click reaction

5.6. References

1. F. D. Tropper, A. Romanowska and R. Roy, *Methods Enzymol.*, 1994, **242**, 257-271.

2. M. A. Findeis, C. H. Wu and G. Y. Wu, *Methods Enzymol.*, 1994, **247**, 341-351.

3. V. Ladmiral, E. Melia and D. M. Haddleton, *Eur. Polym. J.*, 2004, **40**, 431-449.

4. S. R. S. Ting, G. J. Chen and M. H. Stenzel, *Polym. Chem.*, 2010, **1**,

1392-1412.

5. M. Ambrosi, N. R. Cameron, B. G. Davis and S. Stolnik, *Org. Biomol. Chem.*, 2005, **3**, 1476-1480.

6. J. J. Lundquist and E. J. Toone, *Chem. Rev.*, 2002, **102**, 555-578.

7. M. Ambrosi, N. R. Cameron and B. G. Davis, *Org Biomol Chem*, 2005, **3**, 1593-1608.

8. J. E. Gestwicki, C. W. Cairo, L. E. Strong, K. A. Oetjen and L. L. Kiessling, *J. Am. Chem. Soc.*, 2002, **124**, 14922-14933.

9. E. A. Smith, W. D. Thomas, L. L. Kiessling and R. M. Corn, *J Am Chem Soc*, 2003, **125**, 6140-6148.

10. L. L. Kiessling, J. E. Gestwicki and L. E. Strong, *Angew. Chem. Int. Ed.*, 2006, **45**, 2348-2368.

11. A. V. Pukin, H. M. Branderhorst, C. Sisu, C. A. G. M. Weijers, M. Gilbert, R. M. J. Liskamp, G. M. Visser, H. Zuilhof and R. J. Pieters, *Chembiochem*, 2007, **8**, 1500-1503.

12. G. T. Noble, S. L. Flitsch, K. P. Liem and S. J. Webb, *Org Biomol Chem*, 2009, **7**, 5245-5254.

13. Q. Wang, J. S. Dordick and R. J. Linhardt, *Chem. Mater.*, 2002, **14**, 3232-3244.

14. C. R. Bertozzi and L. L. Kiessling, *Science*, 2001, **291**, 2357-2364.

15. K. Kobayashi, A. Tsuchida, T. Usui and T. Akaike, *Macromolecules*, 1997, **30**, 2016-2020.

16. S. J. Novick and J. S. Dordick, *Chem. Mater.*, 1998, **10**, 955-958.

17. T. Miyata, T. Uragami and K. Nakamae, *Adv. Drug Deliver Rev.*, 2002, **54**, 79-98.

18. S. K. Choi, M. Mammen and G. M. Whitesides, *J Am Chem Soc*, 1997, **119**, 4103-4111.

19. A. W. Kawaguchi, H. Okawa and K. Hashimoto, *J. Polym. Sci., Part A: Polym. Chem.*, 2009, **47**, 2032-2042.

20. S. G. Spain and N. R. Cameron, *Polym. Chem.*, 2011, **2**, 60-68.

21. J. Li, S. Zacharek, X. Chen, J. Q. Wang, W. Zhang, A. Janczuk and P. G. Wang, *Biorg. Med. Chem.*, 1999, **7**, 1549-1558.

22. M. G. Garcia-Martin, C. Jimenez-Hidalgo, S. S. J. Al-Kass, I. Caraballo, M. V. de Paz and J. A. Galbis, *Polymer*, 2000, **41**, 821-826.

23. Y. H. Yun, D. J. Goetz, P. Yellen and W. L. Chen, *Biomaterials*, 2004, **25**, 147-157.

24. L. Zhang, J. Bernard, T. P. Davis, C. Barner-Kowollik and M. H. Stenzel, *Macromol. Rapid Commun.*, 2008, **29**, 123-129.

25. S. Pearson, N. Allen and M. H. Stenzel, *J. Polym. Sci., Part A: Polym. Chem.*, 2009, **47**, 1706-1723.

26. X. C. Liu and J. S. Dordick, *J. Polym. Sci., Part A: Polym. Chem.*, 1999, **37**, 1665-1671.

27. H. Schlaad, L. C. You, R. Sigel, B. Smarsly, M. Heydenreich, A. Mantion and A. Masic, *Chem. Commun.*, 2009, 1478-1480.

28. G. Pasparakis and C. Alexander, *Angew. Chem. Int. Ed.*, 2008, **47**, 4847-4850.

29. S. G. Spain, M. I. Gibson and N. R. Cameron, *J. Polym. Sci., Part A: Polym. Chem.*, 2007, **45**, 2059-2072.

30. A. Narumi and T. Kakuchi, *Polym. J.*, 2008, **40**, 383-397.

31. W. J. Ye, S. Wells and J. M. DeSimone, *J. Polym. Sci., Part A: Polym. Chem.*, 2001, **39**, 3841-3849.

32. J. Bernard, M. Schappacher, A. Deffieux, P. Viville, R. Lazzaroni, M. H. Charles, M. T. Charreyre and T. Delair, *Bioconjug Chem*, 2006, **17**, 6-14.

33. K. Yamada, M. Minoda and T. Miyamoto, *J. Polym. Sci., Part A: Polym. Chem.*, 1997, **35**, 751-757.

34. K. Tsutsumiuchi, K. Aoi and M. Okada, *Macromolecules*, 1997, **30**, 4013-4017.

35. K. Aoi, K. Tsutsumiuchi, E. Aoki and M. Okada, *Macromolecules*, 1996, **29**, 4456-4458.

36. K. Aoi, K. Tsutsumiuchi and M. Okada, *Macromolecules*, 1994, **27**, 875-877.

37. C. H. Lu, Q. Shi, X. S. Chen, T. C. Lu, Z. G. Xie, X. L. Hu, J. Ma and X. B. Jing, *J. Polym. Sci., Part A: Polym. Chem.*, 2007, **45**, 3204-3217.

38. K. Nomura and R. R. Schrock, *Macromolecules*, 1996, **29**, 540-545.

39. C. Fraser and R. H. Grubbs, *Macromolecules*, 1995, **28**, 7248-7255.

40. K. H. Mortell, M. Gingras and L. L. Kiessling, *J. Am. Chem. Soc.*, 1994,

116, 12053-12054.

41. S. J. Hou, X. L. Sun, C. M. Dong and E. L. Chaikof, *Bioconjug Chem*, 2004, **15**, 954-959.

42. K. Ohno, Y. Tsujii, T. Miyamoto, T. Fukuda, M. Goto, K. Kobayashi and T. Akaike, *Macromolecules*, 1998, **31**, 1064-1069.

43. H. Gotz, E. Harth, S. M. Schiller, C. W. Frank, W. Knoll and C. J. Hawker, *J. Polym. Sci., Part A: Polym. Chem.*, 2002, **40**, 3379-3391.

44. K. Ohno, Y. Tsujii and T. Fukuda, *J. Polym. Sci., Part A: Polym. Chem.*, 1998, **36**, 2473-2481.

45. M. Ejaz, K. Ohno, Y. Tsujii and T. Fukuda, *Macromolecules*, 2000, **33**, 2870-2874.

46. Z. C. Li, Y. Z. Liang, G. Q. Chen and F. M. Li, *Macromol Rapid Commun*, 2000, **21**, 375-380.

47. O. Abdelkader, S. Moebs-Sanchez, Y. Queneau, J. Bernard and E. Fleury, *J. Polym. Sci., Part A: Polym. Chem.*, 2011, **49**, 1309-1318.

48. M. Ahmed and R. Narain, *Biomaterials*, 2011, **32**, 5279-5290.

49. V. Percec, T. Guliashvili, J. S. Ladislaw, A. Wistrand, A. Stjerndahl, M. J. Sienkowska, M. J. Monteiro and S. Sahoo, *J Am Chem Soc*, 2006, **128**, 14156-14165.

50. G. Lligadas and V. Percec, *J. Polym. Sci., Part A: Polym. Chem.*, 2008, **46**, 6880-6895.

51. G. Lligadas, B. M. Rosen, M. J. Monteiro and V. Percec, *Macromolecules*,

2008, **41**, 8360-8364.

52. N. H. Nguyen, B. M. Rosen, G. Lligadas and V. Percec, *Macromolecules*, 2009, **42**, 2379-2386.

53. M. J. Monteiro, T. Guliashvili and V. Percec, *J. Polym. Sci., Part A: Polym. Chem.*, 2007, **45**, 1835-1847.

54. B. M. Rosen and V. Percec, *Chem. Rev.*, 2009, **109**, 5069-5119.

55. R. Dhamodharan, S. H. Subramanian and R. P. Babu, *Macromolecules*, 2008, **41**, 262-265.

56. N. Haridharan, K. Ponnusamy and R. Dhamodharan, *J. Polym. Sci., Part A: Polym. Chem.*, 2010, **48**, 5329-5338.

57. N. Haridharan and R. Dhamodharan, *J. Polym. Sci., Part A: Polym. Chem.*, 2011, **49**, 1021-1032.

58. H. C. Kolb, M. G. Finn and K. B. Sharpless, *Angew. Chem. Int. Ed.*, 2001, **40**, 2004-2021.

59. C. J. Hawker and K. L. Wooley, *Science*, 2005, **309**, 1200-1205.

60. A. Dag, H. Durmaz, E. Demir, G. Hizal and U. Tunca, *J. Polym. Sci., Part A: Polym. Chem.*, 2008, **46**, 6969-6977.

61. R. K. Iha, K. L. Wooley, A. M. Nystrom, D. J. Burke, M. J. Kade and C. J. Hawker, *Chem. Rev.*, 2009, **109**, 5620-5686.

62. C. R. Becer, R. Hoogenboom and U. S. Schubert, *Angew. Chem. Int. Ed.*, 2009, **48**, 4900-4908.

63. G. Z. Li, R. K. Randev, A. H. Soeriyadi, G. Rees, C. Boyer, Z. Tong, T. P.

Davis, C. R. Becer and D. M. Haddleton, *Polym. Chem.*, 2010, **1**, 1196-1204.

64. M. J. Kade, D. J. Burke and C. J. Hawker, *J. Polym. Sci., Part A: Polym. Chem.*, 2010, **48**, 743-750.

65. X. Li, *Chem. Asian J.*, 2011, **6**, 2606-2616.

66. G. Z. Li and D. M. Haddleton, *Polym. Prepr. (Am. Chem. Soc., Div. Polym. Chem.)*, 2010, **51**, 555-556.

67. A. H. Soeriyadi, G. Z. Li, S. Slavin, M. W. Jones, C. M. Amos, C. R. Becer, M. R. Whittaker, D. M. Haddleton, C. Boyer and T. P. Davis, *Polym. Chem.*, 2011, **2**, 815-822.

68. M. A. Tasdelen, *Polym. Chem.*, 2011, **2**, 2133-2145.

69. C. W. Tornoe, C. Christensen and M. Meldal, *J. Org. Chem.*, 2002, **67**, 3057-3064.

70. V. V. Rostovtsev, L. G. Green, V. V. Fokin and K. B. Sharpless, *Angew. Chem. Int. Ed.*, 2002, **41**, 2596-2599.

71. V. Ladmiral, G. Mantovani, G. J. Clarkson, S. Cauet, J. L. Irwin and D. M. Haddleton, *J. Am. Chem. Soc.*, 2006, **128**, 4823-4830.

72. M. A. Gauthier, M. I. Gibson and H. A. Klok, *Angew. Chem. Int. Ed.*, 2009, **48**, 48-58.

73. B. S. Sumerlin, N. V. Tsarevsky, G. Louche, R. Y. Lee and K. Matyjaszewski, *Macromolecules*, 2005, **38**, 7540-7545.

74. E. Lallana, R. Riguera and E. Fernandez-Megia, *Angew. Chem. Int. Ed.*,

2011, **50**, 8794-8804.

75. J. M. Ren, J. T. Wiltshire, A. Blencowe and G. G. Qiao, *Macromolecules*, 2011, **44**, 3189-3202.

76. B. J. Adzima, Y. H. Tao, C. J. Kloxin, C. A. DeForest, K. S. Anseth and C. N. Bowman, *Nat. Chem.*, 2011, **3**, 256-259.

77. R. N. Keller, H. D. Wrcoff and L. E. Marchi, *Inorg. Synth.*, 1946, **2**, 1-4.

78. D. M. Haddleton, M. C. Crossman, B. H. Dana, D. J. Duncalf, A. M. Heming, D. Kukulj and A. J. Shooter, *Macromolecules*, 1999, **32**, 2110-2119.

79. M. Ciampolini and N. Nardi, *Inorg. Chem.*, 1966, **5**, 41-44.

80. J. Queffelec, S. G. Gaynor and K. Matyjaszewski, *Macromolecules*, 2000, **33**, 8629-8639.

81. G. Mantovani, F. Lecolley, L. Tao, D. M. Haddleton, J. Clerx, J. J. L. M. Cornelissen and K. Velonia, *J. Am. Chem. Soc.*, 2005, **127**, 2966-2973.

82. S. Perrier, C. Barner-Kowollik, J. F. Quinn, P. Vana and T. P. Davis, *Macromolecules*, 2002, **35**, 8300-8306.

83. M. T. Stone and J. S. Moore, *Org. Lett.*, 2004, **6**, 469-472.

84. S. H. Chanteau and J. M. Tour, *J. Org. Chem.*, 2003, **68**, 8750-8766.

85. D. Quemener, M. Le Hellaye, C. Bissett, T. P. Davis, C. Barner-Kowollik and M. H. Stenzel, *J. Polym. Sci., Part A: Polym. Chem.*, 2008, **46**, 155-173.

86. W. Zhang, Z. Zhang, J. Zhu and X. Zhu, *Macromol. Rapid Commun.*,

2010, **31**, 1354-1358.

87. J. Geng, G. Mantovani, L. Tao, J. Nicolas, G. J. Chen, R. Wallis, D. A. Mitchell, B. R. G. Johnson, S. D. Evans and D. M. Haddleton, *J Am Chem Soc*, 2007, **129**, 15156-15163.

88. J. Geng, J. Lindqvist, G. Mantovani and D. M. Haddleton, *Angew. Chem. Int. Ed.*, 2008, **47**, 4180-4183.

89. L. Nurmi, J. Lindqvist, R. Randev, J. Syrett and D. M. Haddleton, *Chem. Commun.*, 2009, 2727-2729.

90. C. W. Cairo, J. E. Gestwicki, M. Kanai and L. L. Kiessling, *J. Am. Chem. Soc.*, 2002, **124**, 1615-1619.

91. K. Henriksen, A. C. Bay-Jensen, C. Christiansen and M. A. Karsdal, *Expert Opin. Biol. Ther.*, 2010, **10**, 1617-1629.

92. J. Wang, D. Chow, A. Heiati and W. C. Shen, *J. Controlled Release*, 2003, **88**, 369-380.

93. G. Mantovani, F. Lecolley, L. Tao, D. M. Haddleton, J. Clerx, J. J. L. M. Cornelissen and K. Velonia, *J Am Chem Soc*, 2005, **127**, 2966-2973.

94. D. Bontempo, R. C. Li, T. Ly, C. E. Brubaker and H. D. Maynard, *Chem. Commun.*, 2005, 4702-4704.